# *DEVELOPMENT OF A BRACHYTHERAPY TREATMENT PLANNING MODULE FOR CERVIX CANCER UTILISING BIOLOGICAL DOSE METRICS*

By

Hester Catharina van der Walt

Submitted in fulfilment of the requirements in respect of the MMedSc (Medical Physics) degree qualification in the Department of Medical Physics in the Faculty of Health Sciences at the University of the Free State

**Submission Date:** 7 December 2020

**Supervisor:** Dr William Shaw, PhD (Medical Physics)

Medical Physicist, Department of Medical Physics, University of the Free State, Bloemfontein, South Africa

## Declaration

"I, Hester Catharina Oosthuizen (van der Walt) , declare that the Master's Degree research dissertation or interrelated, publishable manuscripts/published articles, or coursework Master's Degree mini-dissertation that I herewith submit for the Master's Degree qualification MedSc (Medical Physics) at the University of the Free State is my independent work, and that I have not previously submitted it for a qualification at another institution of higher education."

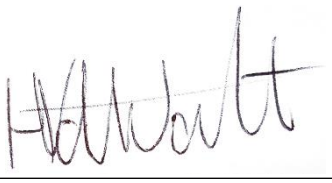

Hester Catharina van der Walt (2009003209)

## Abstract

Key words: Image-Guided Adaptative Brachytherapy, biological, equivalent uniform dose, optimisation, interstitial.

The contouring uncertainties associated with the use of computed tomography imaging for brachytherapy planning creates the need to investigate an alternative planning method for Image-Guided Adaptative Brachytherapy. This alternative method needs to be more robust against imaging and contouring uncertainties compared to the original GEC-ESTRO prescription regarding dose-volume histogram criteria. This study evaluates the utilisation of biological dose metrics (equivalent uniform dose (EUD)) during Image-Guided Adaptive Brachytherapy (IGABT) treatment planning and optimisation. A retrospective planning study was conducted. The eighteen patients that were included in the planning study received CT-based Image-Guided Brachytherapy (IGBT) in combination with external beam radiotherapy (EBRT) between 2014 and 2015. A novel biological optimisation model was developed and used to efficiently and automatically optimise brachytherapy (BT) plans by utilising either dose-volume, biological metrics/indexes or both for fast treatment plan generation. The module was refined to allow forward and inverse planning and optimisation of combined interstitial and intracavitary brachytherapy.

Additionally, the utilisation of OAR total dose constraints during the planning process was applied and evaluated. The results of the study showed that the inverse optimisation tool could produce better target volume coverage compared to the manual optimisation tool. In some cases, the inverse optimisation tool led to higher OAR doses; however, the values recorded were still within set constraints. When comparing the conventional and biological planning methods, the biological planning produced superior CTV-T doses and dose distributions within the CTV-T. The inverse biological approach reported significantly higher average CTV-$T_{HR}$ $D_{98\,\%}$ , $D_{100\,\%}$ values and CTV-$T_{IR}$ EUD, $D_{90\,\%}$ $D_{98\,\%}$ and $D_{100\,\%}$ values compared to inverse conventional planning approach. With this, the inverse biological approach also had the ability to record significant lower average bladder wall EUD and $D_{0.1cm^3}$ $D_{0.1cm^3}$ values. Even though the inverse conventional planning approach reported significant lower average small bowel $D_{2cm^3}$ values compared to the IBG approach, both approaches were still well below the $D_{2cm^3}$ hard constraint of 75 Gy. Dose escalation was achieved in the CTV-T with a reduction in OAR dose with the combination of interstitial/intracavitary brachytherapy. It was concluded from the study that the incorporation and utilisation of biological metrics, which incorporates the entire dose distribution in the organ of interest, is the preferred approach when compared to the conventional physical dose-volume approach.

## Table of Contents

## Glossary

| | |
|---|---|
| 3D-CRT | Three-Dimensional Conformal Radiation Therapy |
| AAPM | American Association of Physicists in Medicine |
| ABS | American Brachytherapy Society |
| AP | Anterior-Posterior |
| BT | Brachytherapy |
| CT | Computed Tomography |
| CTV | Clinical Target Volume |
| CTV-T | Clinical Target Volume for the Primary Tumour |
| $CTV\text{-}T_{adapt}$ | Adaptive Clinical Target Volume |
| DFS | Disease-Free Survival |
| DOH | Department of Health |
| DVH | Dose-Volume Histogram |
| $D_{90\,\%}$ | The minimum dose delivered to 90% of the respective volume |
| $D_{98\,\%}$ | The minimum dose delivered to 98% of the respective volume |
| $D_{100\,\%}$ | The minimum dose delivered to 100% of the respective volume |
| $D_{0.1cm^3}$ | The minimum dose in the most irradiated 0.1cm$^3$ tissue volume |
| $D_{1cm^3}$ | The minimum dose in the most irradiated 1.0cm$^3$ tissue volume |
| $D_{2cm^3}$ | The minimum dose in the most irradiated 2.0cm$^3$ tissue volume |
| $D_{5cm^3}$ | The minimum dose in the most irradiated 5.0cm$^3$ tissue volume |
| $D_{10cm^3}$ | The minimum dose in the most irradiated 10.0cm$^3$ tissue volume |
| EBRT | External Beam Radiotherapy |
| $EQD_2$ | Equivalent Dose in 2 Gy fractions |
| EUD | Equivalent Uniform Dose |
| FIGO | International Federation of Gynaecology and Obstetrics |
| GEC - ESTRO | Groupe Européen de Curiethérapie and the European SocieTy for Radiotherapy & Oncology |

| | |
|---|---|
| gEUD | Generalized Equivalent Uniform Dose |
| GI | Gastrointestinal |
| $GTV_{init}$ | Initial Gross Tumour Volume |
| GTV-$N_{init}$ | Gross Tumour Volume with involved regional node(s) |
| GTV-$M_{init}$ | Gross Tumour Volume with known distant metastases |
| GTV-$T_{init}$ | Gross Tumour Volume for the primary Tumour |
| GTV-$T_{res}$ | Residual Gross Tumour Volume at Brachytherapy |
| $GTV_B$ | Gross Tumour Volume at Brachytherapy |
| GU | Genitourinary |
| HDR | High Dose Rate |
| HIPO | Hybrid Inverse treatment Planning and Optimization algorithm |
| HIV | Human Immunodeficiency Virus |
| CTV-$T_{HR}$ | High Risk Clinical Target Volume |
| HR-QoL | Health–Related Quality of Life |
| HPV | Human Papilloma Virus |
| ICBT | Intracavitary Brachytherapy |
| IC-IS | Intracavitary-Interstitial |
| ICRU | International Commission on Radiation Units and Measurements |
| IGABT | Image Guided Adaptive Brachytherapy |
| IGBT | Image Guided Brachytherapy |
| IGRT | Image Guided Radiotherapy |
| IHDM | In-house Developed Module |
| IMRT | Intensity Modulated Radiation Therapy |
| IPSA | Inverse Planning Simulated Annealing |
| IR-192 | Iridium-192 |
| CTV-$T_{IR}$ | Intermediate Risk Clinical Target Volume |
| ISBT | Interstitial Brachytherapy |

| | |
|---|---|
| LACC | Locally Advanced Cervical Cancer |
| LC | Local Control |
| LDR | Low Dose Rate |
| LMIC | Low- and middle-income countries |
| LQ | Linear Quadratic model |
| MDR | Medium Dose Rate |
| MRI | Magnetic Resonance Imaging |
| NTCP | Normal Tissue Complication Probability |
| OAR | Organs at Risk |
| OS | Overall Survival |
| OTT | Overall Treatment Time |
| PET | Positron Emission Tomography |
| PFS | Progression-Free Survival |
| PRO | Patient Reported Outcome |
| PRS | Patient Reported Symptoms |
| PTV | Planned Target Volume |
| RAKR | Reference Air Kerma Rate |
| RT | Radiation Therapy |
| SF | Surviving fraction |
| SCC | Squamous cell carcinoma |
| SOC | Standard of Care |
| SBRT | Stereotactic Body Radiation Therapy |
| TCP | Tumour Control Probability |
| TG | Task Group |
| TPS | Treatment Planning System |
| TRAK | Total Reference Air Kerma |
| $V_{100}$ | Volume Receiving 100% of the Prescribed Physical Dose |

| | |
|---|---|
| VMAT | Volumetric Modulated Arc Therapy |
| VOI | Volume of Interest |

## List of Tables

## List of Figures

## List of Appendices

# Chapter 1 - Introduction

## 1.1 Origin and occurrence of cervical cancer

Cervical cancer is a malignant growth or tumour at the entrance of the uterus resulting from an uncontrolled division of abnormal cells. This disease is listed as the fourth most frequent cancer in women worldwide, with an estimated 570 000 new cases in 2018 [1]. The majority of new cases and deaths (approximately 85% and 90%, respectively) occur in low- and middle-income countries (LMIC) [2].

A cancer profile of South Africa, which is classified as a LMIC, indicates that the annual number of cervical cancer cases are about 12,983 and the annual number deaths are roughly 5 595 (estimates for 2018) [3]. The unfortunate reasons for the alarmingly high prevalence of this disease in South Africa include the absence of a properly implemented population-based screening programme, a poorly controlled human immunodeficiency virus (HIV) epidemic with high HIV occurrence, late diagnosis and incomplete access to timely and effective treatment [4]. Treatment received is mainly ineffective as it is primarily 3D-External beam radiotherapy and 2D based brachytherapy.

The human papillomavirus (HPV) infection is a well-established cause of cervical cancer and causes nearly 100 % of cervical cancers. There are 15 high-risk (oncogenic) HPV, with just two, HPV-16 and HPV-18, responsible for 70 % of all cervical cancer cases worldwide [5]. The majority of cases are squamous cell carcinoma (SCC) which originate from cells in the exocervix and commonly linked to the HPV-16. Adenocarcinoma, which develops from gland cells, are usually linked with HPV-18 [6]. HPV commonly spreads through sexual contact; however, it can spread without sexual contact, by skin-to-skin contact with an infected area of the body. Most of these infections are transient, and 90 % resolve spontaneously within 2 to 5 years. A newly diagnosed HPV infection in young women lasts on average for between 8 to 13 months [7]. So, it is well known that HPV seldom leads to cancer. However, if HPV is addressed, the resulting cancer is also addressed.

Even though HPV infection is a necessary cause of cervical cancer, it is an insufficient cause. Additional cofactors are present for progression from cervical HPV infection to cancer. Dietary habits, tobacco

[1] (WHO, 2018)
[2] (WHO, 2018; Bhatla et al., 2019)
[3] (Bruni et al., 2019)
[4] (Denny, 2008)
[5] (Smith et al., 2007; Frumovitz, 2015)
[6] (Pirog et al., 2000; Altekruse et al., 2003; Pandey, 2017; Robadi, Pharaon and Ducatman, 2018)
[7] (Jason D Wright, 2019)

smoking, long-term hormonal contraceptive use, teenage pregnancy, multiples pregnancies, family history and HIV have been identified as established cofactors [8].

In 2018, the South African population was estimated at 57.73 million, while approximately 13 % (around 7.52 million) of the population are people living with HIV. A projected 19.0 % of the adult population aged between 15 and 49 years, is HIV positive [9]. HIV-positive patients have an increased risk of persistent HPV infection, premalignant lesions and cervical cancer compared with uninfected women. [10] Local data suggests that cervical cancer occurs up to a decade earlier in HIV-infected women [11]. Moreover, the characteristics of invasive cervical carcinoma could take a more aggressive clinical course in HIV-positive women [12]. It also has a higher recurrence and mortality rate with shorter intervals to recurrence and death than women who are HIV-negative [13].

## 1.2 Screening programmes and vaccinations in South Africa

It has been established that a well-organised cervical cancer screening programme or widespread good quality cytology is the most powerful prevention tool for the reduction of cervical cancer incidence and/or mortality [14]. Cervical cytology testing, also known as a pap smear, involves collecting exfoliated cells from the cervix and examining these cells microscopically [15].

The national cervical cancer prevention programme, presently, offers three cervical cytology smears per lifetime at public health facilities, starting from the age of 30, every ten years. Patients with HIV infection undergo more frequent cytology tests, at diagnosis and every five years [16]. However, the call and recall systems are insufficient, and the number of women lost to follow-up, before treatment, is high. In the private sector, cytology-based opportunistic screening is well accepted, but are implemented inconsistently. Some women undergo screening yearly, thus over-serviced; while, many others do not undergo screening at all. The disease prevalence is lower, but tolerance for incorrect tests is also lower [17].

[8] (Jason D Wright, 2019)
[9] (StatsSA, 2018)
[10] (Snyman et al., 2006; Batra, Kuhn and Denny, 2010)
[11] (Snyman et al., 2006; Simonds, Neugut and Jacobson, 2015)
[12] (Maiman, 1998; Nappi et al., 2005)
[13] (Maiman, 1998; Nappi et al., 2005)
[14] (Denny, 2008)
[15] (Denny and Kuhn, 2017)
[16] (Botha and Dreyer, 2017; Bruni et al., 2019)
[17] (Botha and Dreyer, 2017)

High-risk HPV testing is widely available and offers improved sensitivity for existing and future cervical pre-cancer lesions over a single round of cytology. This approach has been accepted as an alternative primary screening test to the traditional cervical cytology [18].

There are currently vaccines, offering protection against persistent HPV infection. In 2014, a national school-based HPV routine vaccination program was introduced. In this program girls between the ages of 9 and 10 are vaccinated with a Cervix HPV vaccine. The vaccination protects against the two high-risk HPV types, HPV-16 and -18 and is administered in two dose fractions at least six months apart [19].

## 1.3 Staging and different treatment regimens

The International Federation of Gynaecology and Obstetrics (Figo) staging system is used mostly for the staging of cancers within the female reproductive organs, including cervical cancer. Until recently, The FIGO staging was primarily based on clinical examination with the addition of certain procedures that were allowed by FIGO to change the staging. The latest FIGO staging for cervical cancer was revised in 2018 to allow stage assignments based on pathological and imaging findings, when available [20]. The stage of the disease comprises of its size, depth of invasion and how far it has spread. Cross-sectional imaging, such as magnetic resonance imaging (MRI) or Computed Tomography (CT), is used to obtain measurements of tumour size volume, and extent of disease. A pelvic MRI is the best single imaging method for assessing primary tumours over 10 mm in size, since it can accurately determine tumour location and size, pelvic sidewall invasion, parametrial involvement and lymph node metastasis [21] Although MRI is seen as the gold standard, CT imaging is more widely available and can produce adequate clinical information. Positron emission tomography (PET) has become the standard tool for nodal involvement evaluation. The involvement of para-aortic and/or pelvic lymph nodes could be used to guide clinical decisions related to radiation treatment planning, such as the delivered dose and field size [22].

The stage of cervical cancer dictates the treatment regimen for each individual case, and a distinction is made between early stage disease and locally advanced disease (LACC).

### Early stage disease

Early stage disease comprises of FIGO Stage IA, IB1, IB2 and IIA1 [23]. Surgical treatment is the preferred treatment modality. Radiotherapy provides equally good results in terms of local control and survival

[18] (Kitchener et al., 2014; Huh et al., 2015; Botha and Dreyer, 2017)
[19] (Mbulawa et al., 2018; Bruni et al., 2019)
[20] (Bhatla et al., 2019)
[21] (Sala et al., 2013; Dappa et al., 2017)
[22] (Viswanathan, Beriwal, et al., 2012)
[23] (Bhatla et al., 2019)

in cases with contraindications for anaesthesia or surgery [24]. The primary treatment for cases with lymph-node involvement is radiochemotherapy, including brachytherapy [25]. The choice of treatment in early stage disease should be made by considering anatomic, clinical and social factors [26]

### Locally advanced disease

Locally advanced cervical cancer (LACC) consists of FIGO stage IB3 – IVA. The standard of care (SOC) for treatment and management of LACC includes pelvic EBRT with concomitant cisplatin chemotherapy followed by BT [27].

The combination of BT and EBRT maximizes the probability of locoregional control whilst minimizing the risk of treatment complications [28]. Several studies of the combination of EBRT and BT treatment have shown a decline in local recurrence rates [29] and improved overall survival (OS) [30] was observed when BT is a component of treatment compared to pelvic external beam radiotherapy (EBRT) alone.

According to [31], patients receiving SOC treatment had significantly improved OS in contrast to a patient not receiving the standard of care treatment. It has also been reported that no additional treatment, including sophisticated EBRT techniques like Intensity modulated radiation therapy (IMRT) or Stereotactic body radiation therapy (SBRT), can make up for the survival decrement from lack of BT as a component of definitive care [32].

The addition of chemotherapy to the SOC treatment has been found to improve survival and local control among women with LACC. However, concurrent chemotherapy increases the severity of acute side effects but without increasing the risk of severe late treatment-related side effects [33]. The American Brachytherapy Society (ABS) recommends that chemotherapy should be administered on EBRT day and not on a BT day, due to the potential for increase complications due to normal-tissue sensitization [34].

The overall treatment time (OTT) is also important. Treatment should be completed within eight weeks; wherein better local tumour control and survival can be expected [35]. Before the era of

[24] (Bhatla et al., 2019)
[25] ('Prescribing, Recording, and Reporting Brachytherapy for Cancer of the Cervix', 2013)
[26] (Bhatla et al., 2019)
[27] (Haie-Meder et al., 2005; L. T. Tan, 2011; Tanderup et al., 2014; Bhatla et al., 2019)
[28] (Logsdon and Eifel, 1999; Bhatla et al., 2019)
[29] (Hanks, Herring and Kramer, 1983; Delgado et al., 2019)
[30] (Han *et al.*, 2013; Tanderup *et al.*, 2014; 2016; Delgado *et al.*, 2019)
[31] (Robin et al., 2016)
[32] (Han et al., 2013; Robin et al., 2016)
[33] (Morris et al., 1999; Eifel et al., 2004; Eifel, 2006)
[34] (Viswanathan, Beriwal, et al., 2012)
[35] (Mahmoud et al., 2017; Bhatla et al., 2019)

concomitant chemotherapy, the impact of overall treatment time was demonstrated with loss of local control and OS of between 7–8% per week of prolonged treatment [36]. The retroEMBRACE study established that an additional dose of 5 Gy $EQD2_{10}$ ($D_{90}$ CTV-$T_{HR}$) is required to compensate for a delay in OTT by one week [37].

The Universitas Annex Hospital is a public facility that provides radiotherapy services to all public patients in the Free State, Northern Cape and Lesotho. This facility treats roughly between 300 to 400 cervical patients per annum, resulting in an average of more than one new cervix case daily. This high number of cervix patients forces the facility to investigate and implement the most effective treatment techniques, which is balanced with regard to the quality of treatment and the time needed to prepare and deliver the treatment. While other methods are being investigated, the facility's, main goal is still to deliver quality treatment to all patients.

## 1.4 Aim

The study aims to develop a novel biological optimization model which can be used to efficiently and automatically optimize BT plans utilizing either dose-volume or biological metrics/indexes or both for fast treatment plan generation.

[36] (Girinsky et al., 1993; Perez et al., 1995)
[37] (Tanderup et al., 2016)

# Chapter 2 - Theory

The most clinically significant effect of radiation therapy is the production of irreparable DNA cell damage which results in the loss to sustain adequate cell division. In tumours, the main goal is the complete loss of proliferative ability by all the tumour cells, which is a needed for cancer cure. In the case of normal cells, the goal is to maintain the proliferative ability of as many normal cells as possible. Proliferative sterilisation is often referred to as cell kill [38].

## 2.1 Cell survival curves

The linear-quadratic model (LQ) is most often used in describing the cell surviving fraction *SF, a*s illustrated in Figure 1.

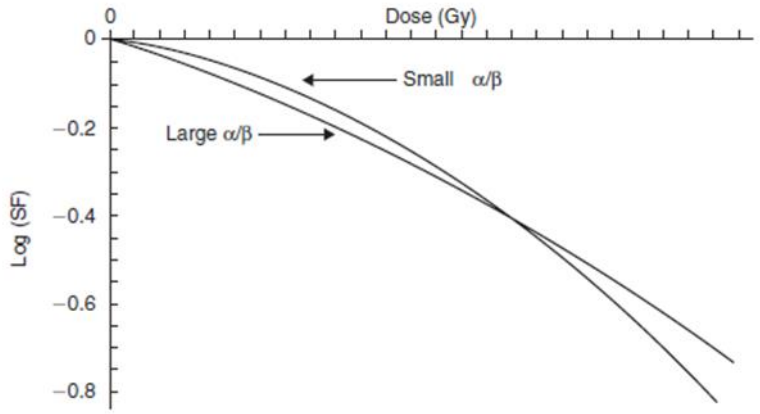


**Figure 1 - Cell survival curves in radiotherapy. "Adapted with permission from (McMahon, S.J., The linear quadratic model: usage, interpretation and challenges, Phys. Med. Biol., 64 (2019) 1-24). Copyright © (2018) Institute of Physics and Engineering in Medicine".**

SF is defined as the proportion of cells that retain the ability to proliferate (relative to an unirradiated control population) with the assumption that there are two components to cell kill, namely:

- Lethal (non-repairable) lesions, with a survival fraction SF = exp (-αD), represented by the tangent to the survival curve at its origin.
- Sub-lethal lesions, non-lethal and potentially repairable, but the accumulation of which can cause cell death, with a survival fraction SF = ($-\beta D^2$)

Equation (1) can be used to calculate the SF:

$$SF = \exp(-\alpha d - \beta d^2) \quad (1)$$

Where

[38] (E.B.Podgorsak, 2005; Barrett et al., 2009)

SF - the surviving fraction

α and β - parameters which characterise the cells involved

d - single dose given

The ratio α/β gives the relative importance of the quadratic dose term and the linear dose term for the cells involved, this ratio controls the shape of the survival curve, as illustrated in Figure 1:

- Large α/β - indicates that the linear term dominates and results in a relative straight cell survival curve with a small repair capacity (Tumour and early responding normal tissues α/β - 10 Gy).
- Small α/β - indicates that the quadratic term is more dominant with a large repair capacity (late responding normal tissues α/β - 3 Gy). In this case, doubling the dose will lead to more than doubling of the effect on the surviving fraction. Such cells will be particularly sensitive to changes in fraction size when radiation is given as a fractionated schedule.

Typically, survival curves are continuously bending, with a slope that steepens as the dose increases.

## 2.2 Equivalent dose in 2 Gy fractions ($EQD_2$)

The radiobiological effects of a different dose per fraction size differ from those of a 2 Gy per fraction for the same radiation dose distribution in an organ. Therefore, the LQ model is used to convert doses per fraction into the biologically equivalent physical dose of 2 Gy per fraction ($EQD_2$), as illustrated in Equation (2):

$$EQD_2 = (nf \times d_1) \times \frac{\left(d_1 + {}^{\alpha}/_{\beta}\right)}{(d_2 + {}^{\alpha}/_{\beta})} \quad (2)$$

Where

$nf$ - Number of fractions

$d_1$ - fractional dose received (Gy)

$d_2$ - 2Gy

${}^{\alpha}/_{\beta}$ - Tissue-specific parameters

The $EQD_2$ gives the ability to compare different treatment techniques and fractionation schedules.

## 2.3 Radiotherapy Treatment techniques

The clinical stage, the size of tumour volume, lymphovascular space involvement, nodal involvement, and histological subtype at the beginning of radiotherapy are well-known prognostic factors [39]. Risk factors for local control (LC) and survival have been identified as large tumour size (>5 cm), young age (≤40 years), non-squamous histology, positive lymph node on MRI, as well as the advanced stage of all risk factors for locoregional failure after definitive platinum-based chemoradiation in patients with locally advanced cervical cancer [40].

The presence of bilateral parametrial invasion decreases the 10-year disease-free survival (DFS) rate in Stage IIIB patients. The presence of central bulky disease (tumour size ≥5 cm in diameter) decreases the DFS and increases the pelvic failure rate by about 11 % for all patients [41]. Wang et al. suggested that the ratio between the tumour volume and regression provide essential information that could guide early intervention for patients at high risk of treatment failure [42]. The 5-year survival rate, including progression-free survival (PFS) and OS in node-negative disease, compared to node-positive disease is significantly higher [43].

Radiotherapy techniques used in the treatment of cervical cancer can be subdivided into two main categories:

1. External beam radiotherapy (EBRT) – This technique will be discussed briefly.
2. Brachytherapy (BT) – This technique is the focus of this study and will be discussed in detail.

### 2.3.1 External beam radiotherapy (EBRT)

External beam radiotherapy (EBRT) plays a vital role in the management of patients diagnosed with cervical cancer. The role of EBRT is to shrink bulky endocervical tumours, to treat paracentral infiltration and nodal disease that lies beyond the reach of the BT system and thus preventing optimal BT treatment.

In general, EBRT can be delivered with orthovoltage, particle therapy or using a linear accelerator. The latter is applicable to cervical cancer treatment. Cervical EBRT is delivered using a machine that produces high energy photons or/and electrons, known as a linear accelerator. The radiation source

[39] (Delgado et al., 1990; Kovalic et al., 1991; Eifel et al., 1994; Fyles et al., 1995; Perez et al., 1998; Morice et al., 2003; Van De Putte et al., 2005; Barbera and Thomas, 2009; Bae et al., 2016; Cho and Chun, 2018)
[40] (Bae et al., 2016)
[41] (Kovalic et al., 1991)
[42] (J. Z. Wang et al., 2010)
[43] (Choi et al., 2018)

is located outside the patient, and the target (tumour) within the patient is irradiated with an external radiation beam.

Conventionally, EBRT planning was based on bony anatomy landmarks visible on X-rays and treatment was delivered by using parallel opposed fields or the four-field box technique. The parallel opposed fields achieved adequate dose coverage to the target, but with an increase in dose to the bladder and rectum and inferior dose to the parametrium. The four-field box technique was introduced and have led to reduced dose in normal tissues and an improvement in dose distribution compared to parallel opposed fields [44]. The risk associated with conventional EBRT is that the actual tumour volume can fall outside the field borders determined by standard bony landmarks; resulting in underdosage of the target volume.

Since the 1990s, 3D-conformal EBRT (3D-CRT) in combination with CT-based treatment planning, has been implemented internationally [45]. CT/MRI/PET imaging gives the ability to visualise and delineate target and normal tissue volumes. However, all commercially available treatment planning systems (TPS) use CT images to provide information regarding electron density of tissues which is required for the dose calculation algorithms. The dose and volumetric coverage of all structures are measured and evaluated by calculating the necessary dose-volume histograms (DVH) [46].

EBRT is designed to treat the clinical target volume (CTV), which include the following:

1. The gross disease (gross tumour volume (GTV), known as the primary tumour with local extensions (if not removed surgically);
2. The entire cervix and uterus;
3. Parametrial and uterosacral ligaments;
4. The upper vagina or at least 3 to 4 cm inferior to the most inferior extent of the tumour;
5. Pre-sacral nodes and all other nodal volumes at risk.

The prescribed dose must encompass the planned target volume (PTV), which consists of the CTV plus a safety margin of between 7 to 10 mm to account for uncertainties in the daily patient set-up [47]. The primary tumour and regional lymph nodes at risk are treated with definitive EBRT to a total dose of approximately 45 Gy (i.e. 40 to 50 Gy). If present, the nodal disease can be optimally boosted with an additional 10 to 15 Gy by the integration of IMRT into the patient's treatment [48].

[44] (Gulia et al., 2013)
[45] (Vordermark, 2016)
[46] (Elshaikh et al., 2006)
[47] (Management of Cervical Cancer: Strategies for Limited-resource Centres - A Guide for Radiation Oncologists, 2013)
[48] (Wagner, Jhingran and Gaffney, 2013)

IMRT, an advanced form of 3D-CRT, has recently been developed and utilized. In contrast to the uniform radiation intensity used in 3D-CRT, the uniform intensity of each beam is purposely altere to produce a variable intensity/fluence across each beam. Each beam consists of hundreds of beamlets, with an individual intensity level. The use of multiple beams can produce a highly conformal dose distribution, allowing precise shaping to the target volume and thus further sparing of the normal tissues.

IMRT or Volumetric Modulated Arc Therapy (VMAT) is associated with exceptional PTV coverage, with considerable sparing of normal tissues, reduced gastrointestinal (GI) and genitourinary (GU) acute toxicity and reduced late overall toxicity compared to 3D-CRT without compromising the clinical outcome [49]. Pelvic IMRT has been reported to improve the quality of life with regards to physical functioning and other treatment effects during treatment [50]. However, the replacement of BT with smaller EBRT fields to deliver a central dose of between 60 to 70 Gy resulted in higher complication rates, while more reduced survival rates were evident [51]. IMRT was shown to be inferior to BT with respect to the specific target volume doses when dose constraints to the bladder, rectum and sigmoid are obeyed. [52]

However, the female pelvis is known to have significantly associated tumour motion, normal organ motion and tumour deformation/shrinkage, which result in intra-and inter-fraction cervical motion, unwanted exposure to OARs and a reduction in treatment accuracy which should be taken into account [53]. IMRT and more conformal techniques require investment in rigorous Image-Guided Radiotherapy (IGRT) as these techniques can only be performed by implementing IGRT. Improvement in treatment accuracy can be obtained by implementing IGRT adaptive approaches. Applying relevant PTV margins can be one way to account for intra-fraction cervical motion [54].

During the past few years, IGRT has become the new standard of care in several tumour types [55]. This technique uses in-room imaging techniques to obtain 3D images before/after treatment daily, reliant on what imaging protocol is followed. The images are used to determine the changes in target, OAR volumes and positioning since the initial treatment plan. The initial plan is then adapted accordingly to optimize dose delivery and achieve safe dose escalation throughout the course of the treatment.

[49] (Mundt et al., 2002; Gandhi et al., 2013; Chen et al., 2015; Deng et al., 2017)
[50] (Klopp et al., 2016)
[51] (Logsdon and Eifel, 1999; Tanderup et al., 2014)
[52] (Fokdal et al., 2016)
[53] (Haripotepornkul et al., 2011)
[54] (Tyagi et al., 2011; Jadon et al., 2014; Heijkoop et al., 2015)
[55] (Martinez et al., 2001; Barker et al., 2004; van de Bunt et al., 2006)

At the same time, advances in diagnostic imaging, as well as image guidance during radiation delivery, permits for more precisely defined treatment delivery [56].

### 2.3.2 Brachytherapy (BT)

The ability of BT to deliver between 80 to 85 Gy ($EQD_2$) to the tumour periphery while the central cervix receives even higher doses (> 120 Gy $EQD_2$) undoubtedly explains the excellent LC rates that can be achieved when cervical cancers are treated with a combination of EBRT and BT. This is one of the many reasons why BT is not optional in the treatment of cervical cancer [57].

BT is a form of radiotherapy treatment where small, encapsulated radioactive sources are placed within or adjacent to the tumour. The two main types of BT are interstitial and intracavitary BT (ICBT). The type of BT selected depends on the extent of the disease in combination with the patient's anatomy. Interstitial BT (ISBT) is based on the temporary or permanent implantation of the sources within the tumour volume (with the aid of needles) and is mainly used to treat prostate, gynaecological and breast tumours. Intracavitary BT is based on the placement of sources temporarily within body cavities, such as the cervix/uterus, close to the tumour volume (with the aid of an applicator) and is mainly used to treat gynaecological tumours such as tumours in the uterus, cervix and vagina [58].

Most common ICBT applicators widely available include two variations on the Tandem and Ring design and Tandem and Ovoid design. As the name suggests, the Tandem and Ring applicator consist of a tandem, an intrauterine tube placed through the cervix to the level of the uterine fundus, and a ring that sits on either side of the cervix. The Tandem and Ovoid applicator consist of a tandem and two ovoids (colpostats) that are placed on either side of the cervix in the lateral vaginal fornices. Both applicators result in comparable treatment outcome, although differences exist in the distribution of radiation dose and ease of use, the choice of use ultimately resides on the user [59].

BT treatment dose rates fall into three categories [60]:

1. Low dose rate (LDR) - from 0.4 to 2.0 Gy/h;
2. Medium dose rate (MDR) - more than 2.0 to 12.0 Gy/h. MDR is not in common use;
3. High dose rate (HDR) - more than 12.0 Gy/h.

[56] (Taylor and Powell, 2004; Elshaikh et al., 2006)
[57] (Tanderup *et al.*, 2013; 2014)
[58] (E.B.Podgorsak, 2005, pp. 451–452)
[59] (Banerjee and Kamrava, 2014)
[60] (E.B.Podgorsak, 2005, p. 454)

The most common radiation source used for high dose rate (HDR) afterloading is Iridium-192 (Ir-192), due to its medium average γ ray energy of 400 keV and its high specific activity. The only downfall of Ir-192 is its relatively short half-life of 73.8 days, which requires several replacements throughout the year [61]. As illustrated in Figure 2, the Ir-192 source is a platinum/iridium alloy (3.5 mm long and 0.6 mm in diameter) with a high concentration of Ir-192, resulting in the high activity. The 1 mm platinum coating attenuates any electrons that are generated through decay. The capsule is welded to the end of a wire, which enables retraction and deployment from within an HDR remote afterloading machine.

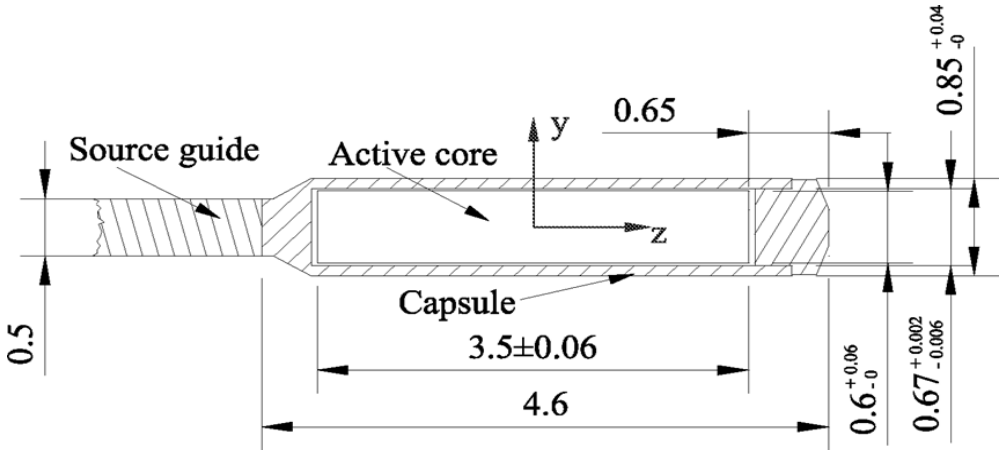


**Figure 2 - Flexisource Ir-192 HDR. "Reproduced with permission from (Granero, D., Pérez-Calatayud, J., Casal, E., Ballester, F. and Venselaar, J.. A dosimetric study on the high dose rate Flexisource, Med. Phys., 33 (2006) 4578–4582). Copyright © (2006), John Wiley & Sons".**

## Conventional 2D Intracavitary brachytherapy

Brachytherapy is seen as one of the oldest treatment modalities in radiotherapy. In 1903, soon after Marie and Pierre Curie discovered radium in 1898, radium sources were successfully used in ICBT for the treatment of cancer of the cervix. The dose prescription was mainly subjective due to the lack of knowledge and data about the biological effects of radiation on the tumour volume and the adjacent normal tissues. Different dosimetric systems were formulated and used as guidelines to reach the required treatment outcome. These guidelines focused on the treatment duration, loading and arrangement patterns for a specific set of radioisotopes and the amount of radium required to deliver the desired prescription, specified in mg-hours. The dose received by normal tissues during treatment was neglected [62].

The Manchester system was formulated in 1938 and subsequently modified by Tod et al. in 1953. The modification attempted to overcome the shortfalls and issues as mentioned above [63]. The treatment was defined in terms of dose to a point, which was considered to be a representative of the target

[61] (E.B.Podgorsak, 2005, p. 457,464)
[62] (Srivastava and Datta, 2014)
[63] (Tod and Meredith, 1938; 1953)

volume itself, being reproducible from one patient to the next. After calculating the dose (in Roëntgen) at several points within the pelvis, Tod et al. determined that the initial site of necrosis was within the paracervical triangle, this triangle was categorized as the dose-limiting region where the uterine vessels cross the ureter. Keeping the paracervical triangle in mind, they defined point A, 2 cm lateral to the central canal of the uterus and 2 cm superior to the mucosa of the lateral fornix, in the plane of the uterus. The combination of applicators used for treatment, loading and source arrangement patterns, as well as applicator design, were specified to deliver the same dose-rate to point A. The constancy of dose rate at point A was believed to be a major strength of the Manchester system point A dose prescription. However, this original defined point A were not visible on orthogonal planar radiographs, therefore point A were redefined in relation to the applicator which was easily visualized on a radiograph. As seen in Figure 3, the newly defined point A was described by Tod and Meredith as a point 2 cm above the external os of the uterus and lateral to the uterine tandem in the plane of the uterus, respectively. Point B was defined 2 cm above the external os and 5 cm laterally to the midline; in other words, 3 cm lateral to point A. This point was seen as a representative of the dose delivered to the obturator nodes and pelvic wall [64]. This point A dose prescription was suitable in clinical practice with limited imaging modalities available.

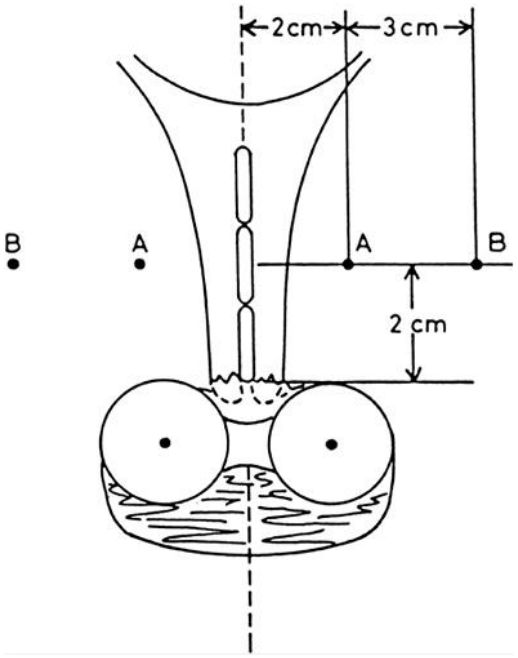


**Figure 3 - Original definition of points A and B, according to the Manchester system [65].**

Questions were raised of how well the BT point A (BPA) correlated with the anatomical point A (APA). Lewis et al. showed that the BPA and APA were at a minimum distance of 0.8 cm from one another in

[64] (Tod and Meredith, 1953)
[65] (Tod and Meredith, 1938)

93 % of their observations [66]. A study by Wang et al. showed that the average distances between the APA and BPA were 5.4 ± 1.1 cm on the left and 5.2 ± 1.0 cm on the right, this led to the dose received by the APA to be 30 % and 35.2 % of the prescribed dose to the left and right BPA, respectively. From these results, they concluded that the BPA provided an inaccurate dose estimate of the APA and indicated the need to revisit the current BPA [67]. In 1985, the International Commission on Radiation Units and Measurements (ICRU) published a report in which the sole use of point A was frowned upon as this reference point was situated in a very high dose gradient. Thus, resulting in any errors and inaccuracy in the determination of distance with considerable uncertainties in the absorbed dose calculated at these specific points.

Recommendations were made regarding the dose and volume specifications to achieve common ground in reporting ICBT for cervical cancer [68]. In addition to Point A and B, it was recommended that the dose received during treatment to be specified in terms of:

1. Total reference air Kerma (TRAK);
2. Description of a reference volume;
3. OAR reference points to estimate the risk of late complications.

**1. Total reference air kerma (TRAK)**

The Total Reference Air Kerma Rate (TRAK) is defined as the air kerma rate in the air to air at a distance of 1 m from the source, corrected for attenuation and scatter. As illustrated in Equation (3), the TRAK value is the sum of the products of the reference air kerma rate and the dwell time of each source:

$$TRAK = \sum_{i} RAKR_i \times w_i \tag{3}$$

**2. The reference volume**

For the target dose, an additional and different approach was recommended; rather than reporting the dose at a point. It was suggested that at an agreed dose level, the dimensions of the volume included in the subsequent isodose should be reported as the reference volume. The recommended dose level was 60 Gy.

[66] (Lewis, Raventos and Hale, 1960)
[67] (Wang et al., 2007)
[68] (Chassagne et al., 1985)

## 3. OAR reference points

At the time of the ICRU Report 38 publication, an approximation of the dose to OARs could only be derived from standard orthogonal radiographs of the applicator. Hence, reference points were defined in relation to the sources visible on radiographs [69].

As seen in Figure 4, the bladder reference point was defined in terms of the Foley balloon filled with 7 $cm^3$ radio radiopaque fluid inserted into the trigone of the bladder. The catheter was pulled downwards to bring the balloon alongside the urethra:

1. On the AP radiograph, the reference point is taken at the centre of the balloon.
2. On a lateral radiograph, the reference point is obtained on an Anterior Posterior (AP) line drawn through the centre of the balloon. The reference point is taken on this line at the posterior surface of the balloon.

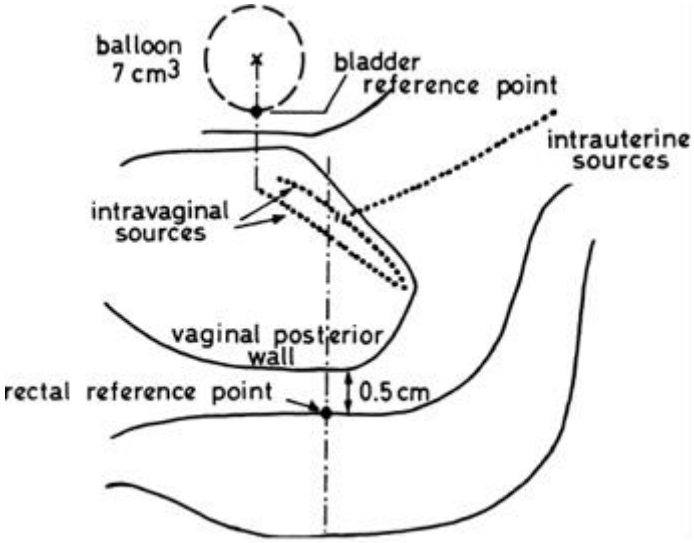


**Figure 4 – The localization of rectum and bladder points. (Reprinted with permission from ICRU. Dose and Volume specification for reporting intracavitary therapy in gynaecology. ICRU Report No. 38. Bethesda, MD: International Commission on Radiation Units and Measurements, 1985.)**

The rectal reference point was related to the applicator, as illustrated in Figure 4:

3. On an anterior radiograph, the reference point is taken at the intersection of the intrauterine source through the plane of the vaginal sources.
4. On a lateral radiograph, an anterior-posterior line is drawn from the lower end of the intrauterine source. The point is located on this line, 5 mm behind the posterior vaginal wall.

[69] (Chassagne and Horiot, 1977)

5. The posterior vaginal wall can be visualised, depending upon the technique, using an intravaginal mould or by opacification of the vaginal cavity with radio-opaque gauze used for packing.

Nonetheless, these points do not take the particular normal tissue anatomy into account, which could be more subject to day-to-day variation affected by fluctuating extents of bowel and bladder filling [70].

**Dose rate**

In the past, ICBT was delivered by using LDR, which involves the source of relatively low activity. The treatment was delivered in phases that ranged from hours to several days, dependent on the dose prescribed. The radiation sources were manually loaded after the applicators/catheters were placed in the target position; this led to unnecessary radiation exposure to staff members.

The introduction of computer-driven remote after loading systems over the recent years, in which radiation sources are controlled with the use of a computer, has made it possible to deliver BT with high activity sources [71]. This has led to the ICBT practice changing from LDR to HDR, and this was done by taking several advantages of HDR over LDR in consideration [72]:

1. Shorter treatment times
    - Smaller risk of applicator movement during treatment
    - Opportunity for outpatients to be treated – no hospitalization needed
    - A greater amount of patient to be treated
2. Eliminates unnecessary radiation exposure to radiation workers and visitors
3. No shielded inpatient hospital rooms required
4. Smaller diameter sources
    - Reduces the need to dilate the cervix
    - Insertion of applicator physically easier
5. The ability to vary dwell positions and dwell times allows the possibility of dose distribution optimization

During HDR-ICBT, the Ir-192 source is moved through the applicator along a specific route; along this route, the source is brought to rest at several positions. The position and the duration in which the source is stationary determine the dose distribution within the patient. HDR-ICBT delivers a high radiation dose concentrated to the local tumour volume while consequently sparing normal tissue,

[70] (Koom et al., 2007)
[71] (E.B.Podgorsak, 2005, p. 454)
[72] (Stewart and Viswanathan, 2006)

due to the inverse square law that causes a rapid dose fall-off outside the tumour [73]. Based on existing prospective and retrospective studies, it was proven that HDR-ICBT is comparable to LDR-ICBT with regard to complications rates, loco-regional control and survival outcomes [74]. A study by Romano et al. reported, as stated above no significant difference in overall survival rates or LC rates between the two approaches, but acute as well as chronic toxicity was higher in HDR-BT compared to LDR-BT outcome [75].

Due to the loss in dose rate effect in HDR-ICBT, multiple HDR fractions are necessary to reach the required treatment outcome; a well-balanced ratio between the rate of tumour control and late normal tissue complications. The applicator placement may vary from one treatment fraction to the other leading to a variation in the applicator spatial position in relation to pelvic bony anatomy, pelvic organs and adjacent organs at risk [76]. Subsequently, this results in the varying location of point A and the 60 Gy ICRU volume [77]. Therefore, multiple HDR fractions lead to a different set of Point A's for the left and right side for each treatment fraction, thus point A changes into a volume A for a single patient [78]. This also results in multiple ICRU volumes in a given patient during multiple HDR fractions [79] and lead to variation in several reporting parameters such as ICRU volumes and TRAK in the same patient during the course of HDR-ICBT treatment [80]. Das et al. stated that these uncertainties in reporting as per ICRU Report 38 guidelines or to Point A, calls for the guidelines to be revised [81].

### Image-Guided Brachytherapy (IGBT)

The limitation of BT based on point A/reference volumes and orthogonal radiographs have focused investigation on BT treatment based on the actual position of the tumour volume and OARs in relation to the applicator.

The availability of CT and MRI has facilitated more detailed anatomic information and the ability to visualize the soft tissues of the pelvis with higher resolution, permitting a closer approximation of the location of the uterus, cervix, vagina, or the OARs, including the sigmoid, rectum, bladder, and small bowel [82]. The combination of 3D imaging and intracavitary applicators that are CT/MRI compatible came more available in the 90's, this combination allowed for accurate localization of intracavitary

[73] (Viswanathan, Beriwal, et al., 2012)
[74] (Teshima et al., 1993; Patel et al., 1994; Hareyama et al., 2002; Lertsanguansinchai et al., 2004; X. Wang et al., 2010)
[75] (Romano et al., 2017)
[76] (Grigsby et al., 1993; Hoskin et al., 1996; Datta et al., 2001)
[77] (Datta *et al.*, 2001; 2004)
[78] (Srivastava and Datta, 2014)
[79] (Datta, 2005)
[80] (Datta *et al.*, 2001; Datta, Das, *et al.*, 2003; Datta, Basu, *et al.*, 2003)
[81] (Datta, Basu, et al., 2003)
[82] (Koom et al., 2007; Viswanathan and Erickson, 2010)

applicators in relation to all necessary neighbouring structures, and with this the ability to obtain the actual dose delivered to the tumour volume and surrounding organs [83].

Plan comparisons were performed by Shin et al., for the conventional point A plan and a CT-guided CTV based plan. A fractional 100 % dose was prescribed to the outermost point to cover all CTV's in the CTV plan and to point A in the conventional plan. The CT-guided CTV planning of ICBT was found to be superior to conventional point A planning in terms of avoidance of overdosed normal tissue volumes and conformity of target coverage[84].

A CT assisted dosimetry study conducted by Kapp et al. showed that the doses received by OARs, specifically focusing on the sigmoid, bladder and rectum are often underestimated when using the ICRU system. The study concluded that OAR doses are higher than traditional 2D planning techniques document [85]. Another study confirmed that prescription based on point A doses, lead to tumour volume uncertainty and underdosage. The maximum ICRU 38 bladder and rectum doses significantly underestimate the maximum doses to OARs and denotes the 90$^{th}$ and 95$^{th}$ percentile of the maximum doses to the rectum and bladder, respectively [86]. The maximum dose to the bladder and rectum was found to be 1.4 and 1.5 times higher in CT-based treatment planning than represented by the ICRU bladder and rectum point in 2D base planning [87]. Other studies have found the same results, some reporting doses higher by approximately two-fold on average [88]. Charra-Brunaud et al. studied the effect of 3D image-based BT on treatment outcomes; for the 2D arm of the study, dosimetry was planned on orthogonal x-rays, and for the 3D arm, dosimetry was planned on CT images. Improved LC and toxicity rates were found with 3D image-based BT [89]. These findings have led to the development of 3D image-guided BT guidelines, to increase the dose to target volume, while reducing the dose to the OARs. The Gynecologic Groupe Européen de Curiethérapie and the European Society for Therapeutic Radiology and Oncology (GYN GEC-ESTRO) Working Group published their recommendations in 2005 and 2006 [90]. The American Brachytherapy Society (ABS) has also adopted the GEC-ESTRO guidelines for contouring, image-based treatment planning, and dose reporting [91]. A publication by the ICRU, in collaboration with GEC-ESTRO are now considered the guidelines which should be followed for contouring, image-based treatment planning, and dose reporting [92].

[83] (Viswanathan, Beriwal, et al., 2012)
[84] (Shin et al., 2006)
[85] (Kapp et al., 1992)
[86] (Datta et al., 2006)
[87] (Fellner et al., 2001)
[88] (Ling et al., 1987; Schoeppel et al., 1994; Pelloski et al., 2005)
[89] (Charra-Brunaud et al., 2012)
[90] (Haie-Meder et al., 2005; Pötter et al., 2006)
[91] (Viswanathan, Beriwal, et al., 2012; Viswanathan, Thomadsen, et al., 2012)
[92] ('Prescribing, Recording, and Reporting Brachytherapy for Cancer of the Cervix', 2013)

The contouring guidelines provide information in the delineation of the following recommended target and OAR volumes:

- The initial gross tumour volume ($GTV_{init}$) - includes the macroscopic demonstrable extent and location of the tumour before any treatment. It can consist of a primary tumour (GTV-$T_{init}$), known distant metastases (GTV-$M_{init}$), or involved regional node(s) (GTV-$N_{init}$).

The GTV-T is seen as the basis for treatment prescription and planning. It is assessed by imaging, clinical and/or pathological investigations.

- Clinical Target Volume for the Primary Tumour (CTV-T) – includes the GTV-T and a volume of surrounding tissue in which the risk of microscopic disease is deemed so high that this region should be treated with a sufficient dose to control the microscopic disease.
- Residual Gross tumour volume (GTV-$T_{res}$) – is defined as the residual tumour at the time of BT after treatment assumed sufficient to control the microscopic disease.
- Adaptive Clinical Target Volume (CTV-$T_{adapt}$) – can be defined after any treatment phase; it includes the GTV-$T_{res}$ and the residual pathologic tissue that might surround the GTV-$T_{res}$.
- High-risk clinical target volume (CTV-$T_{HR}$) – According to GEC-ESTRO the CTV-$T_{HR}$ is defined as the CTV-$T_{adapt}$ that includes the GTV-$T_{res}$, always the whole cervix, and the adjacent residual pathologic tissue, if present. This is the volume bearing the highest risk for recurrence and is selected by clinical examination and imaging at the time of BT after EBRT and chemotherapy in LACC.
- Intermediate-risk clinical target volume (CTV-$T_{IR}$) – carrying a significant microscopic load, encompasses the CTV-$T_{HR}$ with a safety margin of between 5 to 15 mm. The safety margin is chosen according to the tumour location and size, tumour regression, tumour spread and treatment strategy.
- The delineation of OARs which include the outer wall of the rectum, sigmoid, bladder and bowel.
- The traditional ICRU rectum point can serve as a recto-vaginal reference point.

The CTV-$T_{HR}$ serves as a reference for both prescription and evaluation of IGBT. The total radiation dose is prescribed to the CTV-$T_{HR}$ this dose is suitable to eradicate macroscopic disease and selected according to the stage of the disease, tumour volume and the treatment approach.

The image-based treatment planning and dose reporting guidelines provide the following information:

- The use of cumulative dose-volume histograms (DVH) for the evaluation of complex dose heterogeneity.

Dose-volume parameters for target and OAR volumes can be calculated from a DVH and converted into biologically weighted $EQD_2$ doses by using Equation (2) and are recommended for dose reporting:

- DVH parameters for target volumes (GTV, CTV-$T_{HR}$ and CTV-$T_{IR}$) are defined as the minimum dose delivered to 100 % and 90 % of the respective volume of interest (VOI): $D_{100\,\%}$ and $D_{90\,\%}$.
    - $D_{100\,\%}$ is mainly dependent on accurate target delineation, due to the steep dose gradient; small spikes in the target contour can cause large deviations in $D_{100\,\%}$. $D_{90\,\%}$ has been considered to be a more 'stable' parameter, which is less sensitive to these influences [93].

The near-minimum dose $D_{98\,\%}$ is a more robust metric, in which 2 % of the target volume receives less than this dose. Because of the steep absorbed-dose gradients in BT, and the significant resulting differences between $D_{98\,\%}$ and $D_{100\,\%}$, care must be taken when previously reported values are compared [94]. The use of $D_{98\,\%}$ and $D_{90\,\%}$ parameters are recommended for reporting dose to the CTV-$T_{HR}$. If the CTV-$T_{IR}$ is used for prescription and in the case of clinical trials, these two parameters are also recommended for the CTV-$T_{IR.}$

BT-related morbidity such as fistula, ulceration or circumscribed telangiectasia is frequently related to a small volume receiving high absorbed doses. To assesses such volumes and doses appropriately, the reference volume approach has been suggested [95]:

- The DVH parameters for organs at risk (OAR) are set as the minimum dose in the most irradiated tissue volume: 0.1 $cm^3$ and 2 $cm^3$ ($D_{0.1cm^3}$ and $D_{2cm^3}$). Reporting of 5 and 10 $cm^3$ are optional.
- During the reporting of DVH parameters, it should be mentioned if the applicator is included in the considered volume or not.
- The reference volume, TRAK, prescribed dose, point A dose is also used for dosimetric evaluation.

The underlying assumptions include identical locations during fractionated brachytherapy, the full dose of EBRT in the VOI is considered, contiguous volumes and contouring of organ walls for > 2 $cm^3$.

[93] (Kirisits et al., 2005)
[94] (Schmid et al., 2011)
[95] (Pötter et al., 2016)

The perceived limitations of these recommendations are that GEC-ESTRO suggests the use of MRI, which is seen as the gold standard for imaging in BT [96]. Most clinics are limited in terms of imaging capability, and MRI is not necessarily readily available for BT treatments, especially when several treatment fractions are involved. However, CT is more frequently available in RT clinics and can be used for this purpose.

Nonetheless, MRI has been proven to be superior to CT regarding the assessment of tumour size and configuration. Due to lower contrast, CT tumour contours significantly overestimate the tumour volume, especially in the lateral direction. This result in significant differences in the $D_{100\,\%}$, $D_{90\,\%}$ and volume treated to the prescription dose or greater for the CTV-$T_{HR}$ compared with that using MRI. Therefore, MRI remains the gold standard for tumour definition and delineation, but CT has shown to be adequate for contouring of OAR volumes [97]. Intravenous contrast can enhance the rectum and bladder, as well as the central areas of the cervix more than the peripheral areas. This might help to identify the uterine artery, thus assisting the delineation of the upper border of the cervix and in effect, improve the outcome of CT contouring [98].

### Image-Guided Adaptive Brachytherapy (IGABT)

A perfectly optimized BT treatment delivers a very high boost dose to the primary tumour, however sparing OARs due to a sharp dose fall-off outside the target volume. Due to this sharp dose fall-off, definition and contouring of target and OAR volumes on the specific day of treatment has a pronounced impact on the efficiency and accuracy of the BT treatment. This pronounced impact of contouring target and OAR volumes on a day to day basis have led to the introduction of image-guided adaptive brachytherapy (IGABT) for cervical cancer.

IGABT address the effect of tumour shrinkage and OAR geometrical changes in combination with the dose-fall off associated with BT treatment. The key advantage of IGABT is the possibility to conform and optimize the dose to the anatomy of the specific patient, considering tumour volume, topography, and the position of OARs on the specific day of treatment. IGABT has shown to reduce the incidence of severe late rectal bleeding and the improvement of LC rates, even for advanced disease [99].

The ability to adapt the dose to a regressing tumour volume results in much higher tumour dose delivered compared to conventional methods of point-based treatment planning or IGBT which applies a single treatment plan over all fractions, irrespective of changes in target and OAR volumes

[96] (Dimopoulos, Schard, et al., 2006; Johannes C. A. Dimopoulos et al., 2009)
[97] (Dimopoulos, Schard, *et al.*, 2006; Viswanathan *et al.*, 2007; Johannes C. A. Dimopoulos *et al.*, 2009; Eskander *et al.*, 2010; Krishnatry *et al.*, 2012; Hegazy *et al.*, 2013; Viswanathan *et al.*, 2014)
[98] (Viswanathan et al., 2007; Srivastava and Datta, 2014)
[99] (Johannes C.A. Dimopoulos et al., 2009; Kang et al., 2010; L. Tan, 2011)

and positioning [100]. The dosimetric consequences and differences in dose to the CTV-$T_{HR}$ and OARs were studied by Beriwal et al. using individualised MRI/CT-based 3D treatment plans for each fraction versus plans based on a single scan for all fractions. The study showed that a single-plan approach achieved adequate dosimetry in most of the patients, but individualised treatment plans improved dosimetry by accounting for variations in the position of OARs and applicator geometry [101].

Studies have shown that IGABT contributes to the treatment of pelvic nodes in LACC, at the level of around 5 Gy in the external, internal and obturator areas and 2.5 Gy in the common iliac. However, individual variations have been observed, and therefore the assessment of the genuine BT contribution at the individual level should be recommended [102].

In LACC, the implementation of MRI based 3D treatment planning, which includes dose escalation, dose-volume adaptation and a combination of intracavitary/interstitial brachytherapy if needed, seems to improve LC, LC rates at three years above 85%, with low treatment related morbidity, are reported [103].

The CTV-$T_{HR}$ $D_{90\ \%}$ has been reported to be one of the most noteworthy predictors of LC. Treatment delivered in 7 weeks with a $D_{90}$ CTV-$T_{HR}$ ≥ 85 Gy provides 3-year LC rates, in terms of CTV-$T_{HR}$ volume at the time of BT as follows:

1. In limited size CTV-$T_{HR}$ of 20 $cm^3$ the LC > 94 %
2. In intermediate size CTV-$T_{HR}$ of 30 $cm^3$ the LC > 93 %
3. In large size CTV-$T_{HR}$ of 70 $cm^3$ the LC > 86 %

As mentioned above, an increase in CTV-$T_{HR}$ size are related to poorer LC. To achieve equivalent LC, an additional 5 Gy is required for an increase in CTV-$T_{HR}$ volume by 10 $cm^3$. The extension of OTT is associated with poorer LC, and a CTV-$T_{HR}$ dose of 5 Gy is essential to compensate for an increase of OTT by one week. Histology, chemotherapy and dose rate was found to have no significant impact on LC [104].

IGABT's ability to deliver high doses to the CTV-$T_{HR}$ while reducing the dose to OAR volumes and severe toxicity rates have led to numerous studies reporting an improvement in the therapeutic ratio,

[100] (Lindegaard et al., 2013)
[101] (Beriwal et al., 2009)
[102] (Bacorro et al., 2017)
[103] (Pötter *et al.*, 2007; 2011; Lindegaard *et al.*, 2013; Rijkmans *et al.*, 2014; Sturdza *et al.*, 2016)
[104] (Tanderup et al., 2016)

improved LC, DFS and OS. [105]. With all this said, IGABT should preferably be the standard of care at every organisation.

### Interstitial Brachytherapy (ISBT)

Studies have shown that even though ICBT is mostly used for HDR-BT, standard ICBT applicators, like the Vienna-type ring applicator or the Utrecht-type ovoid applicator, do not ensure sufficient coverage of the target volume in all patients with advanced cervical cancer [106]. In cases where CTV-$T_{HR}$ volumes are irregular and bulky, or a significant residual disease is present, the recommended minimum CTV-$T_{HR}$ dose is difficult to achieve. ISBT is recommended in cases where ICBT is not technically possible due to the patient's anatomy, or it is expected to deliver a suboptimal dose distribution [107]. With ISBT, a Perspex template is used to guide and maintain the needles in a parallel position within the cervix and its paracervical tissue. Saha et al. reported a high tumour response, better parametrial coverage and better 3-year LC in Stage IIIB, compared to ICBT [108].

The availability of combined interstitial-intracavitary applicators, allow for a combination of intracavitary and interstitial BT treatment (IC-IS BT), which lead to a higher total target dose, superior dosimetric target coverage and treated volume in patients, which translate into higher LC rates and reduction in pelvic recurrence, without increasing the dose to critical structures and maintaining a low rate of morbidity [109].

Studies have shown that the application of adaptive IC-IS treatment improves the LC in locally advanced cervical cancer, by enabling tumour dose escalation in large tumours > 30 $cm^3$ without adding to treatment related late morbidity [110]. It results in 3-year LC rates of 95 to 100 % in limited/favourable (IB/IIB) and 85 to 90 % in large/poor response (IIB/III/IV) cervix patients linked to a moderate rate of treatment related morbidity scored using LENT/SOMA Score. This approach has led to a decrease of 65 to 70 % in pelvic recurrence and in major morbidity, compared to the historical Vienna series [111].

[105] (Pötter *et al.*, 2007; Tanderup *et al.*, 2010; Pötter *et al.*, 2011; Charra-Brunaud *et al.*, 2012; Wanderås *et al.*, 2012; Nomden *et al.*, 2013; Rijkmans *et al.*, 2014)
[106] (Tanderup et al., 2010; Mohamed et al., 2015)
[107] (Nag et al., 2000; Kuipers et al., 2001; Viswanathan, Thomadsen, et al., 2012)
[108] (Saha et al., 2008)
[109] (Kirisits *et al.*, 2006; Dimopoulos, Kirisits, *et al.*, 2006; Jürgenliemk-Schulz *et al.*, 2009; 2010; Pötter *et al.*, 2011; Fokdal *et al.*, 2013; Tan, Koh and Tang, 2015; Fokdal *et al.*, 2016)
[110] (Fokdal et al., 2016)
[111] (Pötter et al., 2011)

The use of IC-IS BT treatment has been investigated as an alternative to the usual parametrial EBRT boost in patients with substantial parametrial involvement at the time of BT. This alternative method was reported to be superior in target coverage as well as OAR sparing [112].

**Total dose and fractionation schedule**

Direct comparisons between dose and fractionation schedules for BT are limited. Therefore, the chosen fractionation schemes are mostly affected by resource and practicalities constraints. A variety of schedules are used in clinical practice for HDR-ICBT. Frequently used treatment regimens in the United States were published by the ABS and fractions are usually delivered 1 to 2 times per week [113]. Due to limited published experience regarding ISBT; the number of implant procedures and the fractions per implant session are not standardized, due to this, it is delivered by a variety of treatment regimens.

A study by Sharma et al. proved the clinical feasibility of a weekly HDR-ICBT schedule of 10 Gy × 2, in terms of LC, survival rates and low toxicity [114]. Kumar et al. studied the impact of four different dose fractionation schedules on $EQD_2$ in HDR-IGBT. The CTV-$T_{HR}$ $D_{90\%}$ and Point A were similar for 5.5 Gy × 5 fractions, 6.5 Gy × 4 fractions, and 7 Gy × 4 fractions, as well as $EQD_2$ for OARs - bladder, rectum, and sigmoid. The fourth dose fractionation schedule, 9 Gy × 2 fractions were found to produce significantly unfavourable $EQD_2$ values compared to the other three fractionation schedules investigated [115].

At Universitas Annex Hospital, a maximum rectum dose of 2 Gy per fraction was prescribed and applied for five BT fractions. Standard loading patterns were used and the dose at point A varied based on the rectal 2 Gy normalization point.

Nowadays, with the implementation of IGABT which produce a plan of the day and OAR volumes that vary in spatial position from day-to-day in relation to the target volume and have distinct geometrical configurations and, the possibility of fractionation compensation exists. This approach focuses on the total treatment OAR constraint, rather than the constant per-fraction treatment planning constraints. This allows OARs to receive higher than the average dose in one fraction if compensated for in upcoming fractions [116].

Normally, the fractional OAR constraints, of one or more, could limit the prescribed target dose, while other OAR constraints have not been reached in the same fraction. On the other hand, the target dose

[112] (Mohamed et al., 2015)
[113] (Viswanathan, Beriwal, et al., 2012)
[114] (Sharma et al., 2011)
[115] (Kumar et al., 2019)
[116] (Shaw, Rae and Alber, 2017)

aim could be achieved without any of the OARs constraints being violated, or equally, only at the expense of one or more OAR constraint violations. However, this scenario can change in the following fractions and the possibility of adjusting per-fraction OAR constraints optimally throughout the course of treatment to reach a rigorous total treatment OAR constraint exists. Lang et al. proposed that a difference between the total dose constraint and the already delivered dose to be split, equally, between the remaining fractions. Thus, the new fractional dose becomes the new per fraction dose constraint[117]. This is a conservative and optimistic concept that bet on favourable future geometries as opposed to obtaining the maximum benefit at the current fraction. This relates to the belief that geometric changes are mainly due to time trends instead of random changes such as tumour shrinkage. It assumes that future fractions will have no worse geometry than the current situation. Shaw et al. proposed a more greedy and pessimistic approach that does not rely on better chances in the future and exploit any chance of compensation. It assumes that the fractions delivered, which includes the current one, are the best predictors for future ones. The proposal aims to achieve the entire compensation in the current fraction, while the conservative approach allocates it over all undelivered fractions [118].

Shaw et al. compared the two approaches and found no statistically significant differences, as a result of the detected time trend of a shrinking CTV-$T_{HR}$. It is believed that the greedy approach will be more beneficial when BT is applied after or at the end of the EBRT treatment when major tumour shrinkage has already occurred [119].

## 2.4 Optimization in HDR brachytherapy

The ideal outcome and most significant challenge of radiotherapy is the ability to create a treatment plan in which all targets have received at least at least a prescribed dose, without compromising any normal tissue dose limits. To make this challenge even harder, not all normal tissues respond the same to radiation, and therefore, several clinical objectives should be applied to address this issue. To obtain a well-balanced plan, optimization is necessary. Optimization in HDR-BT is referred to as the tool which is used to adjust source dwell times and positions within the applicator and catheters to achieve the desired dose distribution.

There are two main optimization approaches, namely, forward and inverse optimization. The forward optimization process requires the following as a starting point:

1. Anatomy of the patient (CTV and OAR volumes).

[117] (Lang *et al.*, 2007a)
[118] (Shaw, Rae and Alber, 2017)
[119] (Shaw, Rae and Alber, 2017)

2. A standard template of defined source positions and dwell times.

Dwell time and dwell positions of the template plan are altered by the user by means of a trial and error method. The user assesses the changes by calculating and evaluating the dose distribution utilizing a DVH to evaluate if the desired target and organ dose prescribed by the radiation oncologist has been met. If not, the process is repeated until the necessary criteria have been met. This type of optimization requires continuous user input, and in complex anatomy cases, this approach can be time-consuming, and the outcome can be acceptable, but, in most cases, not optimal. A more advanced optimization approach known as inverse optimization has been developed which address the shortfalls and limitations of the forward optimization approach.

The inverse optimization approach is based on the user defining the desired outcome; this user-defined outcome is reached by using an optimization engine to determine the values of the dwell times and times of the sources within the applicator/catheter.

The inverse optimization process requires the following as a starting point:

1. Anatomy (CTV and OAR volumes).
2. A standard template of defined source positions and dwell times.
3. A user-defined desired outcome - The target and OAR dose prescribed by the radiation oncologist in terms of an ideal 3D dose distribution.
4. A user-defined criterion which defines the quality of the dose distribution.
5. A user-defined penalty mechanism that must be applied when these criteria are not met or are violated.

Two types of inverse optimization algorithms have been proposed in radiation therapy planning, deterministic and heuristic algorithms. The former follows the same search path with the same starting point and tend to get trapped in local minima. The latter follows a random search path in each optimization run and has the ability to find the global optimum solution by escaping local minima. A well-known algorithm is Simulated annealing [120]. The two most common algorithms in HDR Brachytherapy will be discussed briefly in the following section.

[120] (Mohammadi et al., 2015)

### 2.4.1 Hybrid Inverse treatment Planning and Optimization algorithm (HIPO)

The Hybrid Inverse treatment Planning and Optimization algorithm (HIPO) is an anatomy-based 3D inverse optimization algorithm developed by Karabis et al. [121]. By setting dosimetric constraints, HIPO has the ability to optimise the source/needle placement and dwell times. The user has two options when HIPO is used as the selected optimization algorithm:

1. Optimization of source positions and dwell times.
2. Optimization of dwell times for a given applicator/needle configuration.

A stochastic optimization algorithm (simulated annealing) is used to select and determine the source placement, for which the corresponding dwell times are optimized by applying a deterministic method known as the Limited Memory Broyden–Fletcher–Goldfarb–Shanno algorithm (L-BFGS), which is part of the quasi-Newton method family.

It is not realistic and practical to define the complete desired 3D dose distribution. As an alternative, the user defines a range [$D_L$, $D_H$] within which the dose value at any sampling point $d_i$ must lie. Low and high objective functions are used Equation (4) and (5):

$$f_L(\mathbf{x}) = \frac{1}{N}\sum_{i=1}^{N}[\emptyset\left(D_L - d_i(\mathbf{x})\right)[D_L - d_i(\mathbf{x})]^{\alpha}] \tag{4}$$

$$f_H(\mathbf{x}) = \frac{1}{N}\sum_{i=1}^{N}[\,\emptyset(d_i(\mathbf{x}) - D_H)[(d_i(\mathbf{x}) - D_H)]^{\alpha}] \tag{5}$$

Where:

$\emptyset$ is the transition/step function Equation (6):

$$\begin{aligned} \emptyset(x) &= 1 \qquad x > 0 \\ \emptyset(x) &= \frac{1}{2} \qquad x = 0 \\ \emptyset(x) &= 0 \qquad x < 0 \end{aligned} \tag{6}$$

N is the total number of dose sampling points in the corresponding VOI.

[121] (Karabis, Giannouli and Baltas, 2005)

$D_L$ and $D_H$ are low and high dose limits, respectively.

$d_i(\mathbf{x})$ is the dose of the i[th] sampling point.[122]

A common characteristic between the two functions is that dose values below and/or above the specified upper and lower dose limits for anatomical structures are penalized and defined for any VOI. The objective functions differ in how the violation is penalized and what dose normalization is applied. Parameter α specifies the type of objective function. For variance-based objective functions with $\alpha$ = 2, dose values exceeding a critical dose value are penalized quadratically, for Lessard–Pouliot objectives linearly with $\alpha$ = 1 and for DVH-based objectives independent of the dose value with $\alpha$ = 0.

When describing the range of dose required for target volumes, such as CTV-$T_{HR}$ and CTV-$T_{IR}$, both low and high objective functions are relevant. The role of the low objective for target volumes is to ensure that a minimum dose level is kept. The role of the high objective for target volumes is to avoid overdosage within the target volumes. To protect the OAR volumes from overdosage, only the high objective function for each individual OAR is considered. Dose optimization in BT considers the simultaneous optimization of many competing objectives and is, therefore, a true multi-objective optimization problem. Competing objectives exist, and it is, in most cases, impossible to meet all the objectives simultaneously. This can be solved by combining objectives functions using penalty/weight factors (w).

The objective function can be defined as the weighted sum of individual objective functions for the different structures. This function is given by Equation (7):

$$f = w_1 f_L^{CTV} + w_2 f_H^{CTV} + w_3 f_H^{NT} + \sum_{j=1}^{OARs} w_{j+3} f_H^{jOAR} \qquad (7)$$

These penalty factor values are dependent on the importance of the specific objective within the optimization process, and it is advantageous to know what the effect of the different values will have on the dose distribution.

This algorithm was tested for the use in HDR-BT, and the outcome compared with clinical data was found to be satisfactory [123].

[122] (Lahanas, Baltas and Zamboglou, 2003)
[123] (Karabis, Giannouli and Baltas, 2005; Trnková et al., 2009)

### 2.4.2 Simulated Annealing

Kirkpatrick et al. first introduced simulated annealing (SA) [124]. It is a heuristic global optimization technique, which is suitable for cases with many variables, as in HDR-BT. This algorithm can process objective functions with arbitrary boundary conditions with the statistical guarantee of finding a global optimum of a given function [125]. SA mimics the physical process of heating a material before slowly cooling the temperature while allowing wider sampling and uphill transitions (hill-climbing) in a controlled fashion. Thus, each transition can transform one configuration into a worse one, and as a result, it is possible to jump out of local minima [126]. Lessard et al. described the use of SA for anatomy-based dose optimization in prostate HDR-BT [127]:

The optimization process starts with an initial dose (dwell time) distribution at step 'k', the current step. A transition is generated (step 'k+1') by randomly increasing/decreasing on randomly chosen dwell times. After every iteration, the algorithm decides if the new dose distribution is accepted to become the current one and replace the former distribution. If the selected transition improves/decrease the objective function, then it is always accepted. If the selected transition causes an increase ΔE of the objective function, it is also accepted, but with a probability given by Equation (8):

$$P(\Delta E) = e^{\left[-\frac{\Delta E}{T(k)}\right]} \tag{8}$$

Where *T*(*k*) is the pseudo-temperature parameter which is analogous to temperature in an annealing system and $\Delta E = E_{k+1} - E_k$.

At higher values of T, uphill movement is more likely to occur which permit the system to escape from local minimum with a finite probability. As T tends to zero, transitions become more and more unlikely. In the case where *T* would be set to zero for all *k*, the probability of accepting a transition with a positive $\Delta E$ would be zero and the optimization would behave as a regular local search algorithm. The parameter k is some constant that relates temperature to energy (in nature it is Boltzmann's constant.)

[124] (Kirkpatrick, Gelatt and Vecchi, 1983)
[125] (Lessard and Pouliot, 2001)
[126] (Mohammadi et al., 2015)
[127] (Lessard and Pouliot, 2001)

The standard SA gives consistent results in the search for the global minimum but tends to be too slow [128]. The fast-simulated annealing (FSA) approach was introduced, which reduce the temperature parameter $T(k)$ used to calculate $P$ ($\Delta E$) at every iteration according to the relation in Equation (9):

$$T(k) = \frac{T_0}{k^{\propto}} \tag{9}$$

where $k$ is the iteration number, $T_0$ the initial temperature, and α the speed parameter. The initial pseudo-temperature is set proportional to the mean $\Delta E$ values of 500 random transitions $E(k)$ to $E$ ($k_1$ + 1).

The objective function is used to translate the clinical criteria into mathematical form and allows comparison of a given dwell time distribution $k$ relative to the next ($k_1$+1). As illustrated in Equation (10), from the dose-rate matrix $d_{ij}$ the dose distribution $D_i$ is given by the sum of the dose-rate contribution from all dwell positions $j$ with a respective dwell time $t_j$:

$$D_i = \sum_j d_{ij} t_j \tag{10}$$

As illustrated in Figure 5, the degree of fulfilment of each clinical criterion is measured using dose potentials. These dose potentials convert the dose distribution to a penalty value $w_i$. This conversion is defined by the relation in Equation (11):

$$\begin{aligned} w_i &= m_L(D_i - L) && \text{if } D_i < L \\ w_i &= m_R(D_i - R) && \text{if } D_i < R \\ w_i &= 0 && \text{if } L \leq D_i \leq R \end{aligned} \tag{11}$$

where the parameters $m_L$, $m_R$ , $L$, and $R$ are the characteristic of the selected dose potentials. Each clinical criterion is controlled by its own potential active on its respective dose calculation points.

[128] (Ingber, 1993)

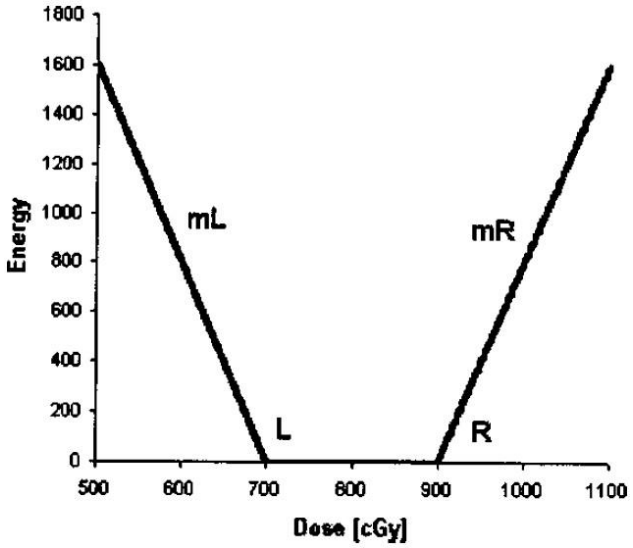


**Figure 5 - Dose potential "Reproduced with permission from (Lessard, E. and Pouliot, J. (2001), Inverse planning anatomy-based dose optimization for HDR-brachytherapy of the prostate using fast simulated annealing algorithm and dedicated objective function. Med. *Phys., 28 (2001) 773-779). Copyright © (2001), The Authors. Published by American Association of Physicists in Medicine and John Wiley & Sons Ltd.".***

Finally, the sum of the penalty values $w_i$ over $m$ dose points is performed, as shown in Equation (12) to obtain the global penalty $E_n$ of a given clinical criterion $n$:

$$E_n = \sum_{i}^{m} \frac{w_i}{m} \tag{12}$$

The objective function $E(k)$ of the dwell time distribution of iteration $k$ is given by the sum of all terms representing the clinical criteria, as shown in Equation (13):

$$E(k) = \sum_{n=1}^{4} E_n(k) \tag{13}$$

This energy value is used to compare a given dwell time distribution $k$ relative to the next ($k_1$+1). The closer to the clinical objective and the physician's prescription, the smaller the energy and the objective function. Agreement with the physician's prescription and the importance of a clinical criterion over the other is adjusted using the parameters of the dose potentials. Thus, the most sensitive part of the algorithm is the choice of these parameters.

## 2.5 Concept of Equivalent Uniform Dose (EUD)

The use of cumulative and differential dose-volume histograms has become a crucial tool in modern 3D treatment planning. However, their usage is limited to a point selection on the DVH to which the prescribed dose is normalized. The use of a single dose-volume-histogram point for dose reporting and specification is adequate when the dose distribution throughout the evaluated volumes is uniform

[129]; this is however not the case in BT treatment especially for normal tissue structures. The concept of equivalent uniform dose (EUD) postulates that two different dose distributions are comparable if they have the ability to produce the same radiobiological effect. The EUD parameter can easily be calculated for target and OAR volumes by using data obtained from DVH's.

Furthermore, the uncertainties in the delineation of target and OAR volumes lead to uncertainty in derived DVH parameters which leads to the uncertainty in the dose received by both target and OAR volumes during BT treatments. The contouring uncertainties associated with the use of CT imaging for BT planning creates the need to investigate an alternative planning method for IGABT. This alternative method needs to be more robust against imaging and contouring uncertainties compared to the original GEC-ESTRO prescription with reference to DVH criteria.

The EUD-based planning method, which can be categorized as a biological method, has been studied for this purpose and was found to be equivalent to IGBT treatment plans for OARs [130]. Biological optimization was proven to be an effective and easy tool to obtain a large variety of dose distributions, with improved sparing of normal tissues for the same or higher target dose [131]. Doses can be selectively fine-tuned in different regions, with either increased doses to the target, or a reduced dose to critical structures [132]. Furthermore, the summation of EUDs from sequential treatment fractions provides a reliable worst-case approximation for the total treatment dose. This opens possibilities for either simultaneous integrated boost in EBRT or safe dose escalation in IGBT [133].

To perform biological dose optimization in IGABT, biological dose metrics (EUD) for target and OAR volumes need to be calculated. Equation (14) can be used to determine the EUD of target volumes ($EUD_T$) relative to the EBRT dose delivered in 2 Gy fractions (d = 2 Gy), from the surviving fraction:

$$EUD_T = \frac{-\log(SF)}{\alpha + \beta d} \tag{14}$$

The differential DVH of target volumes cane be used to calculate the surviving fraction (SF) of each treatment fraction. SF is calculated from $D_i$, the dose bin for the $v_i$−th fractional tumour volume:

[129] (Niemierko, 1997)
[130] (Shaw, Rae and Alber, 2013)
[131] (Wu et al., 2002; Schwarz, Lebesque and Mijnheer, 2004)
[132] (Wu et al., 2005)
[133] (Sobotta et al., 2011; Shaw, Rae and Alber, 2013)

$$SF = \sum_i v_i SF(D_i) \quad (15)$$

The generalized (gEUD) was used for all OAR volumes and will be calculated using Equation (16):

$$gEUD = \left( \sum_i v_i {D_i}^a \right)^{\frac{1}{a}} \quad (16)$$

where $v_i$ and $D_i$ are bins of the differential DVH and $a$ is a tissue-specific parameter [134]. The tissue-specific parameter for the bladder will be used as 8 and for the rectum and sigmoid as 12, respectively.

The significant advantage of EUD-based planning is that the dose metric considers the entire dose distribution of the organs contrary to a single dose-volume-histogram point, as suggested by GEC-ESTRO.

## 2.6 Toxicities in normal tissues

The therapeutic ratio declines as a result of large tumour volumes lying closer to OAR volumes. To maintain the dose to the target volume, OAR doses are increased, and this can lead to an increase in OAR morbidity. Although BT allows for rapid dose fall-off, OARs may still receive high doses of radiation because of their proximity to the target. The implementation of IGABT has made it possible to adapt treatment volumes and in effect, the ability for dose escalation. Even though dose escalation is performed in the tumour volume, severe morbidity is reduced and kept low in OARs while moderate treatment related morbidity is still evident [135]. Therefore, acute and late toxicities remain a valid concern even in the era of IGABT. Acute toxicities usually appear within three months of treatment and are usually reversible and resolve within a few months [136]. Late toxicities occur after three months of treatment and are usually irreversible.

Quantitative, objective scoring systems that explicitly consider multiple patient- and physician-based endpoints, such as the LENT-SOMA system, are suggested to avoid ambiguity given the multiple endpoints used to score toxicity[137].

[134] (Shaw, Rae and Alber, 2013)
[135] (Pötter et al., 2011)
[136] (Viswanathan et al., 2010; Morris, 2015)
[137] (Viswanathan et al., 2010)

**Bladder**

Dose to the bladder range from 40 to 50 Gy in EBRT. However, if combined with BT bladder dose estimates to a total of between 70 to 90 Gy and can reach > 100 Gy for the regions closest to the radiation source. This region is likely to vary between fractions; therefore, the true maximum bladder dose in patients is unknown. As discussed, the ICRU assigned a bladder dose point; conversely, studies have found that this point is not representative of the CT-based or ultrasound-based volumetric dose maximum and surface area of normal tissue irradiated [138]. A previous report revealed that a high bladder $D_{2cm^3}$ is a vital risk factor for moderate to severe grade bladder bleeding, fistula and cystitis [139].

A large prospective study [140] found that severe bladder morbidity, mainly frequency/urgency, incontinence, and cystitis after IGABT is limited and compares favourably to 2D brachytherapy. However, mild to moderate morbidity is still evident, especially with a high level of urinary frequency and gradually increasing incontinence. Late bladder morbidity should be further reduced through continuous optimisation of techniques with individualisation of radiotherapy and side effect management .

**Rectum**

Based on long term evidence and results of the large prospective EMBRACE study, significant correlations were established between overall and single endpoints (proctitis, bleeding, fistula), late rectal morbidity and dose-volume ($D_{2cm^3}$ and $D_{0.1cm^3}$) and the ICRU recto-vaginal reference point parameters. The $D_{2cm^3}$ parameter of the rectum should not exceed 75 Gy $EQD_2$ as this is associated with major and more frequent rectal morbidity such as fistulae, where a $D_{2cm^3} \leq 65$ Gy is reported to decrease rectal morbidity such as bleeding and proctitis$D_{2cm^3}$ [141]. The EMBRACE I study also demonstrated that G3 and G4 rectal morbidity is very uncommon in IGABT [142].

**Sigmoid/Bowel**

Despite advances in radiotherapy, bowel toxicity remains an enormous issue after the completion of treatment [143]. Late bowel morbidity was assessed in terms of physician reported morbidity and patient reported outcome (PRO) for a large group of patients that underwent MRI-IGABT in locally advanced disease. Grade 1 and 2 bowel morbidity was prominent with occurrence rates of between 28 to 33

[138] (Viswanathan et al., 2010)
[139] (Yen et al., 2018)
[140] (Fokdal et al., 2018)
[141] (Georg *et al.*, 2012; Mazeron *et al.*, 2016)
[142] (Mazeron *et al.*, 2016)
[143] (Denham and Hauer-Jensen, 2013)

% during follow-up. The most frequently reported side effect was flatulence and diarrhoea, which significantly increased after three months. Incontinence gradually worsened with time. PRO revealed higher prevalence rates. The 3/5 years actuarial incidence was investigated, grade 3 and 4 bowel morbidity was limited at 5.0 % and 5.9 %, while the incidence of stenosis, stricture and fistula was 2.0 % and 2.6 %, respectively [144].

No single dose-volume parameter has been reported and validated yet to predict late bowel toxicities in IGABT treatment. However, a study by Bockel et al. reported a positive correlation between bowel morbidity and a TRAK value ≥ 2cGy at 1 m, which can be used as a predictor for late bowel toxicities. They also found a positive correlation between the probability of late bowel morbidity with smoking, a CTV-$T_{HR}$ volume of ≥ 25 $cm^3$ and a TRAK value ≥ 2cGy at 1 m [145].

**Vagina and vulva**

The epithelium of the vagina and vulva is sensitive to the effects of radiation. Acute radiation effects experienced after radiotherapy include vaginal erythema, mucositis and moist desquamation, which usually resolve within 2 to 3 months. Some patient may experience progressive and on-going acute effects which at the end may result in vaginal and vaginal entrance stenosis and fragility [146].

Early to late vaginal morbidity was evaluated during the first two years of follow-up in IGABT. Mild to moderate symptoms were pronounced, with the symptoms developing within six months, grade ≥ 1, 89 % and grade ≥ 2, 29 %. Severe vaginal morbidity was reported to be less than reported from earlier studies. The other reported vaginal symptoms reported were stenosis, followed by vaginal dryness ad vaginal bleeding and mucositis in a lesser extent [147]. Vaginal stenosis develops in 88 % of patients who receive pelvic radiation as a result of radiotherapy [148]. Vaginal stenosis is dominant and correlates with EBRT as well as BT dose; a total treatment dose aim of ≤ 65 Gy $EQD_2$ to the recto-vaginal reference point is recommended [149]. To establish a vaginal dose de-escalation planning strategy, Mohamed et al. reduced the dwell times of sources residing in the ovoid/ring, while maintaining the target dose and increasing dwell times in tandem/needles. In this attempt, the dose to the ICRU recto-vaginal point was reduced by an average of 4 ± 4 Gy $EQD_2$, while $D_{2cm^3}$ doses to bladder and rectum were reduced by an average of 2 ± 2 Gy and 3 ± 2 Gy. This vaginal dose de-escalation planning strategy has the potential to decrease the incidence of vaginal stenosis [150].

[144] (Jensen et al., 2018)
[145] (Bockel et al., 2019)
[146] (Schover, Fife and Gershenson, 1989; Jensen *et al.*, 2003; Denton and Maher, 2003; Silberstein *et al.*, 2013)
[147] (Kirchheiner et al., 2014)
[148] (Mittal and Kaushal, 2015)
[149] (Kirchheiner *et al.*, 2016)
[150] (Mohamed et al., 2016)

**Ureteral stricture**

Ureteral stricture is a well-known but rare severe late complication following cervical cancer treatment [151]. The risk for severe to life-threatening ureteral strictures was reported to be unusual and generally low in Stage I and II tumours, with an increased risk in Stage III and IV tumours treated with IGABT [152].

## 2.7 Dosimetry

In 1995, the American Association of Physicists in Medicine (AAPM) Task Group No. 43 (TG-43) published a protocol, which comprised and introduced a new BT dose calculation formalism to establish the 2D dose distribution around cylindrically symmetric brachytherapy line sources (assumed) such as palladium-103, iodine-125 and Ir-192. In 2004 an updated TG-43 protocol was published [153].

### The general dose-rate formalism

The dose rate at a specific position adjacent to a radioactive $\gamma$ - source depends on several parameters. These parameters include the distance to the source, the source shape, the reference air kerma rate (RAKR) of the source, the thickness and composition of the shielding around the source, the composition of the medium between the calculation and source position.

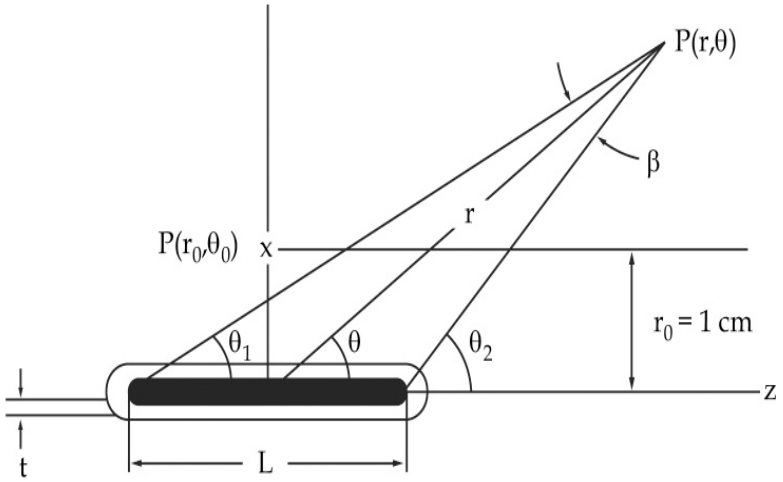


**Figure 6 – The coordinate system utilized for brachytherapy dosimetry calculations.** ***"Reproduced with permission from (Rivard, M.J., Coursey, B.M., DeWerd, L.A., Hanson, W.F., Saiful Huq, M., Ibbott, G.S., Mitch, M.G., Nath, R. and Williamson, J.F.. Update of AAPM Task Group No. 43 Report: A revised AAPM protocol for brachytherapy dose***

[151] (McIntyre et al., 1995; Maier, Ehrenbock and Hofbauer, 1997; Härkki-Sirén, Sjöberg and Tiitinen, 1998; Fokdal et al., 2019)
[152] (Fokdal et al., 2019)
[153] (Rivard et al., 2004)

As illustrated in Figure 6, the dose rate at the point of interest P (r,θ) in water can be calculated by Equation (17):

$$\dot{D}(r,\theta) = S_k \Lambda \frac{G(r,\theta)}{G(r_0\theta_0)} \times g(r) \times F(r,\theta) \quad (17)$$

Where

r - The distance (in cm) from the centre of the source to the point of interest P(r,θ).

P ($r_0$, $\theta_0$) - The reference point that lies on the transverse bisector of the source at a distance of 1 cm from the origin (with $r_0$ = 1 cm)

$\theta_0$ - Defines the source transverse plane and is equal to π/2 radians (90 °)

θ - The angle between the direction of radius vector *r* and the long axis of the source

$S_k$ - The air-kerma strength of the source (cGy.cm$^2$.h$^{-1}$)

Λ - The dose rate constant in water (cGy h$^{-1}$ U$^{-1}$)

$G(r,\theta)$ - The geometry factor

$g(r)$ - The radial dose function

$F(r,\theta)$ - The anisotropy function

**The dose rate constant in water (Λ)**

The dose rate constant is defined as the dose rate to water at a distance of 1 cm on the transverse axis per unit air kerma strength source in water, as illustrated in Equation (18):

$$\Lambda = \frac{\dot{D}(r_0,\theta_0)}{S_k} \quad (18)$$

The dose rate accounts for:

- Spatial distribution of radioactivity within the source encapsulation;
- Scattering in water surrounding the source;
- Self-filtration within the source;

- Effects of source geometry.

**The geometry function G (r, θ)**

The geometry function neglects scattering and attenuation but provides an effective inverse square-law correction based upon an approximate model of the spatial distribution of radioactivity within the source. The geometry function can be calculated for a point and line source and give rise to the following functions:

Equation (19) can be used for a point source approximation:

$$G_P(r,\theta) = r^{-2} \tag{19}$$

Each source can be assumed to be a point source if the distance between the dose calculation point and the source centre is at least twice the active length of the source [154].

Equation (20) can be used for a line source approximation, if $\theta \neq 0°$:

$$G_L(r,\theta) = \frac{\beta}{L\, r \sin\theta} \tag{20}$$

Where β is the angle, in radians, subtended by the tips of the hypothetical line source for the calculation point, P(r, θ). (Refer to Figure 6)

Equation (21) can be used for a line source approximation, If θ = 0 °:

$$G_L(r,\theta) = (r^2 - \frac{L^2}{4})^{-1} \tag{21}$$

**The radial dose function g(r)**

The radial dose function accounts for the effects of attenuation and scatters in the water on the transverse plane of the source (θ = π/2), excluding fall-off, which is included in the geometry function. The radial dose function may also be influenced by filtration of photons by the encapsulation and source materials. This factor can be determined by fitting a fifth-order polynomial fit to the tabulated g(r) data, as shown in Equation (22):

[154] (E.B.Podgorsak, 2005, p. 475)

$$g(r) = a_0 + a_1 r + a_2 r^2 + a_3 r^3 + a_4 r^4 + a_5 r^5 \quad (22)$$

Parameters $a_0$ to $a_5$ should be determined so that they fit the data within ± 2 %.

**The anisotropy function F(r,$\theta$)**

The anisotropy function accounts for the anisotropy of dose distribution around the source, including the effects of absorption and scatter in the water. It gives the angular variation of the dose rate around the source at each distance due to self-filtration, oblique filtration of primary photons through the encapsulating material, and scattering of photons in water as illustrated in Equation (23) :

$$F(r,\theta) = \frac{\dot{D}(r,\theta)}{\dot{D}(r,\theta_0)} \frac{G_L(r,\theta_0)}{G_L(r,\theta)} \quad (23)$$

The anisotropy function decreases:

- As *r* decreases;
- As θ approaches 0 ° or 180 °;
- As the source encapsulation thickness increases;

# Chapter 3 - Methods and Materials

The planning study was conducted on a novel treatment planning module that was specifically developed for the purpose of this study.

## 3.1 Patient data collection and contouring

The existing patient database was used to obtain anonymous patient and treatment data of 18 cervix cancer patients. The patients received CT-based IGBT in combination with EBRT between 1 January 2014 and 30 December 2015. Planning was performed on the Oncentra Brachytherapy Treatment planning system (Version 4.6.0). The planning aim was to deliver a dose of at least 7 Gy to the CTV-$T_{HR}$ $D_{90\,\%}$ per fraction, with a total of five fractions. The patient data consisted of a CT image set of 3 mm axial slices, with the applicator in situ, scanned from L1 to 5 cm below the vaginal introitus, with a Toshiba Aquilion Large Bore CT scanner. The applicators used for treatment were CT/MRI-compatible tandem and ring applicators (Nucletron Systems, Veenendaal, The Netherlands, Elekta AB, Stockholm, Sweden). They were inserted under conscious sedation without the insertion of a Foley catheter and vaginal packing. Due to the extremely high workload in this clinic, foley catheters are not used in general, as well as no vaginal packing. Patients are also treated under conscious sedation, and this also influences decisions about catheter placement and packing. Bowel preparation is performed before the insertion of the applicator to ensure an empty rectum. The selection of patient data is not limited in terms of disease staging, and thus any patient who received five IGBT fractions could be included. The only requirement is that the patients should have different CT datasets for each IGBT treatment. The CT datasets over the entire course of BT are obtained; thus, a total of 90 CT datasets are used in this investigation.

Each CT data set are contoured as per published ICRU 89 [155]and GEC-ESTRO guidelines as described earlier in the Image-Guided Brachytherapy (IGBT) Section Page 34.

The following tumour volumes and dose points are defined and contoured:

- High-risk clinical target volume (CTV-$T_{HR}$)
- Intermediate-risk clinical target volume (CTV-$T_{IR}$) - The CTV-$T_{HR}$ with a safety margin of 10 mm is used;
- Point-A left and right.

The GTV was omitted as it cannot be identified on CT images. Estimated CTV-$T_{HR}$ and CTV-$T_{IR}$ volumes are contoured based on the description of the tumour during clinical examinations recorded before the patients received BT treatment. Variations of these volumes from the actual tumour will have no

[155] ('Prescribing, Recording, and Reporting Brachytherapy for Cancer of the Cervix', 2013)

impact on the study, even if they might have been slightly different when delineated on a MR image set, the reason being that all optimization and planning techniques were performed on the same image datasets.

According to the ICRU 89 report [156], volume selection and delineation of OARs are performed along their walls, either as a wall contour or as an outer contour. Outer contour delineation is sufficient for small absolute volumes, while organ-wall contouring is suggested for volumes larger than 2 $cm^3$ [157]. Both have been contoured in this study, as the EUD constraints applied in this study has been derived from OAR walls by Shaw et al [158].

For OAR's the following organs and dose points were defined and contoured:

- Bladder wall and outer contour with content;
- Rectum wall and outer contour with content;
- Sigmoid wall and outer contour with content;
- Small bowel outer contour with content;
- ICRU Recto-vaginal reference point.

The ICRU bladder point was not defined and reported in any of the patients as there were no Foley catheters inserted before treatment, as stated earlier. The absence of the Foley catheter makes it impossible to define the ICRU bladder point. Several studies have shown that the ICRU bladder point doses are not necessarily a true reflection of the dose received by the bladder and therefore time is rather spent on the contouring of the bladder volumes, to ensure accuracy of all necessary DVH parameters used for planning and reporting purposes.

## 3.2 Dosimetry

IDL, short for Interactive Data Language was used to calculate the 3-D dose distribution around the cylindrically symmetric Ir-192 source. The 2-D dose formalism described in the updated TG-43 protocol, as described in Section 0, was used as a guideline to develop a 3-D dose formalism [159]. The dose distributions were calculated in terms of the source orientation within the tandem and the ring.

### 3.2.1 Calculation of the 3-D dose distribution

An empty 3D dose matrix was created. The matrix size was 40 cm, with a resolution value of 0.25 cm. A 0.35 cm long Ir-192 source was virtually placed in the centre of the matrix, with a position/origin of

[156] ('Prescribing, Recording, and Reporting Brachytherapy for Cancer of the Cervix', 2013)
[157] ('Prescribing, Recording, and Reporting Brachytherapy for Cancer of the Cervix', 2013)
[158] (Shaw, Rae and Alber, 2013)
[159] (Rivard et al., 2004)

(0, 0, 0). As shown below in Figure 7, the sources within the tandem are virtually placed along the y-axis, and the sources within the ring are virtually placed along the z-axis.

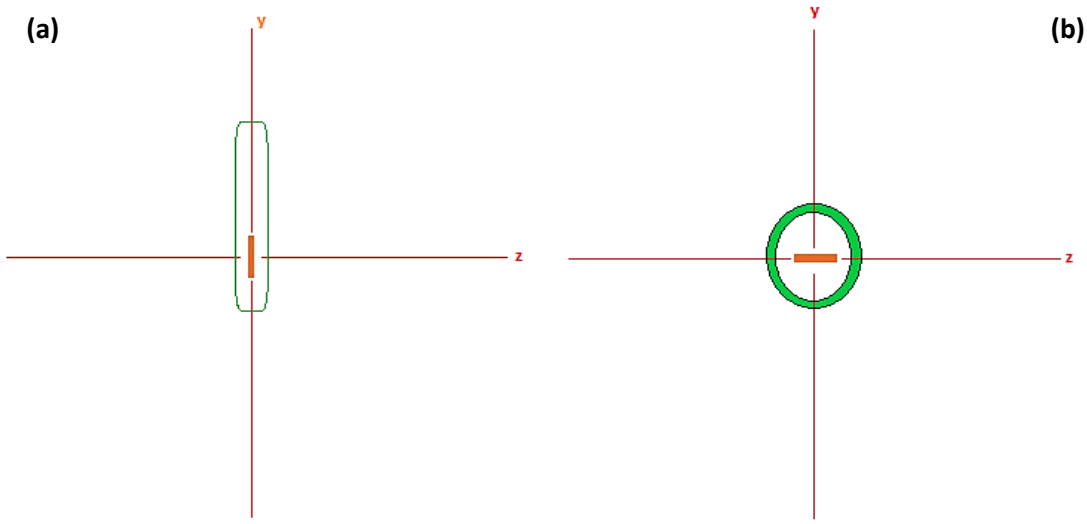


**Figure 7 – Display of the virtual placement of the sources within the dose matrix for dose calculation. a) Tandem sources were placed along the y-axis and b) ring sources were placed along the z-axis. Both these placements had a position of (0, 0, 0) in the centre of the sources.**

The following parameters are calculated in terms of a single source position (0, 0, 0,) and the actual point of interest (Refer to Figure 6):

**The radius ($r_{ijk}$)**

The radius ($r_{ijk}$) between the source origin ($xs_{ijk}$, $ys_{ijk}$, $zs_{ijk}$) and actual point of interest ($xa_{ijk}$, $ya_{ijk}$,$za_{ijk}$) is calculated by:

$$r_{ijk} = \sqrt{\left(xa_{ijk} - xs_{ijk}\right)^2 + \left(ya_{ijk} - ys_{ijk}\right)^2 + \left(za_{ijk} - zs_{ijk}\right)^2} \tag{24}$$

**The angle ($\theta_{ijk}$)**

The angle ($\theta_{ijk}$) between the source origin within the tandem ($xs_{ijk}$, $ys_{ijk}$, $zs_{ijk}$) and actual point of interest ($xa_{ijk}$, $ya_{ijk}$,$za_{ijk}$) is calculated by:

$$\theta_{ijk} = \tan^{-1}\left(\sqrt{\frac{\left(xa_{ijk} - xs_{ijk}\right)^2 + \left(ya_{ijk} - ys_{ijk}\right)^2 + \left(za_{ijk} - zs_{ijk}\right)^2}{\left(ya_{ijk} - ys_{ijk}\right)^2}}\right) \tag{25}$$

The angle ($\theta_{ijk}$) between the source origin within the ring ($xs_{ijk}$, $ys_{ijk}$, $zs_{ijk}$) and actual point of interest ($xa_{ijk}$, $ya_{ijk}$,$za_{ijk}$) is calculated by:

$$\theta_{ijk} = \tan^{-1}\left(\sqrt{\frac{\left(xa_{ijk} - xs_{ijk}\right)^2 + \left(ya_{ijk} - ys_{ijk}\right)^2 + (za_{ijk} - zs_{ijk})^2}{\left(za - zs_{ijk}\right)^2}}\right) \quad (26)$$

**The geometry function G ($r_{ijk}$, $\theta_{ijk}$)**

The geometric function G ($r_{ijk}$, $\theta_{ijk}$) is calculated by using Equation (27) and (28).

For a line source approximation:

If $\theta_{ijk} \neq 0°$:

$$G_L(r_{ijk}, \theta_{ijk}) = \frac{\beta_{ijk}}{L\, r_{ijk} \sin\theta_{ijk}} \quad (27)$$

Where $\beta_{ijk}$ is the angle, in radians, subtended by the tips of the hypothetical line source with respect to the calculation point, P (r, θ). L is the active length of the source, which in this case is 0.35 cm (Refer to Figure 6).

The geometric function is taken as a point source at $\theta_{ijk}$ = 180 ° and 0.0 °

$$G_L(r_{ijk}, \theta_{ijk}) = \frac{1}{{r_{ijk}}^2 - \frac{L^2}{4}} \quad (28)$$

**The radial dose function g ($r_{ijk}$)**

A 5th polynomial fit is done to determine and calculate the radial dose function g($r_{ijk}$) by using Equation (29) The parameters $a_0$ to $a_5$ is chosen to best fit the function:

$$g(r_{ijk}) = a_0 + a_1 r_{ijk} + a_2 {r_{ijk}}^2 + a_3 {r_{ijk}}^3 + a_4 {r_{ijk}}^4 + a_5 {r_{ijk}}^5 \quad (29)$$

Where

- $a_0$ – 0.9918
- $a_1$ – 0.0094
- $a_2$ – -0.0016
- $a_3$ – 0.000006
- $a_4$ – 0.0000009
- $a_5$ – 0.000000007

Thus equation 28 can be rewritten as:

$$g(r_{ijk}) = 0.9918 + 9.4e^{-3}r_{ijk} + (-0.016){r_{ijk}}^2 + 6e^{-6}{r_{ijk}}^3 + 9e^{-7}{r_{ijk}}^4 + 7e^{-9}{r_{ijk}}^5 \quad (30)$$

**The anisotropy function $F(r_{ijk},\theta_{ijk})$**

The anisotropy function values are obtained from published values [160]. The complete table can be found in Appendix 1.

**The dose rate constant ($\Lambda$) and Air Kerma Strenght ($S_k$)**

A dose rate constant of 1.11 cGy $h^{-1}U^{-1}$ for Ir-192 is used [161]. The air kerma strength value $S_k$ will be obtained from the standard plan.

**The dose rate per unit air-kerma strength $\dot{D}(r_{ijk}, \theta_{ijk})$**

All calculated values are substituted into Equation (31) to calculate the 3D dose distribution around the source:

$$\dot{D}(r_{ijk}, \theta_{ijk}) = \Lambda \times \frac{G(r_{ijk}, \theta_{ijk})}{G(r_0\theta_0)} \times g(r_{ijk}) \times F(r_{ijk}, \theta_{ijk}) \quad (31)$$

The two 3D dose rate matrixes, which represents the dose distribution around the sources within the tandem and ring, respectively, are exported and saved as text files. These exported dose distributions will be imported and used during the dose calculation procedure within a patient matrix, which will be explained in Section 3.3.2.

## 3.3 The development of the treatment planning module

The treatment planning module that is developed and described in this section will be referred to as the In-house Developed Module (IHDM) in the rest of the document. The IHDM is solely a research module/tool and has never been used clinically. However, if the tool gives a good distribution, the dwell times and positions on the Oncentra TPS can be made the same to reproduce the distribution on the clinical TPS.

The same IDL software is used to develop the IHDM. The module has the ability to cover a wide range of tasks from importing various DICOM files, displaying CT data to forward and inverse optimization and planning.

[160] (Granero et al., 2006)
[161] (Granero et al., 2006)

### 3.3.1 Import of various DICOM files

The module is developed to import/read various DICOM files which are exported from the commercial Oncentra Brachy treatment planning system:

1. Series of CT image data;
2. RT Structure sets of all contoured structures;
3. Treatment data.

**Series of CT image data**

Information regarding CT images is imported; this information is used to display the CT data in three different anatomical planes as illustrated below in :

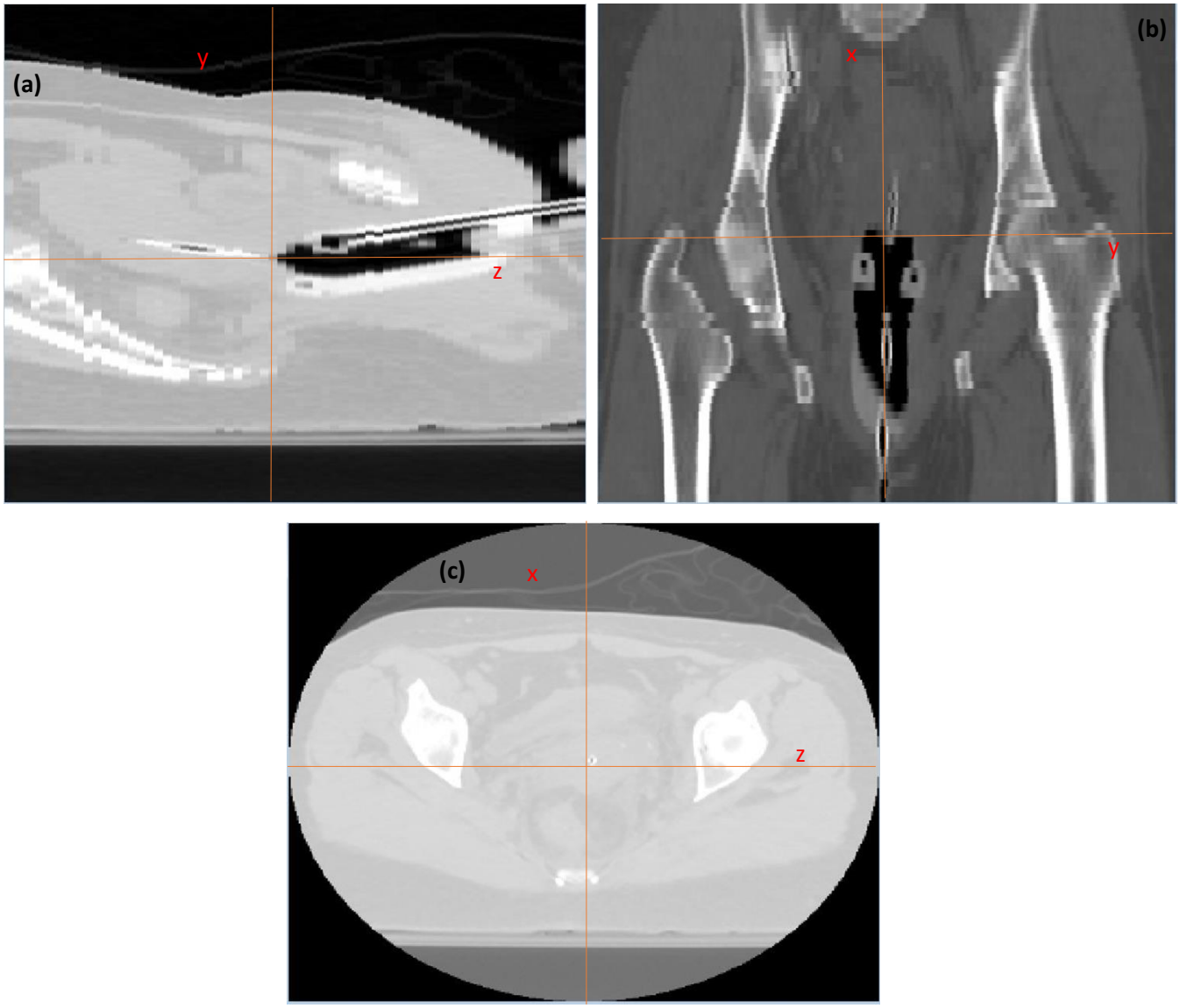


**Figure 8 - Visualisation of CT data with applicator in situ, in three anatomical planes by the IHDM. (a) Sagittal view, (b) Coronal view and (c) Axial view.**

**RT Structure sets of all contoured structures**

The RT structure file is imported; this information is used to relate the position of the contoured target and OAR volumes to the CT data. Figure 9 below displays how the contoured volumes are superimposed on the CT data for all three anatomical planes.

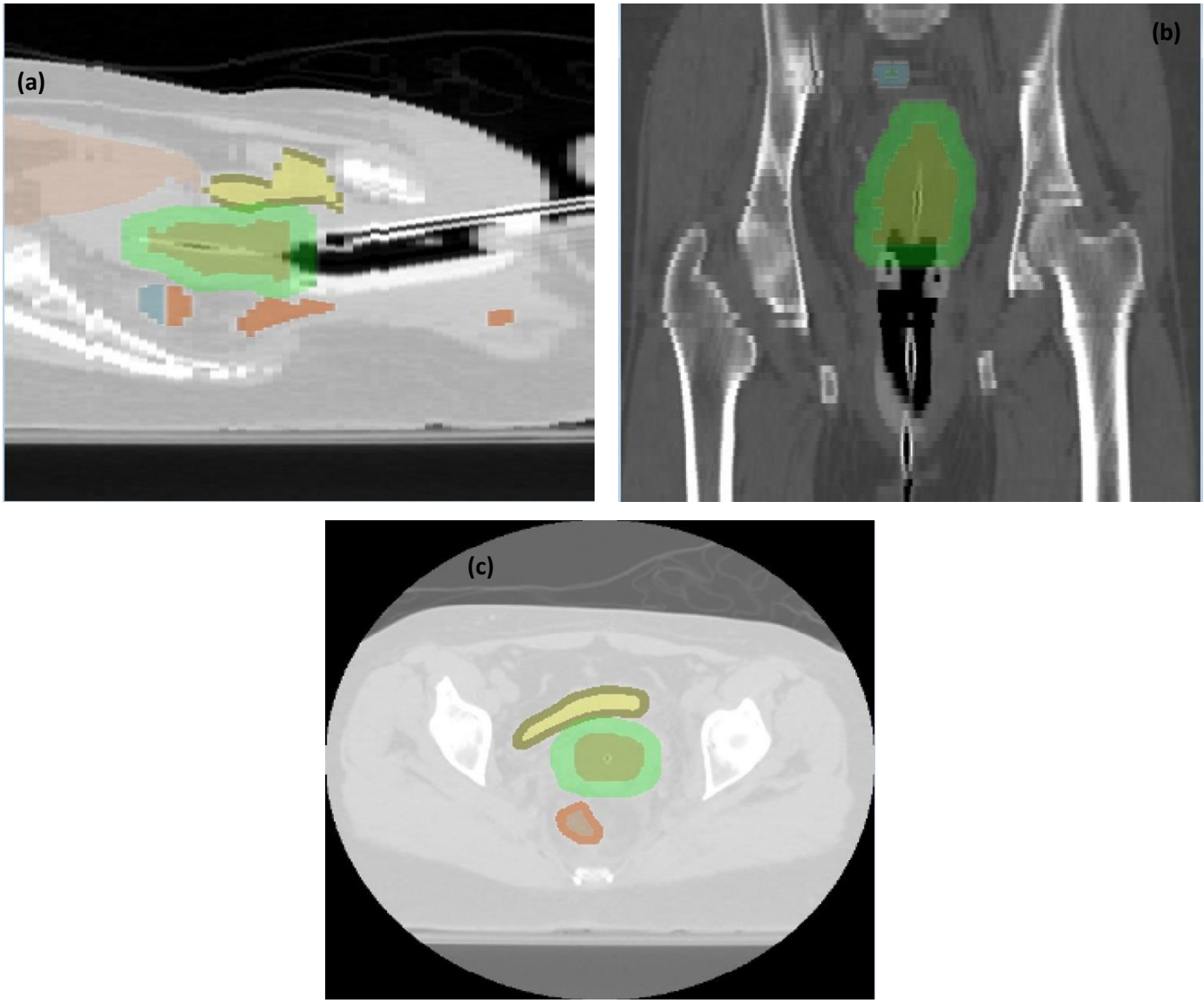


**Figure 9 - Visualisation of contoured volumes superimposed on CT data in three anatomical planes by the IHDM. (a) Sagittal view, (b) Coronal view and (c) Axial view.**

A "slice select" tool, as shown in Figure 10 is created, which gives the user the ability to visualise all relevant structures throughout the CT data in all three projections in increments of 3 mm. During planning and optimization, this tool is used to visualize and evaluate the dose distribution/placement of the applicator in relation to the and target and OAR volumes.


**Figure 10 - "Slice select" tool in the IHDM, which is used to scroll through the patient's anatomy in 3 mm increments.**

**Treatment data**

Treatment data regarding the standard plan is obtained through the RT plan file. This standard plan consists of intra-uterine source positions located at 1 cm intervals from the ring to the tip and the source positions within the ring are fixed and based on a standard source loading pattern currently used within our institution. A standard plan consists of a total of 15 sources, 7 intra-uterine sources and eight ring sources, this can be changed, depending on the complexity of planning geometries. The length of the intra-uterine applicator visible on the CT image was fixed at 6 cm. The source dwell times were individually set to 10 seconds, irrespective of the source strength. The following information is obtained from this file after it is imported into the module:

1. Source activity in terms of Reference Air Kerma Rate (RAKR);
2. Number of sources used;
3. Dwell positions and dwell times of all sources;
4. Dose at point $A_{Left}$ and $A_{Right}$.

### 3.3.2 Calculation of dose distribution within the patient matrix

The actual source coordinates within the patient are extracted from the RT plan. This positional information regarding each individual source is used to ensure that the dose distribution calculated in the Dosimetry Section is correctly imported and positioned within the patient. The calculated dose distribution representing the sources within the tandem is used for all 7 tandem sources. The calculated dose distribution representing the sources within the ring is used for all 8 ring sources. The IDL-calculated dose distributions that were exported and saved as text files (as described in Section 3.2.1) are imported and placed accordingly for each treatment fraction.

The relevant air kerma strength ($S_k$) and dwell times ($t_i$) of the sources are obtained from the RT plan file; however, the dose rate constant value was already incorporated in the calculated dose distributions calculated in Section 3.2.1. The dwell times ($t_i$) of the specific source is multiplied with the relevant dose distribution of each individual source ($Dose_i$). The air kerma strength value is multiplied by the summation of all source dose distributions to reach the total dose distribution:

$$Total\ dose = (\sum_{i=1}^{15}(Dose_i \times t_i)) \times S_k \quad (32)$$

The total dose distribution is superimposed on the CT data in all three projections, as shown in Figure 11 below.

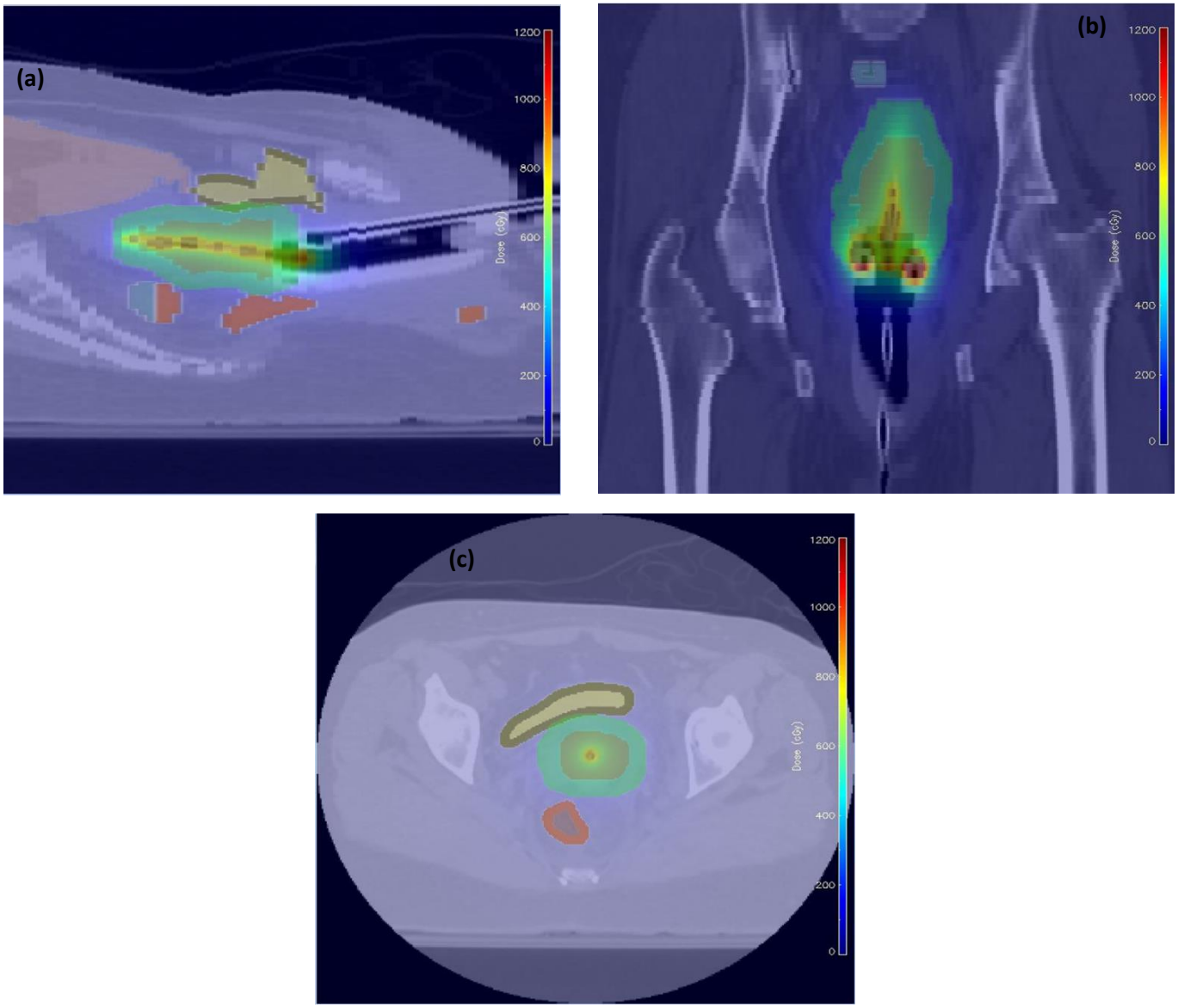


**Figure 11 - Visualisation of the dose distribution superimposed on the CT data and contoured volumes in three anatomical planes by the IHDM. (a) Sagittal view, (b) Coronal view and(c) Axial view.**

### 3.3.3 Calculation and display of relevant target and OAR dose

The total dose distribution is used to calculate the dose distribution in all relevant targets and OAR volumes converted into EQD2 by using Equation (2). The target and OAR dose distributions are used to create differential and cumulative DVHs. EUD values are calculated by using Equation (14) and (16) and $D_{2cm^3}$ and $D_{90\,\%}$ values for OAR and target values are obtained.

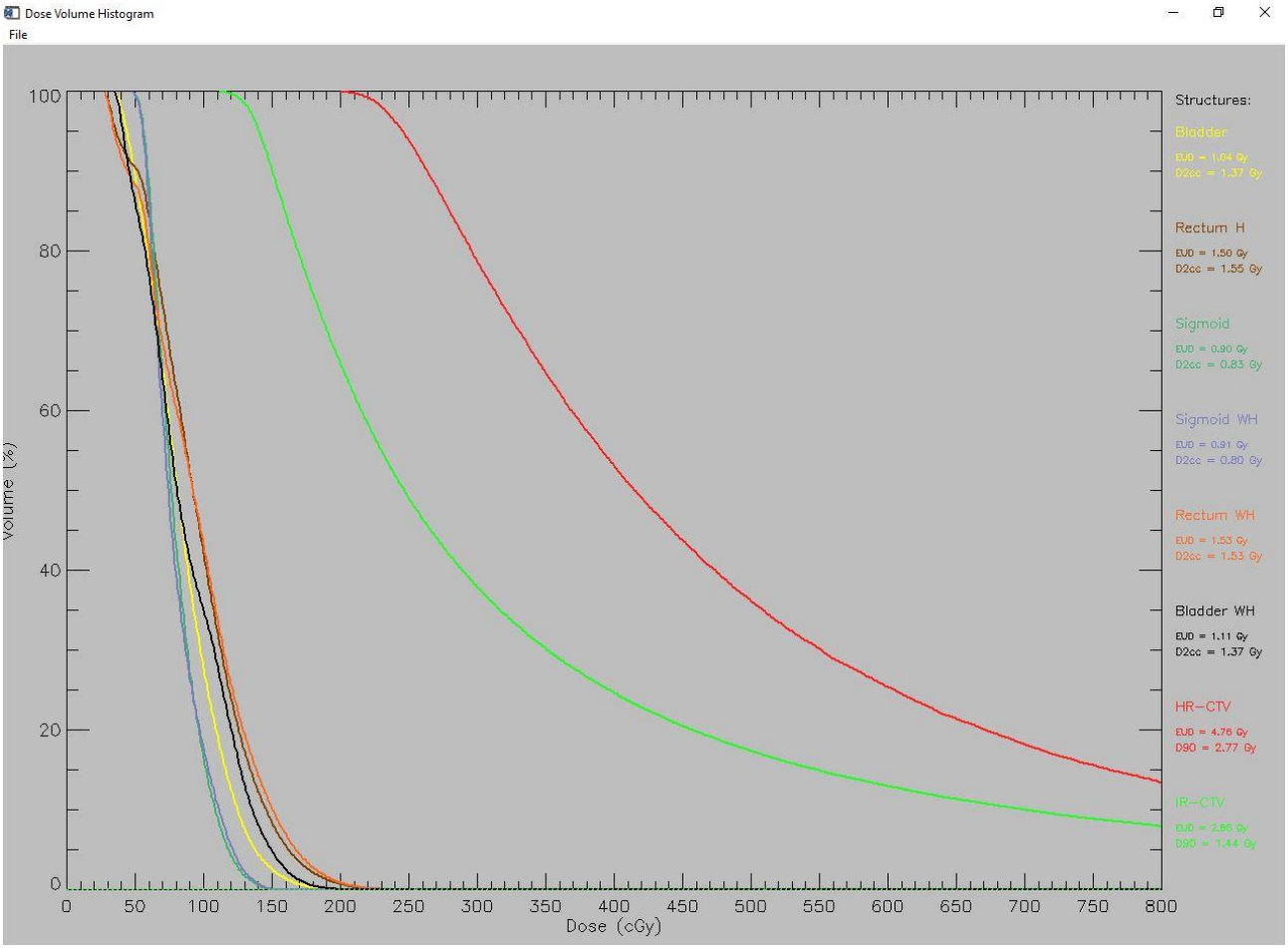


**Figure 12 - Cumulative dose-volume histogram in treatment planning module. All contoured structures are displayed on the same DVH. The legends indicate which structure is displayed, along with Dose-Volume parameters and EUD values.**

The cumulative DVHs (Figure 12) that are plotted and displayed for each individual structure are used as a guideline during the optimization process to determine the increase/decrease effects of source dwell times in relation to the structures.

**Dose files**

The module is developed to read and write text files. Text files are created and saved during each fraction after the plan has been optimized and finalized. The text files consist of the following updated information:

1. DVH parameters of target volumes and OAR volumes;

2. Dwell times of all sources;
3. Total treatment time;
4. TRAK value;
5. ICRU Recto-vaginal reference point doses;
6. Dose to point $A_{Left}$ and $A_{Right}$.

The data of the saved text files are imported into the module before planning of the next fraction commence. This is used to calculate the remaining individual dose to be given to the target and OAR volumes.

## Development of the planning and optimization tools

### 3.3.4 Development of forward planning and optimization tool

A tool was developed to perform forward optimization by manually increasing/reducing the dwell of all 15 sources, individually (Figure 13). After the necessary adjustments are made, the new dwell times can be applied and the dose can re-calculated, an updated dose distribution is/can be displayed on all three projections and a new cumulative DVH with updated DVH parameters can be plotted. This process can be repeated if the user is not satisfied with the outcome of the adjustments made. There is no limit in the number of allowed iterations, and this is solely depended on the user.

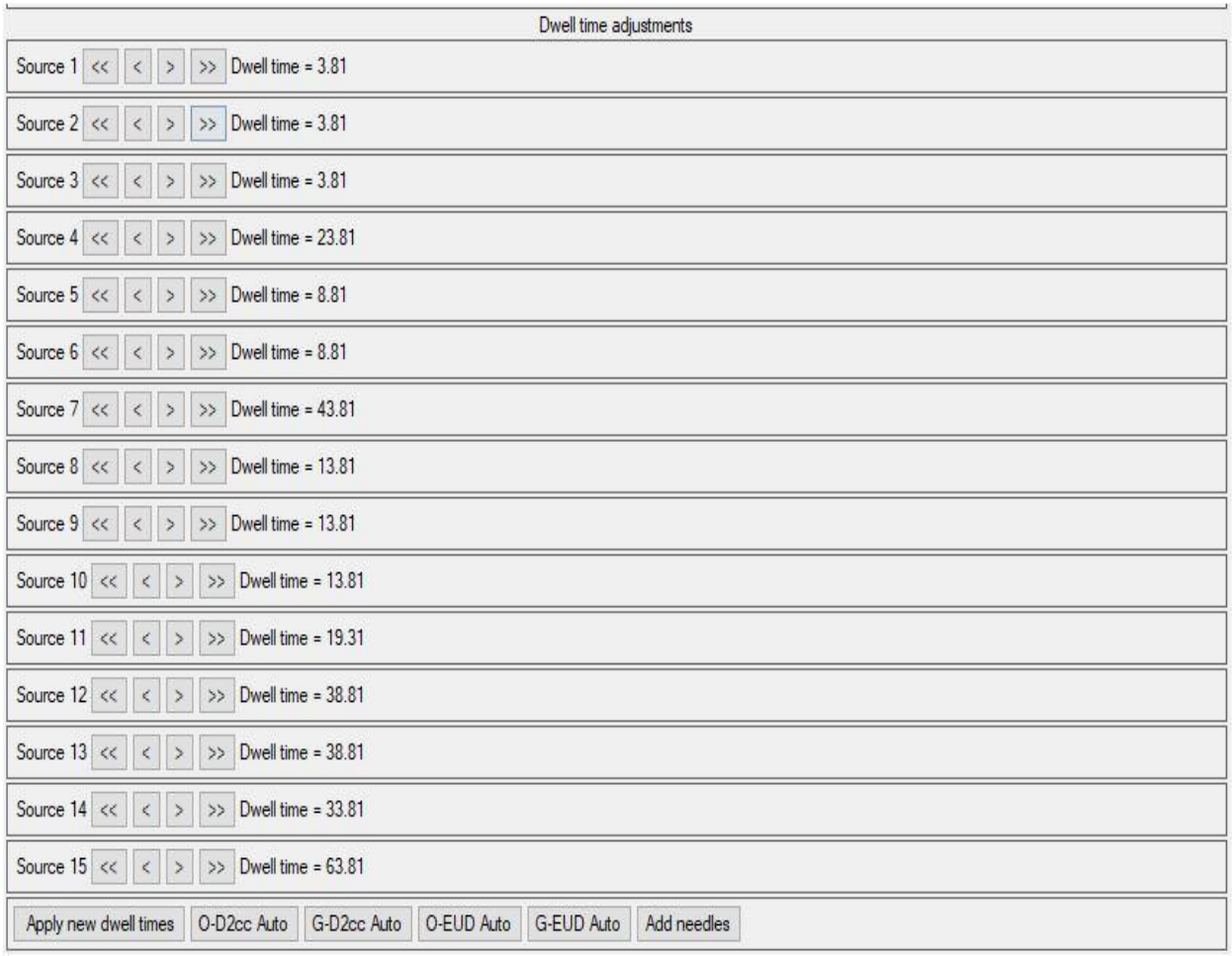


**Figure 13 – Planning interface of the module. Individual dwell time adjustment for each source can be made and applied by the "Apply new dwell times" button.**

A user-defined maximum of 150 seconds is set to an individual source dwell time.

### 3.3.5 Development of inverse planning and optimization tool

A tool was developed that comprise of a novel algorithm which has the ability to perform inverse optimization by automatically increasing/decreasing individual dwell times of all 15 sources until set dose objectives/constraints are reached. Dwell times are increased/decreased while the position of the sources is kept constant. The number of sources used in the inverse optimization process is dependent on the number of sources within the standard plan. If the standard plan is altered to consist of more/less than 15 sources, the inverse optimization tool can easily accommodate the increased or decreased number of sources. The optimization tool also has the ability to switch off sources that possess a very low dwell time and in return, do not contribute to the dose distribution.

**Dose impact analysis**

A dose impact analysis is performed as the starting point of the inverse optimization process. The relative contribution of each individual source towards target and OAR doses are evaluated. This is

done by setting source dwell times to zero (“off”) for 14 sources, while the weight of the 1st source of interest is set to a constant value (“on”), as illustrated in Figure 14 below.

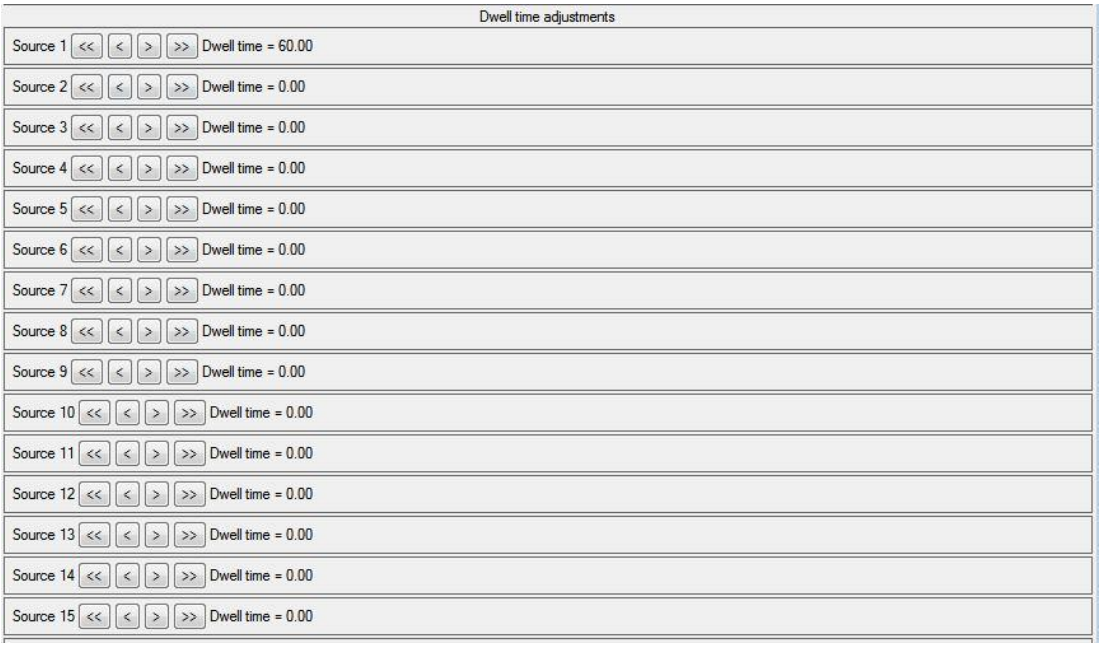


**Figure 14 - Dose impact analysis for the starting point of the inverse optimization process.**

The impact of the “on” source on target and OARs doses is evaluated by obtaining a specific mathematical relationship between the following dose parameters:

1. Target volumes: $D_{90\,\%}$ value;
2. OAR volumes: $D_{2cm^3}$ (conventional) and EUD (biological) values.

Even though the above listed parameters were used to determine the mathematical relation between the target and OAR volumes, the dose impact analysis process can be altered in the future to incorporate other relevant parameters like target volume EUD and $D_{100\,\%}$ values.

After evaluating all sources individually, the sources are arranged in accordance to their importance for each individual VOI. This dose analysis is used to determine the initial individual source dwell times at the start of the optimization process.

**Optimization process:**

Objective functions for the CTV-$T_{HR}$ and all four OARs are created. The objective functions consist of an evaluation of the current structure dose and the required objective/constraint set. Weight factors (s_w) are assigned to each OAR volume and considered as a measure of the importance of this objective in the optimization process. The individual OAR objective functions for the four OAR volumes are weighted and summed to obtain a single OAR objective function (OF_o).

$$OF\_o = (OF\_o\_r + OF\_o\_b + OF\_o\_s + OF\_o\_sbi)/sw\_t \quad (33)$$

Where:

$OF\_o\_r$ – Individual objective function for the rectum

$OF\_o\_b$ – Individual objective function for the bladder

$OF\_o\_s$ – Individual objective function for the sigmoid

$OF\_o\_sbi$ – Individual objective function for the small bowel

$sw\_t$ – Total weight of all OAR volumes:

$$sw\_t = sw(roi\_r) + sw(roi\_b) + sw(roi\_s) + sw(roi\_sbi) \quad (34)$$

Where:

$sw(roi\_r)$ – Weight factor for the rectum

$sw(roi\_b)$ – Weight factor for the bladder

$sw(roi\_s)$ – Weight factor for the sigmoid

$sw(roi\_sbi)$ – Weight factor for the small bowel

The weight factors values are dependent on the importance of the specific objective within the optimization process. If the result for some of the objectives is not satisfactory, then the corresponding weight factor is increased. As this influences the other weights, the result for other objective(s) will, most probably, deteriorate.

The optimization process aims to increase the dose in the target volumes while decreasing the dose in the OAR volumes creating a multi-objective optimization problem. The multi-objective problem is dealt with by combining the two objective functions as a single total objective function (OF):

$$OF = OF\_t + OF\_o \quad (35)$$

Where

$OF\_t$ – Objective function of CTV-$T_{HR}$

$OF\_o$ – Single objective function for all four OARs

A possible optimization solution is reached when the objective function (OF) is at 0 (minimum). If the objective function has not reached its minimum, dwell times are adjusted.

**Dwell time adjustment procedure:**

Objectives per source per structure are constructed. The adjustment (adj) per source weight is determined by combining these objectives:

$$adj = 1 - (eO\_r(n) + eO\_b(n) + eO\_s(n) + eO\_sbi(n)) \quad (36)$$

Where

$eO\_r(n)$ – Rectum objective per source

$eO\_b(n)$ – Bladder objective per source

$eO\_s(n)$ – Sigmoid objective per source

$eO\_sbi(n)$ – Small bowel objective per source

The calculated adjustment values per source are applied to the current source dwell times:

$$dwell\ time(n) = dwell\ time(n) \times adj \quad (37)$$

The newly calculated source dwell times are applied, and the dose is re-calculated. This process is repeated until the objective function has reached its minimum or the maximum number of iterations has been reached. This maximum number of iterations can be set by selecting an appropriate number, or if the difference between two iterations is lower than a pre-set value. In the case where the maximum number of iterations has been reached, the source dwell times that produced the best OF value are selected as the final source dwell times. An updated dose distribution is displayed on all three projections, and a new cumulative DVH with updated DVH parameters are plotted.

As illustrated in Figure 15, different inverse optimization options are developed which is dependent on the type of fractionation compensation scheme to be followed, as well as the planning utilization used, either with biological- or conventional parameters.


**Figure 15 - Different inverse planning options in the IHDM.**

1. O-D2cc Auto: Uses the optimistic fractionation compensation scheme, utilizing $D_{2cm^3}$ parameters;
2. G-D2cc Auto: Uses the greedy fractionation compensation scheme, utilizing $D_{2cm^3}$ parameters;
3. O-EUD Auto: Uses the optimistic fractionation compensation scheme, utilizing EUD parameters;
4. G-EUD Auto: Uses the greedy fractionation compensation scheme, utilizing EUD parameters.

As described earlier, fractionation compensation focuses on the total treatment OAR constraint, rather than the constant per-fraction treatment planning constraints, and this allows OARs to receive higher than the average dose in one fraction, if this can be compensated for in upcoming fractions. A conservative/optimistic approach bet on favourable future geometries instead of obtaining the maximum benefit at the current fraction, the difference between the total dose constraint and the already delivered dose is equally split between the remaining fractions. Thus, this new fractional dose becomes the new per fraction dose constraint [162]. A more greedy and pessimistic approach does not rely on better chances in the future and exploits any chance of compensation. It assumes that the fractions delivered, including the current one, are the best predictors for upcoming ones. It aims to achieve the entire compensation in the current fraction, whereas the conservative approach allocates it over all undelivered fractions [163].

### 3.3.6 Development of Intracavitary-Interstitial IGABT planning and optimization tool

An "Add needles" tool was created to add additional sources to the CTV-$T_{HR}$ volume by means of needles (Figure 16), it gives the user the ability to perform Intracavitary-Interstitial IGABT (IC-IS IGABT) planning, should it be necessary. The tool is not limited to a single needle configuration, and more needles can easily be configured, even though only one needle was configured for this study. In fact, any interstitial or applicator geometry can be re-produced if the coordinates of the possible source positions with reference to the (0, 0, 0) coordinates are known. These can be easily obtained from the CT data sets.

[162] (Lang *et al.*, 2007b)
[163] (Shaw, Rae and Alber, 2017)


**Figure 16 - Interstitial needle planning tool. The tool allows for manual dwell time adjustments of the additional 7 sources used in the IC/IS planning process.**

Figure 16 illustrates the source positions within the single needle, the < and > buttons can be used to decrease/increase the dwell times in small increments, where the << and >> buttons can be used to decrease/increase the dwell times in large increments for all source positions individually.

The position of the sources within the tandem (x_o,y_o,z_o) are used as the initial position of the source positions within the needle. By applying a shift (xc,yc,zc) to the initial position, the sources are shifted to their final position (x_o1, y_o1, z_o1). The final position can be calculated by the below equations:

$$\begin{aligned} x_{o1} &= x_o + xc \\ y_{o1} &= y_o + yc \\ z_{o1} &= z_o + zc \end{aligned} \tag{38}$$

To determine the direction and magnitude of the shift, an evaluation of the reported OAR doses during the intracavitary IGABT planning process is needed. This will allow the user to see which OAR volume dose constraints were violated and which OAR volumes can be exploited. The shift will be in the direction of the OAR volumes, which can be exploited and away from OAR volumes which were violated. The magnitude and direction of the shift applied to the needle are solely user dependant. The initial dwell time of all the needle sources are set to zero.

After the needle sources are inserted, forward planning can commence. Tandem, ring and needle source dwell times can be increased/reduced, individually. After the necessary adjustments are made, the new dwell times can be applied, and the dose can be re-calculated, an updated dose distribution is displayed on all three projections, and a new cumulative DVH with updated DVH parameters are plotted.

The inverse optimization section of IC-IS planning has not been developed in the module yet; however, it can be introduced in a similar way as the IGABT inverse optimization tool that was described earlier. Therefore, the user is restricted to perform forward optimization when planning an IC-IS case. A user-defined maximum of 150 seconds is set to an individual source dwell time. There is no limit in the number of iterations allowed, and this is solely depended on the user.

## 3.4 Verification of treatment planning module

As stated earlier, the in-house developed module (IHDM) planning tool is solely for research purposes, however, several different verifications tests were performed to establish the accuracy of the developed treatment planning module.

### 3.4.1 Comparison between calculated IHDM dose rate versus TG-43 dose rate for a single Ir-192 source

The difference in dose rate calculations between the developed IHDM and published TG-43 absolute dose rate value was evaluated. Several positions of interest were chosen perpendicular to the source axis, parallel (along) to the source axis and at different angles, all assuming rotational symmetry. The relevant dose rates were obtained at the corresponding positions of interest. The 70 different positions of interest used during the verification can be found in Appendix 2.

### 3.4.2 Comparison between calculated IHDM dose rate versus Oncentra TPS dose rate for a single Ir-192 source

The difference in dose rate calculations between the IHDM and the Oncentra TPS was evaluated. Again, the same positions of interest were chosen perpendicular to the source axis, parallel (along) to the source axis and at different angles, all assuming rotational symmetry. The relevant dose rates were obtained at the corresponding positions of interest. The 70 different positions of interest used during the verification can be found in Appendix 3.

Pronounced care was taken during the comparisons to ensure that the orientation of the two system's sources and calculation grids was aligned.

### 3.4.3 Dose distribution and plan comparison

The IHDM were used to optimize three different dose distributions on three different CT data sets with the use of the forward optimisation tool. The plans were optimised to reach an 8 Gy CTV-$T_{HR}$ $D_{90\ \%}$ value. The three CT data and plan sets were transferred to Oncentra and were re-calculated with the same dwell times. The dose distributions of the two systems were compared in the form of an DVH's. The following was compared:

1. Shape of the DVH
2. Parameters obtained from the DVH:
    - For target volumes;
        - $D_{90\%}$
    - For OAR volumes;
        - $D_{2cm^3}$

The same three CT data sets that were used for forward optimization were used to perform inverse optimization on. They were optimised to reach an 8 Gy CTV-$T_{HR}$ $D_{90\%}$ value. The three CT data and plan sets were transferred to Oncentra and were re-calculated with the available inverse optimiser tool, IPSA. The dose distributions of the two systems were compared in the form of an DVH's. The same parameters were compared, as mentioned above.

All verification tests performed was to establish and ensure that the treatment planning module delivered treatment plans that are line with the commercial TPS that is currently used for clinical treatments.

## 3.5 Treatment planning

Before planning and optimization commence, a standard plan is created for each patient on the Oncentra TPS. As mentioned earlier, the standard plan consists of 7 intra-uterine sources and 8 ring sources, that can be changed depending on the complexity of planning geometries. The source dwell times were individually set to 10 seconds, irrespective of the source strength. This information was imported into the IHDM, as the start of the planning and optimisation process.

**Total dose planning aims**

The dose planning aims tabulated below are expressed as a combination of BT and EBRT dose, both converted to EQD2. The planning aims are defined in terms of soft and hard constraints. The dose received from EBRT is assumed to be a total of 50 Gy, for both targets and OAR volumes [164]. Table 1 provides a summary of the CTV-$T_{HR}$ and CTV-$T_{IR}$ dose planning aims defined in terms of soft and hard constraints.[165]

[164] (Shaw, Rae and Alber, 2013)
[165] (Shaw, Rae and Alber, 2013)

**Table 1 - Total target dose planning aims for the CTV-T volumes**

| Target<br>Dose planning aims | CTV-$T_{HR}$ $D_{90\,\%}$<br>$EQD2_{10}$ | CTV-$T_{IR}$ $D_{90\,\%}$<br>$EQD2_{10}$ |
|---|---|---|
| Hard constraint | > 90 Gy | > 60 Gy |
| Soft constraint | > 95 Gy | - |

Table 2 provides a summary of the conventional $D_{2cm}{}^3$ OAR dose planning aims in terms of hard and soft constraints.

**Table 2 – Total OAR dose planning aims (Conventional) [166]**

| OAR<br>Dose planning aims | Rectum $D_{2cm}{}^3$<br>$EQD2_3$ | Bladder $D_{2cm}{}^3$<br>$EQD2_3$ | Bowel $D_{2cm}{}^3$<br>$EQD2_3$ | Sigmoid $D_{2cm}{}^3$<br>$EQD2_3$ |
|---|---|---|---|---|
| Hard constraint | < 75 Gy | < 85 Gy | < 75 Gy | < 75 Gy |
| Soft constraint | < 70 Gy | < 80 Gy | < 65 Gy | < 70 Gy |

The only difference between the tabulated OAR conventional planning aims and that of recent literature is the proposed soft constraint for the rectum, a soft constraint of 70 Gy was used, and literature proposes a constraint of 65 Gy. [167]

Table 3 provides a summary of the biological EUD OAR dose planning aims in terms of hard constraints; these hard constraints were derived by Shaw et al. [168] There are no EUD soft constraints. No bowel EUD value has been derived yet, and therefore the same EUD dose planning aim value was used as for the rectum and sigmoid. [169]

**Table 3 – Total OAR dose planning aims (Biological)**

| OAR<br>Dose planning aims | Rectum EUD<br>$EQD2_3$ | Bladder EUD<br>$EQD2_3$ | Bowel EUD<br>$EQD2_3$ | Sigmoid EUD<br>$EQD2_3$ |
|---|---|---|---|---|
| Hard constraint | 67.8 Gy | 75.95 Gy | 67.8 Gy | 67.8 Gy |
| Soft constraint | - | - | - | - |

[166] (Tanderup *et al.*, 2020)
[167] (Shaw, Rae and Alber, 2013; Tanderup *et al.*, 2020)
[168] (Shaw, Rae and Alber, 2013)
[169] (Shaw, Rae and Alber, 2013)

The hard constraint $D_{90\,\%}$ of the CTV-$T_{HR}$ is given the highest priority and thereafter hard constraints for all OAR volumes. When hard constraints of targets and OARs are realized, the priorities are, to aim for reaching/approaching soft constraints for CTV-$T_{HR}$ and subsequently reaching/approaching soft constraints for the CTV-$T_{IR}$ and OARs [170].

The following values are reported but not used as dose planning aims:

For target volumes, converted to $EQD2_{10}$:

- $D_{98\,\%}$ CTV-$T_{HR}$
- $D_{98\,\%}$ CTV-$T_{IR}$
- Point A

For OARs $EQD2_3$:

- ICRU Recto-vaginal reference point

Literature suggests a soft constraint > 80 Gy and hard constraint of > 75 Gy for the $D_{98\,\%}$ CTV-$T_{HR}$. A $D_{98\,\%}$ CTV-$T_{IR}$ soft constraint > 60 Gy and soft constraint > 65 Gy for Point A are proposed. For OAR dose planning aims a soft and hard constraint for the ICRU recto-vaginal < 65 Gy and < 75 Gy, respectively are also proposed.[171]

**Fractional dose planning aims**

Planning was performed by considering total dose aims and not fractional objectives/constraints. The total dose aims used in the fractional dose calculations for all VOI's are summarized in Table 1, Table 2 and Table 3. The IHDM had the ability to calculate the needed allowed fractional objective/constraint for all VOI's automatically. No additional calculations were needed to be performed by the user outside of the IHDM, and this applies to conventional and biological values.

The allowed fractional objective/constraint for each specific VOI is calculated using the equations below.

**Optimistic dose compensation approach:**

$$D_F = \frac{D_T - \sum_{i=1}^{5} d_i}{nf - tf} \tag{39}$$

[170] (Tanderup *et al.*, 2020)
[171] (Tanderup *et al.*, 2020)

**Greedy dose compensation approach:**

$$D_F = \left( (\frac{tf + cf}{n_f}) \times D_T \right) - \sum_{i=1}^{5} d_i \quad (40)$$

Where

$D_F$ - Calculated allowed dose constraint/objective for current fraction

$D_T$ - Total dose constraint/objective for whole treatment (Table 1, Table 2 and Table 3)

$d_i$ - Dose received by target/OAR in previous fractions

$nf$ - Total number of fractions to be given

$tf$ - Fractions already treated

$cf$ - Current fraction to be treated

**Dose reporting**

The following parameters are reported, this includes Level 1 and Level 2 standards, as per ICRU 89 recommendations. Additional dose reporting parameters are also added that are not listed in the ICRU 89 report [172].

**Table 4 - Level 1 and 2 parameters and additional parameter that will be recorded and reported for each fraction**

| **Level 1*: Minimum standard for reporting*** | **Level 2: *Advanced standard for reporting*** | **Additional dose reporting parameters** |
|---|---|---|
| TRAK | **Dose reporting for defined volumes:** | **Dose reporting for defined volumes:** |
| Point A dose ($A_{Left}$ and $A_{Right}$) | $D_{100\,\%}$, $D_{98\,\%}$ and $D_{90\,\%}$ for $CTV_{HR}$ | EUD for $CTV_{HR}$ and $CTV_{IR}$ |
| Recto-vaginal reference pint dose | $D_{100\,\%}$, $D_{98\,\%}$ and $D_{90\,\%}$ for $CTV_{IR}$ | |
| **Dose reporting for OAR volumes:** | **Dose reporting for OAR volumes:** | **Dose reporting for OAR volumes:** |
| $D_{0.1cm^3}$, $D_{2cm^3}$ for bladder | $D_{0.1cm^3}$, $D_{2cm^3}$ for sigmoid | EUD for bladder, rectum, sigmoid and bowel |

[172] ('Prescribing, Recording, and Reporting Brachytherapy for Cancer of the Cervix', 2013)

| | | |
|---|---|---|
| $D_{0.1cm^3}$, $D_{2cm^3}$ for rectum | $D_{0.1cm^3}$, $D_{2cm^3}$ for bowel | |

### 3.5.1 Intracavitary IGABT treatment planning

Intracavitary IGABT treatment planning was performed on all 18 patients, and all patients received five treatment fractions with daily imaging and contouring. Dose optimization was performed based on two optimization techniques: forward and inverse planning. During the two dose optimization processes, two different dose planning methods were used: conventional (DVH parameter based) and biological (EUD based). The fractional dose limits applied in both the planning methods are calculated by Equation 12 and 13, dependent on the fraction compensation approach used. Figure 17 is a schematic diagram that shows the planning routes that are followed.

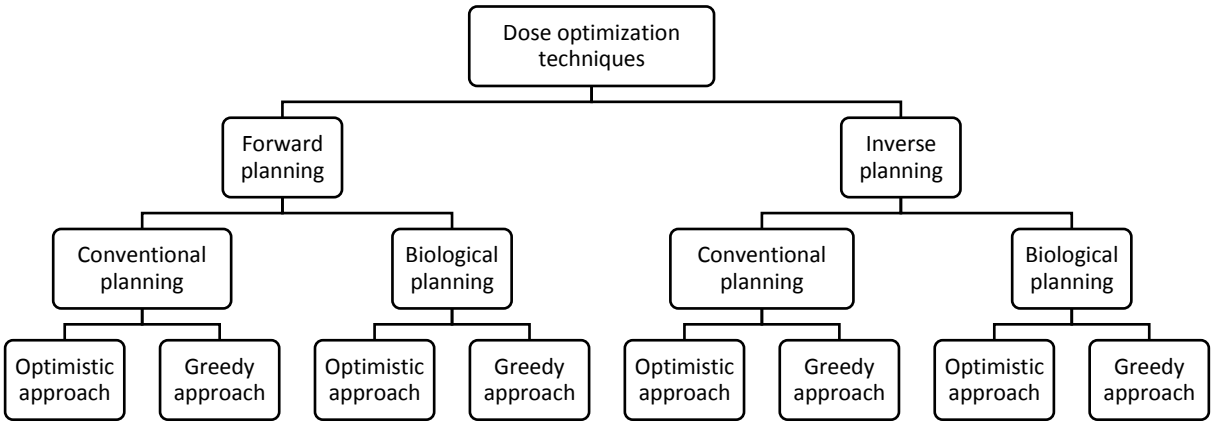


**Figure 17 - IGABT planning routes followed**

From Figure 17, it can be seen that 8 different treatment plans are planned and created per fraction, adding up to 40 different plans in the course of treatment for one patient. A total of 720 different Intracavitary IGABT treatment plans were planned:

360 Forward optimized plans:

1. 90 Conventional ($D_{2cm^3}$) optimistic plans;
2. 90 Conventional ($D_{2cm^3}$) greedy plans;
3. 90 Biological (EUD) optimistic plans;
4. 90 Biological (EUD) greedy plans.

360 Inverse optimized plans:

1. 90 Conventional ($D_{2cm}^3$) optimistic plans;
2. 90 Conventional ($D_{2cm}^3$) greedy plans;
3. 90 Biological (EUD) optimistic plans;
4. 90 Biological (EUD) greedy plans.

This number of plans excludes the number of IC-IS BT treatment plans.

### Forward planning

The forward optimization technique is executed by manual adjustment of source dwell times until the calculated dose planning aims are met. The plan criteria set is dependent on the type of fractionation compensation scheme followed, as well as the planning utilization used, either with biological or conventional parameters. Priority is given to the CTV-$T_{HR}$ dose even if OAR constraints are violated.

### Inverse planning

The inverse optimization technique is executed by setting the dose constraints for the OARs and dose objectives for the targets prior to the onset of optimization. The plan criteria set are the same as listed in Table 1 to Table 3. During the optimization procedure, the dose constraints and objectives will limit/allow the adjustment of source dwell times to a certain extent to meet the specific objectives set. After the inverse optimization process, the dose distribution is visually examined, and if any obvious dwell time adjustments are required, it is manually adjusted.

Priority *is* given to the CTV-$T_{HR}$ dose even if OAR constraints are violated.

### Conventional planning and optimization

During the conventional planning process, DVH parameters, as summarized in Table 2, are used as OAR constraints during the planning and optimization process. Biological parameters of all VOI's are calculated and recorded but are not implemented as constraints during the conventional planning process.

The fractional $D_{2cm}^3$ values of the OAR volumes are calculated by either Equation (39) and (40), dependant on the fractionation compensation scheme used.

### Biological planning and optimization

During the biological planning process, EUD parameters, as summarized in Table 3, are used as OAR constraints during the planning and optimization process. Conventional parameters of all VOI's are calculated and recorded but are not implemented as constraints during the biological planning process.

The fractional EUD values of the OAR volumes are calculated by either Equation (39) and (40), dependant on the fractionation compensation scheme used.

### 3.5.2 IC-IS IGABT treatment planning

**Forward IC-IS IGABT treatment planning**

During the IC-IGABT planning process, several patients may violate one or more OAR total dose constraints to guarantee that the total dose objective of the CTV-$T_{HR}$ is reached. The seven patients that achieved the worse results are handpicked and re-planned by performing IC-IS IGABT planning. It can be seen in Figure 18 that only the forward dose planning technique is used. Patients are planned according to the conventional and biological planning approach while utilizing the optimistic and greedy fractionation dose compensation approaches.

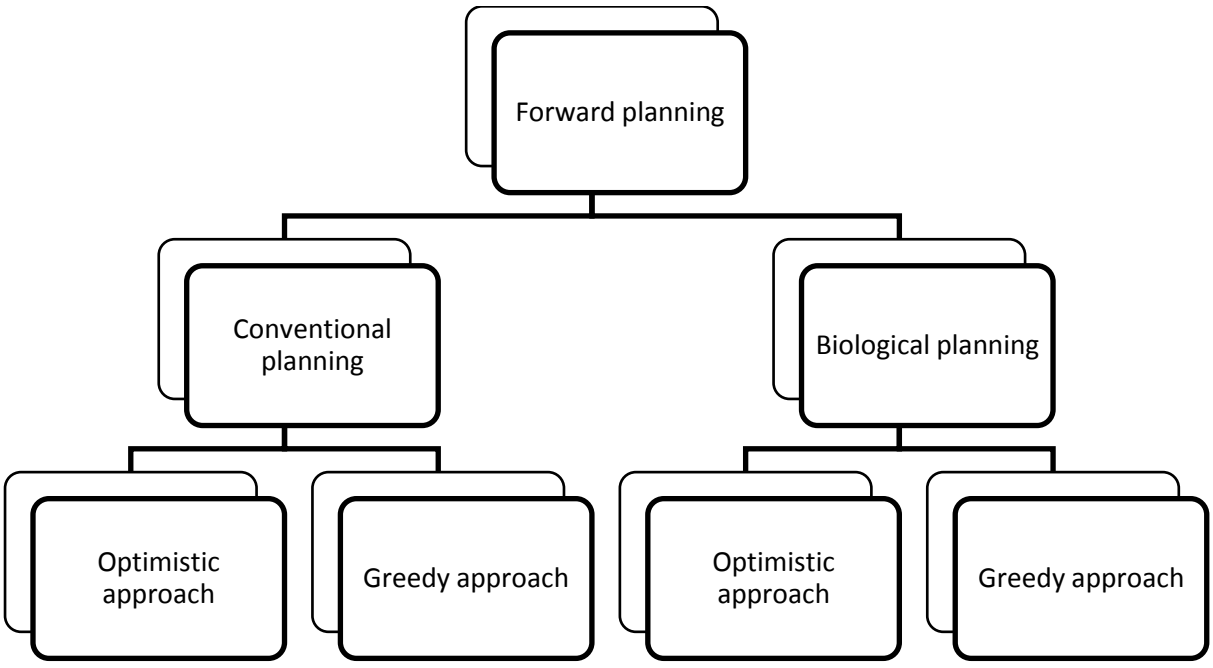


**Figure 18 - IC-IS planning routes followed**

A total of 140 different forward optimized IC-IS IGABT treatment plans are planned:

1. 35 Conventional ($D_{2cm^3}$) optimistic plans;
2. 35 Conventional ($D_{2cm^3}$) greedy plans;
3. 35 Biological (EUD) optimistic plans;
4. 35 Biological (EUD) greedy plans.

The CTV-$T_{HR}$ orientation in relation to the OARs for the specific fraction is evaluated and considered, and this evaluation is used to determine the needed orientations. The insertion of the needle is to avoid the limiting OAR but covering the under-dose region within the CTV-$T_{HR}$ volume. The size of the shift is based on the CTV-$T_{HR}$ size and positioning of the OAR volumes in relation to the CTV-$T_{HR}$ volume.

For example:

Assume the CTV-$T_{HR}$ is under-dosed adjacent to the rectum and sigmoid, due to the bladder or small bowel limiting the increase in intra-uterine source dwell times (blue dots) as illustrated in Figure 19. The rectum and sigmoid dose constraints are not reached due to the intra-uterine sources located far-off. The bladder or/and small bowel constraints are violated to reach CTV-$T_{HR}$ objective.

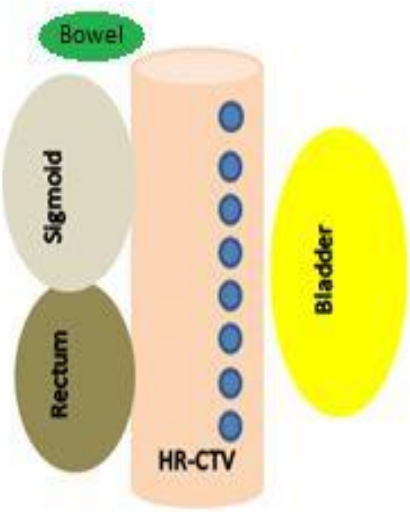


**Figure 19 - Visualisation of IU sources**

In this case, the intra-uterine source positions can be shifted with a constant value (c) in the direction of the sigmoid and rectum by using Equation (38). Thus, becoming the position of the sources within the needle (red dots) as illustrated in Figure 20.

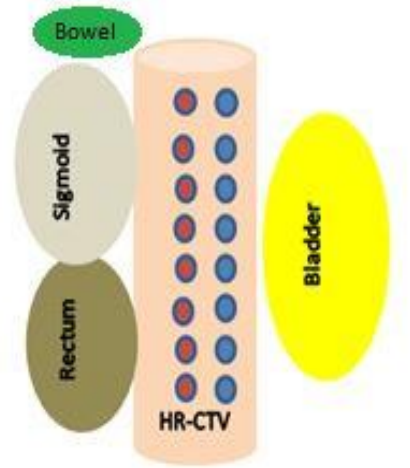


**Figure 20 - Visualisation of IU sources and needle**

The combination of the newly added needle to the existing intra-uterine sources allows for adaption/escalation of CTV-$T_{HR}$ dose. The intra-uterine dwell times are decreased, which allows for a reduction in the bladder dose, dwell times of needle sources are increased, exploiting the fact that the rectum and sigmoid dose constraints are not reached, thus giving some flexibility within the treatment plan. The combination of the two methods may allow for improved dose coverage in the CTV-$T_{HR}$ volume.

The shift applied may vary from patient to patient and fraction to fraction. The same parameters calculated and recorded during the IC-IGABT planning are calculated and recorded during the IC-IS planning.

Dose reporting is done on parameters as set out in Table 4.

### Inverse IC-IS IGABT treatment planning

The patient with the worse outcome during the forward IC/IS IGABT will be selected to perform inverse IC/IS IGABT planning and optimisation. The same needle configuration will be used as was used in the forward optimisation process. The same approach will be used that reported the best results for the forward optimisation technique.

## 3.6 Statistical analysis

Statistical analysis was performed to determine if compared approaches displayed a significant difference in the outcome. During the statistical analysis, normality tests were applied to determine if the data sets were normal distribution. The outcome of the normality test determined the type of statistical test that was applied to the data sets. A Student's *t*-test was applied to the data which followed a normal distribution. The Wilcoxon signed-rank test was applied to data sets that followed skewed distributions. Statistical significance was considered for $p \leq 0.05$. Results that present with p-value $\leq 0.05$ will be mentioned and discussed; otherwise, it can be assumed that there were no statistically significant differences. The SPSS Statistics for Windows, Version 25.0, Armonk, NY: IBM Corp. was used.

# Chapter 4 - Results and discussion

## 4.1 Verification of the In-house developed module (IHDM)

The accuracy of the In-house developed Module (IHDM) was verified with TG-43 and the Oncentra TPS system. The IHDM dose rate per unit air-kerma strength values for a single source was compared with TG-43 and the Oncentra TPS system.

Dose distribution and plan comparison for multiple source positions was also executed for the IHDM and the Oncentra TPS system. These verifications were necessary to establish if the IHDM can perform accurate dose calculation and treatment planning.

### 4.1.1 Comparison between IHDM dose rate versus TG-43 dose rate for a single Ir-192 source

The IHDM dose rate for a single Ir-192 source at 70 different positional coordinates was compared with the TG-43 2D dose rate at the same positional coordinates. The radius between the centre of the Ir-192 source and the positional coordinates chosen ranged from 0.25 cm to 8.50 cm. For simplicity and illustration purposes, the 70 different positional coordinates used for comparison were subdivided into seven coordinate groups. The positional coordinates with the same magnitude but with different direction were grouped. The accuracy results are shown below in Table 5.

**Table 5 – The percentage difference between the IHDM calculated and TG43 dose rate per unit air-kerma strength (%)**

| Coordinates Group | Average difference (%) | STD | Median | Minimum | Maximum |
|---|---|---|---|---|---|
| 1 | 1.20 | 0.20 | 1.13 | 1.02 | 1.51 |
| 2 | 0.96 | 0.13 | 0.96 | 0.74 | 1.19 |
| 3 | 0.99 | 0.15 | 1.06 | 0.70 | 1.09 |
| 4 | 0.90 | 0.14 | 0.81 | 0.76 | 1.16 |
| 5 | 0.65 | 0.13 | 0.61 | 0.46 | 0.91 |
| 6 | 0.57 | 0.34 | 0.63 | 0.13 | 1.06 |
| 7 | 0.76 | 0.46 | 0.71 | 0.29 | 1.43 |

From Table 5, it can be seen that the IHDM dose rate values compared very well with the gold standard – TG 43 dose rate, with a maximum of 1.51 % difference. This difference was noticed in Group 1, where the average differences were less than 2%, which is regarded as the tolerance for acceptable

deviation in dose calculation accuracy [173]. Each individual calculation point with the obtained dose rate values for the IHDM and TG-43 can be found in Appendix 2.

### 4.1.2 Comparison between IHDM dose rate versus Oncentra dose rate for a single Ir-192 source

After the IHDM dose rate for a single Ir-192 source were compared with TG-43. The IHDM dose rate was compared with the Oncentra TPS dose rate. The same 70 different positional coordinates used for comparison were again subdivided into seven coordinate groups, for simplicity and illustration purposes. The results of this comparison are tabulated below in Table 6.

**Table 6 – The difference between the IHDM and TPS dose rate per unit air-kerma strength (%)**

| Coordinates Group | Average difference (%) | STD | Median | Minimum | Maximum |
|---|---|---|---|---|---|
| 1 | 1.33 | 0.84 | 1.44 | 0.03 | 2.42 |
| 2 | 1.15 | 0.76 | 1.01 | 0.45 | 3.08 |
| 3 | 1.19 | 0.71 | 1.01 | 0.65 | 3.07 |
| 4 | 0.91 | 0.81 | 0.48 | 0.42 | 2.54 |
| 5 | 1.49 | 0.81 | 1.77 | 0.57 | 2.89 |
| 6 | 6.16 | 2.69 | 4.46 | 3.29 | 9.60 |
| 7 | 6.89 | 2.64 | 6.25 | 2.32 | 9.77 |

From Table 6, it can be seen that the IHDM dose rate values compared well with the Oncentra TPS system. Groups 6 and 7 displayed significant percentage differences. These points are situated far away from the centre of the source, therefore having a small dose rate value and leading to a big percentage difference. The maximum difference of 9.77 %, can be noted in Group 7, the dose rate values at this specific point are 0.0042 cGy/hU and 0.0047 cGy/hU for the IHDM and Oncentra TPS, respectively. The specific point differed by 9.33 % from TG-43. The difference may be attributed to a small misalignment of the source with the dose calculation grid on the Oncentra TPS system. Each individual calculation point with the obtained dose rate values for the IHDM and TPS Oncentra can be found in Appendix 3**.**

[173] (Nath *et al.*, 1997)

### 4.1.3 Dose distribution and plan comparison for multiple source positions using forward optimisation

To be able to compare dose in 3D on patient CT data, the full 3D dose distribution must be visible in the IHDM. Similar to other 3D TPSs, dose, anatomical geometries and volumes of interest can be displayed in three major planes, axial, sagittal and coronal. Three treatment plans, fully optimised to deliver 8 Gy to the CTV-$T_{HR}$ $D_{90\,\%}$, were devised. The same dwell positions and times were applicable in both systems. An example of such dose distributions planned using the contoured VOIs is displayed in Figure 21. The reason for the IHDM images to appear blue is due to the dose display that was set to blue display for low doses.

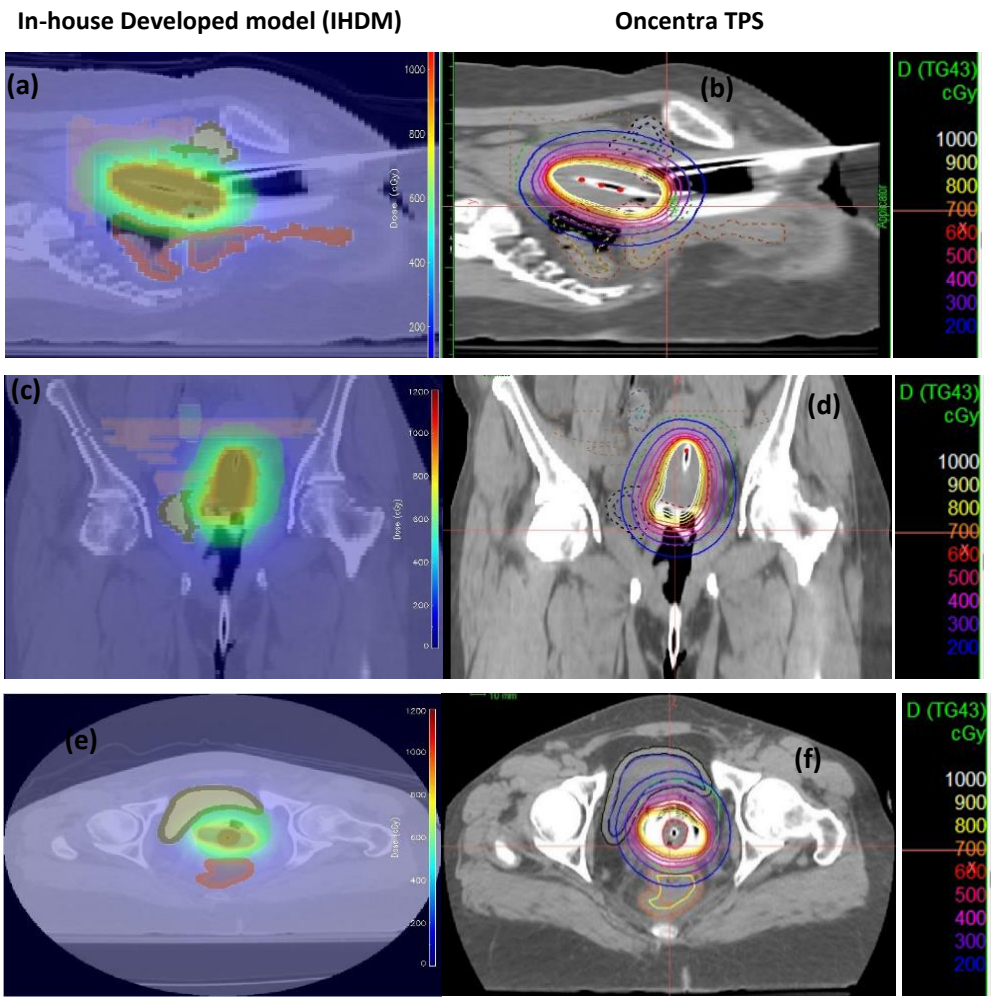


**Figure 21 -Example of the same dose distribution on the two systems in three anatomical planes. (a) IHDM Sagittal (b) Oncentra Sagittal (c) IHDM Coronal (d) Oncentra Coronal (e) IHDM Axial (b) Oncentra Axial.**

To perform an evaluation of dose calculation accuracy of the IHDM, in addition to dose distribution comparisons, cumulative dose-volume histogram comparisons of all three dose distributions were also made.

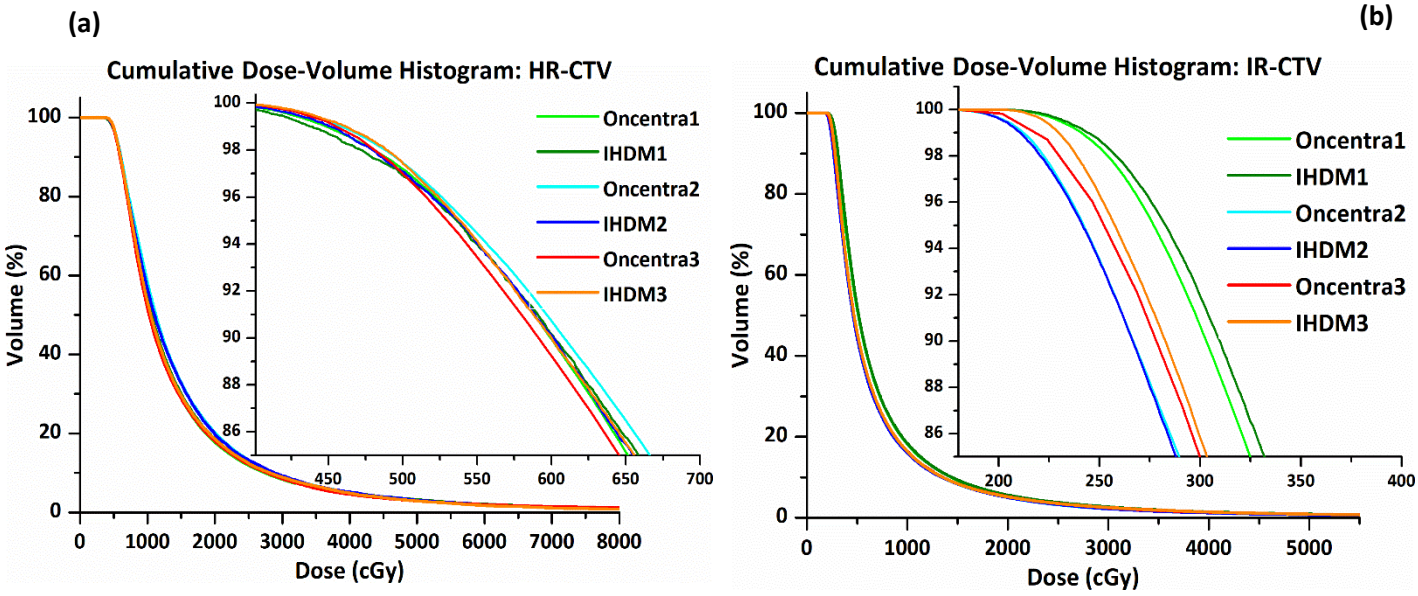


**Figure 22 - Dose distribution comparison between the IHDM and Oncentra for all three forward optimised plans. Three dose distributions in the form of cumulative DVHs for both CTV-T volumes, (a) CTV-$T_{HR}$ and (b) CTV-$T_{IR}$. The graphs are shown in physical dose.**

Figure 22 shows these DVHs for the CTV-$T_{HR}$ and CTV-$T_{IR}$; the two systems show an excellent correlation in the CTV-$T_{HR}$ and CTV-$T_{IR}$. The maximum difference between the two systems' D90% of the CTV-$T_{HR}$ and CTV-$T_{IR}$ was 1.79 % and 2.43 %, respectively. The plans were optimised to be within the tolerance for the OAR volumes, and the planning aim to the CTV-$T_{HR}$ was 8 Gy $EQD2_{10}$. However, some of the OAR constraints were violated in the attempt to reach the 8 Gy dose goal. The limits for the bladder was 7 Gy and 5 Gy for the rectum, sigmoid and small bowel, respectively. Figure 23 shows the correlating DVHs for all the OAR volumes.

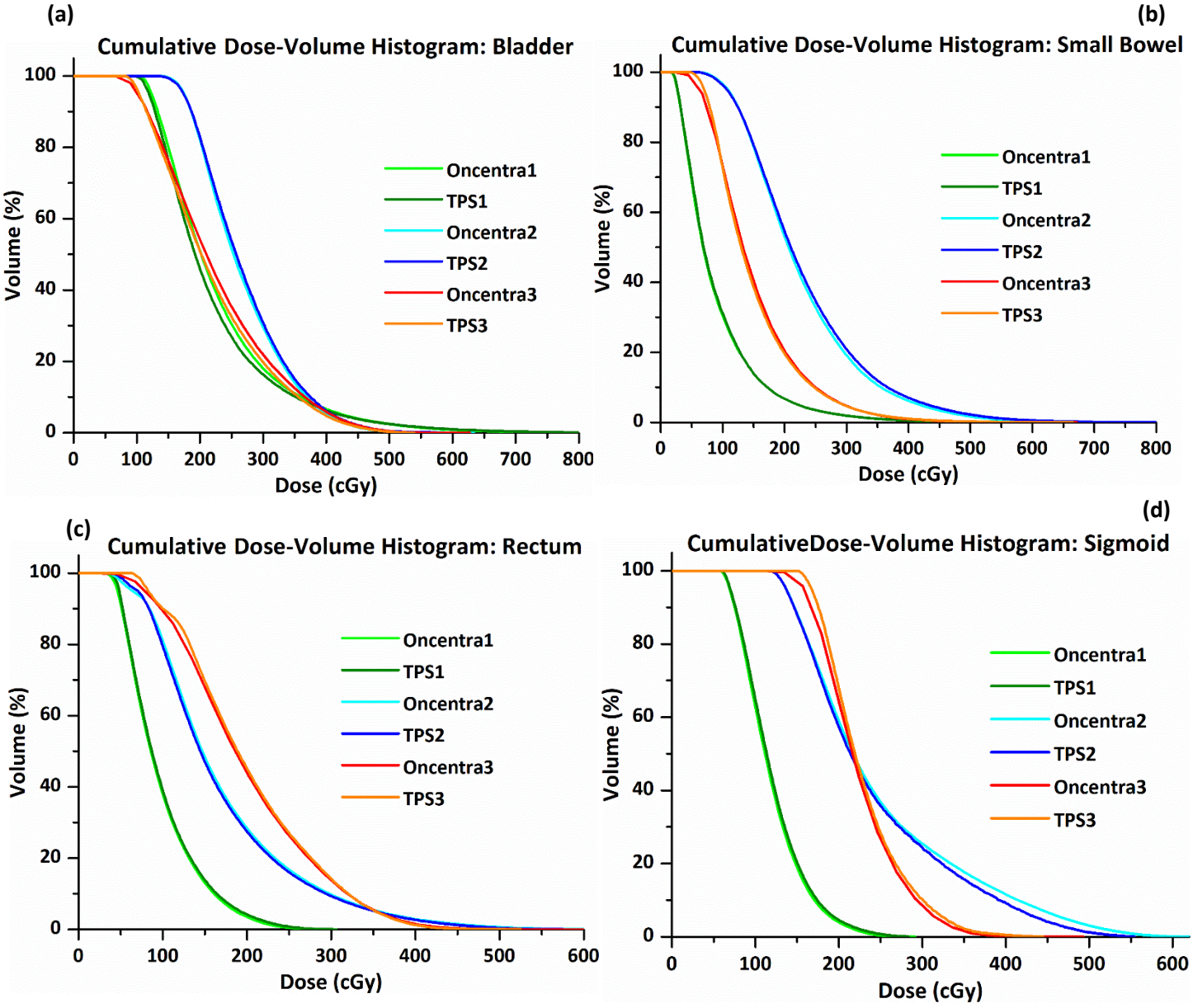


**Figure 23 – Dose distribution comparison between the IHDM and Oncentra for all three forward optimised plans. Three dose distributions in the form of cumulative DVHs for all OAR volumes, (a) Bladder, (b) Small bowel, (c) Rectum and (d) Sigmoid. The graphs are shown in physical dose.**

When comparing the OAR dose distributions, the two systems again showed a very good correlation, as illustrated in Figure 23. In the three treatment plans that were compared, the bladder $D_{2cm^3}$ values were 6.94 Gy, 5.64 Gy and 6.28 Gy for the IHDM, versus 6.94 Gy, 5.47 Gy and 6.41 Gy for Oncentra in plans 1, 2, and 3, respectively. The largest dose deviation was 3.11%. The bladder volume size of plan 1, 2 and 3 was 54.28, 30.98 and 76.45 $cm^3$, respectively. In the case of the rectum, these values were 2.14 Gy, 5.87 Gy and 4.71 Gy for the IHDM, versus 2.02 Gy, 6.03 Gy and 4.68 Gy for Oncentra in plans 1, 2, and 3, respectively, with the largest difference of 5.94 %. The rectum volume size of plan 1,2 and 3 was 60.83, 88.42 and 44.91 $cm^3$, respectively. The sigmoid volume size of plan 1,2 and 3 was 34.18,

10.16 and 9.69 $cm^3$, respectively. The sigmoid $D_{2cm^3}$ values were 1.92 Gy, 4.45 Gy and 3.09 Gy for the IHDM, versus 1.83 Gy, 4.29 Gy and 2.96 Gy for Oncentra in plans 1, 2, and 3, respectively with the largest difference of 5.94 %. The small bowel $D_{2cm^3}$ values were 5.93 Gy, 7.95 Gy and 5.67 Gy for the IHDM, versus 6.05 Gy, 7.39 Gy and 5.55 Gy for Oncentra in plans 1, 2, and 3, respectively, with the largest difference of 7.58 %. The small bowel volume size of plan 1,2 and 3 was 467.83, 81.30 and 206.71 $cm^3$, respectively. Table 7 gives a summary of this comparison.

**Table 7 – Summary of the results of the three forward optimised plans that were used to compare the dose distributions in the IHDM and TPS Oncentra**

| System | CTV-$T_{HR}$ $D_{90\,\%}$ (Gy) | CTV-$T_{IR}$ $D_{90\,\%}$ (Gy) | Bladder $D_{2cm^3}$ (Gy) | Small bowel $D_{2cm^3}$ (Gy) | Rectum $D_{2cm^3}$ (Gy) | Sigmoid $D_{2cm^3}$ (Gy) |
|---|---|---|---|---|---|---|
| | **Plan 1** | | | | | |
| **IHDM** | 8.02 | 3.37 | 6.94 | 5.93 | 2.14 | 1.92 |
| **Oncentra TPS** | 7.99 | 3.29 | 6.94 | 6.05 | 2.02 | 1.83 |
| **Percentage difference (%)** | 0.38 | 2.43 | 0.00 | 1.98 | 5.94 | 4.92 |
| | **Plan 2** | | | | | |
| **IHDM** | 8.02 | 2.81 | 5.64 | 7.95 | 5.87 | 4.45 |
| **Oncentra TPS** | 8.16 | 2.81 | 5.47 | 7.39 | 6.03 | 4.29 |
| **Percentage difference (%)** | 1.69 | 0.00 | 3.11 | 7.58 | 2.65 | 3.73 |
| | **Plan 3** | | | | | |
| **IHDM** | 7.98 | 3.01 | 6.28 | 5.67 | 4.71 | 3.09 |
| **Oncentra TPS** | 7.84 | 2.99 | 6.41 | 5.55 | 4.68 | 2.96 |
| **Percentage difference (%)** | 1.79 | 0.67 | 2.03 | 2.16 | 0.64 | 4.39 |

The differences found were examined thoroughly. The only plausible reason, considering the accuracy attained in the single source comparison results shown in Table 5 and Table 6, may again be attributed to the IHDM dose grid size of 2.5 mm, where Oncentra has a dose calculation grid of 1 mm. Dose averaging leads to variations in the calculated dose when these dose grids are compared. The impact of these differences will be more emphasised when very small or thin structures are contoured, or where the dose gradient is extremely steep. On the DVHs supplied, the dose bin size also influences the comparison of the IHDM and Oncentra. The Oncentra dose bin size for the OAR DVHs is 4 cGy, while the IHDM uses a bin size of 1 cGy. The orientation of sources within the ring in the Oncentra TPS system may differ from that of the IHDM, which will affect the comparison.

Considering the results shown above, the IHDM was deemed to have a dose calculation accuracy level similar to the Oncentra system, and it was therefore accepted that clinically relevant treatment plans could be devised using this module, with expected dose distributions similar to what would be calculated by Oncentra.

### 4.1.4 Dose distribution and plan comparison for multiple source positions using inverse optimisation

The same three CT data sets that were used for forward optimisation were used for inverse optimisation. They were optimised to reach an 8 Gy EQD2 CTV-$T_{HR}$ $D_{90\,\%}$ value. The three CT data and plan sets were transferred to Oncentra and were re-calculated with the available inverse optimiser tool, IPSA. The dose distributions of the two systems were compared in the form of an DVH's. The same parameters were compared, as mentioned above.

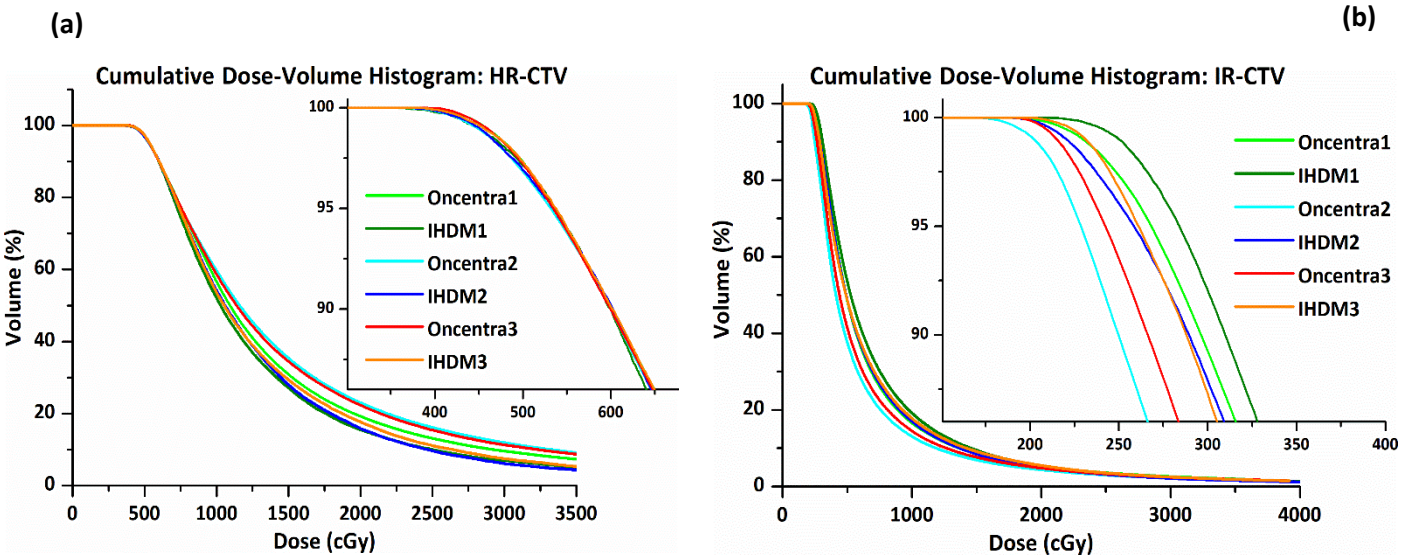


**Figure 24 - Dose distribution comparison between the IHDM and Oncentra for all three inverse optimised plans. Three dose distributions in the form of cumulative DVHs for both CTV-T volumes, (a) CTV-$T_{HR}$ and (b) CTV-$T_{IR}$. The graphs are shown in physical dose.**

The differences between the two systems can be observed in Table 8, Figure 24 and Figure 25. The IHDM optimised plans produce better CTV-$T_{IR}$ coverage with the detriment of higher OAR dose values. However, some OAR dose values were lower for the IHDM compared to the Oncentra TPS, even though better CTV-$T_{IR}$ coverage were produced. If the CTV-$T_{IR}$ weight is reduced during the optimisation process, the probability of the IHDM producing a plan with comparable CTV-$T_{IR}$ and OAR dose are high.

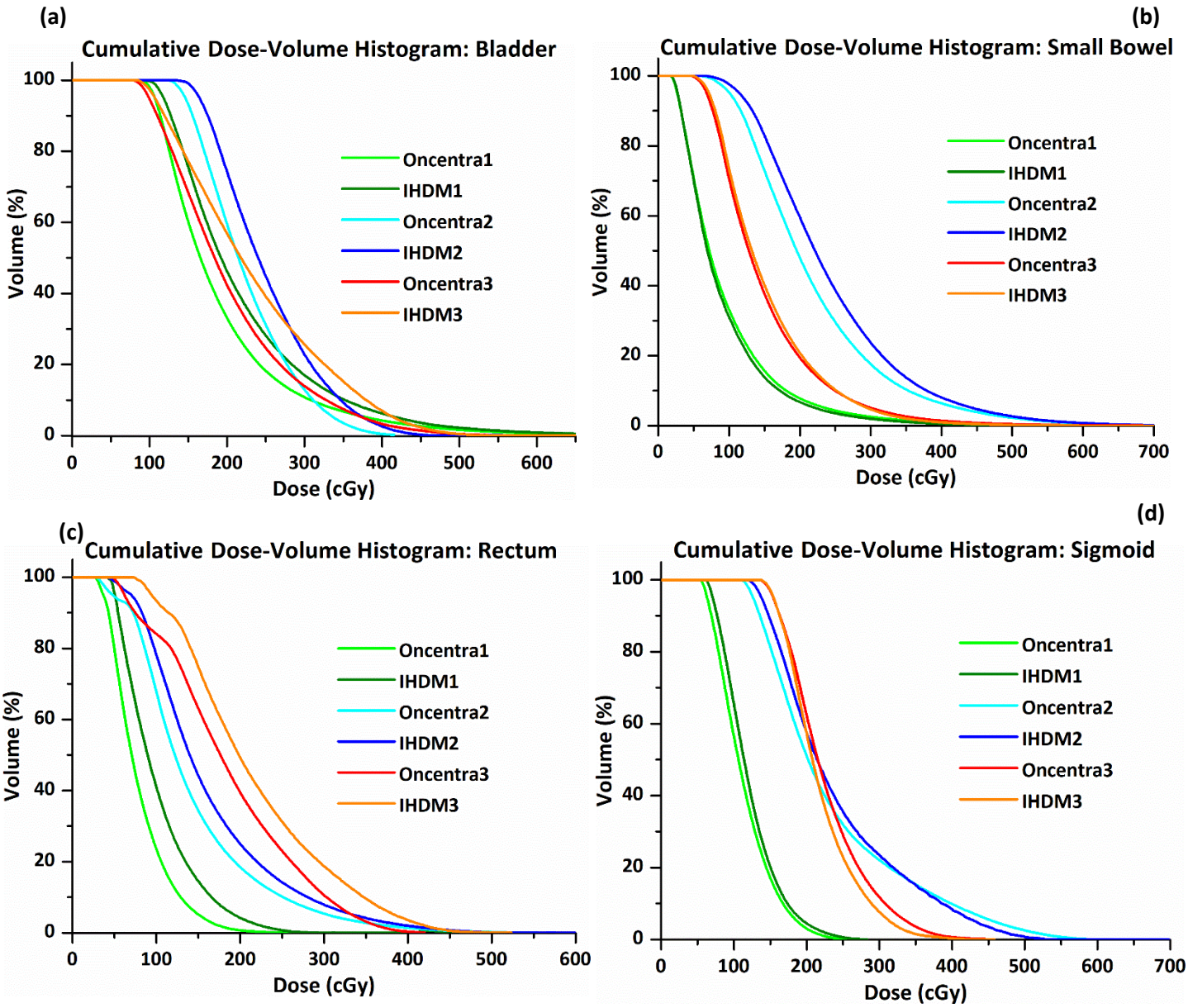


**Figure 25 – Dose distribution comparison between the IHDM and Oncentra for all three inverse optimised plans. Three dose distributions in the form of cumulative DVHs for all OAR volumes, (a) Bladder, (b) Small bowel, (c) Rectum and (d) Sigmoid. The graphs are shown in physical dose.**

**Table 8 - Summary of the results of the three inverse optimised plans that were used to compare the dose distributions in the IHDM and TPS Oncentra.**

| System | CTV-$T_{HR}$ $D_{90\,\%}$ (Gy) | CTV-$T_{IR}$ $D_{90\,\%}$ (Gy) | Bladder $D_{2cm^3}$ (Gy) | Small bowel $D_{2cm^3}$ (Gy) | Rectum $D_{2cm^3}$ (Gy) | Sigmoid $D_{2cm^3}$ (Gy) |
|---|---|---|---|---|---|---|
| | **Plan 1** | | | | | |
| **IHDM** | 7.98 | 3.37 | 6.77 | 6.12 | 2.13 | 1.92 |
| **Oncentra TPS (IPSA)** | 8.01 | 3.20 | 5.95 | 6.81 | 1.50 | 1.63 |
| | **Plan 2** | | | | | |
| **IHDM** | 8.04 | 3.10 | 4.96 | 8.34 | 5.43 | 4.32 |
| **Oncentra TPS (IPSA)** | 7.99 | 2.60 | 4.14 | 7.81 | 4.88 | 5.42 |
| | **Plan 3** | | | | | |
| **IHDM** | 8.02 | 3.09 | 6.63 | 5.58 | 5.40 | 2.91 |
| **Oncentra TPS (IPSA)** | 7.99 | 2.81 | 5.91 | 6.32 | 4.32 | 3.07 |

Differences were expected as the two systems may interpret weights applied to structures differently during the optimisation process as mathematical algorithms differ from optimiser to optimiser.

## 4.2 Treatment planning

### 4.2.1 Reporting of organ and organ wall doses

Although it is widely accepted that organs with contents and organ walls give similar dose metrics irrespective of the contouring method, this assumption might not be applicable when other dose metrics such as the Equivalent Uniform dose (EUD) is used. When comparing the dose-volume metrics for various OARS for the IHDM and Oncentra, all the different executed planning approaches used in this study led to the same $D_{2cm^3}$ and $D_{0.1cm^3}$ values, irrespective of the dose calculation being in the organ or the organ wall. The largest percentage difference between the bladder and bladder wall $D_{2cm^3}$ and $D_{0.1cm^3}$ values were 0.47 % and 0.00 %, respectively. The difference between the rectum and rectum wall $D_{2cm^3}$ and $D_{0.1cm^3}$ values were as low as 0.15 % and 0.06 %, respectively. This is in accordance with the study by Wachter-Gerstner et al.[174] The sigmoid and sigmoid wall $D_{2cm^3}$ and $D_{0.1cm^3}$ differences were 0.59 % and 0.00 %, respectively. Differences were bigger between the organ and

[174] (Wachter-Gerstner *et al.*, 2003)

organ wall considering the $D_{5cm}^3$ values. Differences between the organ and wall of 1.62 %, 0.73 % and 1.27 % were recorded for the bladder, rectum and sigmoid $D_{5cm}^3$ values, respectively.

The same cannot be said about the organ plus content and the organ wall EUDs. Higher organ wall EUD's were consistently calculated in all the patients compared to the organ EUD. The correct method to use EUD dose computation would therefore be to use the organ wall without content as dose in urine or faeces is not dose in the organ. This is also applicable to larger volume dose metrics such as $D_{5cm}^3$ and $D_{10cm}^3$ values. The bladder wall EUD was reported to be up to 2.27 % higher than the bladder EUD itself. The rectum and sigmoid wall EUD were reported to be up to 0.59 % and 0.48 % higher than the rectum and sigmoid EUD itself. Therefore, in this study, only the organ wall doses and EUD's will be reported and discussed.

As mentioned in Section 3.6, to verify the significant differences between the approaches, statistical analysis was performed and compared. Results that presented a statistical significance, $p \leq 0.05$ will be noted and discussed; otherwise, it can be assumed that there were no significant differences.

### 4.2.2 Intracavitary Image-Guided Adaptive Brachytherapy (IGABT) Treatment planning

Intracavitary IGABT treatment planning and optimisation were performed on all eighteen patients. A total of 720 plans were optimised and evaluated. During the optimisation process, priority was given to the hard constraint of the CTV-$T_{HR}$ and subsequently, the hard constraints for all OARs. When hard constraints for targets and OARs were realised, the priorities were, to aim for approaching/reaching the soft constraints for CTV-$T_{HR}$ and thereafter approaching/reaching soft constraints for OARs and CTV-$T_{IR}$. However, if the soft constraint of the CTV-T volumes were reached, but the OAR soft constraint was still not reached, the dose in the CTV-$T_{HR}$ volume was increased up to a maximum of 105 Gy. The local control at 95 Gy and the local control at the given dose > 95 Gy will be evaluated per patient to establish if the dose given beyond 95 Gy will lead to an additional increase in local control.

Before planning and optimisation commenced, a standard plan was created for each patient on the Oncentra TPS. This information was imported into the IHDM, corresponding dose-volume histograms were plotted, and EUD and dose-volume parameters were automatically calculated and displayed for all the CTV-T and OAR volumes. At the onset of optimisation, each OAR volume had an idea what the dose contribution towards their respective $D_{2cm}^3$ and EUD values were, this facilitated the optimisation process. Figure 26, displays an example of the dose-volume histogram, displaying all the automatically calculated EUD and dose-volume parameters for all CTV-T and OAR volumes.

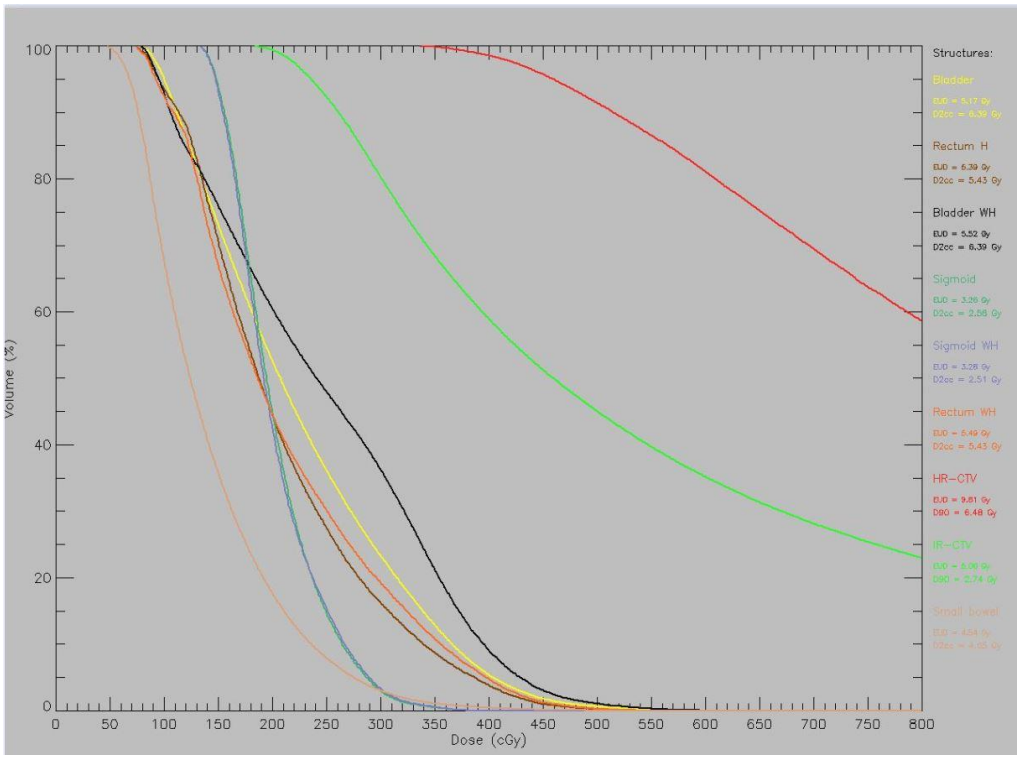


**Figure 26 - Example of the dose-volume histogram displaying all EUD and dose-volume parameters for all CTV-T and OAR volumes.**

The interface of the IHDM is displayed in Figure 27. From this, you can see the variety of tools that were developed. The user had the ability to visualise the CT data with the correlating dose distributions in three different planes, by using the “slice select” tool.

The user had the ability to perform forward optimisation with manual dwell time adjustments of all the sources by using the “Dwell time adjustments” tool. After necessary adjustments were made, the “Apply new dwell times” button were used to display the new dose distribution, plot all corresponding DVH’s and automatically re-calculate and display all dose parameters (conventional and biological).

The user had the option to perform a variety of inverse optimisation techniques. The weights assigned to the different structures could be individually increased or decreased throughout the inverse optimisation processes.

The “Add needles” tools gave the user the ability to add an interstitial needle to the existing intracavitary source configuration to perform IC/IS planning and optimisation. Dwell times of needles

were manually adjusted, or the four different inverse optimisation techniques could be applied by a push of a button to include the needle sources into the inverse optimisation process.

For all optimisation techniques, the IHDM automatically calculated and displayed the allowed fractional dose constraints which where dependent on which fraction compensation approach were utilised.

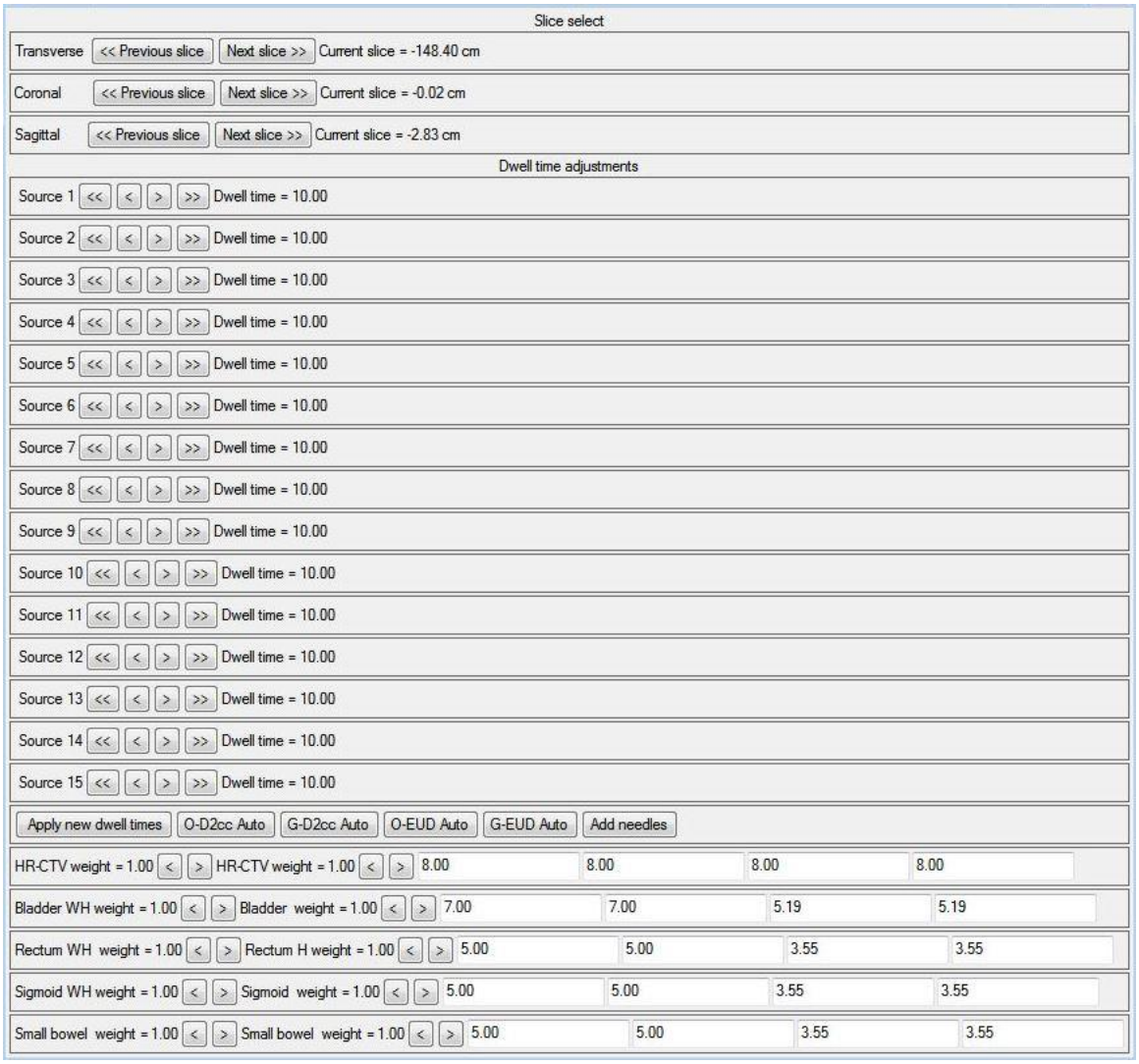


**Figure 27 - Interface of the IHDM displaying the variety of tools available.**

## a) Forward planning and optimisation

The forward planning and optimisation tool as described in Section 3.3.4, was used. Forward planning and optimisation were performed on all eighteen patients, which resulted in a total of 360 Intracavitary IGABT forward optimised plans. The 360 plans consisted of 90 conventional optimistic plans, 90 conventional greedy plans, 90 biological optimistic plans and 90 biological greedy plans.

### a.1) Forward Conventional Optimistic (FCO) vs Forward Conventional Greedy (FCG)

A total of 180 Forward Conventional plans were optimised and planned. During the Forward Conventional Optimistic (FCO) and Forward Conventional Greedy (FCG) approach, the total OAR conventional constraints listed in Table 2 were used as the limiting dose constraints during the optimisation and planning process. Corresponding OAR biological parameters obtained during the conventional optimisation process were only noted and were not incorporated as limiting parameters. The fractional OAR dose constraint was automatically calculated and displayed by the IHDM by using Equation (39) and (40) for the FCO and FCG approach, respectively. The displayed fractional OAR constraints were used and applied during the forward planning approaches.

Table 9 provides the average CTV-$T_{HR}$ and CTV-$T_{IR}$ $D_{90\,\%}$, $D_{98\,\%}$ and $D_{100\,\%}$ values obtained for the Forward Conventional Optimistic (FCO) and Forward Conventional Greedy (FCG) approach.

**Table 9 - Average CTV-T $D_{90\,\%}$, $D_{98\,\%}$ and $D_{100\,\%}$ values for the FCO and FCG approach**

| Approach | CTV-$T_{HR}$ $D_{90\,\%}$ (Gy) | CTV-$T_{HR}$ $D_{98\,\%}$ (Gy) | CTV-$T_{HR}$ $D_{100\,\%}$ (Gy) | CTV-$T_{IR}$ $D_{90\,\%}$ (Gy) | CTV-$T_{IR}$ $D_{98\,\%}$ (Gy) | CTV-$T_{IR}$ $D_{100\,\%}$ (Gy) |
|---|---|---|---|---|---|---|
| **FCO** | 91.50 ± 2.70 | 80.39 ± 2.86 | 73.23 ± 3.23 | 65.90 ± 2.34 | 62.38 ± 2.06 | 60.23 ± 1.86 |
| **FCG** | 91.50 ± 2.71 | 80.41 ± 2.87 | 73.24 ± 3.24 | 65.90 ± 2.23 | 62.38 ± 2.06 | 60.22 ± 1.86 |

The difference in CTV-T values between the FCO and FCG approach was negligible (see

Table 9), considering the patient population as a whole. However, the differences between the two approaches were also evaluated per patient. Figure 28 displays the results for the FCO and FCG approach that was obtained per patient.

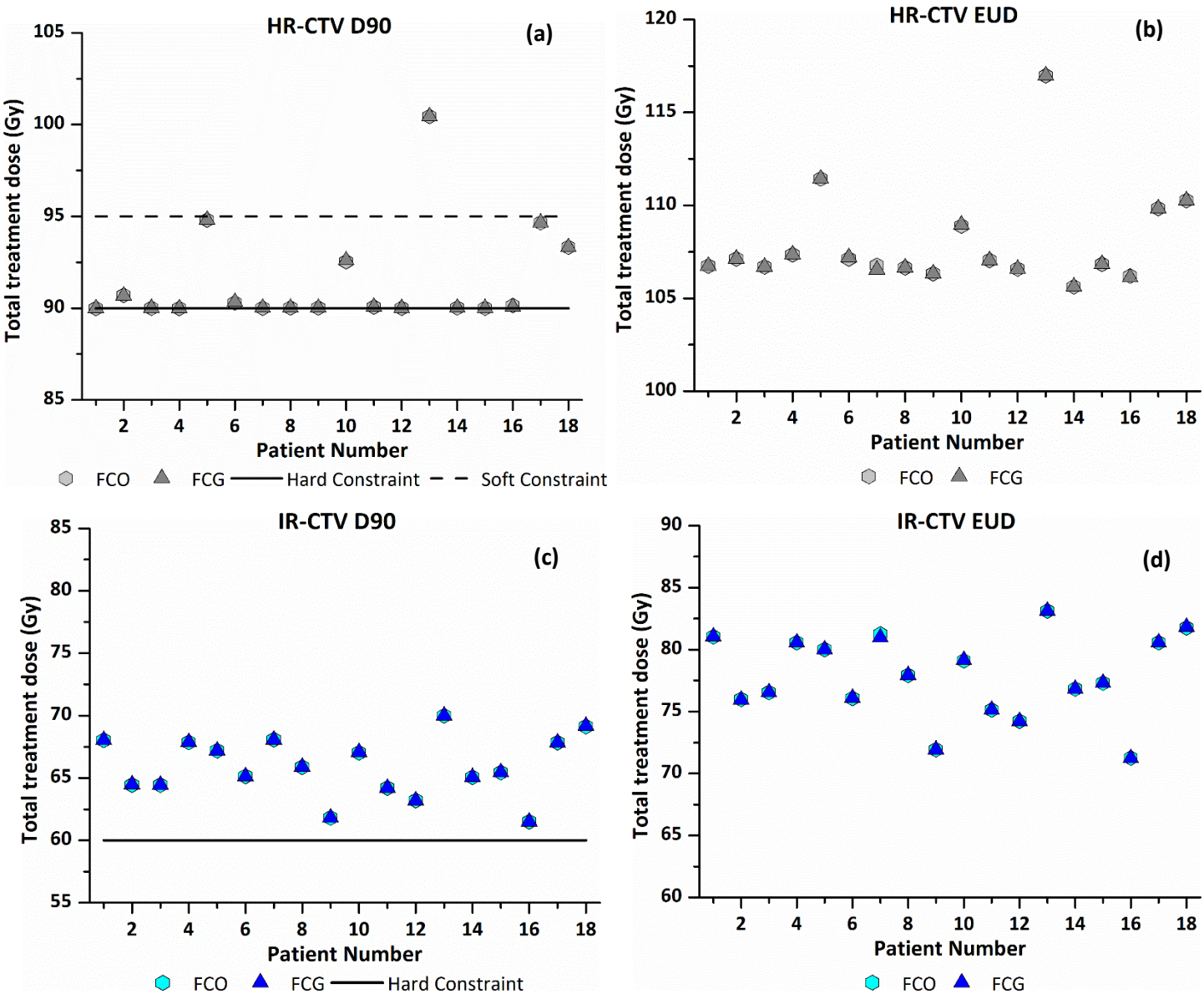


**Figure 28 – Comparison between the FCO and FCG approach per patient. CTV-T HR (a) $D_{90\,\%}$ and (b) EUD, CTV-T IR (c) $D_{90\,\%}$ and (d) EUD. Note: Data points for the FCO and FCG approach are indicated by hexagons and triangles, respectively.**

The solid and dotted lines in Figure 28 and all the CTV-T Figures in the rest of the chapter represent the intended conventional planning aims for the CTV-T volumes in the form of hard and soft constraints as summarised in Table 1 [175]. No significant differences can be observed for both the CTV-$T_{HR}$ and CTV-$T_{IR}$ $D_{90\,\%}$ and EUD values, as seen in Figure 28. The CTV-$T_{HR}$ $D_{90\,\%}$ hard constraint of 90 Gy was given priority and was reached in all the patients. In both approaches, the $D_{90\,\%}$ hard constraint of 60 Gy for the CTV-$T_{IR}$ was reached for all the patients without difficulty. The outcome of the FCO and FCG approach, when assessing the average CTV-T EUD values, were comparable. Average CTV-$T_{HR}$ and

[175] (Shaw, Rae and Alber, 2013; Tanderup et al., 2020)

CTV-$T_{IR}$ EUD values were reported as 108.02 ± 2.65 Gy and 77.81 ± 3.29 Gy for the FCO approach and 108.02 ± 2.66 Gy and 77.80 ± 3.28 Gy for the FCG approach, respectively.

Eight patients received an average CTV-$T_{HR}$ $D_{90\,\%}$ value greater than the set $D_{90\,\%}$ hard constraint of 90 Gy. The $D_{90\,\%}$ soft constraint was surpassed in one patient, Patient 13, with a $D_{90\,\%}$ value of 100.45 Gy without violating any OAR wall $D_{2cm^3}$ constraints, just reaching the small bowel $D_{2cm^3}$ soft constraint (Figure 29). Even though the OAR EUD values were not incorporated as dose-limiting parameters during the FCO and FCG optimisation process, the EUD values were still recorded and evaluated. When evaluating the EUD values of patient 13, it was noticed that the bladder wall EUD hard constraint of 75.95 Gy was reached, while the rectum wall and small bowel EUD hard constraints of 67.75 Gy were both violated (Figure 30). Two patients, Patient 5 and 17, nearly reached the 95 Gy soft constraint with $D_{90\,\%}$ values of 94.80 Gy and 94.65 Gy, respectively. Patient 5 were limited by the $D_{2cm^3}$ of the bladder wall and small bowel, while patient 17 was only restricted by the $D_{2cm^3}$ of the bladder wall (Figure 29). Again, the sigmoid wall EUD of 67.75 Gy was reached in patient 5, and the bladder wall EUD hard constraint was violated in patient 5 and 17 (Figure 30).

Even though patient 13 reached a dose of 100.45 Gy without violating any OAR dose constraints, it has been reported that a CTV-$T_{HR}$ $D_{90\,\%} \geq 85$ Gy and a CTV-$T_{HR}$ size of 29 $cm^3$ already result in a 3-year local control rate > 93 %. Exceptional local control of 96 % has been reported at 95 Gy, with this said it does not seem relevant to further dose escalate beyond 95 Gy, in this case, as it would not translate to higher local control [176].

The $D_{90\,\%}$ hard constraint of the CTV-$T_{HR}$ was also exceeded by five other patients, namely patients 2, 6, 10, 16 and 18. Table 10 below displays the corresponding $D_{2cm^3}$ and $D_{0.1cm^3}$ values for all the OAR walls as well as the recto-vaginal reference point values of the FCO and FCG approach across the whole population.

[176] (Pötter *et al.*, 2018)

**Table 10 - Average $D_{2cm^3}$ and $D_{0.1cm^3}$ values for all OAR walls and the recto-vaginal reference point of the FCO and FCG approach, respectively.**

| | Bladder wall | Small bowel | Rectum wall | Sigmoid wall | Recto-vaginal |
|---|---|---|---|---|---|
| **Approach** | **$D_{2cm^3}$ (Gy) Average ± SD** | **$D_{2cm^3}$ (Gy) Average ± SD** | **$D_{2cm^3}$ (Gy) Average ± SD** | **$D_{2cm^3}$ (Gy) Average ± SD** | **Dose point (Gy) Average ± SD** |
| **FCO** | 78.66 ± 4.35 | 69.51 ± 8.50 | 62.24 ± 3.54 | 61.34 ± 4.74 | 64.50 ± 4.92 |
| **FCG** | 78.54 ± 4.23 | 69.44 ± 8.45 | 62.22 ± 3.53 | 61.36 ± 4.75 | 64.45 ± 4.79 |
| **Approach** | **$D_{0.1cm^3}$ (Gy) Average ± SD** | **$D_{0.1cm^3}$ (Gy) Average ± SD** | **$D_{0.1cm^3}$ (Gy) Average ± SD** | **$D_{0.1cm^3}$ (Gy) Average ± SD** | **-** |
| **FCO** | 99.99 ± 8.32 | 82.85 ± 15.09 | 82.85 ± 15.09 | 70.43 ± 9.87 | - |
| **FCG** | 99.61 ± 8.07 | 82.68 ± 14.97 | 82.68 ± 14.97 | 70.47 ± 9.89 | - |

From these results, the difference in average $D_{2cm^3}$ and $D_{0.1cm^3}$ values for all the OAR volumes considering the FCO and FCG approach is so small it is negligible. The difference between the FCO and FCG approach was once more evaluated per patient, in more detail. Figure 29 and Figure 30 displays the OAR dose results per patient that were obtained for the FCO and FCG approach.

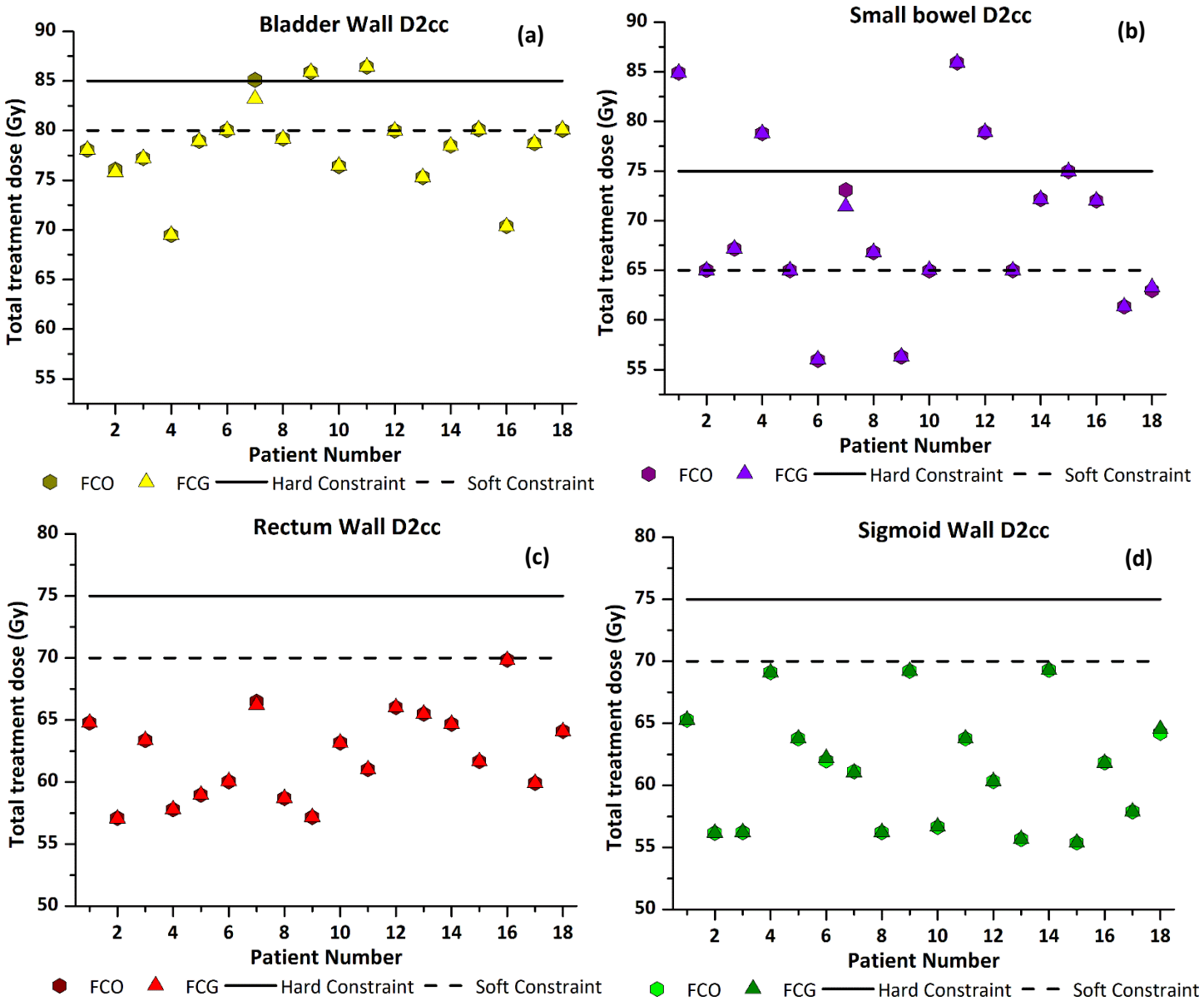


**Figure 29 - Comparison between the FCO and FCG approach per patient. The $D_{2cm^3}$ values for (a) bladder wall, (b) small bowel, (c) rectum wall and (d) sigmoid wall. Note: Data points for the FCO and FCG approach are indicated by hexagons and triangles, respectively.**

The solid and dotted lines in Figure 29 and all the other $D_{2cm^3}$ OAR Figures in the rest of the chapter, represent the intended conventional planning aims for all the OAR volumes in the form of hard and soft constraints as summarised in Table 2 [177]. As illustrated in Figure 29, the $D_{2cm^3}$ hard constraint of the bladder wall was violated in three patients for the FCO approach with an average value of 78.66 ± 4.35 Gy, while only two patients' $D_{2cm^3}$ hard constraint was violated by the FCG approach, with an average value of 78.54 ± 4.23 Gy. In an attempt to reach the CTV-$T_{HR}$ hard constraint of 90 Gy, the bladder wall $D_{2cm^3}$ soft constraint was violated in seven patients, for both approaches. The average

[177] (Shaw, Rae and Alber, 2013; Tanderup et al., 2020)

small bowel $D_{2cm}^3$ were 69.51 ± 8.50 Gy and 69.44 ± 8.45 Gy for the FCO and FCG approach, respectively, while the $D_{2cm}^3$ hard constraint of the small bowel was violated in five patients, for both approaches. The $D_{2cm}^3$ soft constraint of the small bowel was reached/violated in fourteen patients. The $D_{2cm}^3$ hard constraint of the rectum wall was not violated in any of the eighteen patients. The average $D_{2cm}^3$ values of 62.24 ± 3.54 Gy and 62.22 ± 3.53 Gy were reported for the FCO and FCG approach, respectively. The $D_{2cm}^3$ soft constraint of the rectum wall was reached in one patient for both the approaches. Neither the $D_{2cm}^3$ hard or soft constraint of the sigmoid wall was reached and average $D_{2cm}^3$ values of 61.34 ± 4.74 Gy, and 61.36 ± 4.75 Gy were recorded for the FCO and FCG approach, respectively. The results displayed in Figure 29 clearly show that the bladder wall and small bowel are the two most limiting OAR's in both the FCO and FCG approach. Rectum and sigmoid wall constraints were never reached without one or both bladder wall and small bowel constraints reached.

From the results shown in Figure 29, the FCO and FCG display similar outcome, except in the case of patient 7. Patient 7 was the only patient that displayed a significant difference between the FCO and FCG approach. Both the approaches reached the same CTV-$T_{HR}$ $D_{90\,\%}$ value of 90 Gy. The total $D_{2cm}^3$ for the bladder wall for this patient was recorded as 85.11 Gy and 83.23 Gy, respectively. The total $D_{2cm}^3$ for the small bowel was recorded as 73.09 Gy and 71.41 Gy for the FCO and FCG approach, respectively. For this specific patient, the FCG approach led to a difference in $D_{2cm}^3$ values of 2.26 % for the bladder wall and 2.35 % for the small bowel, respectively. The FCG approach recorded a 5.37 Gy and 3.88 Gy lower bladder wall and small bowel $D_{0.1cm}^3$ compared to the FCO approach. The difference in the total $D_{2cm}^3$ values for the rectum and sigmoid wall for this patient were negligible. The reason for this difference in patient 7, the FCG approach allowed for a higher small bowel and bladder wall fractional dose limit in fraction 2, which led to an exploitation of the CTV-$T_{HR}$ dose. The FCG approach was able to give a higher dose to the CTV-$T_{HR}$ compared to the FCO approach. This allowed some sparing of the small bowel and bladder wall in the remainder of the fractions. In the case of the FCO approach, small bowel and bladder wall limits were violated in the remainder of fractions to be able to reach the CTV-$T_{HR}$ dose. This is the reason why patient 7 benefitted more from the FCG approach compared to the FCO approach.

The corresponding EUD values that were recorded for all the OAR are visualised in Figure 30. The solid lines in Figure 30 and all the other EUD OAR Figures in the rest of the chapter, represent the intended biological planning aims for all the OAR volumes in the form of hard constraints as summarised in Table 3 [178].

[178] (Shaw, Rae and Alber, 2013)

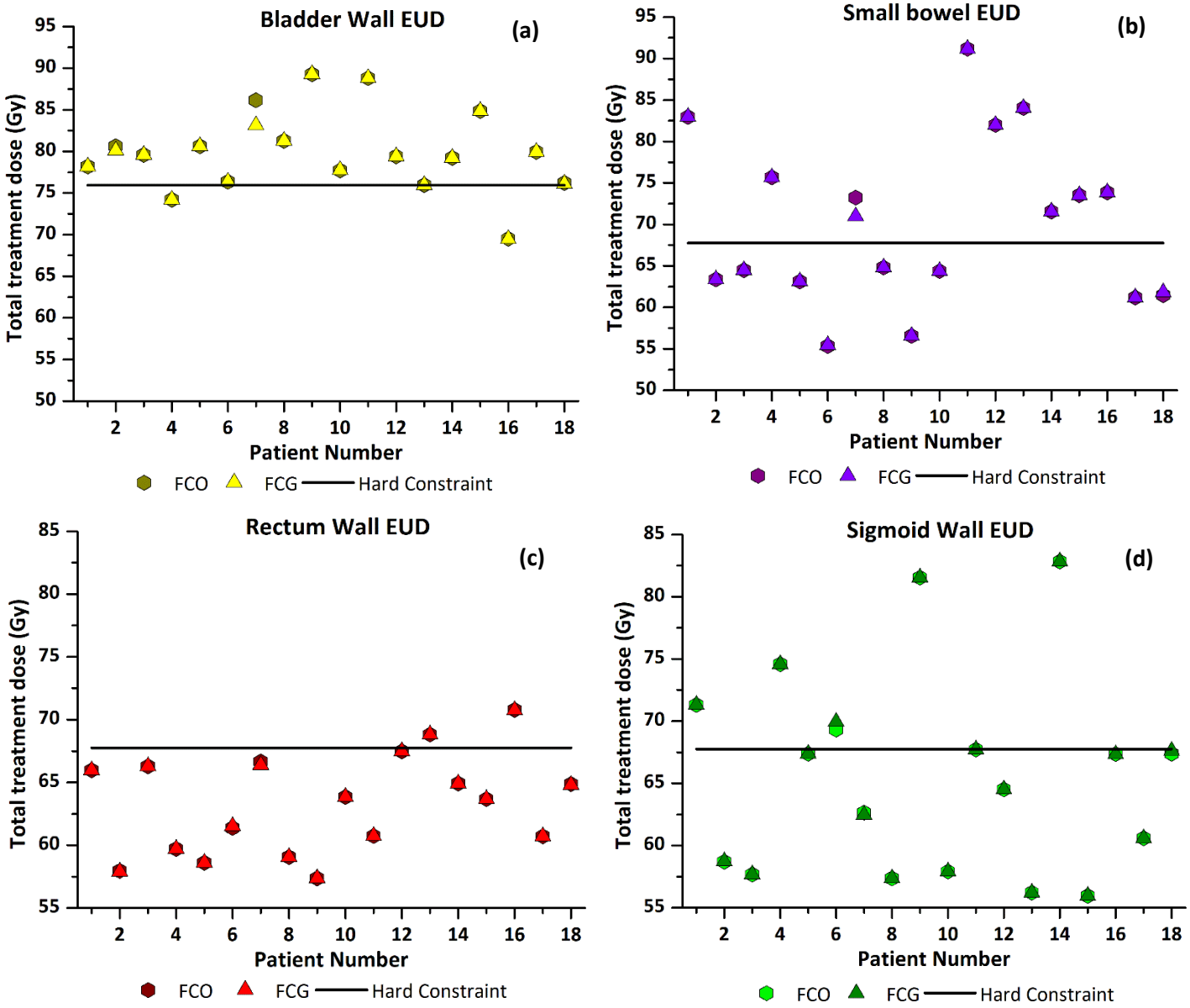


**Figure 30 - Comparison between the FCO and FCG approach per patient. The EUD values for (a) bladder wall, (b) small bowel, (c) rectum wall and (d) sigmoid wall. Note: Data points for the FCO and FCG approach are indicated by hexagons and triangles, respectively.**

As seen in Figure 30, the EUD hard constraint of the bladder wall was violated in sixteen patients, with average values of 79.88 ± 4.85 Gy and 79.68 ± 4.69 Gy for the FCO and FCG approach, respectively. The EUD hard constraint of the small bowel was violated in nine patients, with average values of 70.15 ± 9.87 Gy and 70.05 ± 9.82 Gy for the FCO and FCG approach, respectively. The average reported small bowel values were higher than the EUD hard constraint of 67.75 Gy. The EUD hard constraint of the rectum wall, 67.75 Gy, was reached in one patient and violated in two patients, with average values of 63.27 ± 3.88 Gy and 63.25 Gy ± 3.86 Gy for the FCO and FCG approach, respectively. The EUD hard constraint of the sigmoid wall was reached in four patients and violated in 5 patients, with average values of 65.61 ± 7.98 Gy and 65.65 ± 8.00 Gy for the FCO and FCG approach, respectively. Patient 6 had the most significant difference in sigmoid wall EUD among the whole patient population, with the FCO approach recording a value of 69.32 Gy and the FCG approach a value of 69.94 Gy. Even though

this patient represents the patient with the biggest sigmoid wall EUD difference between the two approaches, the difference is still very small and therefore, negligible.

As displayed in Figure 30, again, the only patient with a significant difference between the FCO and FCG approach was patient 7. The total EUD for the bladder wall were recorded as 86.14 Gy and 83.15 Gy, while the total EUD for the small bowel was recorded as 73.24 Gy and 70.98 Gy for the FCO and FCG approach, respectively. For this specific patient, the FCG approach led to a difference in EUD values of 3.60 % for the bladder wall and 3.18 % for the small bowel, respectively. The reason for the differences in EUD values is similar to the recorded $D_{2cm^3}$ values for this patient stated above. The difference in the total EUD for the rectum and sigmoid wall values for this patient was negligible, while the CTV-$T_{HR}$ dose recorded was as stated previously, 90 Gy for both approaches. When considering the obtained conventional and biological doses for all the OAR and CTV-T volumes for this patient, it can be concluded that patient 7 greatly benefitted from the FCG approach.

**Other parameters that were recorded:**

As summarised in Table 11, the average dose to point $A_{Left}$ and $A_{Right}$ for both the FCO and FCG approach had minimal differences. The dose to point $A_{Left}$ and $A_{Right}$ was not set as a limiting parameter in the optimisation processes, these values were only reported and evaluated retrospectively. This applies to the rest of the reported point A values in this chapter. The average dose to point $A_{Left}$ and $A_{Right}$ was higher than the proposed > 65 Gy soft constraint [179].

No significant difference was recorded between the FCO and FCG average TRAK values. Recorded TRAK values for the FCO and FCG approach were lower than the average TRAK value of 1.74 cGy at 1 m published by Bockel et al [180].

**Table 11 - Average dose to point A and TRAK values of FCO and FCG approach**

| Approach | $A_{Left}$ (Gy) | $A_{Right}$ (Gy) | TRAK (cGy at 1 m) |
|---|---|---|---|
| **FCO** | 76.97 ± 8.27 | 77.26 ± 10.19 | 1.59 ± 0.25 |
| **FCG** | 77.02 ± 8.32 | 77.20 ± 10.23 | 1.58 ± 0.25 |

If the patient population is evaluated as a whole, the difference between FCO and FCG approach is almost negligible. However, when the impact of the approaches is evaluated based on individual response, some patients do benefit more from the FCG approach; for instance, patient 7. When

[179] (Tanderup *et al.*, 2020)
[180] (Bockel et al., 2019)

considering the evaluation, the FCG approach can be proposed to be always used instead of the FCO approach.

### a.2) Forward Biological Optimistic (FBO) vs Forward Biological Greedy (FBG)

A total of 180 Forward Biological plans were optimised and planned. During the Forward Biological Optimistic (FBO) and Forward Biological Greedy (FBG) approach, the total OAR biological constraints listed in Table 3 were used as the limiting dose constraints during the optimisation and planning process. Corresponding OAR conventional parameters obtained during the biological optimisation process were only noted and were not incorporated as limiting parameters. The fractional OAR dose constraint was automatically calculated and applied by the IHDM by using Equation (39) and (40) for the FBO and FBG approach, respectively.

Table 12 provides the average CTV-$T_{HR}$ and CTV-$T_{IR}$ $D_{90\,\%}$ $D_{98\,\%}$ and $D_{100\,\%}$ values obtained for the Forward Biological Optimistic (FBO) approach versus the Forward Biological Greedy (FBG) approach.

**Table 12 - Average CTV-T $D_{90\,\%}$ $D_{98\,\%}$ and $D_{100\,\%}$ values for the FBO and FBG approach**

| Approach | CTV-$T_{HR}$ $D_{90\,\%}$ (Gy) | CTV-$T_{HR}$ $D_{98\,\%}$ (Gy) | CTV-$T_{HR}$ $D_{100\,\%}$ (Gy) | CTV-$T_{IR}$ $D_{90\,\%}$ (Gy) | CTV-$T_{IR}$ $D_{98\,\%}$ (Gy) | CTV-$T_{IR}$ $D_{100\,\%}$ (Gy) |
|---|---|---|---|---|---|---|
| **FBO** | 91.96 ± 2.97 | 81.04 ± 3.48 | 73.75 ± 3.63 | 66.25 ± 2.47 | 62.69 ± 2.24 | 60.49 ± 1.96 |
| **FBG** | 91.77 ± 2.91 | 80.90 ± 3.38 | 73.59 ± 3.51 | 66.20 ± 2.42 | 62.63 ± 2.19 | 60.43 ± 1.91 |

Average CTV-$T_{HR}$ and CTV-$T_{IR}$ doses over the whole patient population were the same for the FBO and FBG approach as summarised in Table 12. The results per patient were depicted in Figure 31 to Figure 33.

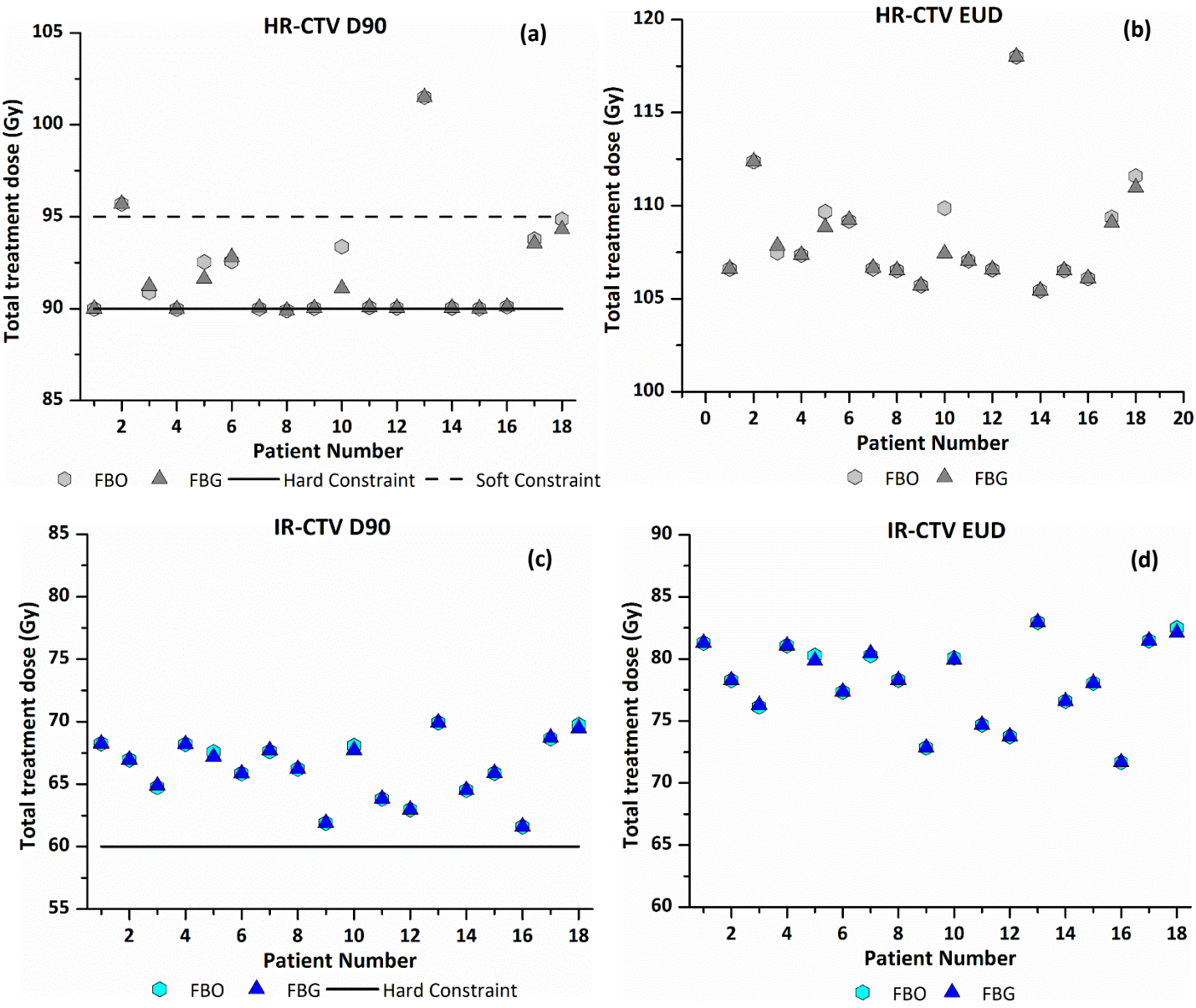


**Figure 31 - Comparison between the FBO and FBG approach per patient. CTV-T HR (a) $D_{90\,\%}$ and (b) EUD, CTV-T IR (c) $D_{90\,\%}$ and (d) EUD. Note: Data points for the FBO and FBG approach are indicated by hexagons and triangles, respectively.**

From Figure 31, it was found that only one patient recorded a significant higher CTV-$T_{HR}$ EUD with the FBO approach compared to the FBG approach, patient 10 recorded a 2.43 Gy difference between the FBO and FBG approach. The average CTV-$T_{HR}$ EUD values reported were similar for the FBO approach and FBG approach, with values of 108.44 ± 3.03 Gy and 108.23 ± 2.96 Gy, respectively. When considering the CTV-$T_{IR}$ EUD values per patient for both approaches, no significant difference was reported. Therefore, the FBO and FBG approach reported similar average CTV-$T_{IR}$ EUD values of 78.19 ± 3.27 Gy and 78.16 ± 3.23 Gy, respectively.

The $D_{90\,\%}$ hard constraint of the CTV-$T_{HR}$ was once again reached in all the patients. The $D_{90\,\%}$ hard constraint of the CTV-$T_{IR}$ was reached for both approaches in all the patients without any difficulty. Eight patients received an average $D_{90\,\%}$ value greater than the set $D_{90\,\%}$ hard constraint of 90 Gy. Two patients reached the 95 Gy soft constraint, patient 2 and 13, with $D_{90\,\%}$ values of 95.69 Gy and 100.45 Gy, respectively for both the approaches. Patient 2 and 13 reached the CTV-$T_{HR}$ soft constraint of 95 Gy without violating any of their OAR wall EUD constraints, just reaching the bladder wall EUD constraint for patient 2 and the small bowel EUD constraint for patient 13 (Figure 32). Even though the OAR $D_{2cm^3}$ values were not incorporated as dose-limiting parameters during the FBO and FBG optimisation process, the $D_{2cm^3}$ values were still recorded and evaluated. However, from the $D_{2cm^3}$ values for patient 2 and 13 that were recorded, the small bowel $D_{2cm^3}$ soft constraint was violated (Figure 33). Six other patients exceeded the $D_{90\,\%}$ hard constraint of the CTV-$T_{HR}$, namely patients 3, 5, 6, 10, 17 and 18, without violating any of their OAR EUD and $D_{2cm^3}$ hard constraints, however violating/reaching some of their $D_{2cm^3}$ soft constraints.

Table 13 displays the corresponding $D_{2cm^3}$ and $D_{0.1cm^3}$ values for all the OAR walls, as well as the recto-vaginal reference point values of the FBO and FBG approach across the whole population.

**Table 13 - Average $D_{2cm^3}$ and $D_{0.1cm^3}$ values for all OAR walls of the FBO and FBG approach**

| | **Bladder wall** | **Small bowel** | **Rectum wall** | **Sigmoid wall** | **Recto-vaginal** |
|---|---|---|---|---|---|
| **Approach** | **$D_{2cm^3}$ (Gy) Average ± SD** | **$D_{2cm^3}$ (Gy) Average ± SD** | **$D_{2cm^3}$ (Gy) Average ± SD** | **$D_{2cm^3}$ (Gy) Average ± SD** | **Dose point (Gy) Average ± SD** |
| **FBO** | 78.05 ± 4.22 | 69.84 ± 7.91 | 62.61 ± 3.27 | 61.42 ± 4.50 | 65.05 ± 4.06 |
| **FBG** | 78.10 ± 4.23 | 69.81 ± 7.88 | 62.64 ± 3.29 | 61.42 ± 4.48 | 65.11 ± 4.12 |
| **Approach** | **$D_{0.1cm^3}$ (Gy)** | **$D_{0.1cm^3}$ (Gy)** | **$D_{0.1cm^3}$ (Gy)** | **$D_{0.1cm^3}$ (Gy)** | **-** |
| **FBO** | 97.07 ± 7.33 | 82.43 ± 13.45 | 69.15 ± 4.93 | 70.12 ± 8.76 | - |
| **FBG** | 97.00 ± 7.36 | 82.29 ± 13.37 | 69.23 ± 4.93 | 70.12 ± 8.74 | - |

As displayed in Table 13, virtually no difference between the average $D_{2cm^3}$ and $D_{0.1cm^3}$ values for all the OAR volumes was recorded for the FBO and FBG approach. The OAR dose results per patient that were obtained for the FBO and FBG approach are displayed below in Figure 32 and Figure 33.

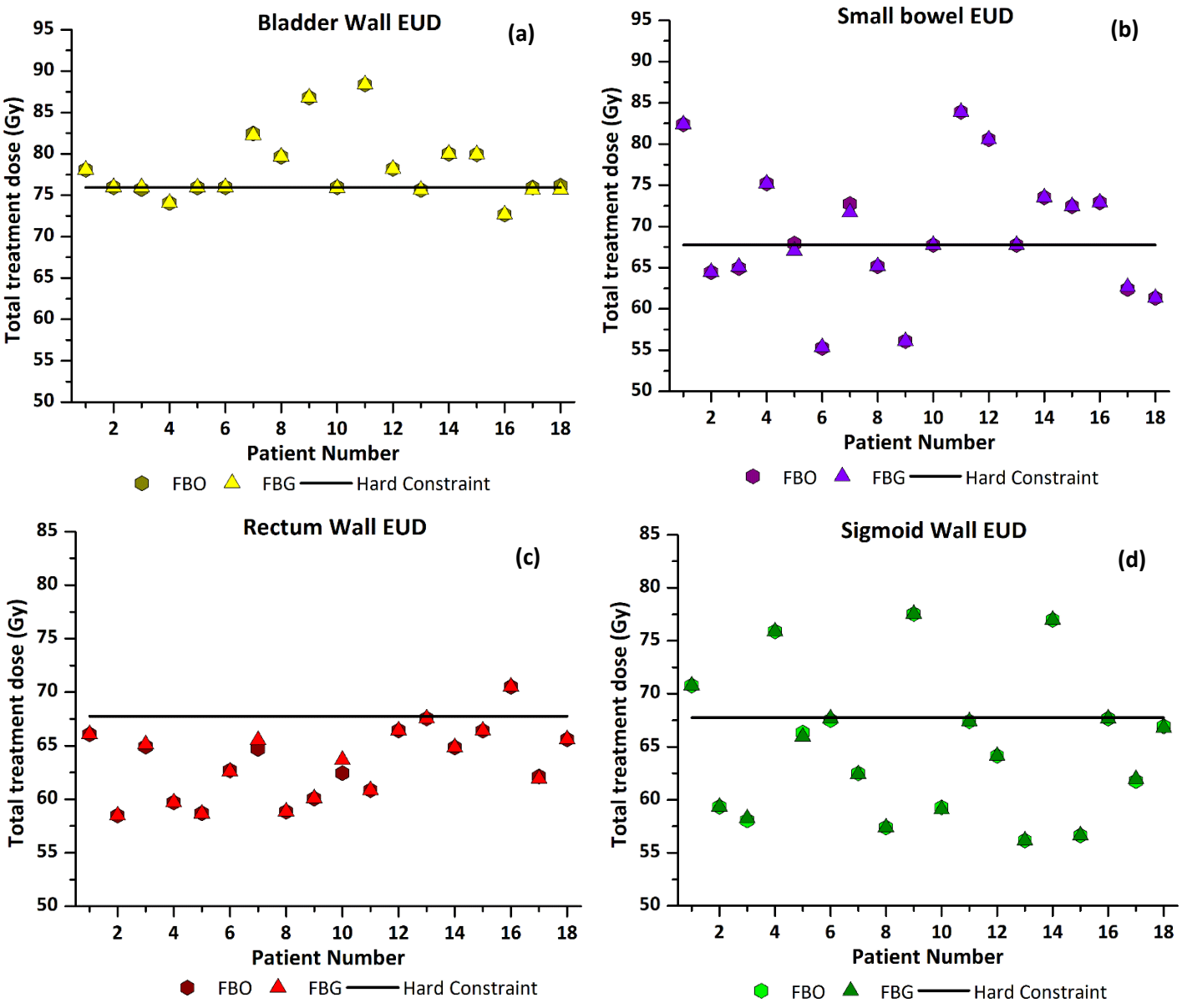


**Figure 32 - Comparison between the FBO and FBG approach per patient. The EUD values for (a) bladder wall, (b) small bowel, (c) rectum wall and (d) sigmoid wall. Note: Data points for the FBO and FBG approach are indicated by hexagons and triangles, respectively.**

As seen in Figure 32, the 75.95 Gy EUD hard constraint of the bladder wall was reached in 7 patients and violated in nine patients, with average values of 78.19 ± 4.04 Gy and 78.14 ± 4.05 Gy for the FBO and FBG approach, respectively. The EUD hard constraint of the small bowel was reached in three patients and violated in eight patients, with average values of 69.26 ± 7.99 Gy and 69.18 ± 7.88 Gy for the FBO and FBG approach, respectively. The EUD hard constraint of the rectum wall was reached in one patient and violated in one patient with average values of 63.38 ± 3.38 Gy and 63.48 ± 3.41 Gy for the FBO and FBG approach, respectively. The EUD hard constraint of the sigmoid wall, 67.75 Gy, was reached in three patients and violated in four patients, with average values of 65.12 ± 6.72 Gy and 65.11 ± 6.71 Gy for the FBO and FBG approach, respectively. The violation of OAR EUD hard constraints

occurred in patients because priority was given to the CTV-$T_{HR}$ hard constraint of 90 Gy. These would then be patients that could potentially benefit from intracavitary/interstitial IGABT. The corresponding $D_{2cm^3}$ values recorded for the OAR's are visualised in Figure 33. There were 12 patients in which the bladder wall EUD constraint was reached/violated without the bladder wall $D_{2cm^3}$ soft constraint of 80 Gy of the same patient being reached.

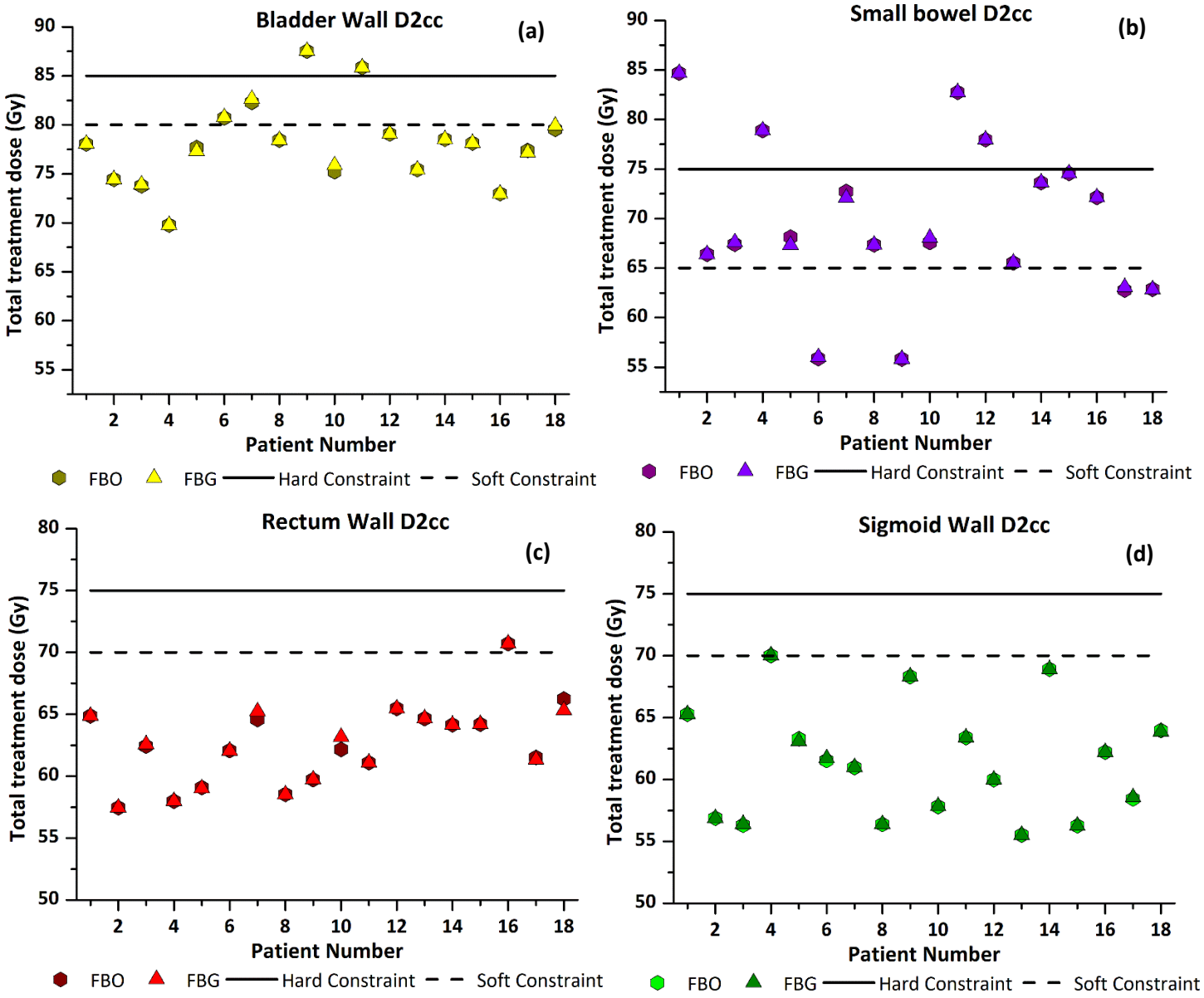


**Figure 33 - Comparison between the FBO and FBG approach per patient. The $D_{2cm^3}$ values for (a) bladder wall, (b) small bowel, (c) rectum wall and (d) sigmoid wall. Note: Data points for the FBO and FBG approach are indicated by hexagons and triangles, respectively.**

As seen in Figure 33, the $D_{2cm^3}$ hard constraint of the bladder wall was violated in two patients. The $D_{2cm^3}$ soft constraints were reached in one patient and violated in four patients. The average bladder wall $D_{2cm^3}$ were 78.05 ± 4.22 Gy and 78.10 ± 4.23 Gy for the FBO and FBG approach, respectively. The $D_{2cm^3}$ hard constraint of the small bowel was reached in one patient and violated in four patients. The

$D_{2cm}^3$ soft constraint of the small bowel was violated in fourteen patients. The average small bowel $D_{2cm}^3$ were 69.84 ± 7.91 Gy and 69.81 ± 7.88 Gy for the FBO and FBG approach, respectively. The $D_{2cm}^3$ hard constraint of the rectum wall was not reached nor violated. The $D_{2cm}^3$ soft constraint of the rectum wall was violated in one patient. The average rectum wall $D_{2cm}^3$ were 62.61 ± 3.29 Gy and 62.64 ± 3.27 Gy for the FBO and FBG approach, respectively. The $D_{2cm}^3$ hard constraint of the sigmoid wall was neither reached nor violated. The $D_{2cm}^3$ soft constraint of the sigmoid wall was reached in one patient. The average sigmoid wall $D_{2cm}^3$ were 61.42 ± 4.50 Gy and 61.42 ± 4.48 Gy for the FBO and FBG approach, respectively.

Considering Figure 31 to Figure 33, the only patients with some significant difference between the two approaches are patients 5, 7 and 10. The rest of the patient population showed no significant difference between the approaches.

The outcome in patient 5 for the two approaches was the same in all CTV-T and OAR parameters, except in the small bowel $D_{0.1cm}^3$ value, where the FBG approach led to a 1.70 Gy lower value compared to the FBO approach. The bladder wall and small bowel EUD hard constraints were reached in both approaches; however, reporting the same values. The sigmoid and rectum wall EUD hard constraints were not reached in any of the approaches; however, the same values were reported. None of the bladder, rectum and sigmoid wall $D_{2cm}^3$ constraints was reached, again the same values were reported. The small bowel $D_{2cm}^3$ soft constraint of 65 Gy was violated in both approaches.

In patient 7, the small bowel and bladder wall $D_{2cm}^3$ soft constraints and EUD hard constraints were violated in both approaches; the same values were reported in both OAR. The small bowel $D_{0.1cm}^3$ value was 1.76 Gy lower in the FBG approach. None of the rectum and sigmoid wall $D_{2cm}^3$ or EUD constraints were reached, again the same values were reported, but the rectum wall $D_{0.1cm}^3$ value was 1.15 Gy higher in the FBG approach. The rest of the CTV-T and OAR results showed no difference between the two approaches.

Patient 10 obtained higher CTV-$T_{HR}$ values for the FBO approach compared to the FBG approach, and the FBO approach led to 2.43 Gy, 2.27 Gy, 1.76 Gy and 1.56 Gy higher CTV-$T_{HR}$ EUD, $D_{90\,\%}$, $D_{98\,\%}$ and $D_{100\,\%}$ values, respectively. Not only did the FBO approach obtain higher CTV-$T_{HR}$ values but also allowed lower rectum wall EUD, $D_{2cm}^3$ and $D_{0.1cm}^3$ values of 1.24 Gy, 1.02 Gy and 1.72 Gy, respectively. The rest of the CTV-T and OAR results showed no difference between the two approaches. The FBO approach led to a higher CTV-$T_{HR}$ $D_{90\,\%}$ and lower OAR EUD and $D_{2cm}^3$ values, compared to the FBG approach.

Parameters like the CTV-$T_{HR}$ $D_{90\,\%}$ and $D_{98\,\%}$ and CTV-$T_{IR}$ $D_{98\,\%}$ have been proven to be associated with better local control (LC) [181]. The CTV-$T_{HR}$ volume size of the patient was classified between limited and intermediate size. According to published data, a tumour volume of 30 $cm^3$ and a CTV-$T_{HR}$ dose of 93.37 Gy recorded by the FBO approach, LC of more or less 94 % has been reported, and this is better LC compared to the 91.10 Gy dose reported by the FBG approach [182]. Considering both OAR and CTV-T values, the FBO approach led to a superior plan compared to the FCG approach.

**Other parameters that were recorded:**

The average dose to Point A (left and right) and TRAK values for the FBO and FBG approach are tabulated below in Table 14. The difference in average dose to point $A_{Left}$ and $A_{Right}$ in both FBO and FBG approach was minimal. No significant difference was recorded between the FBO and FBG average TRAK values.

**Table 14 - Average dose to point A and TRAK values of FBO and FBG approach**

| Approach | $A_{Left}$ (Gy) | $A_{Right}$ (Gy) | TRAK (cGy at 1 m) |
|---|---|---|---|
| **FBO** | 77.56 ± 8.51 | 75.80 ± 8.53 | 1.62 ± 0.23 |
| **FBG** | 77.24 ± 8.98 | 75.35 ± 8.91 | 1.62 ± 0.23 |

Considering the average dose to the CTV-T and OAR volumes over the whole patient population, the FBO and FBG approach outcome seem the same. In three patients, the FBO approach led to better plans compared to the FBG approach. In patient 5 and 7, the same CTV-T values and lower OAR dose in some of the OAR volumes were reported; however, differences were small. Therefore, if an individual scores lower OAR dose in the one approach, but all the CTV-T doses were the same in both approaches, then that approach could be advocated. In patient 10, however noteworthy higher CTV-$T_{HR}$ values and lower dose in some of the OAR volumes were recorded. Taking this into account, the FBO approach can be considered to be superior to the FBG approach.

[181] (Johannes C A Dimopoulos *et al.*, 2009; Mazeron *et al.*, 2015; Tanderup *et al.*, 2016)
[182] (Tanderup *et al.*, 2016)

### a.3) Forward Conventional Greedy (FCG) vs Forward Biological Optimistic (FBO)

The most preferred Forward Conventional (FC) approach and Forward Biological (FB) approach are compared with one another, the Forward Conventional Greedy (FCG) approach versus Forward Biological Optimistic (FBO) approach (discussed in sections a.1 and a.2).

Table 9 provides the average CTV-$T_{HR}$ and CTV-$T_{IR}$ $D_{90\,\%}$ $D_{98\,\%}$ and $D_{100\,\%}$ values obtained for the FCG and FBO approach.

**Table 15 - Average CTV-T $D_{90\,\%}$ $D_{98\,\%}$ and $D_{100\,\%}$ values for the FCG and FBO approach**

| Approach | CTV-$T_{HR}$ $D_{90\,\%}$ (Gy) | CTV-$T_{HR}$ $D_{98\,\%}$ (Gy) | CTV-$T_{HR}$ $D_{100\,\%}$ (Gy) | CTV-$T_{IR}$ $D_{90\,\%}$ (Gy) | CTV-$T_{IR}$ $D_{98\,\%}$ (Gy) | CTV-$T_{IR}$ $D_{100\,\%}$ (Gy) |
|---|---|---|---|---|---|---|
| **FCG** | 91.50 ± 2.71 | 80.41 ± 2.87 | 73.24 ± 3.24 | 65.90 ± 2.23* | 62.38 ± 2.06 | 60.22 ± 1.86 |
| **FBO** | 91.96 ± 2.97 | 81.04 ± 3.48 | 73.75 ± 3.63 | 66.25 ± 2.47* | 62.69 ± 2.24 | 60.49 ± 1.96 |

***Tested for the significant difference with a p-value ≤ 0.05.**

From the CTV-$T_{HR}$ and CTV-$T_{IR}$ results provided in Table 15, it can be concluded that the $D_{90\,\%}$ $D_{98\,\%}$ and $D_{100\,\%}$ parameters reported were similar for the FBO and FCG approach across the whole patient population. The FBO approach, however, produced a higher average CTV-$T_{IR}$ $D_{90\,\%}$ value compared to the FCG approach, which was of significant difference. Table 16 displays the average OAR $D_{2cm^3}$ and $D_{0.1cm^3}$ values reported for the FCG and FBO approach.

**Table 16 - Average $D_{2cm^3}$ and $D_{0.1cm^3}$ values for all OAR walls for the FCG and FBO approach**

| | Bladder wall | Small bowel | Rectum wall | Sigmoid wall | Recto-vaginal |
|---|---|---|---|---|---|
| **Approach** | $D_{2cm^3}$ (Gy) Average ± SD | $D_{2cm^3}$ (Gy) Average ± SD | $D_{2cm^3}$ (Gy) Average ± SD | $D_{2cm^3}$ (Gy) Average ± SD | Dose point (Gy) Average ± SD |
| **FCG** | 78.54 ± 4.23 | 69.44 ± 8.45 | 62.22 ± 3.53 | 61.36 ± 4.75 | 64.45 ± 4.79 |
| **FBO** | 78.05 ± 4.22 | 69.84 ± 7.91 | 62.61 ± 3.29 | 61.42 ± 4.50 | 65.05 ± 4.06 |
| **Approach** | $D_{0.1cm^3}$ (Gy) Average ± SD | $D_{0.1cm^3}$ (Gy) Average ± SD | $D_{0.1cm^3}$ (Gy) Average ± SD | $D_{0.1cm^3}$ (Gy) Average ± SD | - |
| **FCG** | 99.61 ± 8.07* | 82.68 ± 14.97 | 68.88 ± 5.52 | 70.47 ± 9.89 | - |
| **FBO** | 97.07 ± 7.33* | 82.43 ± 13.45 | 69.15 ± 4.93 | 70.12 ± 8.76 | - |

***Tested for the significant difference with a p-value ≤ 0.05.**

The difference in the average bladder wall $D_{0.1cm^3}$ values obtained by the FCG and FBO approach were of significant difference with a p-value ≤ 0.05. The FBO approach led to 2.55 % higher bladder wall $D_{0.1cm^3}$ values compared to the FCG approach. All other average $D_{2cm^3}$ and $D_{0.1cm^3}$ values for the OAR had no significant difference between the approaches. The difference between the two approaches was again evaluated per patient, in Figure 34 through Figure 36.

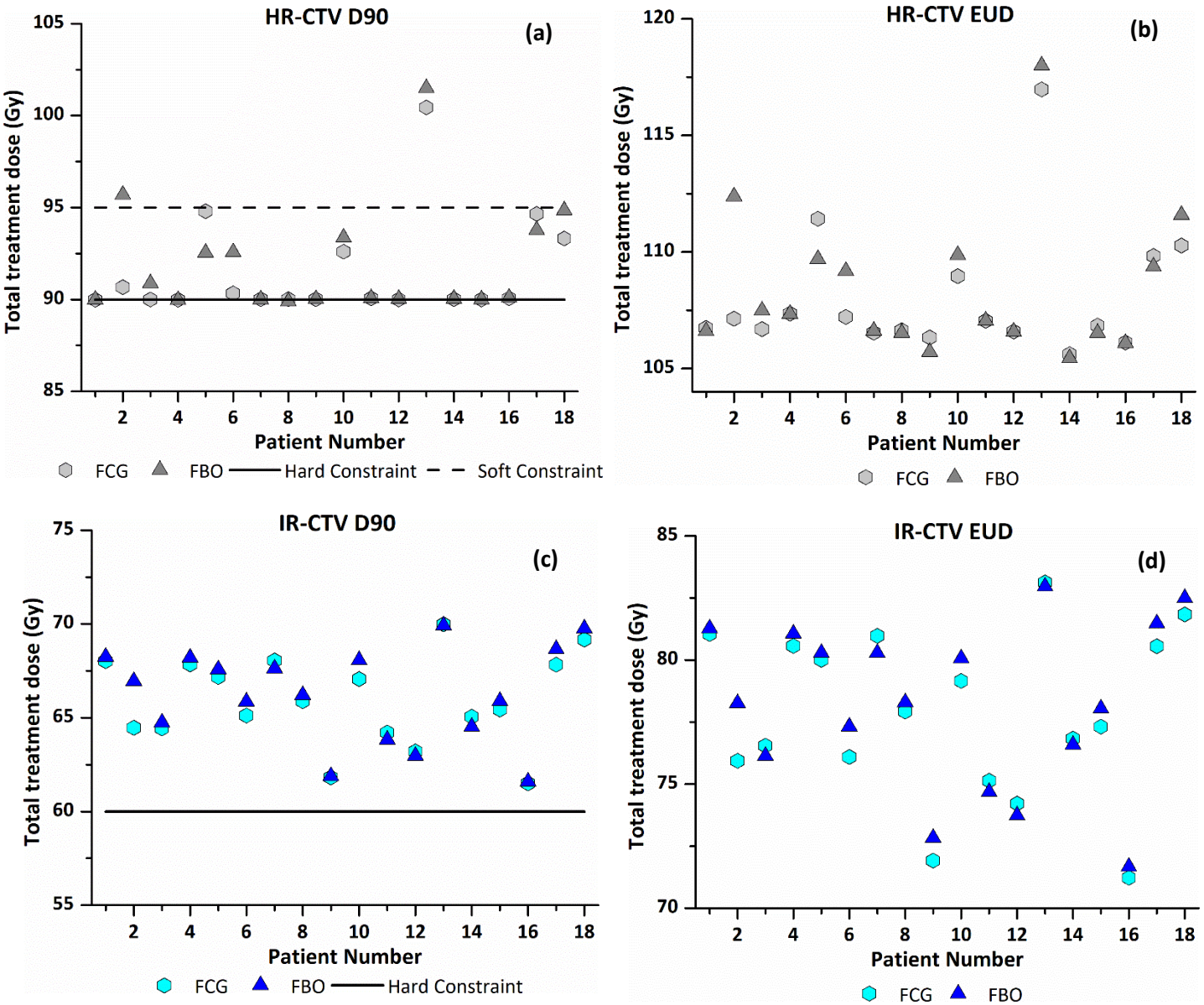


**Figure 34 - Comparison between the FCG and FBO approach per patient. CTV-$T_{HR}$ (a) $D_{90\,\%}$ and (b) EUD, CTV-$T_{IR}$ (c) $D_{90\,\%}$ and (d) EUD. Note: Data points for the FCG and FBO approach are indicated by hexagons and triangles, respectively.**

Figure 34 displays significant differences in CTV-$T_{HR}$ and CTV-$T_{IR}$ $D_{90\,\%}$ and EUD values per patient. The average CTV-$T_{HR}$ EUD values were 108.02 ± 2.66 Gy and 108.44 ± 3.03 Gy. The difference in average CTV-$T_{IR}$ EUD values was 77.80 ± 3.28 Gy and 78.19 ± 3.27 Gy for the FCG and FBO approach, respectively, which was tested for significant difference, with a $p \leq 0.05$.

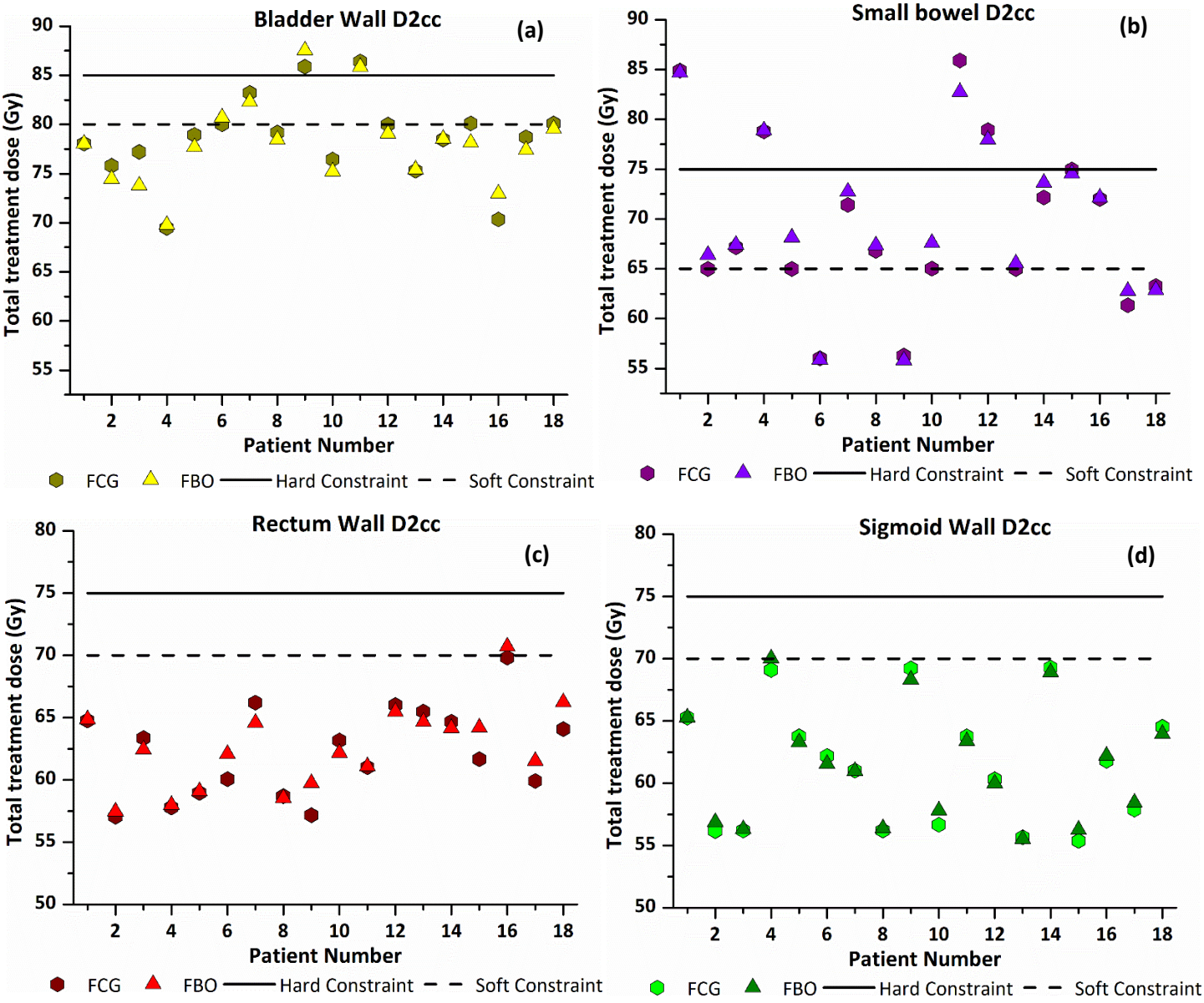


**Figure 35 - Comparison between the FCG and FBO approach per patient. The $D_{2cm^3}$ values for (a) bladder wall, (b) small bowel, (c) rectum wall and (d) sigmoid wall. Note: Data points for the FCG and FBO approach are indicated by hexagons and triangles, respectively.**

The difference between the two approaches was evaluated by considering all the reported OAR and CTV-T dose simultaneously, as illustrated in Figure 34 through Figure 36.

In patient 1, the hard constraint of 90 Gy CTV-$T_{HR}$ $D_{90\,\%}$ was reached in both approaches. No significant difference was observed in the CTV-T values and all the OAR EUD and $D_{2cm^3}$ values between the two approaches. Although small, the FBO approach recorded a lower $D_{0.1cm^3}$ value of 1.0 Gy compared to the FCG approach. The $D_{2cm^3}$ small bowel hard constraint of 75 Gy was excessively violated by both approaches. A TRAK value ≥ 2 cGy at 1 m and a CTV-$T_{HR}$ volume ≥ 25 $cm^3$ have been associated with late bowel toxicity [183]. Both the approaches recorded a TRAK value ≥ 2 cGy, and the CTV-$T_{HR}$ volume was a large volume of ≥ 70 $cm^3$. This violation will cause an increased risk in late bowel toxicity, and therefore the patient is a candidate for the application of intracavitary/interstitial IGABT, in the attempt to lower the dose in the small bowel.

In patient 2, the EUD hard constraint of the bladder wall was reached by the FBO approach and violated by the FCG approach, the FBO approach however recorded lower bladder wall EUD, $D_{2cm^3}$ and $D_{0.1cm^3}$ values of 4.13 Gy, 1.36 Gy and 7.16 Gy compared to FCG approach. The EUD hard constraint of the small bowel was not reached in any of the approaches. The $D_{2cm^3}$ soft constraint of the sigmoid wall was reached in both approaches, but the FCG approach recorded lower small bowel EUD, $D_{2cm^3}$ and $D_{0.1cm^3}$ values of 1.08 Gy, 1.43 Gy and 1.73 Gy compared to FBO approach. No significant difference was observed for the rectum and sigmoid wall values between the two approaches. Significant higher CTV-T values were reported for the FBO approach compared to the FCG approach. The FBO approach led to higher CTV-$T_{HR}$ EUD, $D_{90\,\%}$ and $D_{98\,\%}$ values of 5.24 Gy, 5.02 Gy and 6.21 Gy. CTV-$T_{HR}$ $D_{90\,\%}$ values of 90.67 Gy and 95.69 Gy were recorded for the FCG and FBO approach, respectively. The FBO approach also led to higher CTV-$T_{IR}$ EUD, $D_{90\,\%}$ and $D_{98\,\%}$ values of 2.32 Gy, 2.50 Gy and 2.82 Gy. Parameters like the CTV-$T_{HR}$ $D_{90\,\%}$ and $D_{98\,\%}$ and CTV-$T_{IR}$ $D_{98\,\%}$ are associated with better local control [184]. The CTV-$T_{HR}$ volume size of the patient was classified between limited and intermediate size. According to published data with regards to LC, a tumour volume of 22 $cm^3$ and a CTV-$T_{HR}$ dose ≥ 95 Gy, ensure LC of 96 %, this is better than a LC of 95 % at 90 Gy reported in the FCG approach [185]. Considering both OAR and CTV-T values, the FBO approach led to a superior plan compared to the FCG approach.

In patient 3, none of the sigmoid or rectum wall constraints were reached in any of the two approaches. Still, the FBO approach led to lower EUD and $D_{2cm^3}$ values of 1.35 Gy and 2.07 Gy compared to the FCG approach. The EUD hard constraint of the bladder wall was reached in the FBO

[183] (Bockel *et al.*, 2019)
[184] (Johannes C A Dimopoulos *et al.*, 2009; Mazeron *et al.*, 2015; Tanderup *et al.*, 2016)
[185] (Pötter *et al.*, 2018)

approach and violated in the FCG approach. The FBO approach recorded lower bladder wall EUD, $D_{2cm^3}$ and $D_{0.1cm^3}$ values of 3.84 Gy, 3.44 Gy and 6.51 Gy compared to FCG approach. The bladder wall $D_{2cm^3}$ was still below the soft constraint value of 80 Gy for both approaches. A higher CTV-$T_{HR}$ $D_{98\,\%}$ value of 1.74 Gy was recorded for the FBO approach as well. No significant difference was observed in the other OAR and CTV-T values between the two approaches. In this case, the results show clearly that the FBO approach was superior to the FCG approach.

In patient 4, the CTV-T values had no significant difference between the two approaches. None of the rectum and bladder wall constraints was reached, and no difference in the values was observed between the two approaches. The small bowel EUD and $D_{2cm^3}$ hard constraints were violated in both approaches; however, no significant difference in small bowel EUD values was observed between the two approaches. The $D_{2cm^3}$ soft constraint of the sigmoid wall, 70 Gy, was only reached in the FBO approach. The EUD hard constraint of the sigmoid wall, 67.75 Gy, was violated in both approaches; however, the FCG approach recorded lower EUD and $D_{0.1cm^3}$ values of 1.28 Gy and 1.71 Gy. The small bowel hard constraints that were violated showed no difference between the two approaches, as mentioned earlier. The planning aims were (1) to reach the hard constraint of the CTV-T values, then (2) to obey the OAR hard constraint and (3) then the soft constraints of the CTV-T volumes and OAR becomes a priority. With this said, the FCG approach led to a superior outcome compared to the FBO approach.

In patient 5, lower CTV-$T_{HR}$ $D_{90\,\%}$ and EUD values of 1.74 Gy and 2.26 Gy was recorded for the FBO approach compared to the FCG approach. The EUD hard constraint of the bladder wall was reached in the FBO approach but violated by the FCG approach. The FBO approach led to lower bladder wall EUD, $D_{2cm^3}$ and $D_{0.1cm^3}$ values of 4.69 Gy, 1.26 Gy and 7.75 Gy compared to FCG approach. The EUD hard constraint of the sigmoid wall was reached by the FCG approach. Lower sigmoid wall EUD and $D_{0.1cm^3}$ values of 1.05 Gy and 1.54 Gy were recorded for the FBO approach. The EUD hard constraint of the small bowel was violated by the FBO approach only, while the FCG approach managed to record lower small bowel EUD, $D_{2cm^3}$ and $D_{0.1cm^3}$ values of 4.79 Gy, 3.16 Gy and 9.20 Gy. The small bowel $D_{2cm^3}$ soft constraint of 65 Gy was violated by both approaches. The significant lower small bowel doses and some increase in the CTV-T values recorded by the FCG approach outweigh the lower bladder wall values recorded by the FBO approach.

In patient 6, higher CTV-$T_{HR}$ values were recorded by the FBO approach, with CTV-$T_{HR}$ $D_{90\,\%}$, $D_{98\,\%}$ and EUD values of 1.97 Gy, 2.24 Gy and 1.97 Gy higher. The FBO approach reported a lower bladder wall $D_{0.1cm^3}$ value of 1.11 Gy compared to the FCG approach. The FCG approach led to lower rectum wall EUD, $D_{2cm^3}$ and $D_{0.1cm^3}$ values of 1.17 Gy, 2.02 Gy and 1.67 Gy, however, none of the rectum wall constraints were reached by any of the approaches. A higher recto-vaginal reference point of 2.80 Gy

was reported for the FBO approach; however, the value was still well below the 65 Gy soft constraint. The FBO approach exploited the flexibility of the rectum wall dose values to its advantage to produce a plan with higher CTV-T values which will have an impact, although small on the LC of the patient.

In patient 7, no significant difference was observed in the CTV-T values between the two approaches. Both approaches violated the EUD hard constraint and $D_{2cm^3}$ soft constraint values of the bladder wall. The FBO approach reported a lower bladder wall $D_{0.1cm^3}$ value of 1.08 Gy compared to the FCG approach. Even though none of the rectum wall constraints was reached, the FBO approach still led to lower rectum wall EUD, $D_{2cm^3}$ and $D_{0.1cm^3}$ values of 1.67 Gy, 1.62 Gy and 2.34 Gy. The EUD hard constraint of the small bowel was violated by both approaches, while both approaches reached the $D_{2cm^3}$ soft constraint. The FCG approach produced a plan with lower small bowel EUD, $D_{2cm^3}$ and $D_{0.1cm^3}$ values of 1.77 Gy, 1.33 Gy and 2.95 Gy. A lower recto-vaginal reference point of 3.35 Gy was reported for the FBO approach, with the FCG approach violating the proposed hard constraint of 75 Gy. The recto-vaginal reference point hard constraint of 75 Gy proposed was only reached by the ICG approach. The probability of developing vaginal stenosis (G ≥ 2) in this case is 27 % [186]. This probability rates for the FCG approach are very high, and in this case, any approach that recorded lower rectum wall values and in effect lower the probability of developing vaginal stenosis will be superior. Therefore, the FBO approach led to a superior plan compared to the FCG approach.

In patient 8, no significant difference was observed in the CTV-T values between the two approaches. Both approaches violated the EUD hard constraint of the bladder wall; however, the FBO approach led to lower EUD and $D_{0.1cm^3}$ values of 1.60 Gy and 2.75 Gy. The rest of the OAR values recorded reported no significant difference between the two approaches. When considering these results, the FBO approach led to a better plan compared to FCG approach.

In patient 9, the bladder wall EUD and $D_{2cm^3}$ hard constraints of 85 Gy was violated by both approaches. The FBO approach reported lower bladder wall EUD and $D_{0.1cm^3}$ values of 4.02 Gy and 7.29 Gy, compare to the FCG approach. However, the FCG approach reported a 1.65 Gy lower $D_{2cm^3}$ value to compare to the FBO approach. The EUD hard constraint of 67.75 Gy for the sigmoid wall was violated by both approaches. The FBO approach delivered a plan with lower sigmoid wall EUD and $D_{0.1cm^3}$ values of 4.01 Gy and 4.13 Gy. A higher dose was recorded by the FBO approach in the rectum wall and recto-vaginal reference point. None of the rectum wall constraints was reached by any of the approaches. Still, the FCG recorded lower EUD, $D_{2cm^3}$ and $D_{0.1cm^3}$ values of 2.71 Gy, 2.57 Gy and 3.83 Gy. A higher recto-vaginal reference point of 3.90 Gy was reported for the FBO approach; however, it was still below the 65 Gy soft constraint. The bladder wall was the OAR volume of main concern due to the violation of

[186] (Kirchheiner *et al.*, 2016)

the EUD and $D_{2cm^3}$ hard constraint by both approaches. With this said, the FBO approach had the ability to recorded lower values for the bladder wall, but the FCG approach also led to lower values. Therefore, both approaches had their advantages, and there is no clear evidence to advocate the one approach over the other.

In patient 10, higher CTV-$T_{IR}$ $D_{90\,\%}$ and $D_{98\,\%}$ values of 1.01 Gy and 1.05 Gy were recorded for the FBO approach. No significant difference was observed in the rest of the CTV-T values between the two approaches. The bladder wall EUD hard constraint was violated by the FCG approach but only reached by the FBO approach. The FBO approach recorded lower bladder wall EUD, $D_{2cm^3}$ and $D_{0.1cm^3}$ values of 1.79 Gy, 1.21 Gy and 3.24 Gy compared to FCG approach. None of the small bowel, rectum and sigmoid wall constraints was violated. The FBO approach led to lower rectum wall EUD, $D_{2cm^3}$ and $D_{0.1cm^3}$ values of 1.41 Gy, 1.02 Gy and 2.08 Gy. The FCG approach recorded lower sigmoid wall and small bowel doses compared to the FBO approach. Lower small bowel EUD, $D_{2cm^3}$ and $D_{0.1cm^3}$ values of 3.34 Gy, 2.57 Gy and 5.41 Gy were recorded. Lower sigmoid wall EUD, $D_{2cm^3}$ and $D_{0.1cm^3}$ values of 1.35 Gy, 1.16 Gy and 1.73 Gy were recorded. A lower recto-vaginal reference point of 1.27 Gy was reported for the FBO approach, even though both approaches recorded doses below 65 Gy. Even though the FCG approach led to lower values in the sigmoid and small bowel, no hard constraints were reached or violated in these volumes. The FBO approach exploited the flexibility of the small bowel and sigmoid wall dose values to its advantage to produce a plan with lower bladder wall doses in which the EUD hard constraint was violated and therefore are considered the superior approach in this case.

In patient 11, the hard constraint of 90 Gy CTV-$T_{HR}$ $D_{90\,\%}$ was reached in both approaches, and no significant difference was observed in the CTV-T values between the two approaches. Both approaches violated the EUD and $D_{2cm^3}$ hard constraints of the bladder wall and small bowel. The FBO approach produced a plan with significant lower small bowel EUD, $D_{2cm^3}$ and $D_{0.1cm^3}$ values of 7.28 Gy, 3.16 Gy and 10.12 Gy compared to the FCG approach. The rest of the OAR values recorded had no significant difference between the two approaches. When considering these results, the FBO approach clearly led to a better treatment plan compared to FCG approach.

In patient 12, the FBO approach led to a lower dose in the bladder wall, rectum wall and small bowel. The FCG approach did not record any significant lower doses in any of the OAR volumes. The bladder wall and small bowel EUD hard constraints were violated by both approaches, and the rectum wall EUD hard constraint was only reached by the FCG approach. The FBO, however, recorded lower EUD and $D_{0.1cm^3}$ values in these OAR volumes. The small bowel $D_{2cm^3}$ hard constraint was also violated by both approaches. The FCG approach only reached the bladder wall $D_{2cm^3}$ soft constraint. The FBO approach recorded lower bladder wall EUD and $D_{0.1cm^3}$ values of 1.20 Gy and 2.29 Gy, respectively. Again, the FBO approach led to lower rectum wall EUD and $D_{0.1cm^3}$ values of 1.05 Gy and 1.15 Gy. The

FBO approach produced a plan with lower small bowel EUD and $D_{0.1cm^3}$ values of 1.41 Gy and 1.71 Gy compared to the FCG approach. No significant difference was observed in the CTV-T values between the two approaches. With this said, the FBO approach led to a better plan compared to the FCG approach.

In patient 13, the EUD hard constraints of the small bowel and rectum wall were violated by the FCG approach and only reached by the FBO approach. Both the approaches reached only the $D_{2cm^3}$ soft constraint of the small bowel. A lower rectum wall EUD and $D_{0.1cm^3}$ values of 1.27 Gy and 1.52 Gy, and a lower recto-vaginal reference point of 1.52 Gy was reported for the FBO approach. The FBO approach produced a plan with lower small bowel EUD and $D_{0.1cm^3}$ values of 16.29 Gy and 11.68 Gy compared to the FCG approach. Higher CTV-$T_{HR}$ values of 1.02 Gy and 1.04 Gy was also recorded by the FBO approach. When considering these results, the FBO approach was superior to the FCG approach in this case.

In patient 14, no significant difference was observed in the CTV-T values between the two approaches. Both approaches violated the EUD hard constraints of the sigmoid wall and small bowel. The FCG approach led to higher sigmoid wall EUD and $D_{0.1cm^3}$ values of 5.84 Gy and 4.42 Gy. The small bowel $D_{2cm^3}$ soft constraint was reached by both approaches. The FCG approach managed to report lower small bowel EUD, $D_{2cm^3}$ and $D_{0.1cm^3}$ values of 1.98 Gy, 1.47 Gy and 3.59 Gy compared to the FCG approach. A lower recto-vaginal reference point of 1.23 Gy was reported for the FBO approach, with both approaches violating the soft constraint of 65 Gy. Both approaches led to lower OAR dose in one of the two OAR, small bowel and sigmoid wall. According to published data, the small bowel dose constraints take priority over the sigmoid constraints, and for this reason, the FCG approach can be chosen as the superior approach in this case [187].

In patient 15, no significant difference was observed in the CTV-T values between the two approaches. The bladder wall $D_{2cm^3}$ soft constraint was only reached by the FCG approach, while both approaches violated the EUD hard constraint. Significant lower bladder wall EUD, $D_{2cm^3}$ and $D_{0.1cm^3}$ values of 4.90 Gy, 1.96 Gy and 8.54 Gy was reported by the FBO approach compared to the FCG approach. None of the rectum and sigmoid wall constraints was reached by any of the approaches. Still, the FCG approach led to lower rectum wall EUD, $D_{2cm^3}$ and $D_{0.1cm^3}$ values of 2.73 Gy, 2.55 Gy and 3.66 Gy. The $D_{2cm^3}$ values reported for the rectum was well below the 70 Gy soft constraint. The small bowel $D_{2cm^3}$ hard constraint of 75 Gy was reached by both approaches, while both approaches violated the EUD hard constraint. The FBO approach managed to record lower small bowel EUD and $D_{0.1cm^3}$ values of 1.07 Gy, and 1.95 Gy. A higher recto-vaginal reference point of 3.82 Gy was reported for the FBO approach,

[187] (Tanderup *et al.*, 2020)

with only the FBO approach reaching the soft constraint of 65 Gy. The FBO approach recorded lower bladder wall and small bowel values which were violated in both approaches. With all this said, the FBO approach led to a superior outcome compared to the FCG approach.

In patient 16, none of the bladder wall constraints was reached by any of the approaches. However, the FCG approach managed to report lower bladder wall EUD, $D_{2cm^3}$, and $D_{0.1cm^3}$ values of 3.17 Gy, 2.63 Gy and 5.18 Gy compared the FBO approach. Both approaches violated the EUD hard and $D_{2cm^3}$ soft constraint of the small bowel, the FBO approach only managed to report a lower $D_{0.1cm^3}$ value of 1.26 Gy. The FCG approach produced a plan that was 1.85 Gy lower for the recto-vaginal point, and this will, in effect, lead to a lower probability of developing vaginal stenosis (G ≥ 2) [188]. No significant difference was observed in the CTV-T values between the two approaches. The bladder wall constraints were not reached by any approaches and therefore was not the OAR of main concern. In this case, the FCG approach seems to be superior, which led to a lower recto-vaginal point.

In patient 17, the EUD hard constraint of the bladder wall was violated by the FCG approach and only reached by the FBO approach. Significant lower bladder wall EUD, $D_{2cm^3}$ and $D_{0.1cm^3}$ values of 4.02 Gy, 1.31 Gy and 7.29 Gy was reported by the FBO approach. None of the small bowel, rectum and sigmoid wall constraints was reached by any of the approaches. However, the FCG approach recorded lower small bowel, rectum and sigmoid wall values compared to the FBO approach. The FCG approach led to lower sigmoid wall EUD and $D_{0.1cm^3}$ values of 1.16 Gy and 1.47 Gy. The FCG approach led to lower rectum wall EUD, $D_{2cm^3}$ and $D_{0.1cm^3}$ values of 1.42 Gy, 1.61 Gy and 2.01 Gy. The FCG approach also managed to record lower small bowel EUD, $D_{2cm^3}$ and $D_{0.1cm^3}$ values of 1.24 Gy, 1.44 Gy and 1.88 Gy, respectively. A higher recto-vaginal reference point of 2.90 Gy was reported for the FBO approach; however, no approach reached the soft constraint of 65 Gy. A higher CTV-$T_{HR}$ $D_{98\,\%}$ value of 1.34 Gy was recorded by the FBO approach. The FBO approach exploited the flexibility of the small bowel, rectum and sigmoid wall dose values to its advantage to produce an approach that lowered the dose in the OAR of main concern, in this case, the bladder wall.

In patient 18, higher CTV-$T_{HR}$ EUD and $D_{90\,\%}$ values of 1.32 Gy and 1.53 Gy were recorded by the FBO approach. None of the OAR values showed a significant difference between the two approaches, except for the rectum wall and recto-vaginal reference point. The FBO approach recorded higher rectum wall $D_{2cm^3}$ and $D_{0.1cm^3}$ values of 2.17 Gy and 2.14 Gy, however, no rectum wall constraints was reached for both approaches. A higher recto-vaginal reference point of 2.34 Gy was reported for the FBO approach, with only the FBO approach violating the 65 Gy soft constraint, by a very small margin.

[188] (Kirchheiner *et al.*, 2016)

None of the approaches reached the OAR hard constraints, while the FCG approach reported a lower rectum wall and recto-vaginal reference point values. The reported rectum wall values for both approaches still fall within the same sub-group of 65-70 Gy regarding the probability of late rectal effect; therefore, the FBO approach may be advocated for due to some increase in CTV-T dose [189].

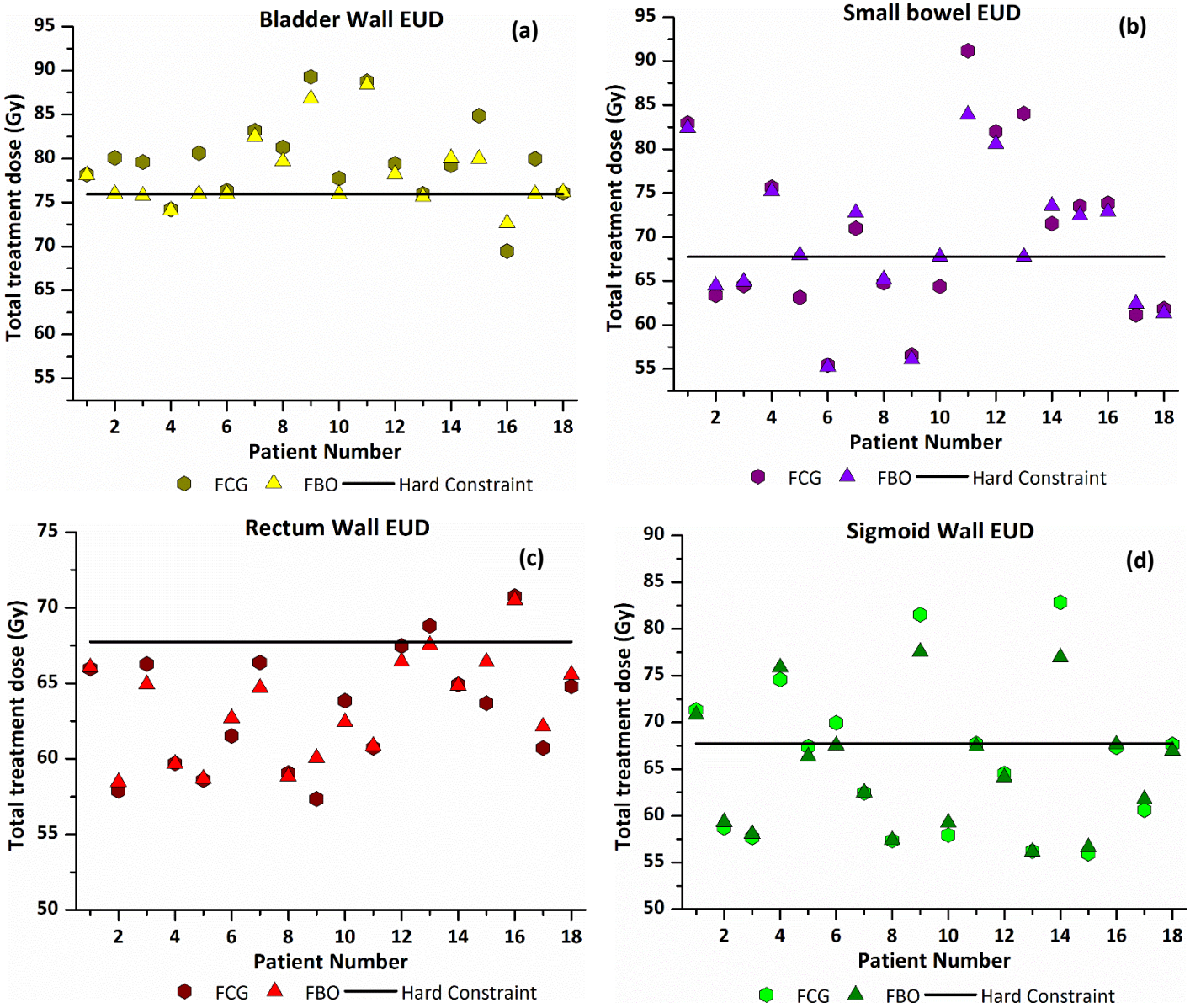


**Figure 36 - Comparison between the FCG and FBO approach per patient. The EUD values for (a) bladder wall, (b) small bowel, (c) rectum wall and (d) sigmoid wall. Note: Data points for the FCG and FBO approach are indicated by hexagons and triangles, respectively.**

The difference in the average bladder wall EUD values was of significant difference with a $p \leq 0.05$. The average bladder wall EUD was 79.68 ± 4.69 Gy and 78.19 ± 4.04 Gy, a 1.86 % difference between the FCG and FBO approach, respectively. No significant difference between the two approaches was reported for the average EUD values of the small bowel, sigmoid and rectum wall. The average small bowel EUD values of 70.05 ± 9.82 Gy and 69.26 ± 7.99 Gy were reported for the FCG and FBO approach,

[189] (Mazeron *et al.*, 2016)

respectively. The average rectum wall EUD values were recorded as 63.25 ± 3.86 and 63.38 ± 3.38 Gy Gy for the FCG and FBO approach, respectively. The average sigmoid wall EUD was recorded as 65.65 ± 8.00 Gy and 65.12 ± 6.72 Gy, for the FCG and FBO approach, respectively.

**Other parameters that were recorded:**

As displayed in Table 17, the dose to $A_{Left}$ and $A_{Right}$ is more comparable for both the approaches. The FBO approach led to significantly higher average TRAK values.

**Table 17 - Average dose to point A and TRAK values of FCG and FBO approach**

| Approach | $A_{Left}$ (Gy) | $A_{Right}$ (Gy) | TRAK (cGy at 1 m) |
|---|---|---|---|
| **FCG** | 77.02 ± 8.32 | 77.20 ± 10.23 | 1.58 ± 0.25* |
| **FBO** | 77.56 ± 8.51 | 75.80 ± 8.53 | 1.62 ± 0.23* |

***Tested for the significant difference with a p-value ≤ 0.05.**

The FBO approach led to significant higher CTV-$T_{IR}$ $D_{90\ \%}$ and EUD values combined with significant lower bladder wall EUD and $D_{0.1cm^3}$ values. Aside from these differences, when patient plans were individually assessed, the FBO approach also led to more superior plans in more patients compared to the FCG approach.

## b) Inverse planning and optimisation

The inverse planning and optimisation tool, as described in Section 3.3.5, were used to plan all 18 patients. A total of 360 inverse Intracavitary IGABT plans were optimised and planned. The 360 plans consist of 90 conventional optimistic plans, 90 conventional greedy plans, 90 biological optimistic plans and 90 biological greedy plans. The priorities set for the target and OAR volumes during the planning and optimisation process were the same as the forward planning and optimisation method, as described in Section 0.

### b.1) Inverse Conventional Optimistic (ICO) vs Inverse Conventional Greedy (ICG)

A total of 180 Inverse Conventional plans were optimised and planned. The Inverse Conventional Optimistic (ICO) approach was executed, and the total OAR conventional constraints listed in Table 2 were used as the dose constraints during the optimisation and planning process. Corresponding OAR biological parameters obtained during the conventional optimisation process were only noted and were not incorporated as limiting parameters. The fractional OAR dose constraint was automatically calculated and applied by the IHDM by using Equation (39) and (40), for the ICO and ICG approach, respectively.

Table 18 provides the average CTV-$T_{HR}$ and CTV-$T_{IR}$ $D_{90\,\%}$ $D_{98\,\%}$ and $D_{100\,\%}$ values obtained for the Inverse Conventional Optimistic (ICO) approach versus the Inverse Conventional Greedy (ICG) approach. Evaluating these results below no significant differences can be seen in all the CTV-T parameters for the ICG approach compared to the ICO approach considering the whole patient population.

**Table 18 - Average CTV-T $D_{90\,\%}$ $D_{98\,\%}$ and $D_{100\,\%}$ values for the ICO and ICG approach**

| Approach | CTV-$T_{HR}$ $D_{90\,\%}$ (Gy) | CTV-$T_{HR}$ $D_{98\,\%}$ (Gy) | CTV-$T_{HR}$ $D_{100\,\%}$ (Gy) | CTV-$T_{IR}$ $D_{90\,\%}$ (Gy) | CTV-$T_{IR}$ $D_{98\,\%}$ (Gy) | CTV-$T_{IR}$ $D_{100\,\%}$ (Gy) |
|---|---|---|---|---|---|---|
| **ICO** | 91.24 ± 2.58 | 80.69 ± 2.96 | 73.70 ± 3.29 | 66.46 ± 2.44 | 62.81 ± 2.11 | 60.59 ± 1.85 |
| **ICG** | 91.22 ± 2.57 | 80.67 ± 2.93 | 73.66 ± 3.25 | 66.44 ± 2.42 | 62.79 ± 2.10 | 60.57 ± 1.82 |

Again, the difference in approaches was evaluated per patient. Results are displayed in Figure 37 to Figure 39. As illustrated in Figure 37, the $D_{90\,\%}$ hard constraint of the CTV-$T_{HR}$ were reached in all the patients. No significant difference in the CTV-T $D_{90\,\%}$ and EUD values can be noted between the ICO and ICG approach. Average CTV-$T_{HR}$ and CTV-$T_{IR}$ EUD values of 107.57 ± 2.57 Gy and 78.75 ± 3.18 Gy were reported for the ICO approach, whereas values of 107.55 ± 2.55 Gy and 78.73 ± 3.15 Gy were recorded for the ICG approach.

Six patients received an average $D_{90\,\%}$ value greater than the set $D_{90\,\%}$ hard constraint of 90 Gy. The $D_{90\,\%}$ soft constraint was reached in one patient, patient 13, with a $D_{90\,\%}$ value of 100.64 Gy. This was without violating any OAR walls $D_{2cm^3}$ constraints, just reaching the small bowel $D_{2cm^3}$ soft constraint. Even though the OAR EUD values were not incorporated as dose-limiting parameters during the ICO and ICG optimisation process, the EUD values were still recorded and evaluated. When the corresponding OAR EUD values for patient 13 are evaluated, it is noted that the small bowel and rectum wall EUD hard constraint was violated. The violation of the small bowel and rectum wall EUD hard constraint is not justified, because even though patient 13 reached a dose of 100.45 Gy, it has been reported that a CTV-$T_{HR}$ $D_{90\,\%} \geq 85$ Gy and a CTV-$T_{HR}$ size of 29 $cm^3$ already result in a 3-year local control rate > 93 %. Exceptional local control of 96 % has been reported at 95 Gy, with this said it does not seem relevant to further dose escalate beyond 95 Gy, in this case, as it would not translate to higher local control [190].

[190] (Pötter *et al.*, 2018)

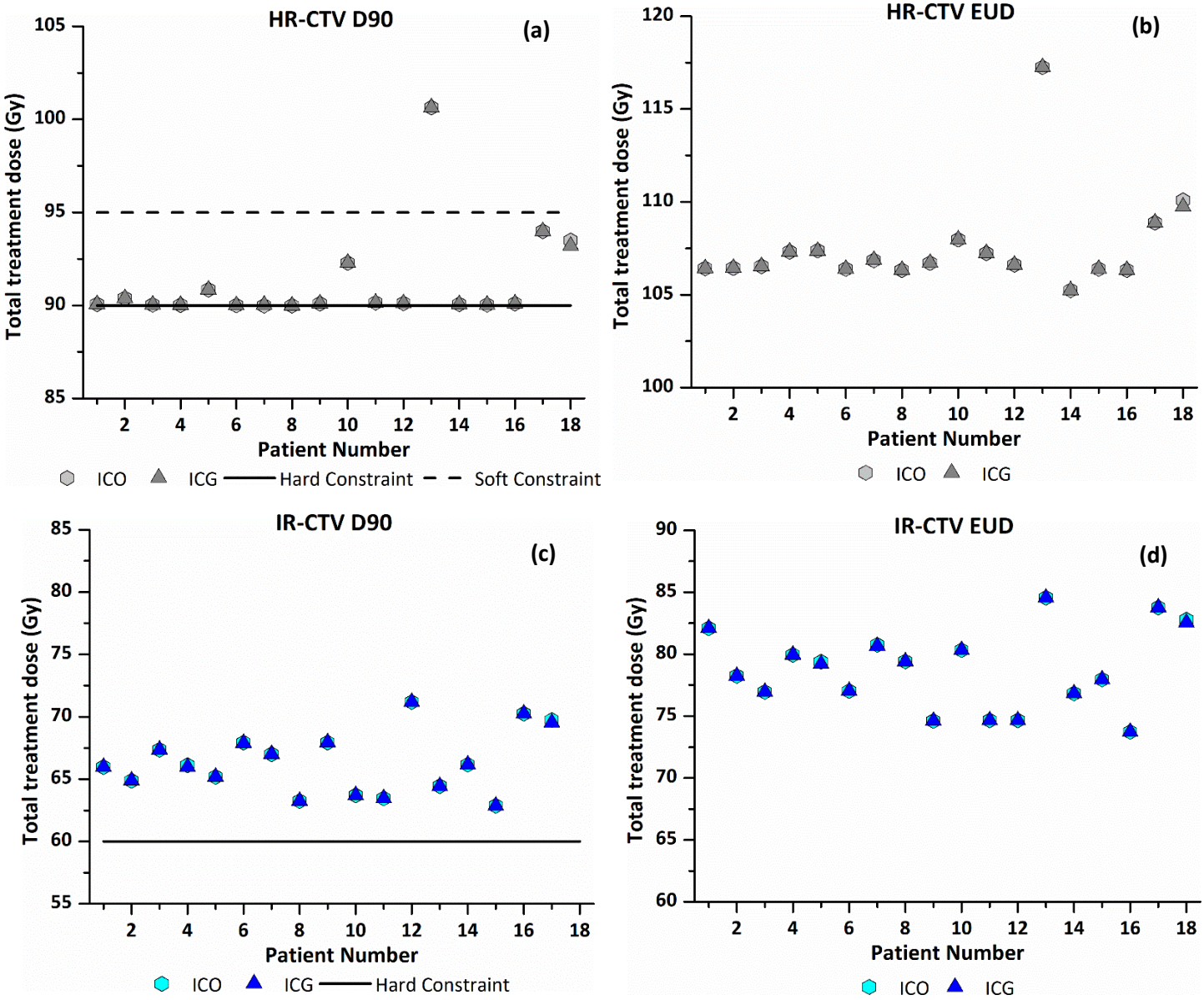


**Figure 37 - Comparison between the ICO and ICG approach per patient. CTV-$T_{HR}$ (a) $D_{90\,\%}$ and (b) EUD, CTV-$T_{IR}$ (c) $D_{90\,\%}$ and (d) EUD. Note: Data points for the ICO and ICG approach are indicated by hexagons and triangles, respectively.**

As illustrated in Figure 37, the $D_{90\,\%}$ hard constraint of the CTV-$T_{HR}$ was exceeded in five other patients, patient 2, 5, 10, 17 and 18. Table 19 displays the corresponding $D_{2cm^3}$ and $D_{0.1cm^3}$ values for the OAR walls as well as the recto-vaginal reference point values for the ICO and ICG approach across the whole population.

**Table 19 - Average $D_{2cm^3}$ and $D_{0.1cm^3}$ values for all OAR walls of the ICO and ICG approach.**

| | Bladder wall | Small bowel | Rectum wall | Sigmoid wall | Recto-vaginal |
|---|---|---|---|---|---|
| **Approach** | **$D_{2cm^3}$ (Gy) Average ± SD** | **$D_{2cm^3}$ (Gy) Average ± SD** | **$D_{2cm^3}$ (Gy) Average ± SD** | **$D_{2cm^3}$ (Gy) Average ± SD** | **Dose point (Gy) Average ± SD** |
| **ICO** | 78.88 ± 4.68 | 69.39 ± 7.77 | 64.17 ± 3.92 | 69.39 ± 7.77 | 67.35 ± 4.12 |
| **ICG** | 78.89 ± 4.69 | 69.39 ± 7.79 | 64.15 ± 3.92 | 69.39 ± 7.79 | 67.31 ± 4.11 |
| **Approach** | **Bladder wall $D_{0.1cm^3}$ (Gy)** | **Small bowel $D_{0.1cm^3}$ (Gy)** | **Rectum wall $D_{0.1cm^3}$ (Gy)** | **Sigmoid wall $D_{0.1cm^3}$ (Gy)** | **-** |
| **ICO** | 97.86 ± 9.60 | 81.84 ± 13.57 | 71.69 ± 6.17 | 71.25 ± 12.00 | -- |
| **ICG** | 97.86 ± 9.59 | 81.84 ± 13.61 | 71.63 ± 6.17 | 71.21 ± 12.00 | - |

The difference in the $D_{2cm^3}$, $D_{0.1cm^3}$, dose point values (see Table 19) for the ICO and ICG approach, for the whole patient population, are of no significant value. Figure 38 and Figure 39 display the OAR dose results that were obtained for the ICO and ICG approach per patient.

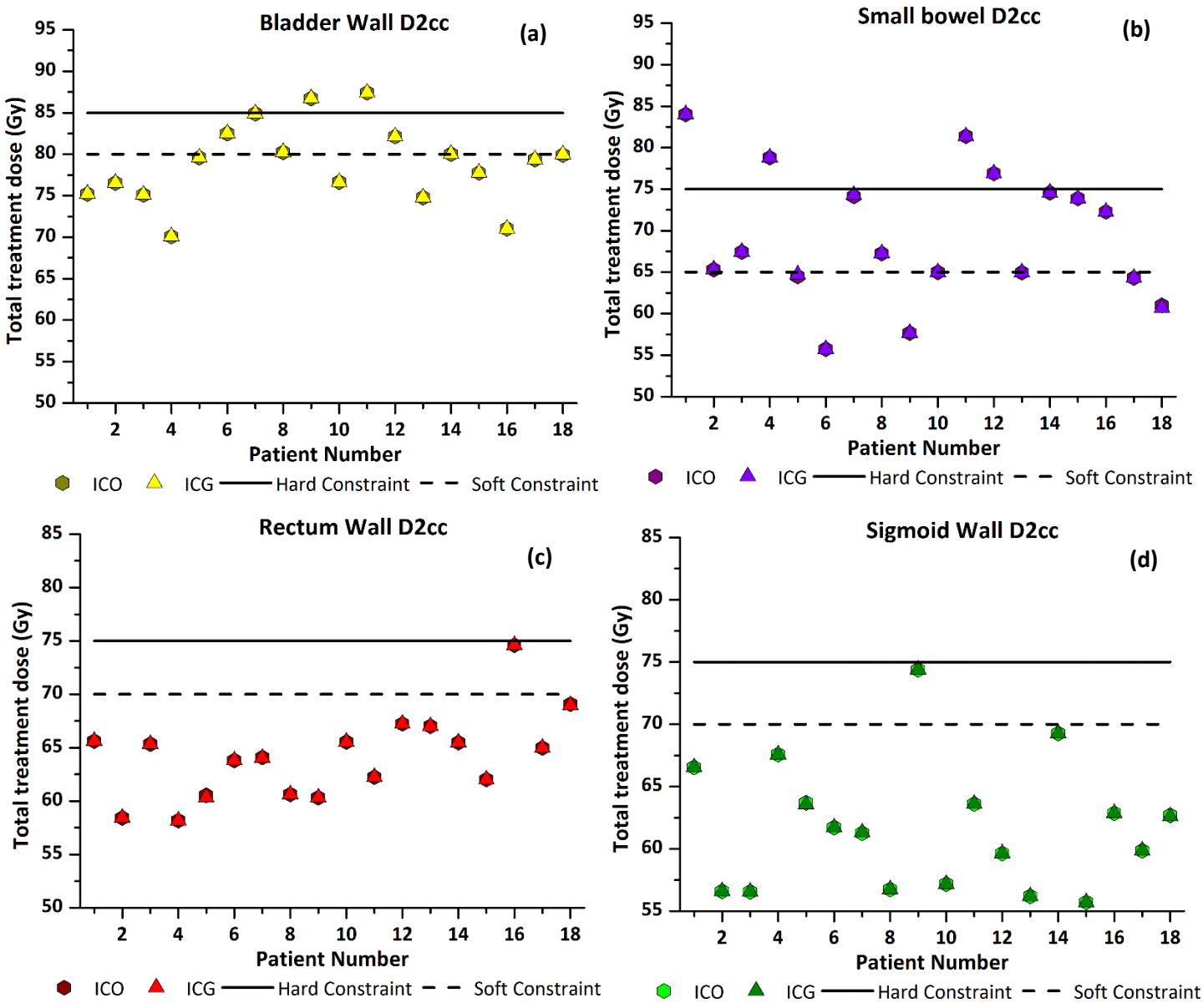


**Figure 38 - Comparison between the ICO and ICG approach per patient. The $D_{2cm^3}$ values for (a) bladder wall, (b) small bowel, (c) rectum wall and (d) sigmoid wall. Note: Data points for the ICO and ICG approach are indicated by hexagons and triangles, respectively.**

The $D_{2cm^3}$ hard constraint of the bladder wall was reached in one patient and violated in two patients, while the $D_{2cm^3}$ soft constraint was reached in five patients and violated in five patients. The average bladder wall $D_{2cm^3}$ were 78.88 ± 4.68 Gy and 78.89 ± 4.69 Gy for the ICO and ICG approach, respectively. The $D_{2cm^3}$ hard constraint of the small bowel was violated in four patients, while the soft constraint was reached/violated in thirteen patients. The average small bowel $D_{2cm^3}$ was 69.39 ± 7.77 Gy and 69.39 ± 7.79 Gy for the ICO and ICG approach, respectively. The $D_{2cm^3}$ hard constraint of the rectum and sigmoid wall were not reached/violated. One patient violated the $D_{2cm^3}$ soft constraint of the rectum and sigmoid wall. The average rectum wall $D_{2cm^3}$ was 64.17 ± 3.92 Gy and 64.15 ± 3.92 Gy for the ICO and ICG approach, respectively. The average sigmoid wall $D_{2cm^3}$ was 61.78 ± 5.04 Gy and

61.77 ± 5.04 Gy for the ICO and ICG approach, respectively. From these results, no significant difference between the two optimisation techniques is recorded. The corresponding OAR EUD values are illustrated in Figure 39. Again, it is evident from Figure 38 and Figure 39 that the bladder wall and small bowel are the most limiting OAR volumes.

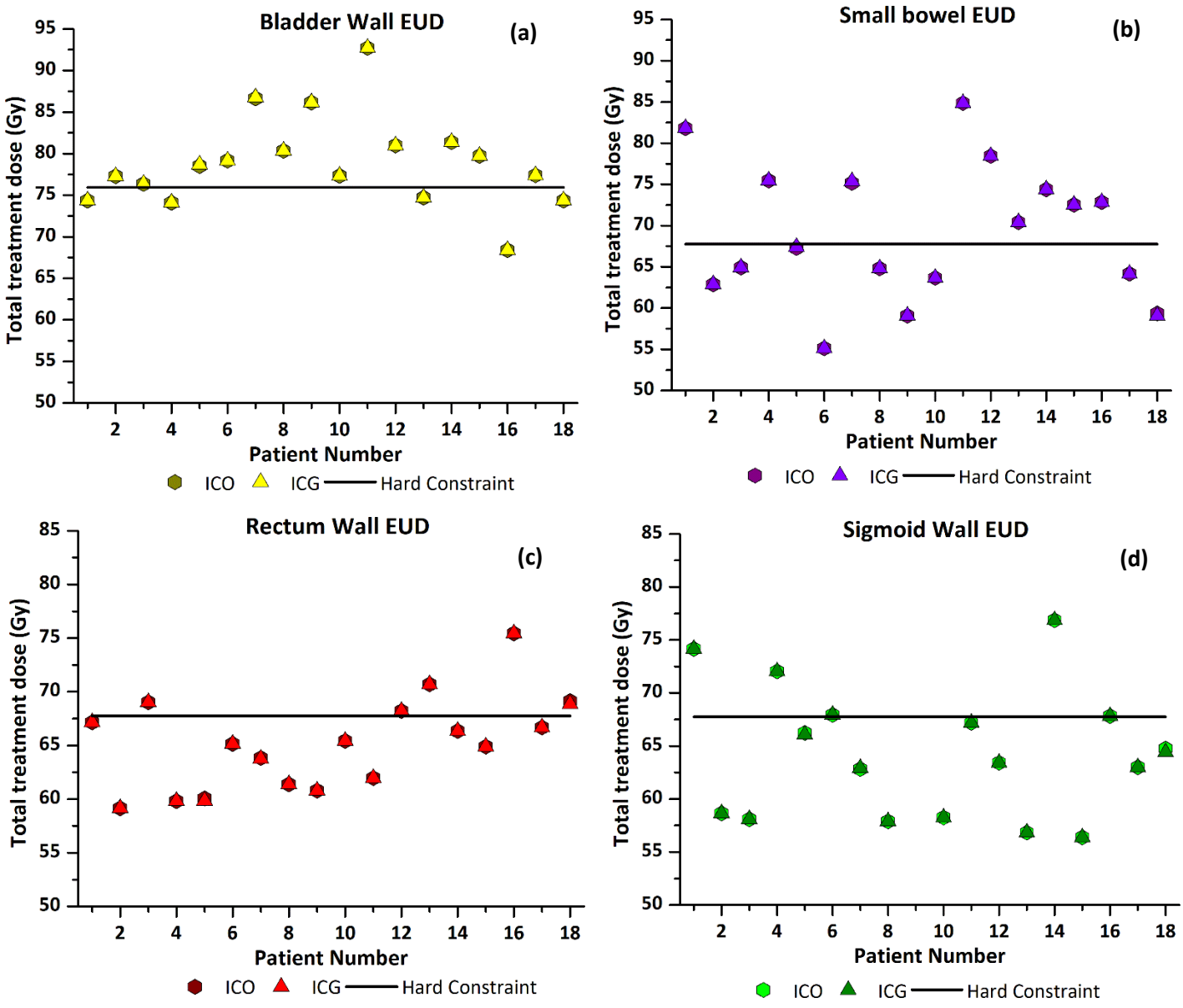


**Figure 39 - Comparison between the ICO and ICG approach per patient. The EUD values for (a) bladder wall, (b) small bowel, (c) rectum wall and (d) sigmoid wall. Note: Data points for the ICO and ICG approach are indicated by hexagons and triangles, respectively.**

As illustrated in Figure 39, the EUD hard constraint of the bladder wall was reached/violated in thirteen patients, while the small bowel was reached/violated in ten patients. The average bladder wall EUD was 78.88 ± 5.39 Gy and 78.90 ± 5.40 Gy for the ICO and ICG approach, respectively. The average small bowel EUD was 69.28 ± 8.00 Gy and 69.29 ± 8.03 Gy for the ICO and ICG approach, respectively. The

EUD hard constraint of the rectum and the sigmoid wall was respectively reached/violated in five and six patients. The average rectum wall EUD was 65.29 ± 4.22 Gy and 65.25 ± 4.22 Gy for the ICO and ICG approach, respectively. Also, the average sigmoid wall EUD was 66.07 ± 9.55 Gy and 66.05 ± 9.55 Gy for the ICO and ICG approach, respectively. However, no significant difference in OAR $D_{2cm^3}$ and EUD values per patient was observed for the ICO and ICG approach in Figure 38 and Figure 39.

**Other parameters that were recorded:**

The dose to point A and TRAK values are summarised in Table 20. The average dose to point $A_{Left}$ and $A_{Right}$ reported minimal differences between the two approaches. No significant difference between the ICO and ICG average TRAK values was recorded.

**Table 20 - Average dose to point A and TRAK values of ICO and ICG approach**

| Approach | $A_{Left}$ (Gy) | $A_{Right}$ (Gy) | TRAK (cGy at 1 m) |
|---|---|---|---|
| **ICO** | 85.47 ± 22.63 | 81.77 ± 15.94 | 1.73 ± 0.24 |
| **ICG** | 85.50 ± 22.64 | 81.77 ± 15.99 | 1.73 ± 0.24 |

The difference between ICO and ICG approach, in terms of the whole patient population or per patient, is negligible. Therefore, there is no preferred approach when considering the ICO and ICG approach.

### b.2) Inverse Biological Optimistic (IBO) vs Inverse Biological Greedy (IBG)

A total of 180 Inverse Biological plans were optimised and planned. The Inverse Biological Optimistic (IBO) approach was executed; the total OAR biological constraints listed in Table 3 were used as the dose constraints during the optimisation and planning process. Corresponding OAR conventional parameters obtained during the biological optimisation process were only noted and were not incorporated as limiting parameters. The fractional OAR dose constraint was automatically calculated and applied by the IHDM by using Equations (39) and (40), for the IBO and IBG approach, respectively.

Table 21 provides the average CTV-$T_{HR}$ and CTV-$T_{IR}$ $D_{90\,\%}$ $D_{98\,\%}$ and $D_{100\,\%}$ values obtained for the Inverse Biological Optimistic (IBO) approach compared to the Inverse Biological Greedy (IBG) approach.

**Table 21 - Average CTV-T $D_{90\,\%}$ $D_{98\,\%}$ and $D_{100\,\%}$ values for the IBO and IBG approach**

| Approach | CTV-$T_{HR}$ $D_{90\,\%}$ (Gy) | CTV-$T_{HR}$ $D_{98\,\%}$ (Gy) | CTV-$T_{HR}$ $D_{100\,\%}$ (Gy) | CTV-$T_{IR}$ $D_{90\,\%}$ (Gy) | CTV-$T_{IR}$ $D_{98\,\%}$ (Gy) | CTV-$T_{IR}$ $D_{100\,\%}$ (Gy) |
|---|---|---|---|---|---|---|
| **IBO** | 91.82 ± 3.18 | 81.53 ± 3.41 | 74.41 ± 3.57 | 67.14 ± 2.52 | 63.46 ± 2.31 | 61.14 ± 2.01 |
| **IBG** | 91.86 ± 3.13 | 81.53 ± 3.38 | 74.39 ± 3.57 | 67.13 ± 2.47 | 63.43 ± 2.27 | 61.11 ± 1.97 |

The outcome between the two approaches, considering the results in Table 21, are comparable. No major differences were recorded for the average CTV-T volumes between the two approaches. These results were evaluated in more detail in Figure 40.

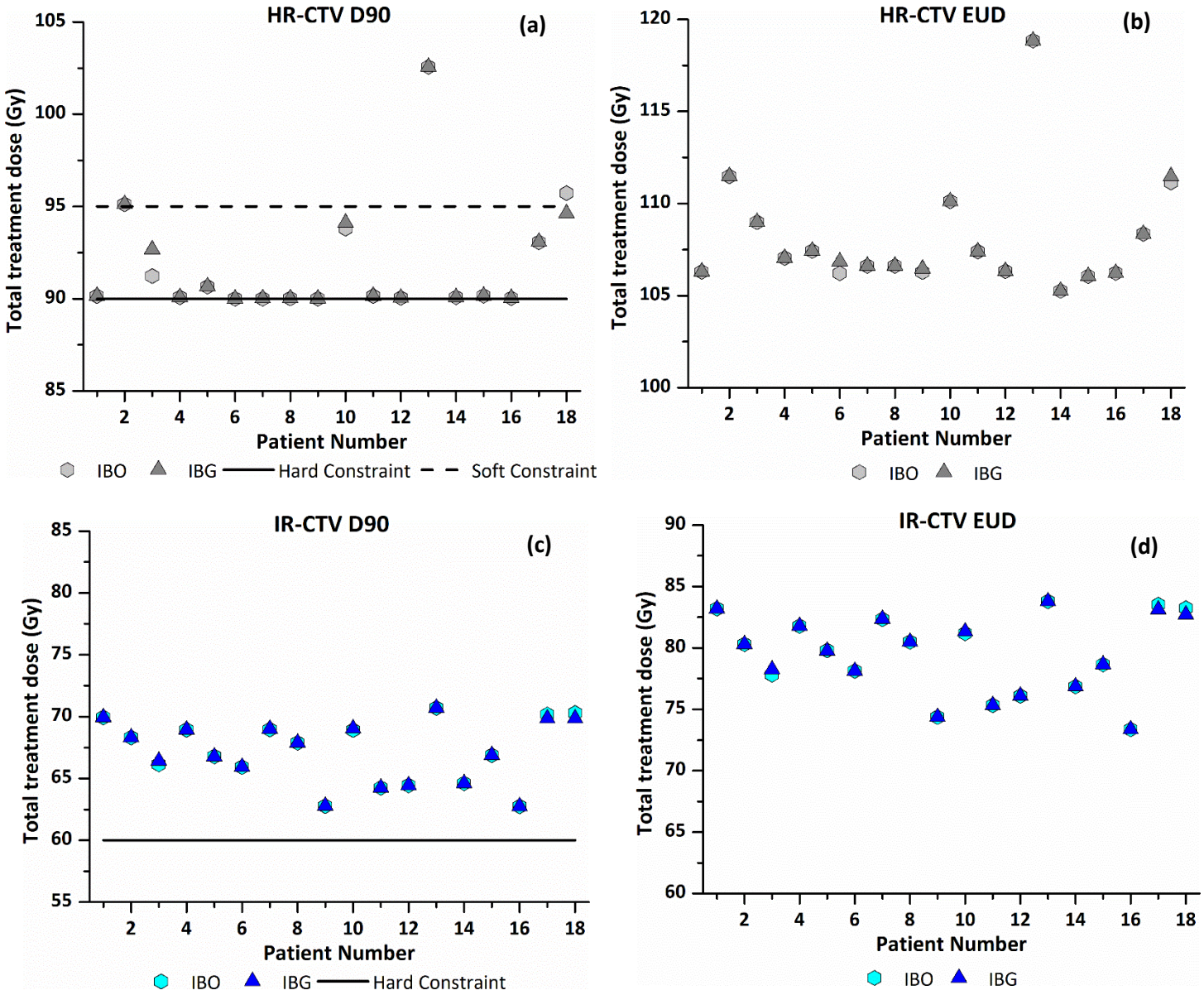


**Figure 40 - Comparison between the IBO and IBG approach per patient. CTV-$T_{HR}$ (a) $D_{90\,\%}$ and (b) EUD, CTV-$T_{IR}$ (c) $D_{90\,\%}$ and (d) EUD. Note: Data points for the IBO and IBG approach are indicated by hexagons and triangles, respectively.**

As illustrated in Figure 40, the CTV-$T_{IR}$ $D_{90\,\%}$ and EUD values were the same, with virtually no difference in patient 17 and 18 for the IBO and IBG approach. Average CTV-$T_{IR}$ EUD values of 79.46 ± 3.21 Gy and 79.44 ± 3.15 Gy were recorded for the IBO and IBG approach, respectively. The CTV-$T_{HR}$ EUD values were also comparable for the two approaches, except for patient 6 and 18, who recorded a higher value for the IBG approach compared to the IBO approach. Average CTV-$T_{HR}$ EUD values of 108.10 ± 3.20 Gy and 108.15 ± 3.13 Gy were recorded for the IBO and IBG approach, respectively. Considering the differences in CTV-$T_{HR}$ $D_{90\,\%}$ per patient, patient 3 and 18 reported differences in their CTV-$T_{HR}$ $D_{90\,\%}$ values. Patient 3 reported higher values for the IBG approach, in contrast to patient 18, who reported higher values for the IBO approach.

Seven patients received an average CTV-$T_{HR}$ $D_{90\,\%}$ value greater than the set $D_{90\,\%}$ hard constraint of 90Gy. The $D_{90\,\%}$ soft constraint of 95 Gy was reached in three patients. Patient 2 and 13 reached the 95 Gy constraint for both approaches, while patient 18 only reached the $D_{90\,\%}$ soft constraint for the IBO approach, with the IBG approach just falling short. The $D_{90\,\%}$ soft constraints for these three patients were reached without violating any OAR wall EUD constraints. Even though the OAR $D_{2cm^3}$ values were not incorporated as dose-limiting parameters during the IBO and IBG optimisation process, the $D_{2cm^3}$ values were still recorded and evaluated. When the corresponding OAR $D_{2cm^3}$ values for patient 2 and 13 are evaluated, it is noted that the small bowel hard constraint was violated. For patient 18, the bladder wall $D_{2cm^3}$ value was violated.

As mentioned earlier, the excessive CTV-$T_{HR}$ dose reported in patient 13 will not contribute to even better local control rates, and with this, the violation of the small bowel constraint is not justified.

The $D_{2cm^3}$, $D_{0.1cm^3}$, recto-vaginal reference point values for the IBO and IBG approach for the whole patient population are given in Table 22

**Table 22 – Average $D_{2cm^3}$ and $D_{0.1cm^3}$ values for all OAR walls of the IBO and IBG approach**

| | **Bladder wall** | **Small bowel** | **Rectum wall** | **Sigmoid wall** | **Recto-vaginal** |
|---|---|---|---|---|---|
| **Approach** | **$D_{2cm^3}$ (Gy) Average ± SD** | **$D_{2cm^3}$ (Gy) Average ± SD** | **$D_{2cm^3}$ (Gy) Average ± SD** | **$D_{2cm^3}$ (Gy) Average ± SD** | **Dose point (Gy) Average ± SD** |
| **IBO** | 78.73 ± 4.55 | 70.09 ± 7.69 | 64.30 ± 3.39 | 61.81 ± 4.39 | 67.67 ± 3.83 |
| **IBG** | 78.72 ± 4.50 | 70.07 ± 7.69 | 64.28 ± 3.44 | 61.77 ± 4.39 | 67.61 ± 3.93 |
| **Approach** | **Bladder wall $D_{0.1cm^3}$ (Gy)** | **Small bowel $D_{0.1cm^3}$ (Gy)** | **Rectum wall $D_{0.1cm^3}$ (Gy)** | **Sigmoid wall $D_{0.1cm^3}$ (Gy)** | **-** |
| **IBO** | 95.61 ± 8.18 | 81.67 ± 12.20 | 71.55 ± 4.95 | 70.64 ± 8.98 | - |
| **IBG** | 95.58 ± 8.10 | 81.66 ± 12.28 | 71.52 ± 5.03 | 70.53 ± 8.96 | - |

The IBO and IBG approach led to the same average $D_{2cm^3}$ and $D_{0.1cm^3}$ values for all the OAR walls, as summarised in Table 22. The outcome was again evaluated per patient Figure 41 and Figure 42.

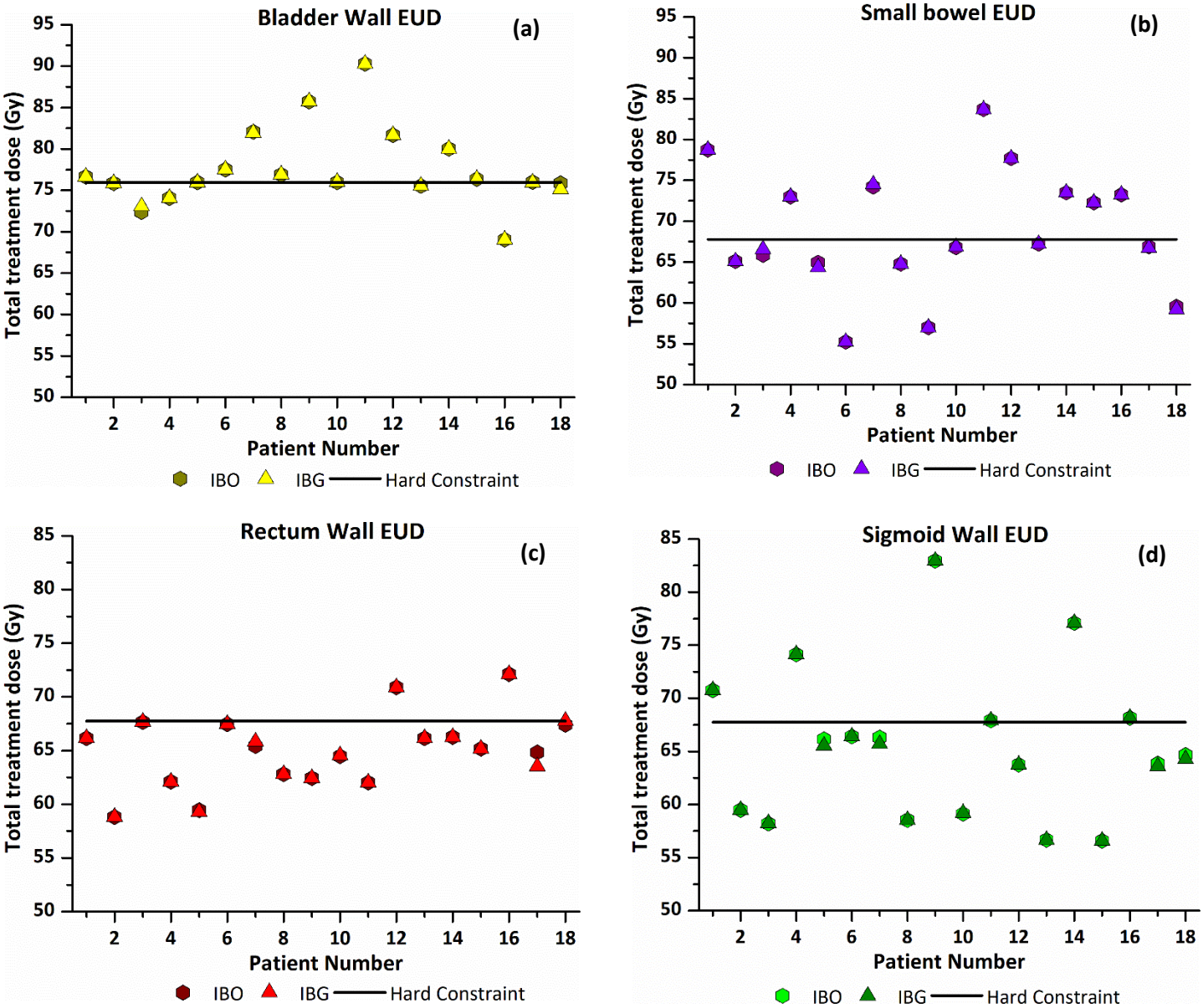


**Figure 41 - Comparison between the IBO and IBG approach per patient. The EUD values for (a) bladder wall, (b) small bowel, (c) rectum wall and (d) sigmoid wall. Note: Data points for the IBO and IBG approach are indicated by hexagons and triangles, respectively.**

As seen in Figure 41, the EUD hard constraint of the bladder wall was reached/violated in fifteen and fourteen patients, for the IBO and IBG approach, respectively. The average bladder wall EUD values of 77.66 ± 4.73 Gy and 77.64 ± 4.70 Gy were recorded for the IBO and IBG approach, respectively. The small bowel EUD hard constraint was reached/violated in eight patients for both approaches, with average small bowel EUD values of 68.87 ± 7.35 Gy and 68.86 ± 7.39 Gy for the IBO and IBG approach, respectively. The EUD hard constraint of the rectum wall was reached/violated in three patients with the IBO approach and in four patients with the IBG approach. The average rectum wall EUD values of 65.09 ± 3.39 Gy and 65.06 ± 3.44 Gy recorded for the IBO and IBG approach, respectively. The sigmoid wall was reached/violated in six patients for both approaches. The average sigmoid wall EUD was

65.59 ± 7.06 Gy and 65.49 ± 7.06 Gy for the IBO and IBG approach, respectively. The corresponding $D_{2cm^3}$ OAR values were recorded and plotted in Figure 42 below.

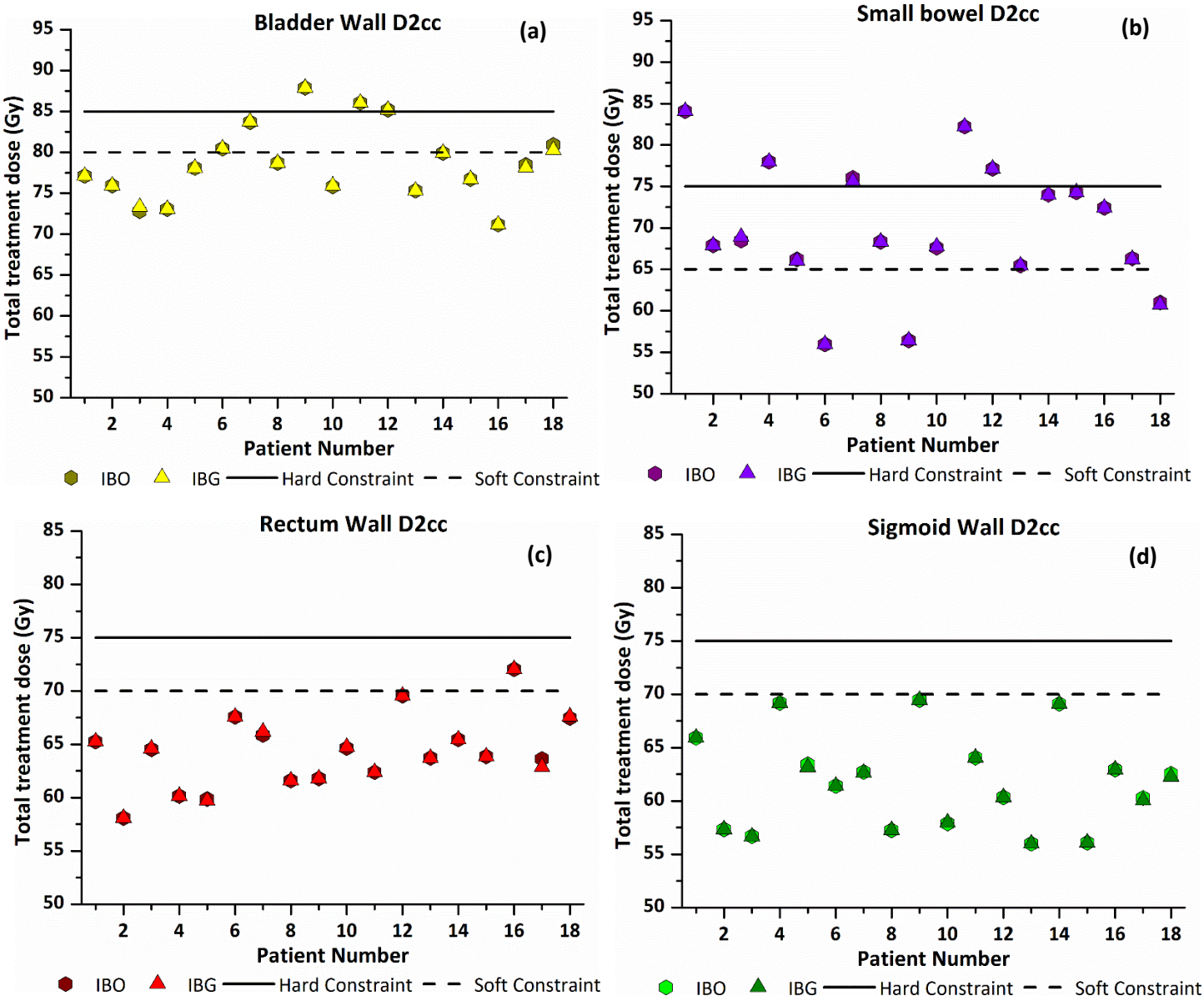


**Figure 42 - Comparison between the IBO and IBG approach per patient. The $D_{2cm^3}$ values for (a) bladder wall, (b) small bowel, (c) rectum wall and (d) sigmoid wall. Note: Data points for the IBO and IBG approach are indicated by hexagons and triangles, respectively.**

As illustrated in Figure 42, the $D_{2cm^3}$ hard constraint of the bladder wall was reached/violated in three patients, while the $D_{2cm^3}$ soft constraint was reached/violated in seven patients for both approaches. The average bladder wall $D_{2cm^3}$ were 78.73 ± 4.55 Gy and 78.72 ± 4.50 Gy for the IBO and IBG approach, respectively. The $D_{2cm^3}$ hard constraint of the small bowel was reached/violated in five patients, while the $D_{2cm^3}$ soft constraint of the small bowel was reached/violated in fifteen patients. The average small bowel $D_{2cm^3}$ were 70.09 ± 7.69 Gy and 70.07 ± 7.69 Gy for the IBO and IBG approach, respectively. The $D_{2cm^3}$ hard constraint of the rectum wall was not reached, while one patient violated the soft constraint of the rectum wall. The average rectum wall $D_{2cm^3}$ was 64.30 ± 3.39 Gy and 64.28 ± 3.44 Gy for the

IBO and IBG approach, respectively. The $D_{2cm^3}$ hard and soft constraint of the sigmoid wall were not reached/violated. The average sigmoid wall $D_{2cm^3}$ were 61.81 ± 4.39 Gy and 61.77 ± 4.39 Gy for the IBO and IBG approach, respectively.

When considering Figure 40 to Figure 42, the only patients with some significant difference between the two approaches is patient 3, 17 and 18. The rest of the patient population showed no significant difference between the approaches.

In patient 3, the IBG approach led to higher CTV-$T_{HR}$ EUD, $D_{90\,\%}$ and $D_{98\,\%}$ values of 1.49, 1.43 and 1.00 Gy. The small bowel $D_{2cm^3}$ soft constraint of 65 Gy was violated by both approaches; both approaches recorded the same small bowel $D_{2cm^3}$ value. All the other OAR $D_{2cm^3}$ constraints were still intact. None of the OAR EUD constraints was violated, but both approaches reached the rectum wall EUD hard constraint. The bladder wall and sigmoid wall $D_{0.1cm^3}$ values recorded were 1.05 and 1.13 Gy lower for the IBO approach. The recto-vaginal reference point recorded by the IBG approach was also 1.26 Gy higher than compared to the IBO approach, however still below the soft constraint of 65 Gy. No difference was noted between any other CTV-T or OAR parameters for this patient.

In patient 17, lower rectum wall EUD and $D_{0.1cm^3}$ values of 1.31 and 1.70 Gy were recorded by the IBG approach. The small bowel $D_{2cm^3}$ soft constraint of 65 Gy was violated by both approaches; both approaches recorded the same small bowel $D_{2cm^3}$ value. None of the OAR EUD constraints was violated, but both approaches reached the bladder wall EUD hard constraint. All the other OAR $D_{2cm^3}$ constraints were still intact. No difference was noted between any other CTV-T or OAR parameters for this patient.

In patient 18, the IBO approach led to higher CTV-$T_{HR}$ EUD and $D_{90\,\%}$ values of 1.22 and 1.09 Gy. The bladder wall $D_{2cm^3}$ soft constraint of 80 Gy was violated by both approaches with similar bladder wall $D_{2cm^3}$ values. None of the OAR EUD constraints was violated, but both approaches reached the rectum and bladder wall EUD hard constraint. The bladder wall $D_{0.1cm^3}$ values recorded were 1.45 Gy lower for the IBG approach. All the other OAR $D_{2cm^3}$ constraints were still intact. No difference was noted between any other CTV-T or OAR parameters for this patient.

**Other parameters that were recorded:**

The dose to point A and TRAK values are summarised in Table 23. No difference was recorded between the ICO and ICG average TRAK and dose to point A values.

**Table 23 - Average dose to point A and TRAK values of IBO and IBG approach**

| Approach | $A_{Left}$ (Gy) | $A_{Right}$ (Gy) | TRAK (cGy at 1 m) |
|---|---|---|---|
| **IBO** | 83.54 ± 13.42 | 82.02 ± 15.45 | 1.77 ± 0.24 |
| **IBG** | 83.87 ± 13.54 | 82.22 ± 15.54 | 1.77 ± 0.24 |

The difference between the IBO and IBG approach is negligible; however, some individuals did benefit more from the IBG approach. For this reason, between the two reported approaches, the IBG approach is selected as the preferred approach in this study.

### b.3) Inverse Conventional Greedy (ICG) vs Inverse Biological Greedy (IBG)

The most preferred Inverse Conventional (IC) and Inverse Biological (IB) approach are compared with one another, the Inverse Conventional Greedy (ICG) approach versus Inverse Biological Greedy (IBG) approach (see section b.1) and b.2)). Table 24 provides the average CTV-$T_{HR}$ and CTV-$T_{IR}$ $D_{90\,\%}$ $D_{98\,\%}$ and $D_{100\,\%}$ values obtained for the ICG and IBG approach.

**Table 24 - Average CTV-T $D_{90\,\%}$ $D_{98\,\%}$ and $D_{100\,\%}$ values for the ICG and IBG approach**

| Approach | CTV-$T_{HR}$ $D_{90\,\%}$ (Gy) | CTV-$T_{HR}$ $D_{98\,\%}$ (Gy) | CTV-$T_{HR}$ $D_{100\,\%}$ (Gy) | CTV-$T_{IR}$ $D_{90\,\%}$ (Gy) | CTV-$T_{IR}$ $D_{98\,\%}$ (Gy) | CTV-$T_{IR}$ $D_{100\,\%}$ (Gy) |
|---|---|---|---|---|---|---|
| **ICG** | 91.22 ± 2.57 | 80.67 ± 2.93* | 73.66 ± 3.25* | 66.44 ± 2.42* | 62.79 ± 2.10 | 60.57 ± 1.82 |
| **IBG** | 91.86 ± 3.13 | 81.53 ± 3.38* | 74.39 ± 3.57* | 67.13 ± 2.47* | 63.43 ± 2.27 | 61.11 ± 1.97 |

***Tested for the significant difference with a p-value ≤ 0.05.**

The evaluated results, see Table 24, showed that the IBG approach led to significantly better average CTV-$T_{HR}$ $D_{98\,\%}$ and $D_{100\,\%}$ values and CTV-$T_{IR}$ $D_{90\,\%}$ values, with a significant difference with $p \leq 0.05$. The outcome of the two approaches is also evaluated per patient and displayed in Figure 43 to Figure 45. As illustrated in Figure 43, five patients benefited a great deal from the IBG approach when the CTV-$T_{HR}$ $D_{90\,\%}$ values are evaluated, while only one patient benefited from the ICG approach instead of the IBG approach.

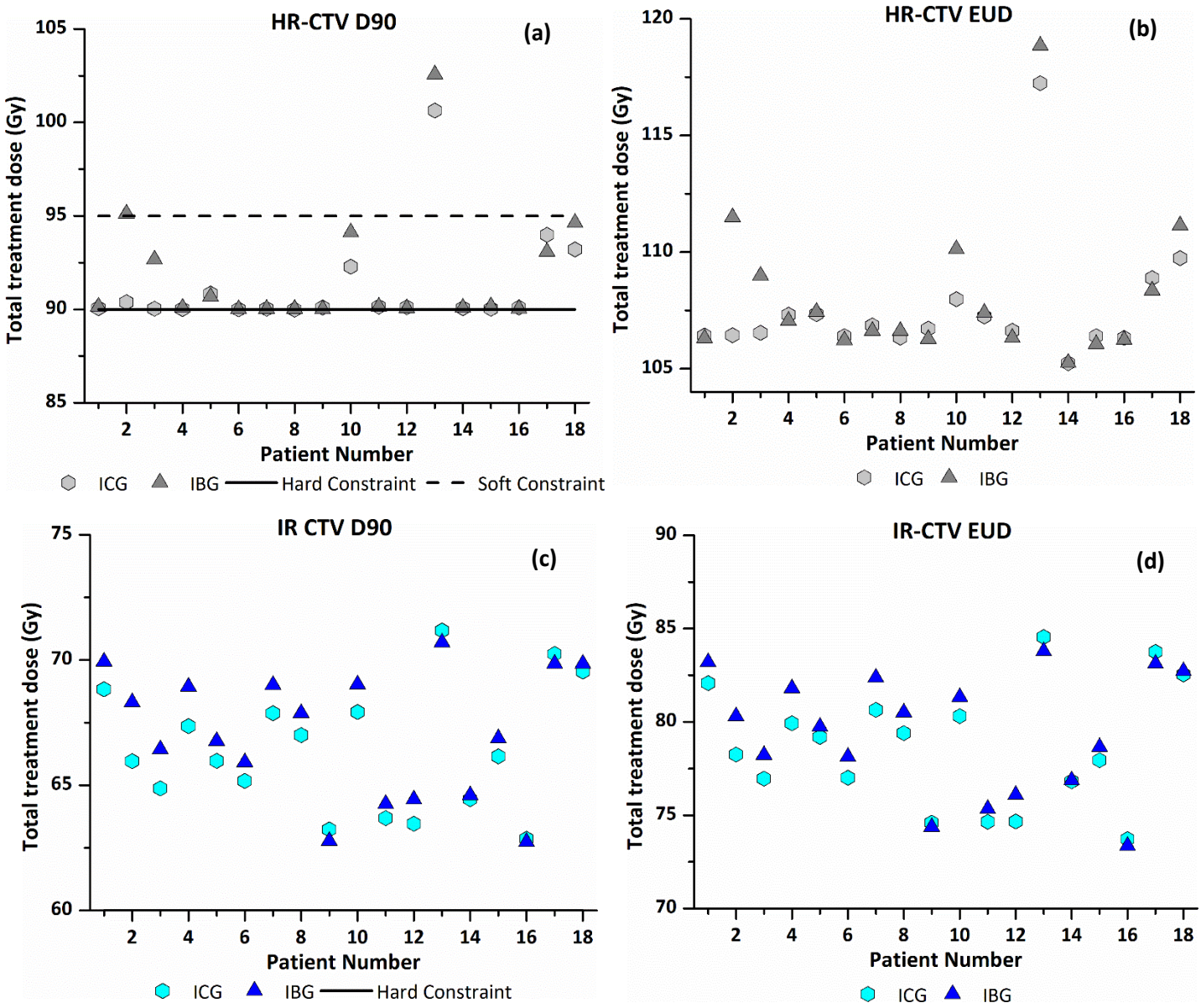


**Figure 43 - Comparison between the ICG and IBG approach per patient. CTV-$T_{HR}$ (a) $D_{90\,\%}$ and (b) EUD, CTV-$T_{IR}$ (c) $D_{90\,\%}$ and (d) EUD. Note: Data points for the ICG and IBG approach are indicated by hexagons and triangles, respectively.**

Patient 2, 3, 10, 13 and 18 recorded higher CTV-$T_{HR}$ $D_{90\,\%}$ and EUD values for the IBG approach compared to the ICG approach. A difference of up to 4.98 % and 4.53 % was recorded for these patients for the CTV-$T_{HR}$ $D_{90\,\%}$ and EUD values, respectively. The difference observed in patient 7, that might appear as if the ICG approach resulted in better CTV-T dose, compared to the IBG approach, was of no significant value. Average CTV-$T_{HR}$ EUD values of 107.55 ± 2.55 Gy and 108.15 ± 3.13 Gy were recorded for the ICG and IBG approach, respectively, which showed no significant difference considering the whole patient population. The average CTV-$T_{IR}$ $D_{90\,\%}$ and EUD values displayed significant differences between the two approaches, with $p \leq 0.05$; therefore, the outcome of the IBG approach led to better CTV-$T_{IR}$ dose compared to the ICG approach. Average CTV-$T_{IR}$ EUD values of

78.73 ± 3.15 Gy and 79.44 ± 3.15 Gy were recorded for the ICG and IBG approach, respectively. Table 25 displays the corresponding $D_{2cm}^3$ and $D_{0.1cm}^3$ values for the OAR walls as well as the recto-vaginal reference point values obtained for the ICG and IBG approach across the whole population.

**Table 25 – Average $D_{2cm}^3$ and $D_{0.1cm}^3$ values for all OAR walls of the ICG and IBG approach**

| | **Bladder wall** | **Small bowel** | **Rectum wall** | **Sigmoid wall** | **Recto-vaginal** |
|---|---|---|---|---|---|
| **Approach** | **$D_{2cm}^3$ (Gy) Average ± SD** | **$D_{2cm}^3$ (Gy) Average ± SD** | **$D_{2cm}^3$ (Gy) Average ± SD** | **$D_{2cm}^3$(Gy) Average ± SD** | **Dose point (Gy) Average ± SD** |
| **ICG** | 78.89 ± 4.69 | 69.39 ± 7.79* | 64.15 ± 3.92 | 61.77 ± 5.04 | 67.79 ± 3.89 |
| **IBG** | 78.72 ± 4.50 | 70.07 ± 7.69* | 64.28 ± 3.44 | 61.77 ± 4.39 | 67.61 ± 3.93 |
| **Approach** | **Bladder wall $D_{0.1cm}^3$ (Gy)** | **Small bowel $D_{0.1cm}^3$ (Gy)** | **Rectum wall $D_{0.1cm}^3$ (Gy)** | **Sigmoid wall $D_{0.1cm}^3$ (Gy)** | **-** |
| **ICG** | 97.86 ± 9.59* | 81.84 ± 13.61 | 71.63 ± 6.17 | 71.21 ± 12.00 | - |
| **IBG** | 95.58 ± 8.10* | 81.66 ± 12.28 | 71.52 ± 5.03 | 70.53 ± 8.96 | - |

***Tested for the significant difference with a p-value ≤ 0.05.**

From the result set out in Table 25, the small bowel $D_{2cm}^3$ values displayed a significant difference between the two approaches. When considering the entire patient population, the ICG approach led to lower small bowel $D_{2cm}^3$ values compared to the IBG approach. The bladder wall $D_{0.1cm}^3$ also tested for a significant difference between the two approaches, with the IBG approach reporting lower values compared to the ICG approach. The rest of the average reported parameters for the OAR volumes showed no significant difference between the approaches.

The OAR dose results per patient that were obtained for the ICG and IBG approach are displayed below in Figure 44 and Figure 45. The variation in OAR dose between the two approaches for all OAR walls is evident.

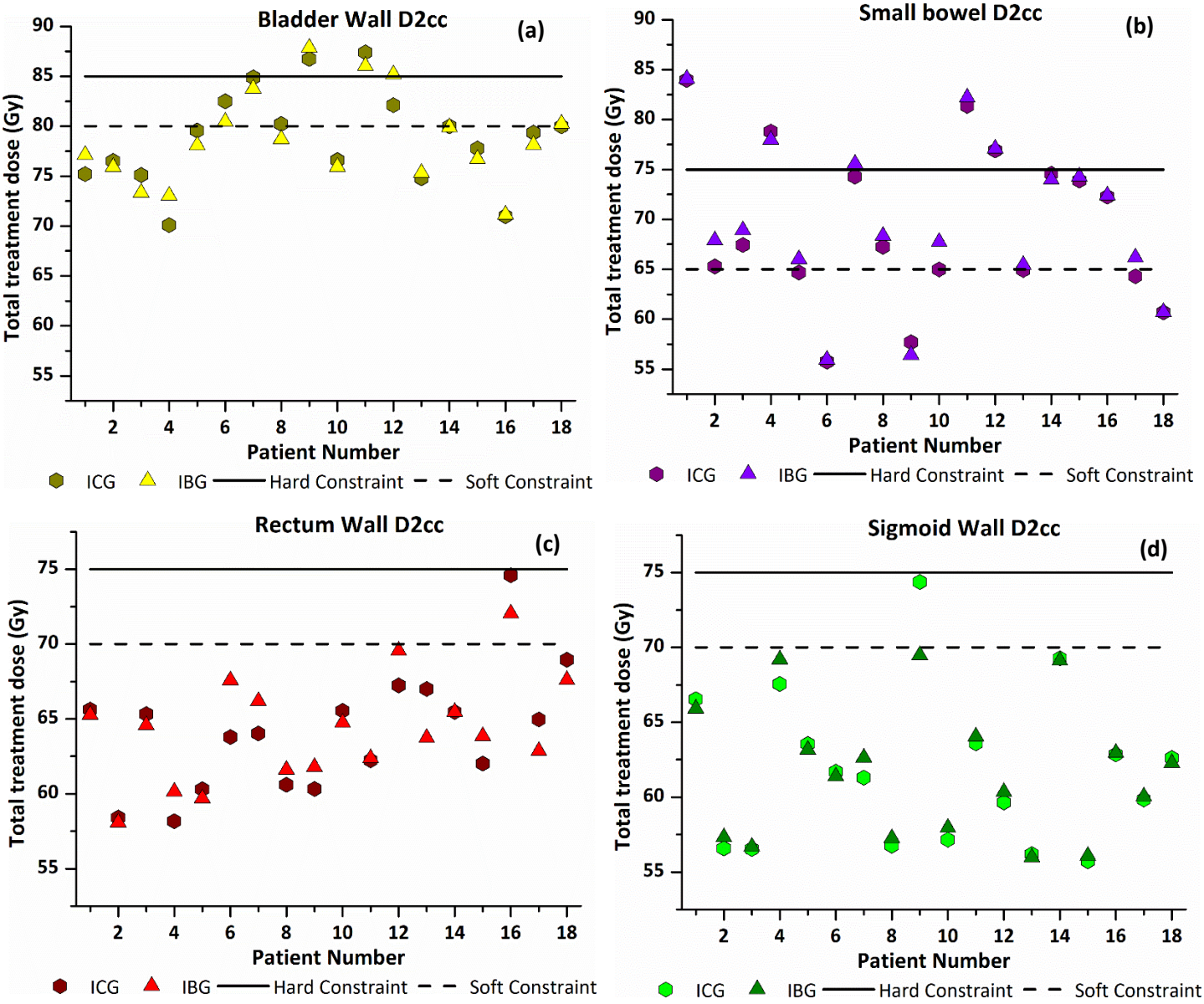


**Figure 44 - Comparison between the ICG and IBG approach per patient. The $D_{2cm^3}$ values for (a) bladder wall, (b) small bowel, (c) rectum wall and (d) sigmoid wall. Note: Data points for the ICG and IBG approach are indicated by hexagons and triangles, respectively**

As illustrated in Figure 44, lower bladder wall $D_{2cm^3}$ values were reported for the ICG approach in seven patients, whereas the IBG approach reported lower bladder wall $D_{2cm^3}$ values in eleven patients. Lower small bowel $D_{2cm^3}$ values were reported for the ICG approach in 14 patients compared to the four patients of the IBG approach. The outcome of the rectum wall $D_{2cm^3}$ values was the same as for the bladder walls, lower rectum wall $D_{2cm^3}$ values were reported for the ICG approach in seven patients, whereas the IBG approach recorded lower rectum wall $D_{2cm^3}$ values in eleven patients.

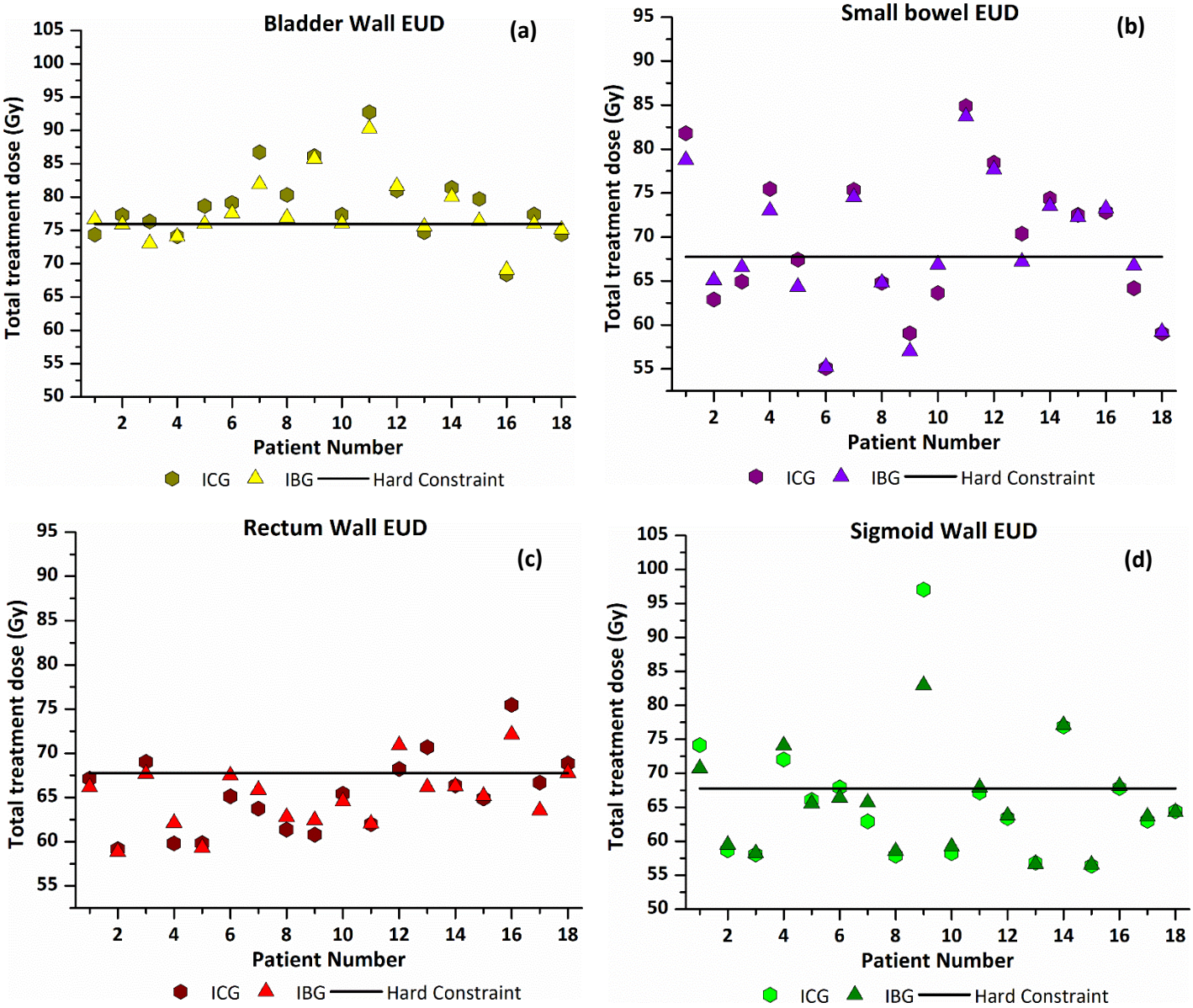


**Figure 45 - Comparison between the ICG and IBG approach per patient. The EUD values for (a) bladder wall, (b) small bowel, (c) rectum wall and (d) sigmoid wall. Note: Data points for the ICG and IBG approach are indicated by hexagons and triangles, respectively.**

Figure 45 displays the comparison between ICG and IBG approach in terms of the EUD values for all OAR walls. Lower bladder wall EUD values were recorded for the ICG approach in five patients. The IBG approach recorded lower bladder wall EUD values in twelve patients, and the same bladder wall EUD value was reported in one patient the approach. The average bladder wall EUD values recorded were 78.90 ± 5.40 Gy and 77.64 ± 4.70 Gy for the ICG and IBG approach, respectively, with the IBG approach reported lower values compared to the ICG approach. The difference in the average bladder wall EUD between the two approaches was of significant value with a p-value ≤ 0.05. The average small bowel EUD values recorded were 69.29 ± 8.03 Gy and 68.86 ± 7.39 Gy for the ICG and IBG approach, respectively. The small bowel EUD values were lower in ten patients with the IBG approach, while seven reported lower values with the ICG approach. The average rectum wall EUD values

recorded were 65.25 ± 4.22 Gy and 65.06 ± 3.44 Gy for the ICG and IBG approach, respectively. The ICG approach led to lower sigmoid wall EUD values in eight patients, where the IBG approach reported lower sigmoid wall EUD values in four patients. Sigmoid wall EUD values were the same in six patients irrespective of the approach. The average sigmoid wall EUD values recorded were 66.05 ± 9.55 Gy and 65.49 ± 7.06 Gy for the ICG and IBG approach, respectively.

The difference between the two approaches was evaluated per patient, by considering all the reported OAR and CTV-T doses simultaneously, as illustrated in Figure 43 to Figure 45.

In patient 1, the sigmoid wall EUD constraint of 67.75 Gy was violated by both approaches. However, the IBG approach ensured a lower sigmoid wall EUD value of 3.42 Gy, compared to the ICG approach. The IBG approach also led to a lower sigmoid wall $D_{0.1cm^3}$ value of 4.37 Gy compared to ICG. The bladder wall EUD constraint of 75.95 Gy was only violated by the IBG approach. The ICG approach produced a plan that presented with lower bladder wall EUD, $D_{2cm^3}$ and $D_{0.1cm^3}$ values of 2.29 Gy, 1.92 Gy and 3.58 Gy, respectively. However, the bladder wall $D_{2cm^3}$ soft and hard constraint was not reached by either of the two approaches and was therefore not the OAR of main concern in this case. The rectum wall EUD and $D_{0.1cm^3}$ values recorded were 1.0 Gy and 1.35 Gy lower for IBG approach compared to the ICG approach. The recto-vaginal reference point hard constraint of 75 Gy proposed by Tanderup et al. was reached only by the ICG approach [191]. The probability of developing vaginal stenosis (G ≥ 2) in this case is 27 % [192] . The IBG produced a plan that was 1.14 Gy lower for the recto-vaginal point, and this will, in effect, lead to a lower probability of developing vaginal stenosis (G ≥ 2). The small bowel $D_{2cm^3}$ hard and soft constraint was violated in both approaches. The small bowel EUD and $D_{0.1cm^3}$ recorded for the IBG approach was 3.06 Gy and 5.61 Gy lower compared to ICG approach. The same CTV-$T_{HR}$ values were recorded, but the EUD, $D_{90\,\%}$ and $D_{98\,\%}$ for the CTV-$T_{IR}$ was 1.12 Gy, 1.1 Gy and 1.03 Gy higher in the IBG approach compared to ICG approach. An increase in CTV-$T_{IR}$ $D_{90\,\%}$ and $D_{98\,\%}$ have been found to affect local control (LC), and even though the difference is relatively small, the IBG approach still outweighs the ICG approach [193]. With this said, the IBG approach reduced the dose in OAR volumes which were of main concern, sigmoid wall, recto-vaginal reference point and small bowel in this case. Therefore, the benefits of the plan produced by the IBG approach in patient 1 outweigh the plan produced by the ICG approach.

In patient 2, the sigmoid wall $D_{0.1cm^3}$ was 1.15 Gy higher for IBG approach compared to ICG approach. However, neither the EUD nor $D_{2cm^3}$ constraints were reached by both the approaches. With the same bladder wall $D_{2cm^3}$, bladder wall EUD and $D_{0.1cm^3}$ were 1.43 Gy and 2.68 Gy lower for IBG approach

[191] (Tanderup *et al.*, 2020)
[192] (Kirchheiner *et al.*, 2016)
[193] (Tanderup *et al.*, 2016)

compared to ICG approach. The small bowel EUD, $D_{2cm^3}$ and $D_{0.1cm^3}$ were 2.20 Gy, 2.59 Gy and 3.87 Gy higher for IBG compared to ICG approach, with the IBG violating the $D_{2cm^3}$ soft constraint of 65 Gy. The CTV-$T_{HR}$ EUD, $D_{90\,\%}$ and $D_{98\,\%}$ were higher by 5.05 Gy, 4.74 Gy and 5.95 Gy for the IBG approach compared to the ICG approach. The LC in this case for limited to intermediate size CTV-$T_{HR}$ volume of 22 $cm^3$ is 96 %, with a CTV-$T_{HR}$ $D_{90\,\%}$ of 95 Gy instead of a LC of 94 % for a 90 Gy CTV-$T_{HR}$ $D_{90\,\%}$.[194] With this said, the IBG approach also produced higher CTV-$T_{IR}$ EUD, $D_{90\,\%}$ and $D_{98\,\%}$ of 2.05 Gy, 2.35 Gy and 2.41 Gy compared to ICG approach. Even though the IBG approach violated the main OAR of concern, in this case, the small bowel $D_{2cm^3}$ soft constraint, the $D_{2cm^3}$ was still far from reaching the hard constraint of 75 Gy. Therefore, the increase in LC for the plan developed by the IBG approach outweigh the plan produced by the ICG approach.

In patient 3, the plan produced by the IBG approach led to lower bladder wall EUD, $D_{2cm^3}$ and $D_{0.1cm^3}$ values of 3.29 Gy, 1.79 Gy, 5.02 Gy compared to ICG approach. The rectum wall EUD and $D_{0.1cm^3}$ was also 1.34 Gy and 1.76 Gy lower for the IBG approach. Both approaches violated the small bowel $D_{2cm^3}$ soft constraint; however, the EUD, $D_{2cm^3}$, and $D_{0.1cm^3}$ values reported was 1.63 Gy, 1.46 Gy and 2.70 Gy higher for the IBG approach compared to ICG approach. Although the small bowel $D_{2cm^3}$ soft constraint was reached, the $D_{2cm^3}$ hard constraint was still far from being reached. The soft constraint of the recto-vaginal point, 65 Gy, was only reached by the ICG approach. The IBG plan recorded a 1.0 Gy lower recto-vaginal point dose compared to the ICG approach. Higher CTV-$T_{HR}$ EUD, $D_{90\,\%}$ and $D_{98\,\%}$ of 2.45 Gy, 2.63 Gy and 2.58 Gy was recorded for the IBG approach compared to ICG approach. Also, higher CTV-$T_{IR}$ EUD, $D_{90\,\%}$ and $D_{98\,\%}$ of 1.27 Gy, 1.55 Gy and 1.39 Gy were recorded for the IBG approach. This will improve the LC, although small. The reduction in the recto-vaginal dose will also reduce the probability of developing vaginal stenosis (G ≥ 2), and in this case, the plan produced by the IBG approach was superior to the ICG approach.

In patient 4, the overall performance of the ICG approach was superior to the IBG approach. Lower sigmoid wall EUD, $D_{2cm^3}$ and $D_{0.1cm^3}$ of 2.08 Gy, 1.63 Gy and 2.56 Gy was reported for the ICG approach. A lower bladder wall $D_{2cm^3}$ of 2.95 Gy was recorded for the ICG approach. Again, lower rectum wall EUD, $D_{2cm^3}$ and $D_{0.1cm^3}$ values of 2.28 Gy, 1.97 Gy, 3.08 Gy was recorded for the ICG approach. Small bowel EUD and $D_{2cm^3}$ hard constraints were violated for both the approaches, values reported had no significant difference between the two approaches. Lower small bowel EUD and $D_{0.1cm^3}$ of 2.48 Gy and 4.61 Gy for the IBG approach was recorded. The recto-vaginal reference point was 3.22 Gy higher in the IBG approach, which will increase the risk of vaginal stenosis (G ≥ 2). The same CTV-$T_{HR}$ $D_{90\,\%}$ value was recorded; however, higher CTV-$T_{IR}$ EUD, $D_{90\,\%}$ and $D_{98\,\%}$ of 1.86 Gy, 1.57 Gy and 1.32 Gy were

[194] (Tanderup *et al.*, 2016)

reported for the IBG approach. The benefits of the ICG approach outweigh the IBG approach in this case.

In patient 5, the same CTV-T values were recorded for both approaches. The ICG approach only reached the bladder wall and small bowel $D_{2cm^3}$ soft constraint. The bladder wall EUD hard constraint was violated by the ICG approach and only reached in the IBG approach. Lower bladder wall EUD, $D_{2cm^3}$ and $D_{0.1cm^3}$ values of 2.73 Gy, 1.49 Gy and 4.28 Gy were recorded for the IBG approach. The EUD hard constraint of the small bowel was only reached by the ICG approach. The reported small bowel EUD value was 3.11 Gy lower for the IBG approach compared to ICG approach, with lower $D_{2cm^3}$ and $D_{0.1cm^3}$ values of 1.31 Gy and 1.77 Gy for the ICG approach. Sigmoid and rectum wall $D_{2cm^3}$ and EUD values reported were well below the set constraints, with no significant difference between the two approaches. The IBG approach reported lower EUD values in the bladder wall and small bowel, which were violated and reached by the ICG approach. Therefore, the IBG approach led to a superior plan in terms of OAR dose compared to the ICG approach.

In patient 6, the ICG approach reached the EUD hard constraint of the sigmoid wall. The plan produced by the IBG approach led to lower sigmoid wall EUD and $D_{0.1cm^3}$ values of 1.54 Gy and 1.64 Gy compared to ICG approach. Both approaches violated the bladder wall $D_{2cm^3}$ soft constraint; however, the IBG approach managed to report lower bladder wall EUD, $D_{2cm^3}$ and $D_{0.1cm^3}$ values of 1.64 Gy, 2.05 Gy and 3.73 Gy compared to ICG approach. None of the rectum wall $D_{2cm^3}$ constraints was reached; however, the IBG approach reached the EUD hard constraint. The ICG approach recorded lower rectum wall EUD, $D_{2cm^3}$ and $D_{0.1cm^3}$ values of 2.33 Gy, 3.79 Gy and 4.49 Gy. No significant difference was observed in the CTV-T values between the approaches.

When evaluating the relationship between the $D_{2cm^3}$ and late grade 2-4 (G2-4) side-effects for both the rectum and the bladder, it is noticed that the rectum has a steeper dose-effect curve compared to the bladder [195]. With this said, the rectum constraints take priority over the bladder during the planning and optimisation process [196]. Rectum wall $D_{2cm^3}$ values of 67.58 Gy and 63.79 Gy were reported by the ICG and IBG approach, respectively. These reported rectum wall $D_{2cm^3}$ values fall in two different sub-groups for the probability of late rectal morbidity and rectal bleeding. The 67.58 Gy $D_{2cm^3}$ value will cause the probability of G2-4 rectal morbidity and rectal bleeding to be 15.1 % and 6.3 %, respectively. With ICG approach value of 63.79 Gy, the probability is lower; therefore, the probability of G2-4 rectal morbidity and rectal bleeding is 8.6 % and 5.2 %, respectively. Taking this into account, the ICG approach outweighs the IBG approach.

[195] (Georg *et al.*, 2012)
[196] (Tanderup *et al.*, 2020)

In patient 7, no significant difference was observed in the CTV-T values between the approaches. None of the sigmoid wall constraints was reached, yet ICG approach led to lower sigmoid wall EUD, $D_{2cm^3}$ and $D_{0.1cm^3}$ values of 2.78 Gy, 1.33 Gy and 3.66 Gy compare to the IBG approach. The bladder wall $D_{2cm^3}$ hard constraint was only reached by the ICG approach, where both approaches reached the bladder wall $D_{2cm^3}$ soft constraint. The IBG approach reported lower bladder wall EUD, $D_{2cm^3}$ and $D_{0.1cm^3}$ values of 4.84 Gy, 1.15 Gy and 8.38 Gy compared to ICG approach. For both approaches, none of the rectum wall constraints was reached; however, the ICG approach recorded lower rectum wall EUD, $D_{2cm^3}$ and $D_{0.1cm^3}$ values of 2.09 Gy, 2.15 Gy, 2.93 Gy. The $D_{2cm^3}$ hard constraint of the small bowel was reached by both approaches, the IBG reporting a higher $D_{2cm^3}$ value of 1.31 Gy, but lower $D_{0.1cm^3}$ value of 1.02 Gy compared to ICG approach. A recto-vaginal reference point of 4.37 Gy higher was reported in the IBG approach compared to ICG approach.

In patient 8, the $D_{2cm^3}$ soft constraint of the bladder wall was only reached by the ICG approach. Both approaches violated the bladder wall EUD hard constraint, while the IBG approach recorded lower bladder wall EUD, $D_{2cm^3}$ and $D_{0.1cm^3}$ values of 3.45 Gy, 1.53 Gy and 6.15 Gy, respectively, compared to ICG approach. No soft or hard constraints of the rectum wall were reached by either approach yet the ICG produced lower EUD, $D_{2cm^3}$ and $D_{0.1cm^3}$ values of 1.41 Gy, 1.0 Gy, 1.86 Gy, respectively, compared to the IBG approach. Both approaches reached the $D_{2cm^3}$ soft constraint of the small bowel, but the ICG delivered a plan which had a lower small bowel $D_{2cm^3}$ value of 1.07 Gy. The ICG approach reported a lower recto-vaginal reference point of 2.42 Gy. The same CTV-T EUD, $D_{90\,\%}$ and $D_{98\,\%}$ values were recorded for both approaches. The bladder constraints take priority in this case; therefore, the IBG approach led to the superior plan compared to the IBG approach.

In patient 9, the EUD hard constraint of the sigmoid wall was violated by both approaches, while the ICG approach only violated the $D_{2cm^3}$ soft constraint. The IBG plan reported lower sigmoid wall EUD, $D_{2cm^3}$ and $D_{0.1cm^3}$ values of 14.09 Gy, 4.9 Gy and 17.09 Gy compared to ICG approach. Both approaches violated the $D_{2cm^3}$ hard constraint, the ICG approach, however, led to a lower bladder wall $D_{2cm^3}$ value of 1.13 Gy. None of the rectum wall or small bowel constraints was reached, yet the ICG approach led to lower rectum wall EUD, $D_{2cm^3}$ and $D_{0.1cm^3}$ values of 1.64 Gy, 1.47 Gy and 2.41 Gy. Small bowel EUD and $D_{2cm^3}$ values of 2.07 Gy and 1.27 Gy lower were recorded for IBG approach. The soft constraint of the recto-vaginal point was only reached by the IBG approach with a value 2.73 Gy higher. The same CTV-T EUD, $D_{90\,\%}$ and $D_{98\,\%}$ values were recorded for both approaches. During the optimisation process, the hard constraint of the CTV-T and OAR was given priority. Therefore, the OAR of main concern, in this case is the sigmoid wall, the IBG approach led to significantly lower values compared to the ICG approach and therefore are chosen as the approach of choice.

In patient 10, the IBG approach produced a plan with higher CTV-T values. Higher CTV-$T_{HR}$ EUD, $D_{90\,\%}$ and $D_{98\,\%}$ values of 2.15 Gy, 1.84 Gy and 1.62 Gy and higher CTV-$T_{IR}$ EUD, $D_{90\,\%}$ and $D_{98\,\%}$ values of 1.02 Gy, 1.09 Gy and 1.14 Gy were recorded for the IBG approach. No constraints were reached for the sigmoid wall; however, the ICG approach led to a lower sigmoid wall $D_{0.1cm^3}$ value of 1.14 Gy. Both approaches reached the EUD hard constraint of the bladder wall, and the IBG approach reported lower bladder wall EUD and $D_{0.1cm^3}$ values of 1.33 Gy and 1.76 Gy, respectively. None of the rectum wall constraints was reached; however, the IBG approach reported a lower rectum wall $D_{0.1cm^3}$ value of 1.31 Gy. Both approaches reached the $D_{2cm^3}$ soft constraint of the small bowel. Small bowel EUD and $D_{2cm^3}$ values of 3.21 Gy and 2.73 Gy higher were reported for the IBG approach. A lower recto-vaginal reference point of 1.0 Gy was recorded for the IBG approach. The reduction of the small bowel values outweighs the reduction in bladder dose as the $D_{2cm^3}$ constraints of the bladder wall was still well intact. The increase in the CTV-T doses does not justify the increase in small bowel dose, as the small increase in CTV-T dose will not have an immense impact on the local control. With this said, the ICG approach produced a plan which was superior to the IBG approach.

In patient 11, no significant difference was observed in the CTV-T values between the approaches. Both approaches violated the $D_{2cm^3}$ hard constraint of 85 Gy; however, the IBG approach led to lower bladder wall EUD, $D_{2cm^3}$ and $D_{0.1cm^3}$ values of 2.44 Gy, 1.37 Gy and 5.1 Gy, compared to ICG approach. The small bowel $D_{2cm^3}$ hard constraint of 75 Gy was also violated by both approaches. The IBG approach leads to lower small bowel EUD and $D_{0.1cm^3}$ values of 1.19 Gy and 2.22 Gy compared to ICG approach. The rest of the OAR volumes had no significant difference between the two approaches, and therefore it is evident that the IBG approach produced a plan superior of the ICG approach.

In patient 12, the ICG approach clearly produced a plan which was superior to the IBG approach. The IBG approach violated the bladder wall $D_{2cm^3}$ hard constraint, where the ICG approach only violated the $D_{2cm^3}$ soft constraint of 80 Gy. The ICG approach recorded a lower bladder wall $D_{2cm^3}$ value of 3.06 Gy. Both approaches violated the rectum wall EUD constraint of 67.75 Gy but with lower rectum wall EUD, $D_{2cm^3}$ and $D_{0.1cm^3}$ values of 2.70 Gy, 2.31 Gy and 3.62 Gy recorded by the ICG approach. The $D_{2cm^3}$ hard constraint of the small bowel was violated by both approaches; however, the IBG recorded lower small bowel $D_{0.1cm^3}$ values of 1.45 Gy compared to ICG approach. A recto-vaginal dose of 3.7 Gy higher was reported for the IBG approach compared to the ICG approach. No significant difference was observed in the CTV-T values between the approaches. Even though the IBG approach led to a lower small bowel $D_{0.1cm^3}$ value, the ICG approach led to more significant benefits when the other OAR volumes were considered.

In patient 13, no significant difference was observed in the CTV-T values between the approaches. However, when considering the outcome of the IBG approach regarding OAR values, it is clear that the IBG produced a superior plan compared to the ICG approach. The bladder wall EUD constraint was reached by both approaches, however with the same value. The IBG recorded a higher bladder wall $D_{0.1cm^3}$ value of 1.82 Gy compared to ICG approach. The rectum wall EUD hard constraint of 67.75 Gy was only violated by the ICG approach, significant lower rectum wall EUD, $D_{2cm^3}$ and $D_{0.1cm^3}$ values of 4.55 Gy, 3.28 Gy and 6.12 Gy were reported for the IBG approach compared to ICG approach. The small bowel EUD hard constraint was only violated by the ICG approach, where the $D_{2cm^3}$ soft constraint was reached by both approaches, yet a small bowel EUD of 3.18 Gy lower was recorded for IBG approach compared to ICG approach. A significant lower recto-vaginal dose of 4.84 Gy was recorded for the IBG approach, which will decrease the risk of vaginal stenosis (G ≥ 2).

Patient 14: Both approaches violated the bladder wall hard constraint; however, the IBG approach recorded lower bladder wall EUD and $D_{0.1cm^3}$ values of 1.34 Gy and 2.7 Gy compared to ICG approach. The small bowel $D_{2cm^3}$ soft constraint and EUD hard constraint was reached/violated by both approaches. The IBG plan produced a lower small bowel $D_{0.1cm^3}$ value of 1.26 Gy compared to ICG approach. The sigmoid wall EUD hard constraint was reached by both approaches, reaching the same EUD values. The same CTV-T dose values were reported for both approaches. When considering these results, the IBG approach led to a better plan compared to the ICG approach.

In patient 15, the small bowel $D_{2cm^3}$ soft constraint and EUD hard constraint was reached/violated by both approaches; however, both approaches recorded the same EUD and $D_{2cm^3}$ values. Both approaches violated the bladder wall EUD hard constraint, but the IBG approach had the ability the record lower bladder wall EUD, $D_{2cm^3}$ and $D_{0.1cm^3}$ values of 3.36 Gy, 1.06 Gy and 7.17 Gy, respectively, compared to ICG approach. The hard and soft constraints of the rectum wall were still intact; nevertheless, the ICG recorded lower rectum wall $D_{2cm^3}$ and $D_{0.1cm^3}$ values of 1.82 Gy and 1.73 Gy compared to IBG approach. A lower recto-vaginal reference point of 2.96 Gy was recorded for the ICG approach. The same CTV-T dose values were reported for both approaches. The aim was to reach CTV-hard constraints with the OAR hard constraints limits still intact, the IBG approach, which led to a lower bladder wall EUD value was selected as the preferred approach.

In patient 16, the same CTV-$T_{HR}$ and CTV-$T_{IR}$ EUD, $D_{90\ \%}$ and $D_{98\ \%}$ values were reported for both approaches. Small bowel $D_{2cm^3}$ soft constraint of 65 Gy and EUD hard constraint was reached/violated by both approaches, though producing the same EUD and $D_{2cm^3}$ values. No bladder wall hard or soft constraints were reached in both approaches; still, the ICG approach led to lower bladder wall $D_{0.1cm^3}$ value of 1.17 Gy compared to the IBG approach. Both approaches violated the EUD hard constraint of the rectum wall. The IBG produced a plan with lower rectum wall EUD, $D_{2cm^3}$ and $D_{0.1cm^3}$ values of 3.33

Gy, 2.55 Gy and 4.97 compared to ICG approach. The IBG also recorded a lower recto-vaginal reference point of 3.97 Gy. The plan produced by the IBG approach was superior to the ICG approach.

In patient 17, the same CTV-$T_{HR}$ and CTV-$T_{IR}$ EUD, $D_{90\,\%}$ and $D_{98\,\%}$ values were reported for both approaches. Both approaches reached the bladder and rectum wall EUD hard constraints. However, the IBG approach produced lower bladder wall EUD, $D_{2cm^3}$ and $D_{0.1cm^3}$ values of 1.44 Gy, 1.25 Gy and 2.68 Gy compared to ICG approach. The IBG approach also produced lower rectum wall EUD, $D_{2cm^3}$ and $D_{0.1cm^3}$ values of 3.16 Gy, 2.12 Gy and 4.19 Gy compared to ICG approach. Even though the IBG produced higher small bowel EUD, $D_{2cm^3}$ and $D_{0.1cm^3}$ values of 2.55 Gy, 1.9 Gy and 4.17 Gy compared to ICG approach, none of the small bowel hard or soft constraints was reached. The ICG approach violated the recto-vaginal soft constraint, while the IBG approach produced a lower recto-vaginal reference point of 3.36 Gy, which will decrease the risk of vaginal stenosis (G ≥ 2). The dose planning aim was to reach (1) target hard constraint, (2) then hard constraints of OAR and (3) then only were there given priority to the soft constraints of both targets and OARs. With this said, the IBG produced a better plan.

In patient 18, it is clear that the IBG approach produced a better plan compared to the ICG approach. The IBG approach led to lower rectum wall EUD, $D_{2cm^3}$ and $D_{0.1cm^3}$ of 1.1 Gy and 1.35 Gy and 1.23 Gy compared to ICG approach. The IBG approach also recorded a lower recto-vaginal reference point of 1.24 Gy. Higher CTV-$T_{HR}$ EUD, $D_{90\,\%}$ and $D_{98\,\%}$ of 1.4 Gy, 1.42 Gy and 1.33 Gy were recorded for the IBG approach. All other CTV-T and OAR parameters had no significant difference.

**Other parameters that were recorded:**

The dose to point A and TRAK values are summarized in Table 26. No significant difference was found between the two approaches.

**Table 26 - Average dose to point A and TRAK values of ICG and IBG approach**

| Approach | $A_{Left}$ (Gy) | $A_{Right}$ (Gy) | TRAK (cGy at 1 m) |
|---|---|---|---|
| **ICG** | 85.50 ± 22.64 | 81.77 ± 15.99 | 1.73 ± 0.24 |
| **IBG** | 83.87 ± 13.54 | 82.22 ± 15.54 | 1.77 ± 0.24 |

The significantly higher average CTV-$T_{HR}$ $D_{98\,\%}$, $D_{100\,\%}$ values and CTV-$T_{IR}$ EUD, $D_{90\,\%}$ $D_{98\,\%}$ and $D_{100\,\%}$ values led to improved dose distributions within the CTV-T; with this, the IBG also managed to record significant lower average bladder wall EUD and $D_{0.1cm^3}$ values. Even though the ICG approach reported significant lower average small bowel $D_{2cm^3}$ values displayed a significant difference compared to the

ICG approach, both approaches were still well below the $D_{2cm^3}$ hard constraint of 75 Gy. Considering these results, the benefits from the IBG approach outweigh the benefits of the ICG approach.

### b.4) Inverse Biological Greedy (IBG) vs Forward Biological Optimistic (FBO)

The best inverse, Inverse Biological Greedy (IBG) and forward approach, Forward Biological Optimistic (FBO) were compared (see sections b.3) and a.3)). The results are evaluated by considering the response on an individual basis between the two approaches, as seen in Figure 46 through Figure 48.

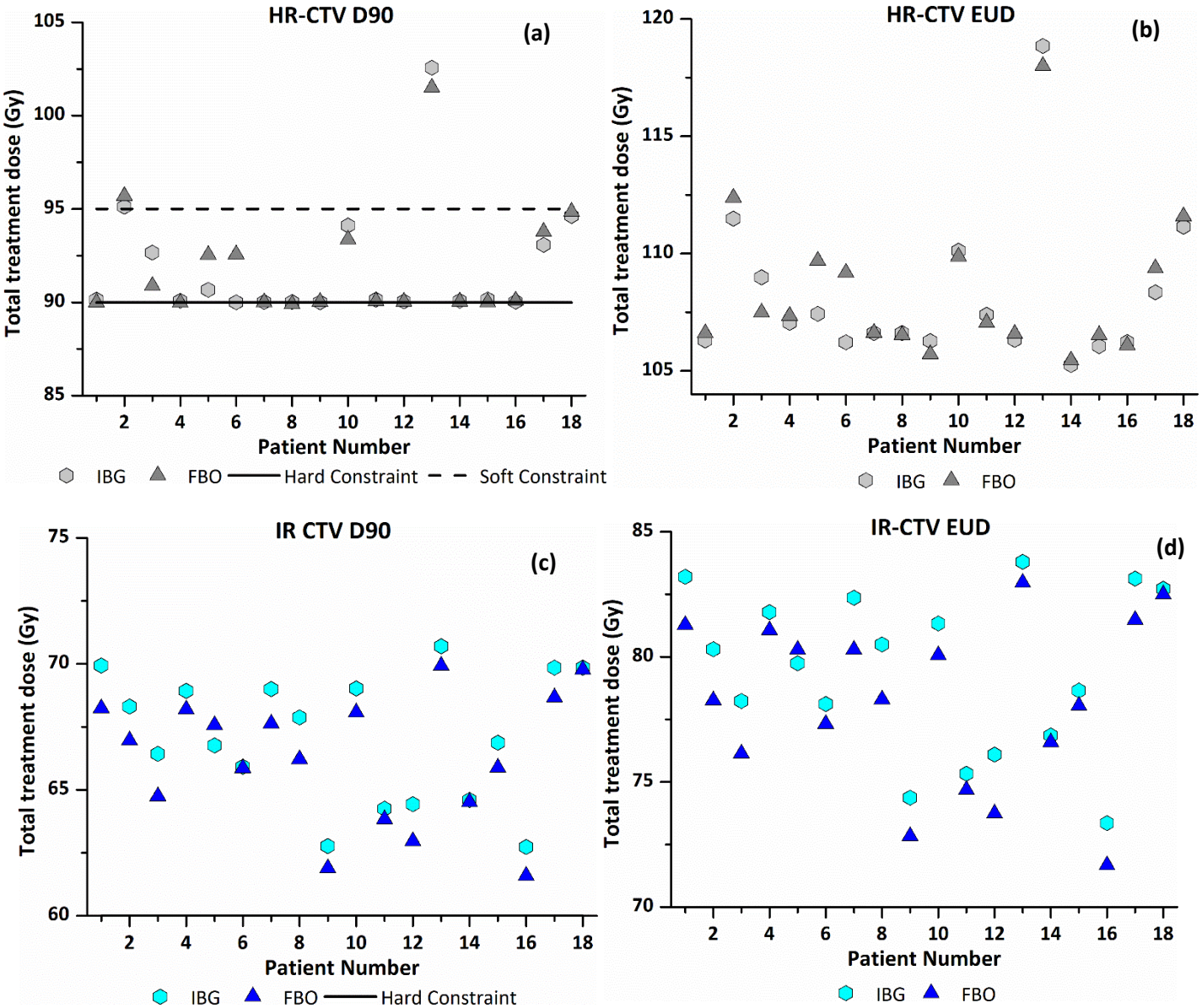


**Figure 46 - Comparison between the IBG and FBO approach per patient. CTV-T HR (a) $D_{90\,\%}$ and (b) EUD, CTV-T IR (c) $D_{90\,\%}$ and (d) EUD. Note: Data points for the IBG and FBO approach are indicated by hexagons and triangles, respectively.**

The results depicted in Figure 46 shows a significant variation in the CTV-T dose values for the IBG and FBO approach. When considering the CTV-$T_{HR}$ $D_{90\,\%}$ values, the same $D_{90\,\%}$ value of 90 Gy was recorded

in ten patients irrespective of the approach. Higher $D_{90\,\%}$ values up to 2.78 % were reported in five patients with the FBO approach, higher $D_{90\,\%}$ values of up to 2.02 % were reported in three patients with the IBG approach. Average CTV-$T_{HR}$ EUD values of 108.15 ± 3.13 Gy and 108.44 ± 3.03 Gy were recorded for the IBG and FBO approach, respectively. Differences of up to 3.19 % and 2.61 % were reported for the CTV-$T_{IR}$ $D_{90\,\%}$ and EUD values. The FBO approach showed a difference in CTV-$T_{IR}$ $D_{90\,\%,}$ and EUD values in only one patient, the IBG approach, on the other hand, reported higher CTV-$T_{IR}$ $D_{90\,\%}$ and EUD values in seventeen patients. The average EUD and $D_{90\,\%}$ values for the CTV-$T_{IR}$ showed significant difference with a p-value ≤ 0.05. Average CTV-$T_{IR}$ EUD values of 79.44 ± 3.15 Gy and 78.19 ± 3.27 Gy were recorded for the IBG and FBO approach, respectively. The IBG approach tends to use the requirement of dose to the CTV-$T_{IR}$ volume more effectively. Therefore, the dose gradient is shallower for the inverse approach compared to the forward approach. Though this is good for tumour dose coverage, it might be bad for OAR volumes or the OAR volumes might receive the same dose as with the forward optimisation approach. The OAR dose results per patient that were obtained for the IBG and FBO approach are displayed in Figure 47 and Figure 48.

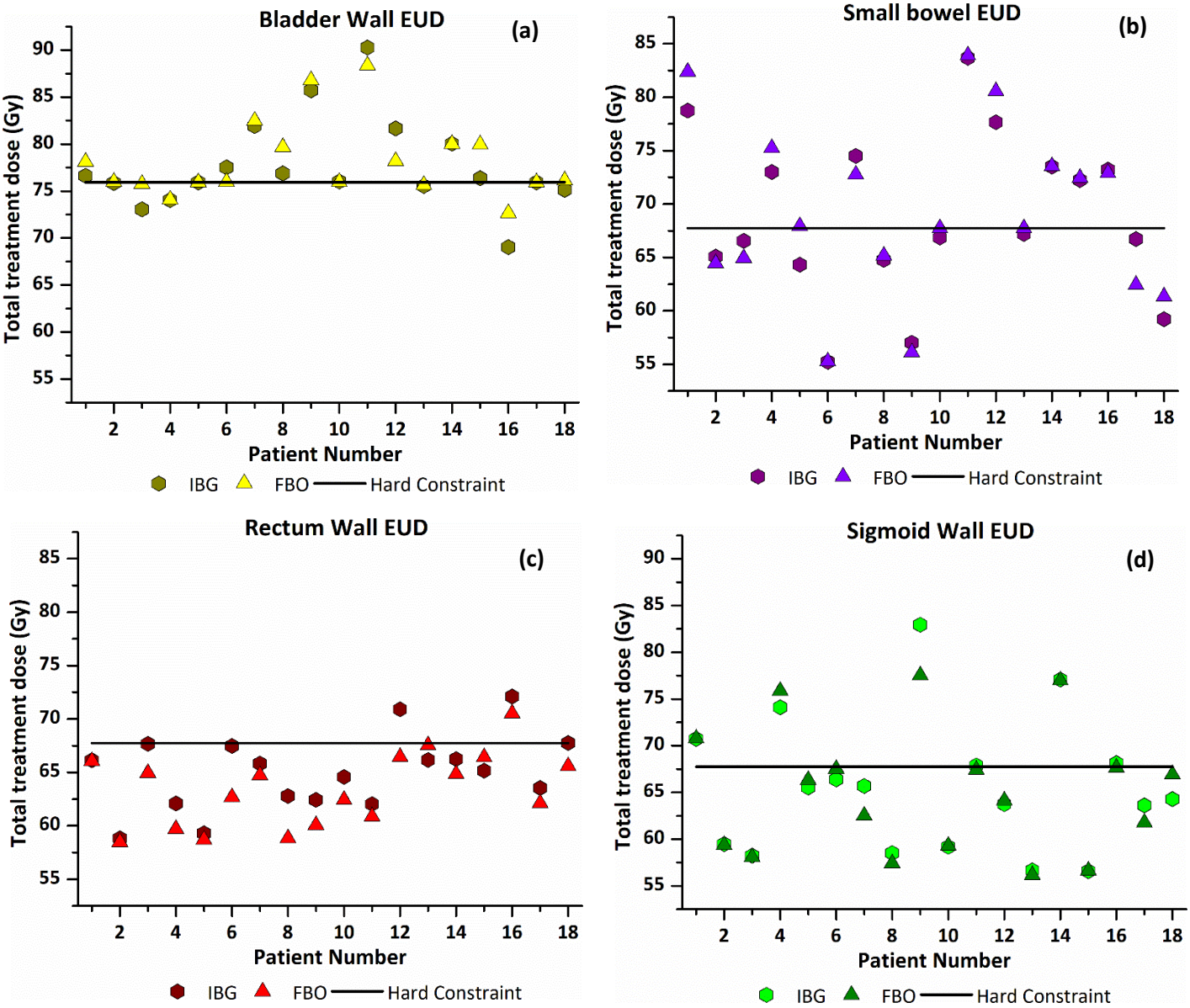


**Figure 47 - Comparison between the IBG and FBO approach per patient. The EUD values for (a) bladder wall, (b) small bowel, (c) rectum wall and (d) sigmoid wall. Note: Data points for the IBG and FBO approach are indicated by hexagons and triangles, respectively.**

The results in Figure 47 shows an ambivalent response to the two different approaches. Average bladder wall EUD values for the whole patient population were reported as 77.64 ± 4.70 Gy and 78.19 ± 4.04 Gy for the IBG and FBO approach, respectively. Average small bowel EUD values for the whole patient population were reported as 68.86 ± 7.39 Gy and 69.26 ± 7.99 Gy for the IBG and FBO approach, respectively. A significant difference with $p \leq 0.05$, was found between the reported average rectum wall EUD values between the approaches. Average rectum wall EUD values for the whole patient population were reported as 65.06 ± 3.44 Gy and 63.38 ± 3.38 Gy for the IBG and FBO approach, respectively. Even though the FBO approach led to lower EUD values for the rectum wall, there was only one hard constraint violation compared to the two violations for the IBG approach. Average sigmoid wall EUD values for the whole patient population were reported as 65.49 ± 7.06 Gy and 65.12

± 6.72 Gy for the IBG and FBO approach, respectively. The IBG approach exploited the EUD hard constraint of the rectum and sigmoid wall, to ensure lower bladder wall and small bowel EUD values, which is seen as the two most violated OAR walls among the four OAR walls.

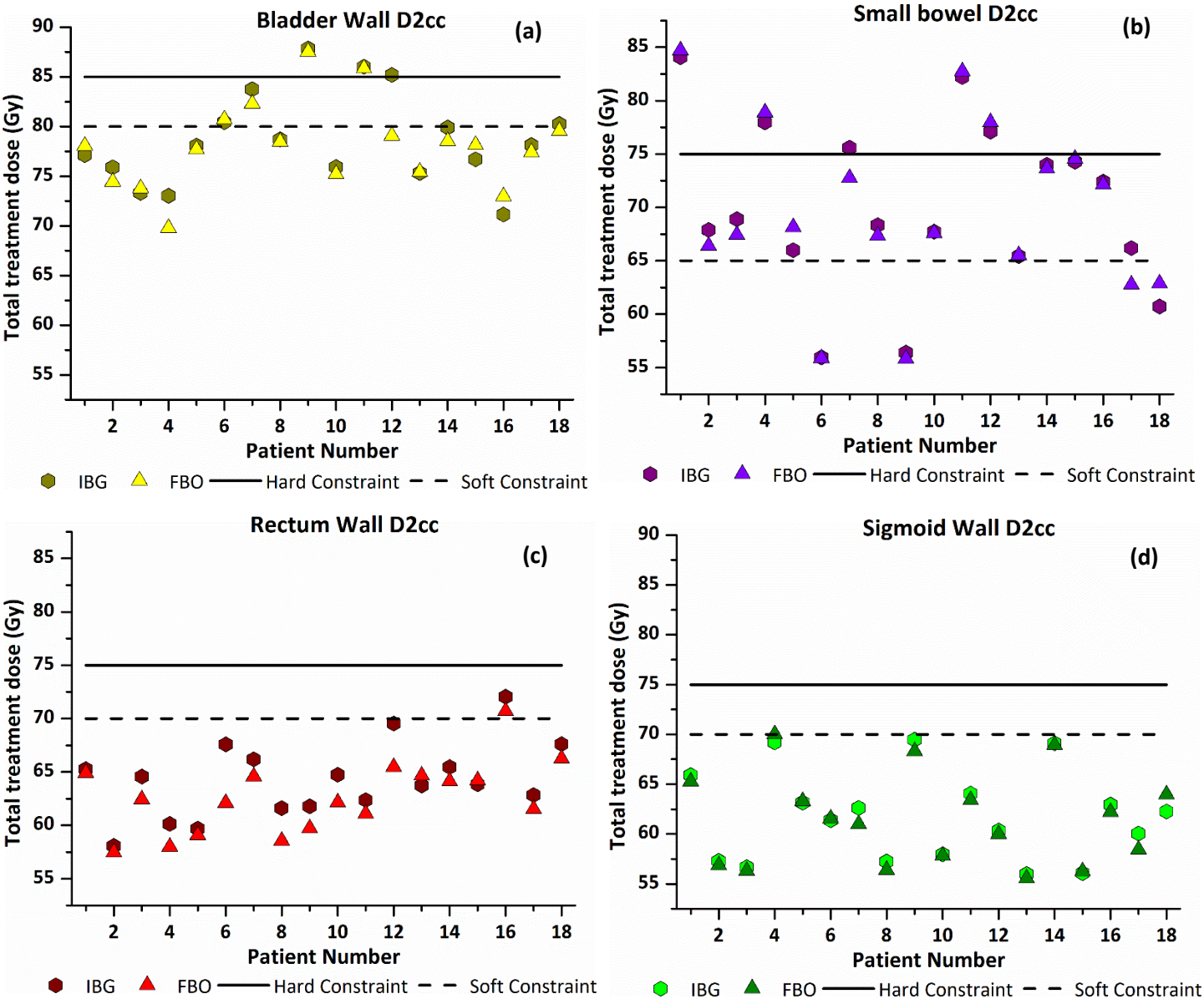


**Figure 48 - Comparison between the IBG and FBO approach per patient. The D 2 cm3 values for (a) bladder wall, (b) small bowel, (c) rectum wall and (d) sigmoid wall. Note: Data points for the IBG and FBO approach are indicated by hexagons and triangles, respectively**

As seen in Figure 48, given the bladder wall $D_{2cm^3}$ hard constraint, it was reached/violated in three patients for the IBG approach and two patients for the FBO approach. The bladder wall $D_{2cm^3}$ soft constraint was reached/violated in seven patients for the IBG approach and in five patients, for the FBO approach. Small bowel $D_{2cm^3}$ hard constraint was reached/violated in five and four patients, for the IBG and FBO approach, respectively. The small bowel $D_{2cm^3}$ soft constraint was reached/violated in fifteen for the IBG approach, and fourteen patients for the FBO approach. The rectum and sigmoid wall $D_{2cm^3}$ values were higher for the IBG approach; however, no hard constraint was ever

reached/violate by the IBG or FBO approach. When considering the $D_{2cm^3}$ soft constraint violation, the rectum wall soft constraint was violated in one patient by both approaches. The sigmoid wall soft constraint was reached by the FBO approach only. The difference between the two approaches was evaluated per patient by considering all the reported OAR and CTV-T doses simultaneously.

In patient 1, the EUD hard constraint of the bladder wall was reached by both approaches. However, the IBG approach produced lower bladder wall EUD and $D_{0.1cm^3}$ values of 1.44 Gy and 2.58 Gy compared to FBO approach. The EUD hard constraint of the sigmoid wall was violated by both approaches, with no difference between them. The $D_{2cm^3}$ hard constraint of 75 Gy for the small bowel was reached, and both approaches violated the EUD hard constraint of 67.75 Gy. However, the IBG approach led to lower small bowel EUD and $D_{0.1cm^3}$ values of 3.64 Gy and 6.28 Gy compared to the FBO approach. No significant difference was observed in the CTV-$T_{HR}$ $D_{90\,\%}$. EUD, $D_{90\,\%}$ and $D_{98\,\%}$ values between the two approaches. Higher CTV-$T_{IR}$ values of 1.93 Gy, 1.69 Gy and 1.07 Gy were recorded for the IBG approach compared to FBO approach. The rest of the OAR values showed no significant difference between the two approaches. Considering the CTV-T and OAR doses, the IBG approach led to a superior plan compared to the FBO approach.

In patient 2, the EUD hard constraint of the bladder wall was reached by both approaches, with no difference between them. Neither approaches reached the $D_{2cm^3}$ bladder wall constraints. Still, the IBG approach, however, recorded a higher bladder wall $D_{2cm^3}$ value of 1.47 Gy compared to FBO approach. The small bowel $D_{2cm^3}$ soft constraint of 65 Gy was violated by both approaches, and the IBG approach recorded higher small bowel $D_{2cm^3}$ and $D_{0.1cm^3}$ values of 1.49 Gy and 1.43 Gy compared to FBO approach. The soft constraint of the recto-vaginal point proposed by Tanderup et al.[197] of 65 Gy, was not reached by either of the two approaches. The IBG approach recorded a higher recto-vaginal reference point of 1.88 Gy compared to the FBO approach. However, the IBG approach led to higher CTV-$T_{IR}$ EUD, $D_{90\,\%}$ and $D_{98\,\%}$ values of 2.04 Gy, 1.35 Gy and 1.27 compared to FBO approach. Parameters like the CTV-$T_{HR}$ $D_{90\,\%}$ and $D_{98\,\%}$ and CTV-$T_{IR}$ $D_{98\,\%}$ have been proven to be associated with better local control [198]. The planning aim was to reach the hard constraint of the targets, which was achieved and then to obey the set of hard constraints of the OAR volumes, after that the soft constraints of the targets took priority above the soft constraints of the OAR volumes. With this said, the higher CTV-$T_{IR}$ values recorded by the IBG approach justify the higher OAR doses as none of the OAR which hard constraints were reached showed no difference between the two approaches.

[197] (Tanderup *et al.*, 2020)
[198] (Johannes C A Dimopoulos *et al.*, 2009; Mazeron *et al.*, 2015; Tanderup *et al.*, 2016)

In patient 3, higher CTV-$T_{HR}$ and CTV-$T_{IR}$ values were observed for the IBG approach, compared to the FBO approach. Higher CTV-$T_{HR}$ EUD, $D_{90\,\%}$ and $D_{98\,\%}$ values of 1.50 Gy, 1.78 Gy and 2.45 Gy was recorded for the IBG approach. Also, higher CTV-$T_{IR}$ EUD, $D_{90\,\%}$ and $D_{98\,\%}$ values of 2.1 Gy, 1.69 Gy and 1.24 Gy was reported for the IBG approach compared to FBO approach. Parameters like the CTV-$T_{HR}$ $D_{90\,\%}$ and $D_{98\,\%}$ and CTV-$T_{IR}$ $D_{98\,\%}$ have been proven to be associated with better local control. [199] The EUD hard constraint of the bladder wall was only reached by the FBO approach. The IBG approach led to lower bladder wall EUD and $D_{0.1cm^3}$ values of 2.69 Gy and 5.42 Gy compared to FBO approach. The small bowel $D_{2cm^3}$ soft constraint was reached by both approaches, with the IBG approach reporting higher small bowel EUD, $D_{2cm^3}$ and $D_{0.1cm^3}$ values of 1.61 Gy, 1.48 Gy and 2.77 Gy compared to FBO approach. The EUD hard constraint of the rectum wall was only reached by the IBG approach, while the FBO approach led to lower rectum wall EUD, $D_{2cm^3}$ and $D_{0.1cm^3}$ values of 2.74 Gy, 2.16 Gy and 4.24 Gy, respectively. The IBG approach also recorded a significant higher recto-vaginal reference point of 3.39 Gy. Even though a higher dose was observed for the rectum and recto-vaginal point by the IBG approach, it was still below the set soft constraint values. The rectum wall $D_{2cm^3}$ value recorded for the IBG approach was below the $D_{2cm^3}$ soft constraint of 70 Gy, it even conformed to the $D_{2cm^3}$ soft constraint proposed by Tanderup et al.[200] of 65 Gy. The recto-vaginal point also conformed to the soft constraint of 65 Gy. No OAR hard constraints were violated to allow higher dose values for CTV-T volumes; therefore, the IBG approach was selected as the preferred approach.

In patient 4, the IBG approach led to a higher CTV-$T_{HR}$ $D_{98\,\%}$ value of 1.61 Gy to FBO approach, the rest of the CTV-T values, however, had no significant difference between the two approaches. The sigmoid wall $D_{2cm^3}$ soft constraint was reached by both approaches, while both approaches violated the EUD hard constraint. The IBG approach produced a plan with lower sigmoid wall EUD and $D_{0.1cm^3}$ values of 1.75 Gy and 1.92 Gy compared to the FBO approach. None of the bladder or rectum wall constraints were reached by any of the two approaches; still, the FBO approach recorded a lower bladder wall $D_{2cm^3}$ value of 3.27 Gy. The FBO approach led to lower rectum wall EUD, $D_{2cm^3}$ and $D_{0.1cm^3}$ values of 2.41 Gy, 2.16 Gy and 3.27 Gy. The $D_{2cm^3}$ values of the rectum wall reported for the IBG and FBO approach were 60.14 and 57.98 Gy, respectively. The probability of grade 2-4 rectal morbidity and the risk of rectal bleeding is 8.6 % and 5.2 %, for the IBG approach. The probability for the FBO approach it is 6.5 % and 3.1 %, respectively [201]. The $D_{2cm^3}$ soft constraint of the small bowel was reached by both approaches, however, reporting the same $D_{2cm^3}$ value. The small bowel EUD hard constraint was violated by both approaches. The FBO approach led to lower small bowel EUD and $D_{0.1cm^3}$ values of

[199] (Johannes C A Dimopoulos *et al.*, 2009; Mazeron *et al.*, 2015; Tanderup *et al.*, 2016)
[200] (Tanderup *et al.*, 2020)
[201] (Mazeron *et al.*, 2016)

2.23 Gy and 4.05 Gy. The soft constraint of 65 Gy was violated by the IBG approach. The probability of developing vaginal stenosis (G ≥ 2) in this case was 20 % [202]. The FBO produced a plan that was 3.58 Gy lower for the recto-vaginal point, and this will, in effect, lead to a lower probability of developing vaginal stenosis (G ≥ 2). With this said, the FBO approach outweighs the IBG approach.

In patient 5, the FBO approach led to higher CTV-$T_{HR}$ EUD, $D_{90\,\%}$ and $D_{98\,\%}$ values of 2.25 Gy, 1.87 Gy and 1.85 Gy with a higher CTV-$T_{IR}$ $D_{98\,\%}$ value of 1.01 Gy as well. However, none of the sigmoid wall constraints were reached by any of the two approaches. Still, the IBG approach led to a lower sigmoid wall $D_{0.1cm^3}$ value of 1.14 Gy. The small bowel $D_{2cm^3}$ soft constraint and EUD hard constraint were violated by both approaches, lower small bowel EUD, $D_{2cm^3}$ and $D_{0.1cm^3}$ values of 3.59 Gy, 2.13 Gy and 7.34 Gy was recorded for the IBG approach. None of the approaches violated the soft constraint, and a higher recto-vaginal reference point of 1.21 Gy was reported by the IBG approach. No significant difference was reported between the approaches regarding the rectum and bladder wall values. The planning aim was to reach the hard constraint of the targets, which was achieved and then to obey the set hard constraints of the OAR volumes. The increase in dose to the CTV-T volumes does not justify the violation of the EUD hard constraint of the small bowel dose. Therefore, one can conclude that the IBG approach led to a superior plan compared to the FBO approach.

In patient 6, the FBO approach led to higher CTV-$T_{HR}$ EUD, $D_{90\,\%}$ and $D_{98\,\%}$ values of 2.96 Gy, 2.57 Gy and 2.14 Gy. Both approaches violated the sigmoid wall EUD constraint. The IBG approach reported lower sigmoid wall EUD and $D_{0.1cm^3}$ values of 1.12 Gy and 1.56 Gy. None of the bladder wall constraints was reached by any of the approaches. Nevertheless, lower bladder wall EUD and $D_{0.1cm^3}$ values of 1.57 Gy and 2.05 Gy were reported for the FBO approach. Again, none of the rectum wall constraints was reached by any of the approaches; still, the FBO approach managed to record significant lower rectum wall EUD, $D_{2cm^3}$ and $D_{0.1cm^3}$ values of 4.78 Gy, 5.5 Gy, 7.92 Gy. The $D_{2cm^3}$ values of the rectum wall reported for the IBG and FBO approach were 66.15 and 61.44 Gy, respectively. The probability of grade 2-4 rectal morbidity and the risk of rectal bleeding are 15.1% and 6.3 % for the IBG approach, however, for the FBO approach, it is 8.6 % and 5.2 %, respectively [203]. A recto-vaginal reference point of 4.73 Gy higher was reported for the IBG approach compared to FBO approach, the IBG approach violating the soft constraint. The lower recto-vaginal reference point value for the FBO approach will, in effect, lead to a lower probability of developing vaginal stenosis (G ≥ 2). When considering the higher CTV-T values and lower rectum wall and recto-vaginal dose point, the FBO approach led to a superior plan compared to the IBG approach.

[202] (Kirchheiner *et al.*, 2016)
[203] (Mazeron *et al.*, 2016)

In patient 7, the IBG approach recorded higher CTV-$T_{IR}$ EUD, $D_{90\,\%}$ and $D_{98\,\%}$ values of 2.08 Gy, 1.38 Gy and 1.18 Gy compared to the FBO approach. The rest of the CTV-T values, however, had no significant difference between the two approaches. The FBO approach led to lower values for all the OAR $D_{2cm^3}$ and EUD values. The EUD and $D_{2cm^3}$ hard constraint of the bladder wall was violated by both approaches, with the IBG approach recording a higher bladder wall $D_{2cm^3}$ value of 1.47 Gy. None of the sigmoid wall constraints was reached by any of the approaches; however, the IBG approach led to higher sigmoid wall EUD, $D_{2cm^3}$ and $D_{0.1cm^3}$ values of 3.20 Gy, 1.66 Gy and 4.31 Gy compared to FBO approach. None of the rectum wall constraints was reached by any of the two approaches; still, the FBO approach recorded lower rectum wall EUD, $D_{2cm^3}$ and $D_{0.1cm^3}$ values of 1.13 Gy, 1.60 Gy and 1.59 Gy. The EUD hard constraint of the small bowel was violated by both approaches; however, the $D_{2cm^3}$ hard constraint was only violated by the IBG approach. Therefore, the FBO approach led to lower small bowel EUD, $D_{2cm^3}$ and $D_{0.1cm^3}$ values of 1.75 Gy, 2.84 Gy and 3.42 Gy compared to IBG approach. Again, the IBG recorded a higher recto-vaginal reference point of 2.97 Gy compared to FBO approach, with only the IBG approach violating the proposed hard constraint of 75 Gy.[204] The benefits of the FBO approach, in this instance, clearly outweighs the IBG approach.

In patient 8, the IBG approach recorded higher CTV-$T_{IR}$ EUD, $D_{90\,\%}$ and $D_{98\,\%}$ values of 2.21 Gy, 1.67 Gy and 1.70 Gy compared to the FBO approach. The rest of the CTV-T values had no significant difference between the two approaches. None of the sigmoid wall constraints was reached by any of the approaches; nevertheless, the FBO approach let to lower sigmoid wall EUD and $D_{0.1cm^3}$ values of 1.12 Gy and 1.68 Gy. Both approaches violated the EUD hard constraint of the bladder wall; still, the IBG approach reported significant lower bladder wall EUD and $D_{0.1cm^3}$ values of 2.77 Gy and 5.36 Gy compared to FBO approach. Significant higher rectum wall EUD, $D_{2cm^3}$ and $D_{0.1cm^3}$ values of 3.96 Gy, 3.07 Gy, 5.52 Gy were recorded for the IBG approach compared to the FBO approach, even though, none of the rectum wall constraints were reached by any of the two approaches. The $D_{2cm^3}$ values of the rectum wall reported for the IBG and FBO approach were 61.61 Gy and 58.54 Gy, respectively. The probability of grade 2-4 rectal morbidity and the risk of rectal bleeding are 8.6 % and 5.2 %, for the IBG approach, however, for the FBO approach it is 6.5 % and 3.1 %, respectively [205]. The small bowel $D_{2cm^3}$ soft constraint was reached by both approaches, while the FBO approach reported a lower small bowel $D_{2cm^3}$ value of 3.42 Gy. A 6.47 Gy higher recto-vaginal reference point was reported by the IBG approach compared to FBO approach, and this led to the IBG approach violating the soft constraint of 65 Gy. The lower recto-vaginal reference point value for the FBO approach will, in effect, lead to a lower probability of developing vaginal stenosis (G ≥ 2). When considering the higher CTV-T values

[204] (Tanderup *et al.*, 2020)
[205] (Mazeron *et al.*, 2016)

and lower rectum wall and recto-vaginal dose point, the FBO approach led to a superior plan compared to the IBG approach.

In patient 9, the CTV-T values had no significant difference between the two approaches, except for a small difference in the CTV-$T_{IR}$ EUD value. The IBG approach led to a higher CTV-$T_{IR}$ EUD value of 1.54 Gy compared to the FBO approach. A higher small bowel $D_{0.1cm^3}$ value of 1.51 Gy was reported for the IBG approach compared to FBO approach. The bladder wall $D_{2cm^3}$ hard constraint of 85 Gy was reached in both approaches. However, both approaches recorded the same $D_{2cm^3}$ value. The EUD hard constraint of the bladder wall was violated by both approaches, with the IBG approach reporting lower bladder wall EUD and $D_{0.1cm^3}$ values of 1.07 Gy and 2.52 Gy compared to the FBO approach. The EUD hard constraint of 67.75 Gy for the sigmoid wall was violated by both approaches, while the FBO approach produced a plan with lower sigmoid wall EUD, $D_{2cm^3}$ and $D_{0.1cm^3}$ values of 5.42 Gy, 1.17 Gy and 5.04 Gy compared to the IBG approach. None of the rectum wall constraints was reached by both approaches. However, lower rectum wall EUD, $D_{2cm^3}$ and $D_{0.1cm^3}$ values of 2.37 Gy, 2.06 Gy and 3.47 Gy were reported for the FBO approach. The $D_{2cm^3}$ values of the rectum wall reported for the IBG and FBO approach were 61.79 Gy and 59.73 Gy, respectively. The probability of grade 2-4 rectal morbidity and the risk of rectal bleeding are 8.6 % and 5.2 % for the IBG approach. The probability is 6.5 % and 3.1 %, respectively, for the FBO approach.[206] Still, below the 65 Gy soft constraint, the IBG approach reported a higher recto-vaginal reference point of 3.81 Gy. The higher CTV-$T_{IR}$ EUD value does not justify the increase in rectal morbidity.

In patient 10, a higher CTV-$T_{IR}$ EUD value of 1.26 Gy was recorded by the IBG approach compared to the FBO approach. The rest of the CTV-T values had no significant difference between the two approaches. None of the rectum wall constraints was reached by both approaches. However, lower rectum wall EUD, $D_{2cm^3}$ and $D_{0.1cm^3}$ values of 2.13 Gy, 2.59 Gy and 3.90 Gy were reported for the FBO approach. The probability of rectal morbidity is the same for both approaches, despite the difference [207]. The $D_{2cm^3}$ soft constraint of the small bowel, 65 Gy, was reached by both approaches, the same value for both. The IBG approach managed to produce a lower small bowel $D_{0.1cm^3}$ values of 1.22 Gy compared to FBO approach. Again, a higher recto-vaginal reference point 2.73 of Gy was recorded for the IBG approach. Even though the IBG led to a higher recto-vaginal reference point, it was still well below the soft constraint of 65 Gy. There is no clear approach superior to the other approach in this case.

[206] (Mazeron *et al.*, 2016)
[207] (Mazeron *et al.*, 2016)

In patient 11, the $D_{2cm}^3$ hard constraints of the bladder wall and small bowel were reached by both approaches; however, recorded the same $D_{2cm}^3$ values between the two approaches. Both approaches also violated the bladder wall EUD hard constraint, and the FBO approach recorded lower a bladder wall EUD value of 1.92 Gy. None of the rectum wall constraints was reached; however, the FBO approach again led to lower rectum wall EUD, $D_{2cm}^3$ and $D_{0.1cm}^3$ values of 1.18 Gy, 1.30 Gy and 1.60 Gy. The probability of rectal morbidity is the same for both approaches, despite the difference [208]. The IBG approach again led to a higher recto-vaginal reference point of 1.12 Gy. Even though the IBG led to a higher recto-vaginal reference point, it was still well below the soft constraint of 65 Gy. The IBG approach managed a higher CTV-$T_{HR}$ $D_{98\%}$ of 1.99 Gy compared to the FBO approach. When considering the higher CTV-$T_{HR}$ $D_{98\%}$ of 1.99 Gy recorded, the IBG approach led to a superior plan compared to the FBO approach.

In patient 12, higher CTV-$T_{IR}$ EUD, $D_{90\%}$ and $D_{98\%}$ values of 2.35 Gy, 1.47 Gy and 1.27 Gy were reported for the IBG approach compared to the FBO approach, with the other CTV-T values no significant difference was recorded. The bladder wall $D_{2cm}^3$ hard constraint of 85 Gy was violated by the IBG approach, where the FBO approach did not manage to reach the 80 Gy constraint. The FBO led to significant lower bladder wall EUD, $D_{2cm}^3$ and $D_{0.1cm}^3$ values of 3.47 Gy, 6.12 Gy and 5.08 Gy. The EUD hard constraint of the rectum wall was violated by the IBG approach, and the FBO approach reported lower rectum wall EUD, $D_{2cm}^3$ and $D_{0.1cm}^3$ values of 4.47 Gy, 4.09 Gy, 5.84 Gy. Both approaches violated the $D_{2cm}^3$ hard constraint of the small bowel while recording the same $D_{2cm}^3$ values between the two approaches. The IBG approach led to lower small bowel EUD and $D_{0.1cm}^3$ values of 2.89 Gy and 5.69 Gy compared to the FBO approach. A higher recto-vaginal reference point of 5.82 Gy was reported for the IBG approach compared to FBO approach. The higher CTV-$T_{IR}$ EUD, $D_{90\%}$ and $D_{98\%}$ values recorded do not justify the serious violation of OAR doses. The rectum and bladder wall constraints take priority above the sigmoid wall constraints; for this reason, the FBO approach led to a superior plan compared to the IBG approach.

In patient 13, the IBG approach produced a plan with a higher CTV-$T_{HR}$ $D_{90\%}$ value of 1.07 Gy, although small. The EUD hard constraint of the rectum wall was reached by the FBO approach. The IBG approach recorded lower rectum wall and recto-vaginal point doses. Rectum wall EUD and $D_{0.1cm}^3$ values of 1.39 Gy and 1.89 Gy lower and a recto-vaginal point value of 1.0 Gy lower. The probability of rectal morbidity is the same for both approaches, despite the difference EUD hard constraints of the bladder wall and small bowel were reached by both approaches, however recording the same EUD values

[208] (Mazeron *et al.*, 2016)

between the two approaches. When considering the outcome of the approaches, the IBG approach led to a superior plan compared to the FBO approach.

In patient 14, no significant difference was observed in the CTV-T values between the approaches. The EUD hard constraint of the bladder, sigmoid wall and small bowel was violated by both approaches, again recording the same EUD values between the approaches. The IBG approach, however, led to a higher bladder wall $D_{2cm^3}$ value of 1.37 Gy, while reaching the $D_{2cm^3}$ soft constraint of 80 Gy. The FBO approach led to lower rectum wall EUD, $D_{2cm^3}$ and $D_{0.1cm^3}$ values of 1.42 Gy, 1.32 Gy and 1.87 Gy to the IBG approach. Again, a higher recto-vaginal reference point of 2.05 Gy was reported for the IBG approach, while the soft constraint was violated only by the IBG approach. A steeper rectum dose-effect curve is observed when the relationship between the $D_{2cm^3}$ and late G2-4 side effects are evaluated, for the rectum and the bladder[209]. With this said, the rectum constraints take priority over the bladder during the planning and optimisation process. From the results, the FBO led to a superior plan compared to the IBG approach.

In patient 15, no significant difference was observed in the CTV-$T_{HR}$ values between the approaches. However, a higher CTV-$T_{IR}$ $D_{90\,\%}$ value of 1.0 Gy was recorded by the IBG approach compared to the FBO approach. Both approaches violated the EUD hard constraints of the bladder wall and small bowel. However, the small bowel EUD values were the same for both approaches. The IBG approach led to lower bladder wall EUD and $D_{2cm^3}$ values of 3.58 Gy and 1.43 Gy compared to the FBO approach. The IBG approach reported a significant lower bladder wall $D_{0.1cm^3}$ value of 6.83 Gy. None of the rectum wall constraints was reached; still, the IBG produced a plan with lower rectum wall EUD and $D_{0.1cm^3}$ values of 1.24 Gy and 1.83 Gy compared to FBO approach. Considering the CTV-T and OAR dose for the patient 15, the IBG approach led to lower bladder wall doses which were of main concern in this case. Therefore, the IBG approach led to a superior plan compared to the FBO approach.

In patient 16, the bladder wall constraints were kept intact by both approaches. However, the IBG approach recorded lower bladder wall EUD, $D_{2cm^3}$ and $D_{0.1cm^3}$ values of 3.60 Gy, 1.81 Gy and 6.82 Gy, compared to FBO approach. The EUD hard constraint and the $D_{2cm^3}$ soft constraint of the rectum wall was violated by both approaches, while the FBO approach reported lower rectum wall EUD, $D_{2cm^3}$ and $D_{0.1cm^3}$ values of 1.61 Gy, 1.33 Gy and 2.64 Gy. The $D_{2cm^3}$ values of the rectum wall reported for both approaches ranged between 70-75 Gy. Therefore, the probability of grade 2-4 rectal morbidity and the risk of rectal bleeding are 18.0 % and 12.8 % for both approaches [210]. This probability rates are very high, and in this case, any approach that recorded lower rectum wall values and in effect lower

[209] (Georg *et al.*, 2012)
[210] (Mazeron *et al.*, 2016)

the probability rates will be superior. Again, a higher recto-vaginal reference point of 2.60 Gy was reported by the IBG approach; both approaches violated the soft constraint of 65 Gy. A lower value for the recto-vaginal point recorded will, in effect, lead to a lower probability of developing vaginal stenosis (G ≥ 2). Higher CTV-$T_{IR}$ EUD, $D_{90\,\%}$ and $D_{98\,\%}$ values of 1.69 Gy, 1.15 Gy and 1.13 Gy were recorded for the IBG approach. Even though the IBG approach led to lower bladder wall dose values, none of the constraints was reached. Therefore, the bladder wall was not the OAR volume of main concern in this case. The FBO approach managed to deliver a plan with lower rectum wall doses, which were violated by both approaches; with this said, the FBO approach was superior to the IBG approach.

In patient 17, no significant difference was observed in the CTV-$T_{HR}$ values between the approaches. However, higher CTV-$T_{IR}$ EUD and $D_{90\,\%}$ values of 1.65 Gy and 1.19 Gy was reached by the IBG approach compared to the FBO approach. None of the sigmoid or bladder wall constraints was violated. The IBG approach led to higher sigmoid wall EUD, $D_{2cm^3}$ and $D_{0.1cm^3}$ values of 1.86 Gy, 1.62 Gy and 2.77 Gy compared to the FBO approach. The EUD hard constraint of the rectum wall was reached by the IBG approach, lower rectum wall EUD, $D_{2cm^3}$ and $D_{0.1cm^3}$ values of 1.40 Gy, 1.32 Gy and 1.87 Gy, respectively, were recorded by the FBO approach. The IBG approach violated the $D_{2cm^3}$ soft constraint of the small bowel, therefore lower small bowel EUD, $D_{2cm^3}$ and $D_{0.1cm^3}$ values of 4.30 Gy, 3.42 Gy and 7.07 Gy were recorded by the FBO approach. A lower recto-vaginal reference point of 1.99 Gy was reported for the FBO approach, with only the IBG violating the 65 Gy soft constraint. The increase in the CTV-$T_{IR}$ by the IBG approach does not justify the OAR doses recorded. The FBO led to a superior plan compared to the IBG approach as it produced lower rectum wall and small bowel doses which were a reached and violated by the IBG approach.

In patient 18, the EUD hard constraint of the bladder wall was reached by the FBO approach, the $D_{2cm^3}$ soft constraint was reached by both approaches but reported the same $D_{2cm^3}$ value. The IBG approach produced lower bladder wall EUD and $D_{0.1cm^3}$ values of 1.0 Gy and 1.39 Gy compared to the IBG approach. None of the sigmoid wall constraints was reached by both approaches; however, the IBG approach led to lower sigmoid wall EUD, $D_{2cm^3}$ and $D_{0.1cm^3}$ values of 2.66 Gy, 1.69 Gy and 3.55 Gy, respectively, compared to FBO approach. The rectum wall EUD hard constraint was reached by the IBG approach, lower rectum wall EUD, $D_{2cm^3}$ and $D_{0.1cm^3}$ values of 2.18 Gy, 1.37 Gy and 2.34 Gy were recorded by the FBO approach. Both approaches reached the recto-vaginal reference point soft constraint of 65 Gy. The probability of developing vaginal stenosis (G ≥ 2) in this case was 20 % [211]. The FBO produced a plan that was 3.76 Gy lower for the recto-vaginal point, and this will lead to a lower probability of developing vaginal stenosis (G ≥ 2). No significant difference was observed in the CTV-T

[211] (Kirchheiner *et al.*, 2016)

values between the approaches. The rectum wall constraints take priority above the bladder wall constraints. For this reason, the FBO approach led to a superior plan compared to the IBG approach.

By evaluating the results displayed in Table 27, it can be seen that the IBG approach also led to significantly higher average CTV-$T_{HR}$ $D_{98\,\%}$ and $D_{100\,\%}$ values compared to the FBO approach. The IBG approach led to significantly higher average CTV-$T_{IR}$ $D_{90\,\%}$, $D_{98\,\%}$, $D_{100\,\%}$ and EUD values compared the FBO approach.

**Table 27 - Average CTV-T $D_{90\,\%}$ $D_{98\,\%}$ and $D_{100\,\%}$ values for the IBG and FBO approach**

| Approach | CTV-$T_{HR}$ $D_{90\,\%}$ (Gy) | CTV-$T_{HR}$ $D_{98\,\%}$ (Gy) | CTV-$T_{HR}$ $D_{100\,\%}$ (Gy) | CTV-$T_{IR}$ $D_{90\,\%}$ (Gy) | CTV-$T_{IR}$ $D_{98\,\%}$ (Gy) | CTV-$T_{IR}$ $D_{100\,\%}$ (Gy) |
|---|---|---|---|---|---|---|
| **IBG** | 91.86 ± 3.13 | 81.53 ± 3.38* | 74.39 ± 3.57* | 67.13 ± 2.47* | 63.43 ± 2.27* | 61.11 ± 1.97* |
| **FBO** | 91.96 ± 2.97 | 81.04 ± 3.48* | 73.75 ± 3.63* | 66.25 ± 2.47* | 62.69 ± 2.24* | 60.49 ± 1.96* |

***Tested for the significant difference with a p-value ≤ 0.05.**

The difference in the average $D_{2cm^3}$, $D_{0.1cm^3}$, recto-vaginal reference point dose point values (see Table 28) for the IBG and FBO approach are summarized. The FBO approach led to significantly lower average rectum wall $D_{2cm^3}$ and $D_{0.1cm^3}$ values and significantly lower average recto-vaginal dose point values. However, the IBG approach led to significantly lower average $D_{0.1cm^3}$ bladder wall values.

**Table 28 - Average $D_{2cm^3}$ and $D_{0.1\,cm^3}$ values for all OAR walls of the IBG and FBO approach**

| | Bladder wall | Small bowel | Rectum wall | Sigmoid wall | Recto-vaginal |
|---|---|---|---|---|---|
| **Approach** | $D_{2cm^3}$ (Gy) Average ± SD | $D_{2cm^3}$ (Gy) Average ± SD | $D_{2cm^3}$ (Gy) Average ± SD | $D_{2cm^3}$ (Gy) Average ± SD | Dose point (Gy) Average ± SD |
| **IBG** | 78.72 ± 4.50 | 70.07 ± 7.69 | 64.28 ± 3.44* | 61.77 ± 4.39 | 67.61 ± 3.93* |
| **FBO** | 78.05 ± 4.22 | 69.84 ± 7.91 | 62.61 ± 3.27* | 61.42 ± 4.50 | 65.05 ± 4.06* |
| **Approach** | $D_{0.1cm^3}$ (Gy) | $D_{0.1cm^3}$ (Gy) | $D_{0.1cm^3}$ (Gy) | $D_{0.1cm^3}$ (Gy) | - |
| **IBG** | 95.58 ± 8.10* | 81.66 ± 12.28 | 71.52 ± 5.03* | 70.53 ± 8.96 | - |
| **FBO** | 97.07 ± 7.33* | 82.43 ± 13.45 | 69.15 ± 4.93* | 70.12 ± 8.76 | - |

***Tested for the significant difference with a p-value ≤ 0.05.**

Table 29 outlined dose to point A and TRAK values for the IBG and FBO approach. The difference in average dose to point $A_{Left}$ and $A_{Right}$ were of significant value, and the IBG approach led to higher

values compared to the FBO approach. The TRAK value recorded for the IBG approach was also higher compared to the FBO approach.

**Table 29 - Average dose to point A and TRAK values of IBG and FBO approach**

| Approach | $A_{Left}$ (Gy) | $A_{Right}$ (Gy) | TRAK (cGy at 1 m) |
|---|---|---|---|
| **IBG** | 83.87 ± 13.54* | 82.22 ± 15.54* | 1.77 ± 0.24 |
| **FBO** | 77.56 ± 8.51* | 75.80 ± 8.53* | 1.62 ± 0.23 |

***Tested for the significant difference with a p-value ≤ 0.05.**

The average treatment time between the two approaches was 8.16 ± 2.98 min and 7.47 ± 2.79 min for the IBG and FBO approach, respectively, which correlate with the reported TRAK values. With the lower average point A doses and CTV-T values reported by the FBO approach, the dose fall-off was quicker for the FBO approach compared to the IBG approach. This also may have led to the significant lower rectum and recto-vaginal reference point doses that were reported. The CTV-T had better dose coverage with the IBG approach. Significantly higher average dose to point A values were reported for the IBG approach, together with significantly higher average CTV-$T_{HR}$ $D_{98\,\%}$ and $D_{100\,\%}$ values. The IBG approach also led to significantly higher average CTV-$T_{IR}$ $D_{90\,\%}$, $D_{98\,\%}$, $D_{100\,\%}$ and EUD values compared the FBO approach. However, it is unsure if the dose outside the tumour was higher for the one approach compared to the other. The addition of a normal tissue constraint outside the tumour should be considered for future optimisation processes, to ensure that normal tissues are not unnecessarily overdosed in the attempt to reach specific CTV-T constraints.

As mentioned before, the optimisation process aims to reach the CTV-T hard constraint, then the OAR hard constraint and if there is room for more dose-escalation the CTV-T soft constraint is of priority and then the soft constraints of the OAR volumes. The IBG approach exploited all OAR constraints to its full protentional, thus ensuring a better CTV-T coverage compared to the FBO approach. Even though the FBO led to lower average rectum wall and recto-vaginal doses**,** the average $D_{2\,cm3}$ values recorded for the IBG approach are still well below the recommended dose constraints. The reduction of average $D_{0.1cm^3}$ values for the bladder wall by the IBG approach is a great benefit.

**Bladder wall**

High bladder $D_{2cm^3}$ was previously established as a significant risk factor for moderate to severe grade bladder bleeding, fistula and cystitis. Therefore, it is crucial to adhere to the bladder wall $D_{2cm^3}$ constraints, as far as possible [212].

[212] (Spampinato et al., 2019)

When the IBG results of the entire patient population are compared to published constraints [213], 83% of the treatment plan total dose conformed to the $D_{2cm^3}$ hard constraint of 85 Gy, and 67% of treatment plan total dose conformed to the soft constraint of 80 Gy. These values fell short of the proposed achievement rates of 70 – 80 % and 90 – 95 % of patients for the soft and hard constraints, respectively [214].

**Small bowel**

The small bowel was the worst-performing and most limiting OAR among all four OARs. Considering the results of the IBG approach, 72 % of the treatment plan total dose conformed to the $D_{2cm^3}$ hard constraint of 75 Gy, while only 17 % of treatment plan total dose conformed to the soft constraint of 65 Gy. Again, falling short of the proposed achievement rates of 70 – 80 % and 90 – 95 % of patients for the soft and hard constraints, respectively [215].

Moreover, it has been found that bowel $D_{2cm^3}$ can be linked to pooled ≥ G3 bowel morbidity. This includes fistulas, diarrhoea, stenosis, necrosis, bleeding, and perforation [216]. TRAK values ≥ 2 cGy at 1 m and a CTV-$T_{HR}$ volume ≥ 25 $cm^3$ have been associated with late bowel toxicity [217]. Out of the entire patient population, TRAK ≥ 2 cGy at 1 m were reported in three patients, while a TRAK value of 1.98 cGy at 1 m was reported in another two patients. Sixteen patients had a CTV-$T_{HR}$ volume of ≥ 25 $cm^3$.

Considering all this, a great number of patients in this study will have a high probability for the risk of late bowel toxicity.

**Rectum wall and Recto-vaginal reference point**

As shown in literature, a rectum $D_{2cm^3}$ ≤ 65 Gy is related with less frequent rectal and more minor morbidity, specifically bleeding and proctitis. Furthermore, $D_{2cm^3}$ ≥ 75 Gy is linked with more recurrent and major rectal morbidity, also with a bigger risk of a fistula [218]. The EMBRACE cohort showed that risk factors for diarrhoea are bowel $D_{2cm^3}$, rectum $D_{2cm^3}$, as well as EBRT components such as para-aortic irradiation, prescribed dose, as well the high-dose regions related to lymph node boosts.49

A soft constraint of 65 Gy was proposed by Tandeup et al [219]. However, a soft constraint of 70 Gy was used in this study. When the IBG results of the entire patient population are compared to published constraints [220], 100% of the treatment plan total dose conformed to the $D_{2cm^3}$ hard constraint of 75

[213] (Tanderup et al., 2020)
[214] (Tanderup *et al.*, 2020)
[215] (Tanderup *et al.*, 2020)
[216] (Bockel *et al.*, 2019)
[217] (Bockel et al., 2019)
[218] (Mazeron *et al.*, 2016)
[219] (Tanderup et al., 2020)
[220] (Tanderup et al., 2020)

Gy, and 61% of treatment plan total dose conformed to the proposed soft constraint of 65 Gy. Evaluating the applied soft constraint of this study, 94.4% of the treatment plan total dose conformed to the $D_{2cm}^3$ soft constraint of 70 Gy. The hard constraint of 75 Gy was well within the proposed achievement rate of 90 – 95 % of patients [221]. The achievement rate of 61 % fell short of the proposed 70 – 80 %.

An increase in the recto-vaginal reference point dose has been related to an increase in the probability of vaginal stenosis G ≥ 2 significantly. Vaginal stenosis ( G ≥ 2) is defined as 'shortening and/or narrowing interfering with function'. The probability of developing vaginal stenosis (G ≥ 2) is 16% with a recto-vaginal reference point dose of 55 Gy, 20 % with 65 Gy, 27 % with 75 Gy, 34 % with 85 Gy and 43 % with 95 Gy [222].

When the IBG results of the entire patient population are compared to published constraints [223], 100% of the treatment plan total dose conformed to the $D_{2cm}^3$ hard constraint of 75 Gy, and only 33% of treatment plan total dose conformed to the proposed soft constraint of 65 Gy. The hard constraint of 75 Gy was well within the proposed achievement rate of 90 – 95 % of patients [224]. Considering the 65 Gy soft constraint, the achievement rate of 33 % fell way short of the proposed 70 – 80 %.

According to the dose received by this study population, 65 Gy or less was reported in six patients, 65 – 75 Gy were reported in 12 patients and in one patient a dose between 75 – 85 Gy was reported. Therefore, the probability of developing vaginal stenosis in these three subgroups will be 20 %, 27 % and 34 %, respectively [225].

**Sigmoid wall**

When the IBG results of the entire patient population are compared to published constraints [226], 100% of the treatment plan total dose conformed to the $D_{2cm}^3$ hard constraint of 75 Gy, and 100 % of treatment plan total dose conformed to the proposed soft constraint of 70 Gy. The hard and soft constraint were well within the proposed achievement rate [227].

[221] (Tanderup *et al.*, 2020)
[222] (Kirchheiner *et al.*, 2016)
[223] (Tanderup et al., 2020)
[224] (Tanderup *et al.*, 2020)
[225] (Kirchheiner *et al.*, 2016)
[226] (Tanderup et al., 2020)
[227] (Tanderup *et al.*, 2020)

**CTV-T**

Low-dose regions in target volumes are assumed to be of the utmost importance when local control is considered. The CTV-$T_{HR}$ $D_{90\,\%}$ and $D_{98\,\%}$ and CTV-$T_{IR}$ $D_{98\,\%}$ have been established to be related to better local control [228].

In this study, the patients CTV-$T_{HR}$ volumes that was contoured in the first fraction varied from intermediate to large size, with no limited size CTV-$T_{HR}$ volumes present. Five patients had intermediate size CTV-$T_{HR}$ volumes (30 $cm^3$). All five intermediate size CTV-$T_{HR}$ volumes were planned with the IBG approach to CTV-$T_{HR}$ $D_{90\,\%}$ values ≥ 92 Gy, without the violation of OAR doses. The outlier in terms of a high CTV-$T_{HR}$ $D_{90\,\%}$ value of 102 Gy, patient 13 recorded a CTV-$T_{HR}$ volume of 22 $cm^3$, which gave the planner the ability to allow for dose escalation in the CTV-$T_{HR}$ without violation of OAR doses. Ten patients CTV-$T_{HR}$ volumes were between 30 - 50 $cm^3$. One of the ten patients had favourable OAR geometries despite a CTV-T volume of 48 $cm^3$, this allowed for a planned dose of just below 95 Gy to the CTV-$T_{HR}$ $D_{90\,\%}$. The other nine patients had a combination of unfavourable OAR and target geometries and sizes which led to OAR violations in an attempt to reach CTV-$T_{HR}$ $D_{90\,\%}$ values of 90 Gy. Three patients had large size CTV-$T_{HR}$ volumes of between 50 – 77 $cm^3$. All three these patients with large CTV-$T_{HR}$ volumes had OAR dose violations to ensure an adequate total dose of 90 Gy to the CTV-$T_{HR}$ $D_{90\,\%}$.

It was reported that a CTV-$T_{HR}$ $D_{90\,\%}$ of ≥ 85 Gy delivered in less than 50 days would provide 3-year local control rates of > 94 % in limited size CTV-$T_{HR}$ (20 $cm^3$), > 93 % in intermediate size (30 $cm^3$), and > 86 % in large size (70 $cm^3$). Based solely on the CTV-$T_{HR}$ $D_{90\,\%}$ recorded for all the patients in the study with the IBG approach, not taking stage and histology into account the predicted LC would be > 93 % for five patients, > 86 % but < 93 % for eleven patients and > 86% for two patients.

Tanderup et al. found that point A may provide a realistic estimate of the average CTV-$T_{HR}$ $D_{90\,\%}$ in a large patient population, but a poor predictor of CTV-$T_{HR}$ $D_{90\,\%}$ in the individual patient [229]. Considering the results of the IBG approach, 83.87 ± 13.54 Gy and 82.22 ± 15.54 Gy for Point $A_{Left}$ and $A_{Right}$ respectively and a CTV-$T_{HR}$ $D_{90\,\%}$ of 91.86 ± 3.13 Gy. The average point A values reported were significantly lower compared to the average target dose and did not provide a good estimate of the average target dose reported for the population. The dose to point $A_{Left}$ and $A_{Right}$ was not set as a limiting parameter in the optimisation processes, these values were only reported and evaluated retrospectively. The average dose to point $A_{Left}$ and $A_{Right}$ was still higher than the proposed > 65 Gy

[228] (Johannes C A Dimopoulos *et al.*, 2009; Mazeron *et al.*, 2015; Tanderup *et al.*, 2016)
[229] (Tanderup *et al.*, 2010)

soft constraint [230]. For future optimisation and planning processes, it would be good to incorporate this parameter into the optimisation process.

The IBG approach lived up to the expectation, showcasing its ability to produce a clinically feasible plan, which is in line with published conventional-dose planning aims, balanced between CTV-T and OAR dose while utilizing biological indexes.

### 4.2.3 Intracavitary/Interstitial (IC/IS) IGABT Treatment planning

Seven patients with the worse intracavitary IGABT treatment planning results were selected for forward intracavity/interstitial IGABT planning and optimisation as described in Section 3.5.2. Patient 1, 7, 8, 9, 11, 12 and 14 were selected.

Forward IC/IS planning and optimisation were executed on all seven patients; a total of 140 plans were optimised and planned. Again, priority was given to the hard constraint of the CTV-$T_{HR,}$ followed by the hard constraints for OARs. When hard constraints for targets and OARs were achieved, the priorities were, to aim for reaching/approaching the soft constraints for CTV-$T_{HR}$ and thereafter reaching/approaching soft constraints for OARs and CTV-$T_{IR}$.

#### 4.2.3.1 Forward IC/IS IGABT planning

The results for all the four approaches are summarized in Table 30 and Table 32. Conventional Interstitial Optimistic (CIO), Conventional Interstitial Greedy (CIG), Biological Interstitial Optimistic (BIO) and Biological Interstitial Greedy (BIG).

**Table 30 - Average CTV-T $D_{90\,\%}$ $D_{98\,\%}$ and $D_{100\,\%}$ values for all interstitial approaches**

| Approach | CTV-$T_{HR}$ $D_{90\,\%}$ (Gy) | CTV-$T_{HR}$ $D_{98\,\%}$ (Gy) | CTV-$T_{HR}$ $D_{100\,\%}$ (Gy) | CTV-$T_{IR}$ $D_{90\,\%}$ (Gy) | CTV-$T_{IR}$ $D_{98\,\%}$ (Gy) | CTV-$T_{IR}$ $D_{100\,\%}$ (Gy) |
|---|---|---|---|---|---|---|
| **CIO** | 92.46 ± 3.22 | 80.56 ± 2.94 | 72.51 ± 3.29 | 65.08 ± 2.69 | 61.52 ± 2.23 | 59.34 ± 1.97 |
| **CIG** | 92.22 ± 2.80 | 80.21 ± 2.44 | 72.04 ± 2.82 | 65.00 ± 2.63 | 61.39 ± 2.12 | 59.22 ± 1.66 |
| **BIO** | 92.22 ± 3.61 | 80.36 ± 3.55 | 72.29 ± 3.58 | 65.00 ± 3.02 | 61.40 ± 2.48 | 59.24 ± 1.96 |
| **BIG** | 92.25 ± 3.63 | 80.46 ± 3.64 | 72.37 ± 3.64 | 64.99 ± 3.06 | 61.41 ± 2.53 | 59.26 ± 2.03 |

Table 31 outlines the average dose to point A and TRAK values for all four interstitial approaches.

[230] (Tanderup *et al.*, 2020)

**Table 31 - Average dose to point A and TRAK values of all interstitial approaches**

| Approach | $A_{Left}$ (Gy) | $A_{Right}$ (Gy) | TRAK (cGy at 1 m) |
|---|---|---|---|
| **CIO** | 80.89 ± 13.99 | 78.65 ± 8.89 | 1.73 ± 0.22 |
| **CIG** | 80.80 ± 14.00 | 78.63 ± 9.02 | 1.73 ± 0.22 |
| **BIO** | 80.99 ± 14.27 | 75.13 ± 5.86 | 1.71 ± 0.22 |
| **BIG** | 80.94 ± 14.28 | 75.03 ± 5.83 | 1.70 ± 0.22 |

The results in Table 30 displays no significant difference between the four approaches when the average CTV-T values are considered. The average OAR dose parameters reported for all four approaches are summarised in Table 32.

**Table 32 - Average $D_{2cm^3}$, EUD and $D_{0.1cm^3}$ values for OAR walls for all interstitial approaches**

| | Bladder wall | Small bowel | Rectum wall | Sigmoid wall | Recto-vaginal |
|---|---|---|---|---|---|
| **Approach** | **$D_{2cm^3}$ (Gy) Average ± SD** | **$D_{2cm^3}$ (Gy) Average ± SD** | **$D_{2cm^3}$ (Gy) Average ± SD** | **$D_{2cm^3}$ (Gy) Average ± SD** | **$D_{2cm^3}$ (Gy) Average ± SD** |
| **CIO** | 76.71 ± 1.65 | 68.83 ± 7.67 | 64.52 ± 3.43 | 65.06 ± 3.64 | 68.39 ± 5.34 |
| **CIG** | 76.76 ± 1.58 | 68.75 ± 7.72 | 64.39 ± 3.41 | 65.02 ± 3.68 | 68.42 ± 5.46 |
| **BIO** | 76.19 ± 0.92 | 68.85 ± 7.74 | 64.04 ± 3.02 | 64.63 ± 2.98 | 68.06 ± 5.43 |
| **BIG** | 75.92 ± 0.75 | 68.86 ± 7.72 | 63.89 ± 2.95 | 64.65 ± 2.95 | 67.90 ± 5.19 |
| **Approach** | **$D_{0.1cm^3}$ (Gy)** | **$D_{0.1cm^3}$ (Gy)** | **$D_{0.1cm^3}$ (Gy)** | **$D_{0.1cm^3}$ (Gy)** | **-** |
| **CIO** | 93.20 ± 2.98 | 79.34 ± 12.01 | 73.75 ± 7.24 | 78.69 ± 8.03 | - |
| **CIG** | 93.33 ± 2.95 | 79.15 ± 12.14 | 73.48 ± 7.16 | 78.59 ± 8.15 | - |
| **BIO** | 91.92 ± 2.62 | 79.52 ± 12.34 | 72.51 ± 5.52 | 77.35 ± 5.89 | - |
| **BIG** | 91.68 ± 2.68 | 79.55 ± 12.30 | 72.24 ± 5.52 | 77.35 ± 5.77 | - |
| **Approach** | **EUD (Gy)** | **EUD (Gy)** | **EUD (Gy)** | **EUD (Gy)** | **-** |
| **CIO** | 76.34 ± 1.83 | 67.44 ± 7.09 | 66.44 ± 5.18 | 72.12 ± 6.95 | - |
| **CIG** | 76.29 ± 1.79 | 67.34 ± 7.17 | 66.43 ± 5.20 | 72.03 ± 7.04 | - |
| **BIO** | 75.33 ± 1.00 | 67.55 ± 7.23 | 65.63 ± 3.87 | 70.74 ± 4.74 | - |

| | | | | | |
|---|---|---|---|---|---|
| **BIG** | 75.17 ± 1.20 | 67.56 ± 7.21 | 65.46 ± 3.87 | 70.75 ± 4.65 | - |

The OAR values reported by the CIG and the BIG approach were tested for significant differences. Even though differences are visually noted between average OAR values of the two approaches, it was not of any statistical significance. It is recommended that all eighteen patients in this study should be planned and optimised with the IC/IS IGABT planning tool and not only seven patients. This will allow reliable results from which conclusions can be made about which approach are superior to the other.

**a) Biological Interstitial Greedy (BIG) vs Inverse Biological Greedy (IBG)**

An intracavitary IGABT approach and IC/IS IGABT approach, IBG and BIG, respectively, was compared to see if the patients did benefit from the IC/IS application compared to intracavitary IGABT only. The needle placement in all seven patients was in the direction of the rectum and sigmoid wall, in the attempt to lower the dose in the small bowel and bladder wall which were severely over-dosed in the IBG approach to reach the desired CTV-$T_{HR}$ $D_{90\,\%}$ hard constraint of 90 Gy.

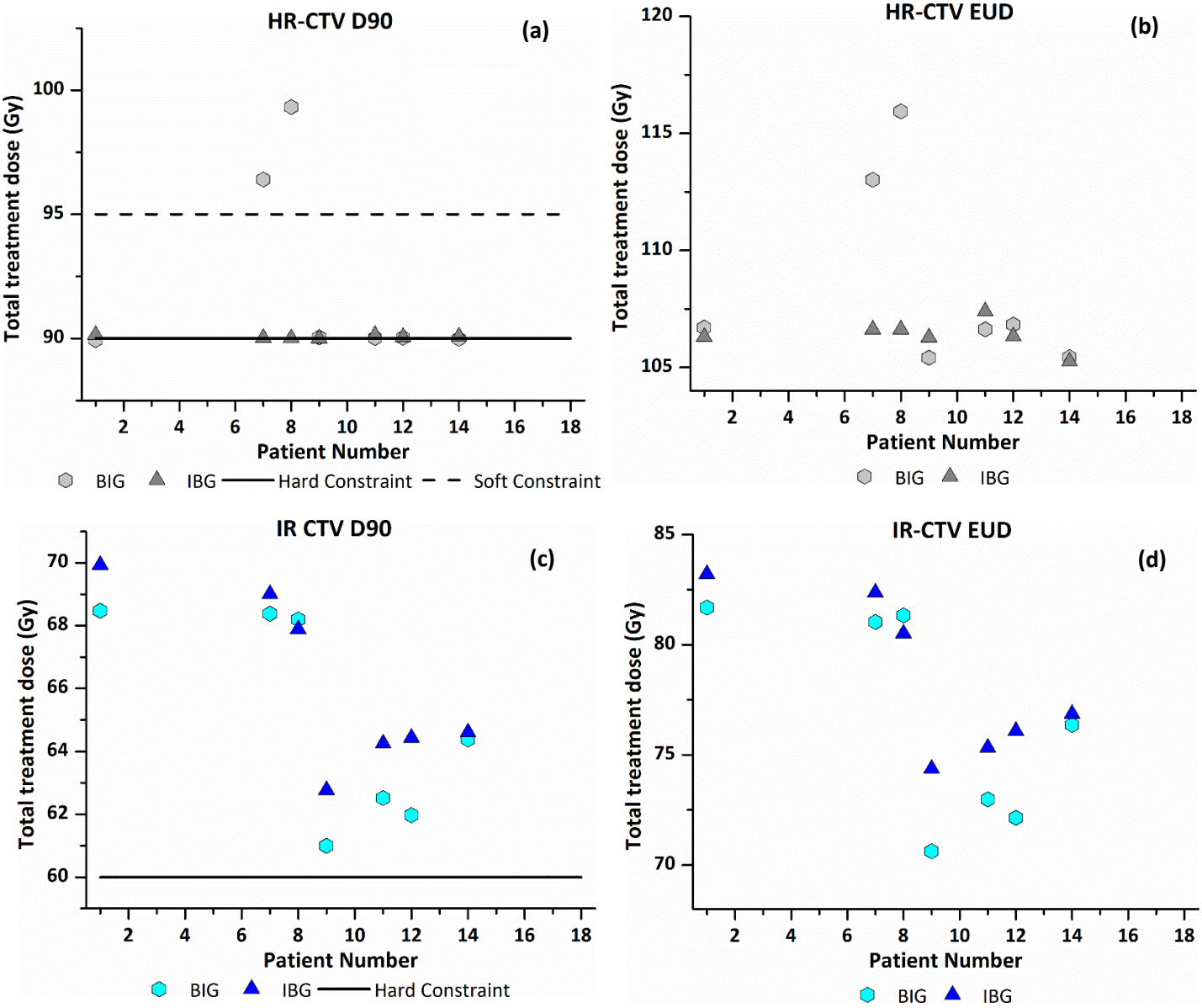


**Figure 49 - Comparison between the BIG and IBG approach per patient. CTV-$T_{HR}$ (a) $D_{90\,\%}$ and (b) EUD, CTV-$T_{IR}$ (c) $D_{90\,\%}$ and (d) EUD. Note: Data points for the BIG and IBG approach are indicated by hexagons and triangles, respectively.**

Figure 49 illustrates that two patients, patient 7 and 8 CTV-$T_{HR}$ $D_{90\,\%}$ were improved significantly with the BIG approach. For patient 7 the CTV-$T_{HR}$ $D_{90\,\%}$ value changed from 90.02 Gy to 96.40 Gy, 7.09 % higher. The CTV-$T_{HR}$ $D_{90\,\%}$ value of patient 8 changed from 90.01 Gy to 99.32 Gy, a 10.34 % change. The CTV-$T_{HR}$ EUD values were higher for the BIG approach for five patients compared to the two for the IBG approach. Average CTV-$T_{HR}$ EUD values of 108.57 ± 3.86 Gy and 106.39 ± 0.59 Gy were recorded for the BIG and IBG approach, respectively. Average CTV-$T_{IR}$ EUD values of 76.59 ± 4.42 Gy and 78.39 ± 3.31 Gy were recorded for the BIG and IBG approach, respectively. The difference in average CTV-$T_{IR}$ EUD values tested for a significant difference with $p \leq 0.05$.

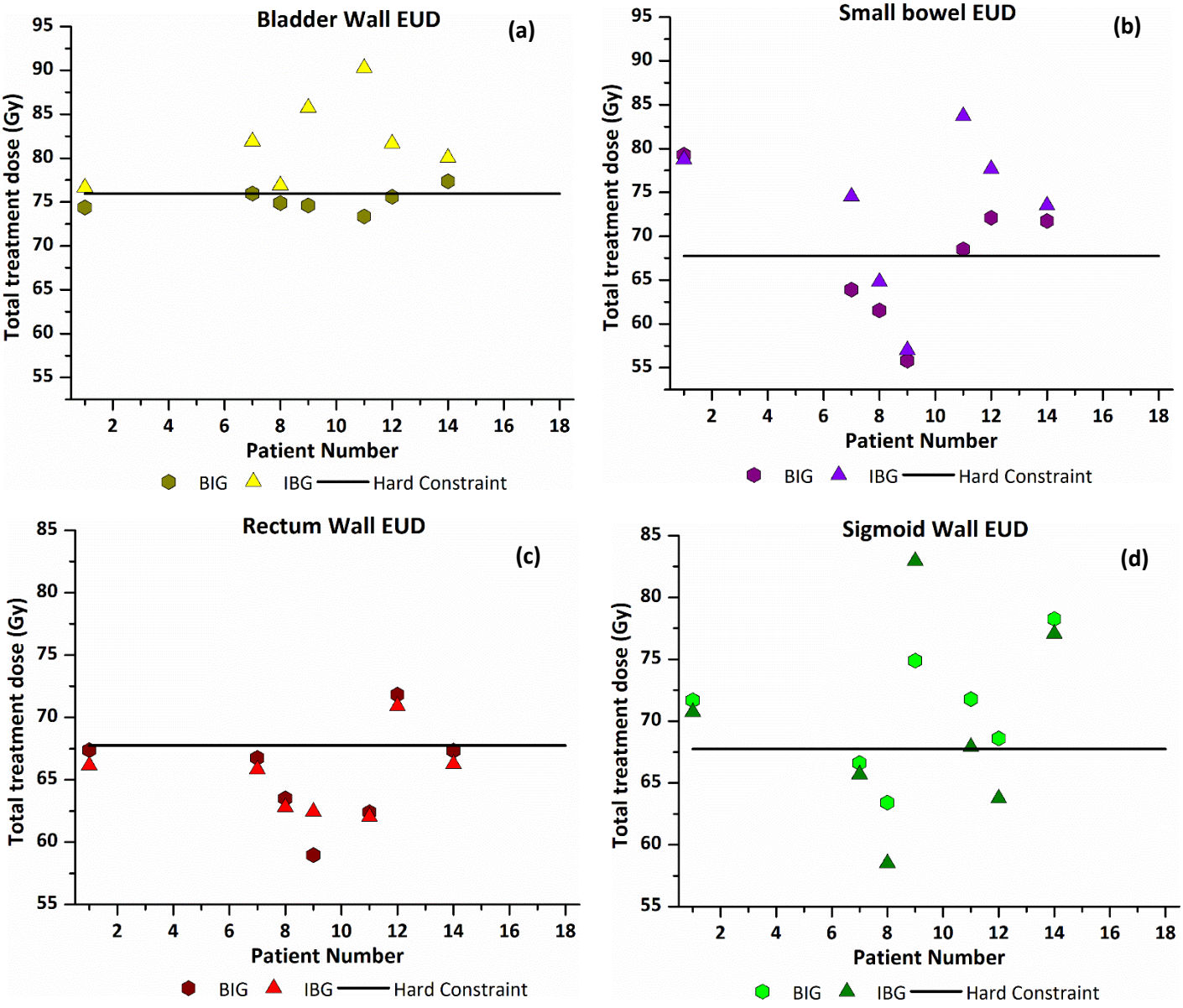


**Figure 50 - Comparison between the BIG and IBG approach per patient. The EUD values for (a) bladder wall, (b) small bowel, (c) rectum wall and (d) sigmoid wall. Note: Data points for the BIG and IBG approach are indicated by hexagons and triangles, respectively.**

The illustration in Figure 50 and data summary provided in Table 33, shows that the BIG approach led to significant lower bladder EUD values. The average bladder wall EUD values recorded were 75.17 ± 1.20 Gy and 81.87 ± 4.49 Gy for the BIG and IBG approach, respectively. Average small bowel EUD values were lower for the BIG approach with recorded values of 72.84 ± 8.41 Gy to 67.56 ± 7.21 Gy. The difference in the average bladder wall and small bowel EUD values tested significant difference with $p \leq 0.05$. Rectum wall EUD values of 65.46 ± 3.87 Gy and 65.20 ± 2.89 Gy were recorded, while sigmoid wall EUD values of 70.75 ± 4.65 Gy and 69.52 ± 7.66 Gy were noted for the BIG and IBG approach, respectively. However, with no significant difference.

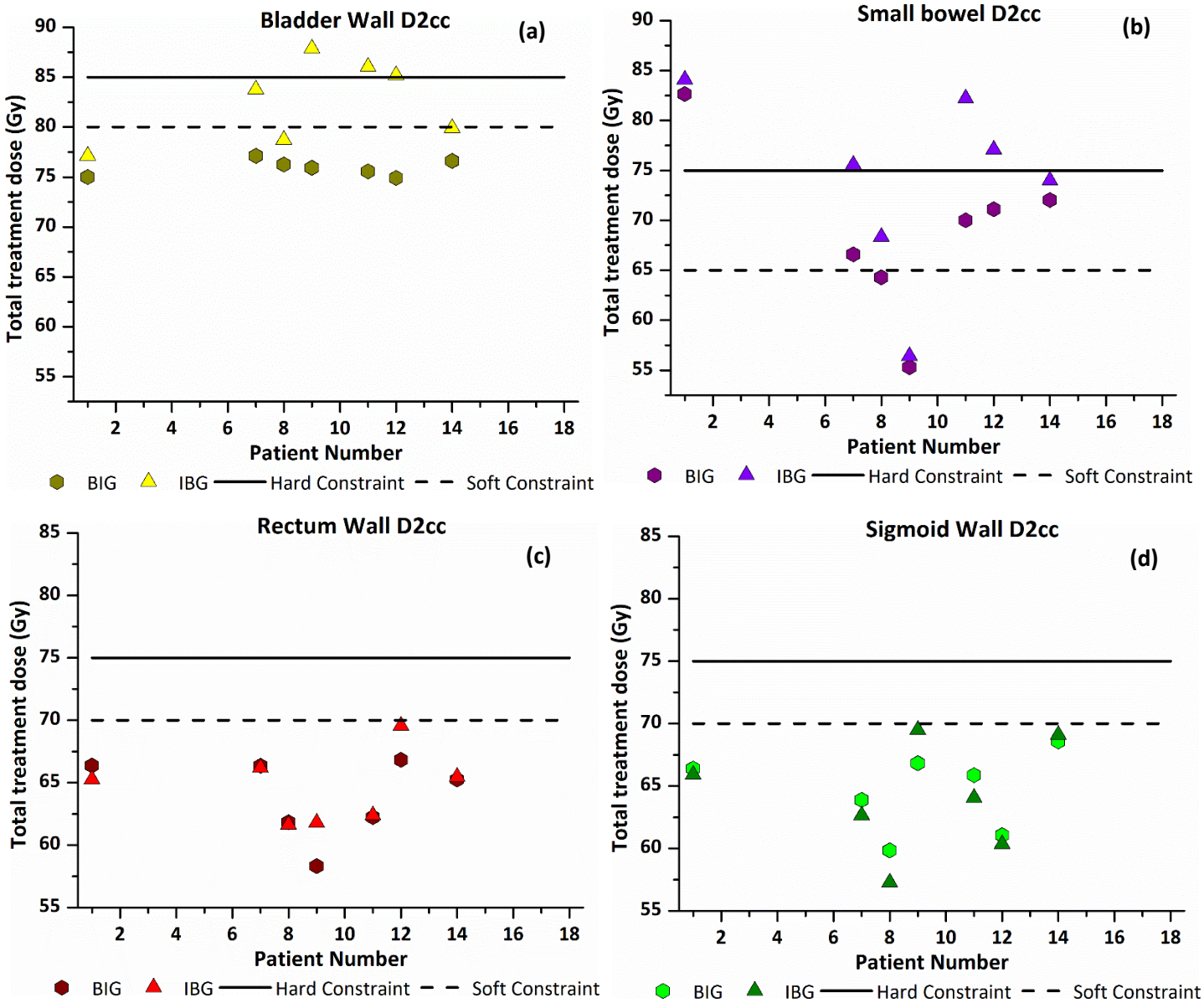


**Figure 51 - Comparison between the BIG and IBG approach per patient. The $D_{2cm^3}$ values for (a) bladder wall, (b) small bowel, (c) rectum wall and (d) sigmoid wall. Note: Data points for the BIG and IBG approach are indicated by hexagons and triangles, respectively**

Figure 51 display the changes in $D_{2cm^3}$ values per patient between the BIG and IBG approach for all OAR volumes. Figure 51, together with Table 33, show that the BIG approach led to a lower bladder wall $D_{2cm^3}$ values in all seven patients compared to the IBG approach. A difference of up to 13.59 % was achieved.

**Table 33 - Comparison between BIG and IBG approach regarding $D_{2cm^3}$ and EUD values for bladder wall**

| Patient | BIG Bladder wall $D_{2cm^3}$ (Gy) | IBG Bladder wall $D_{2cm^3}$ (Gy) | Percentage difference (%) | BIG Bladder wall EUD (Gy) | IBG Bladder wall EUD (Gy) | Percentage difference (%) |
|---|---|---|---|---|---|---|
| **1** | 75.00 | 77.12 | -2.75 | 74.37 | 76.64 | -2.96 |
| **7** | 77.11 | 83.76 | -7.94 | 75.97 | 81.91 | -7.25 |
| **8** | 76.27 | 78.70 | -3.09 | 74.88 | 76.89 | -2.61 |
| **9** | 75.93 | 87.87 | -13.59 | 74.61 | 85.71 | -12.95 |
| **11** | 75.58 | 86.04 | -12.16 | 73.35 | 90.28 | -18.75 |
| **12** | 74.92 | 85.18 | -12.05 | 75.61 | 81.66 | -7.41 |
| **14** | 76.61 | 79.90 | -4.12 | 77.37 | 80.03 | -3.32 |

Positive difference values indicate that the BIG approach led to higher OAR values, where negative values indicate that the BIG approach led to lower OAR values.

As shown in Table 33, the BIG approach reported lower bladder wall EUD values in all seven patients. A difference of up to 18.75 % was achieved for the bladder EUD values.

**Table 34 - Comparison between BIG and IBG approach regarding $D_{2cm^3}$ and EUD values for small bowel**

| Patient | BIG small bowel $D_{2cm^3}$ (Gy) | IBG small bowel $D_{2cm^3}$ (Gy) | Percentage difference (%) | BIG Small bowel EUD (Gy) | IBG Small bowel EUD (Gy) | Percentage difference (%) |
|---|---|---|---|---|---|---|
| 1 | 82.66 | 84.08 | -1.69 | 79.29 | 78.74 | 0.70 |
| 7 | 66.60 | 75.58 | -11.88 | 63.91 | 74.50 | -14.21 |
| 8 | 64.29 | 68.33 | -5.91 | 61.55 | 64.78 | -4.99 |
| 9 | 55.29 | 56.41 | -1.99 | 55.82 | 57.00 | -2.07 |
| 11 | 70.00 | 82.22 | -14.86 | 68.51 | 83.68 | -18.13 |
| 12 | 71.13 | 77.10 | -7.74 | 72.09 | 77.67 | -7.18 |
| 14 | 72.04 | 73.99 | -2.64 | 71.74 | 73.50 | -2.39 |

Positive difference values indicate that the BIG approach led to higher OAR values, where negative values indicate that the BIG approach led to lower OAR values.

When considering the results in Table 34, it can be seen that the small bowel $D_{2cm}^3$ and EUD values for all the patients benefitted from the BIG approach. Differences of up to 14.86 % and 18.13 % were recorded for the $D_{2cm}^3$ and EUD, respectively.

**Table 35 - Comparison between BIG and IBG approach regarding $D_{2cm}^3$ and EUD values for rectum wall**

| Patient | BIG rectum wall $D_{2cm}^3$ (Gy) | IBG rectum wall $D_{2cm}^3$ (Gy) | Percentage difference (%) | BIG rectum wall EUD (Gy) | IBG rectum wall EUD (Gy) | Percentage difference (%) |
|---|---|---|---|---|---|---|
| 1 | 66.38 | 65.26 | 1.72 | 67.37 | 66.14 | 1.86 |
| 7 | 66.36 | 66.18 | 0.27 | 66.77 | 65.83 | 1.43 |
| 8 | 61.83 | 61.61 | 0.36 | 63.50 | 62.79 | 1.13 |
| 9 | 58.32 | 61.79 | -5.62 | 58.97 | 62.43 | -5.54 |
| 11 | 62.23 | 62.38 | -0.24 | 62.41 | 62.03 | 0.61 |
| 12 | 66.83 | 69.55 | -3.91 | 71.84 | 70.90 | 1.33 |
| 14 | 65.26 | 65.46 | -0.31 | 67.33 | 66.26 | 1.61 |

Positive difference values indicate that the BIG approach led to higher OAR values, where negative values indicate that the BIG approach led to lower OAR values.

Table 35 displays the difference between the BIG and IBG approach, given the rectum wall doses. There was an ambivalent response to the BIG and IBG approach. However, all rectum wall $D_{2cm}^3$ values achieved for both approaches were within the $D_{2cm}^3$ soft constraint of 70 Gy. The rectum wall EUD hard constraint of 67.75 Gy was violated for one patient for both approaches.

**Table 36 - Comparison between BIG and IBG approach regarding $D_{2cm^3}$ and EUD values for sigmoid wall**

| Patient | BIG sigmoid wall $D_{2cm^3}$ (Gy) | IBG sigmoid wall $D_{2cm^3}$ (Gy) | Percentage difference (%) | BIG sigmoid wall EUD (Gy) | IBG sigmoid wall EUD (Gy) | Percentage difference (%) |
|---|---|---|---|---|---|---|
| 1 | 66.40 | 65.91 | 0.74 | 71.69 | 70.74 | 1.34 |
| 7 | 63.90 | 62.64 | 2.01 | 66.62 | 65.69 | 1.42 |
| 8 | 59.86 | 57.26 | 4.54 | 63.40 | 58.52 | 8.34 |
| 9 | 66.84 | 69.48 | -3.80 | 74.88 | 82.95 | -9.73 |
| 11 | 65.87 | 64.05 | 2.84 | 71.77 | 67.90 | 5.70 |
| 12 | 61.08 | 60.35 | 1.21 | 68.60 | 63.74 | 7.62 |
| 14 | 68.57 | 69.11 | -0.78 | 78.26 | 77.07 | 1.54 |

Positive difference values indicate that the BIG approach led to higher OAR values, where negative values indicate that the BIG approach led to lower OAR values.

Table 36 shows the results obtained for the sigmoid wall for both approaches. Sigmoid wall values were compromised in the attempt to allow for dose de-escalation in the small bowel and bladder wall. However, no sigmoid wall $D_{2cm^3}$ dose constraint values were reached/violated for both approaches. The EUD hard constraint of the sigmoid wall, in contrast, was violated in numerous cases by the BIG and IBG approach, respectively.

The difference between the two approaches was evaluated per patient by considering all the reported OAR and CTV-T doses simultaneously.

In patient 1, the same CTV-$T_{HR}$ values were reported for both approaches; however, the IBG approach led to higher CTV-$T_{IR}$ $D_{90\,\%}$ and $D_{98\,\%}$ values of 1.52 Gy and 1.45 Gy, respectively. The bladder wall EUD hard constraint was violated only by the IBG approach. The bladder wall $D_{2cm^3}$ values were well below the set $D_{2cm^3}$ soft constraint for both approaches. The BIG approach recorded lower bladder wall EUD, $D_{2cm^3}$ and $D_{0.1cm^3}$ values of 2.27 Gy, 2.12 Gy and 3.64 Gy. Both approaches violated the EUD hard constraint of the small bowel, and both reported the same EUD value. The small bowel $D_{2cm^3}$ hard constraint was also violated by both approaches; the BIG approach recorded a lower small bowel $D_{2cm^3}$ value of 1.42 Gy. The IBG approach recorded lower rectum wall EUD, $D_{2cm^3}$ and $D_{0.1cm^3}$ values of 1.23 Gy, 1.12 Gy and 2.26 Gy. Both approaches violated the sigmoid wall EUD hard constraint, with no significant difference reported. The IBG approach also recorded a lower sigmoid wall $D_{0.1cm^3}$ value of

1.23 Gy. The $D_{2cm^3}$ values of the sigmoid and rectum wall were, however, far from their set $D_{2cm^3}$ constraints. The BIG approach used the rectum and sigmoid wall constraints, that had some flexibility, to its benefit; this allowed a lower dose within the bladder and small bowel volumes.

In patient 7, higher CTV-$T_{HR}$ EUD $D_{90\,\%}$ and $D_{98\,\%}$ values of 6.41 Gy, 6.40 Gy and 4.47 Gy were recorded by the BIG approach. The IBG approach led to a higher CTV-$T_{IR}$ $D_{90\,\%}$ value of 1.33 Gy. The IBG approach only violated the bladder wall $D_{2cm^3}$ soft constraint and EUD hard constraint. The BIG approach recorded lower bladder wall EUD, $D_{2cm^3}$ and $D_{0.1cm^3}$ values of 5.94 Gy, 6.65 Gy and 10.06 Gy, respectively. The small bowel $D_{2cm^3}$ hard constraint was also violated by the IBG approach, and the BIG approach recorded a lower small bowel EUD, $D_{2cm^3}$ and $D_{0.1cm^3}$ values of 10.59 Gy, 8.98 Gy and 18.37 Gy, respectively. The IBG approach recorded a lower rectum wall $D_{0.1cm^3}$ value of 1.35 Gy, while none of the rectum and sigmoid wall constraints was violated. The IBG approach recorded lower sigmoid wall $D_{2cm^3}$ and $D_{0.1cm^3}$ values of 1.26 Gy and 1.37 Gy. The significant higher CTV-$T_{HR}$ values will improve local control in this patient, with a tumour size of 70 $cm^3$ and a dose difference of 6.40 Gy. With a dose of 90 Gy a 3-year local control rate of > 86% were reported, the dose of 96.40 Gy has the potential to improve this local control by ± 4%. [231]

In patient 8, higher CTV-$T_{HR}$ EUD $D_{90\,\%}$ and $D_{98\,\%}$ values of 9.32 Gy, 9.31 and 6.28 Gy were recorded by the BIG approach. The small bowel EUD hard constraint was also violated by the IBG approach, with this said the BIG approach recorded lower bladder wall EUD, $D_{2cm^3}$ and $D_{0.1cm^3}$ values of 2.01 Gy, 2.43 Gy and 3.43 Gy. The EUD and $D_{2cm^3}$ constraints of the small bowel were violated by the IBG approach. The BIG approach recorded lower small bowel EUD, $D_{2cm^3}$ and $D_{0.1cm^3}$ values of 3.23 Gy, 4.04 Gy and 5.64 Gy. None of the rectum and sigmoid wall constraints was violated by any of the approaches. The IBG approach recorded a lower rectum wall $D_{0.1cm^3}$ value of 1.05 Gy and lower sigmoid wall EUD, $D_{2cm^3}$ and $D_{0.1cm^3}$ values of 4.80 Gy, 2.60 Gy and 6.05 Gy. The significant higher CTV-$T_{HR}$ values will improve local control in this patient, with a tumour size of 41 $cm^3$ and a dose difference of 9.32 Gy. With a dose of 90 Gy the 3-year local control rate of ± 93 % were reported, the dose of 99.32 Gy has the potential to improve this local control by ± 4%. [232]

For patient 7 and 8, the BIG approach used the rectum and sigmoid wall constraints that had some flexibility to its benefit, allowing higher doses in this OAR volumes. This allowed lower dose within the bladder and small bowel volumes. Not only did the BIG approach lower OAR of concern, but it also produced a plan which will have an impact on the LC of the patient.

[231] (Tanderup *et al.*, 2016)
[232] (Tanderup *et al.*, 2016)

In patient 9 -12, the bladder wall $D_{2cm^3}$ hard constraint and EUD hard constraint was only violated by the IBG approach.

In patient 9, the same CTV-$T_{HR}$ values were reported for both approaches; however, the IBG approach led to higher CTV-$T_{IR}$ $D_{90\,\%}$ and $D_{98\,\%}$ values of 3.74 Gy and 1.77 Gy. The BIG approach managed to record lower OAR values in all the OAR volumes compared to the IBG approach. Lower bladder wall EUD, $D_{2cm^3}$ and $D_{0.1cm^3}$ values of 11.10 Gy, 11.94 Gy and 17.46 Gy were recorded for the IBG approach. The BIG approach recorded lower small bowel EUD, $D_{2cm^3}$ and $D_{0.1cm^3}$ values of 1.18 Gy, 1.12 Gy and 1.92 Gy, with lower rectum wall EUD, $D_{2cm^3}$ and $D_{0.1cm^3}$ values of 3.46 Gy, 3.47 Gy and 5.00 Gy. The BIG approach recorded lower sigmoid wall EUD, $D_{2cm^3}$ and $D_{0.1cm^3}$ values of 8.07 Gy, 2.64 Gy and 8.73 Gy.

In patient 11, the same CTV-$T_{HR}$ values were reported for both approaches; however, the IBG approach led to higher CTV-$T_{IR}$ $D_{90\,\%}$ and $D_{98\,\%}$ values of 2.35 Gy and 2.46 Gy. The BIG approach recorded lower bladder wall EUD, $D_{2cm^3}$ and $D_{0.1cm^3}$ values of 16.93 Gy, 10.46 Gy and 26.58 Gy. The BIG approach recorded lower small bowel EUD, $D_{2cm^3}$ and $D_{0.1cm^3}$ values of 15.17 Gy, 12.22 Gy and 23.70 Gy. The sigmoid wall EUD hard constraint was violated by both approaches. The IBG approach recorded lower sigmoid wall EUD, $D_{2cm^3}$ and $D_{0.1cm^3}$ values of 3.87 Gy, 1.82 Gy and 5.12 Gy.

In patient 12, the same CTV-$T_{HR}$ values were reported for both approaches; however, the IBG approach led to higher CTV-$T_{IR}$ $D_{90\,\%}$ and $D_{98\,\%}$ values of 3.95 Gy and 2.46 Gy. The BIG approach recorded lower bladder wall EUD, $D_{2cm^3}$ and $D_{0.1cm^3}$ values of 6.05 Gy, 10.26 Gy and 9.22 Gy. The BIG approach recorded a lower small bowel EUD, $D_{2cm^3}$ and $D_{0.1cm^3}$ values of 5.58 Gy, 5.97 Gy and 8.32 Gy.

In patient 9-12, the serious violation of the bladder wall $D_{2cm^3}$ and EUD hard constraint by the IBG approach only, do not justify the higher CTV-$T_{IR}$ $D_{90\,\%}$ and $D_{98\,\%}$ values recorded.

In patient 14, the same CTV-T values were reported for both approaches. The IBG approach reached the bladder wall $D_{2cm^3}$ soft constraint, and the EUD hard constraint was violated by both approaches. The BIG approach recorded lower bladder wall EUD, $D_{2cm^3}$ and $D_{0.1cm^3}$ values of 2.66 Gy, 3.29 Gy and 4.07 Gy. Both approaches violate the small bowel EUD hard constraint; however, the BIG approach recorded lower small bowel EUD, $D_{2cm^3}$ and $D_{0.1cm^3}$ values of 1.76 Gy, 1.95 Gy and 3.17 Gy. The IBG approach recorded lower rectum and sigmoid wall $D_{2cm^3}$ and $D_{0.1cm^3}$ values of 1.07 Gy, 1.36 Gy and 1.19 Gy, 1.32 Gy, respectively. The sigmoid wall EUD hard constraint was violated, with no difference in the recorded values. The rest of the sigmoid and rectum wall constraints were not reached. The BIG approach's ability to recorded lower values for the bladder and small bowel, which were the OAR of main concern ensure the BIG approach to be superior to the IBG approach.

The BIG approach used the rectum and sigmoid wall constraints that had some flexibility to its benefit, which allowed lower dose within the bladder and small bowel volumes, which were mainly the OAR

volumes which hard constraints were violated with the intracavitary IGABT only. Not only did the BIG approach lower OAR of concern, but it also produced a plan in some patients with higher CTV-T values, which will have an impact on the LC of the patient.

A summary of the two approaches is given in Table 37 through Table 39.

**Table 37 - Average CTV-T $D_{90\,\%}$ $D_{98\,\%}$ and $D_{100\,\%}$ values of BIG and IBG approach**

| Approach | CTV-$T_{HR}$ $D_{90\,\%}$ (Gy) | CTV-$T_{HR}$ $D_{98\,\%}$ (Gy) | CTV-$T_{HR}$ $D_{100\,\%}$ (Gy) | CTV-$T_{IR}$ $D_{90\,\%}$ (Gy) | CTV-$T_{IR}$ $D_{98\,\%}$ (Gy) | CTV-$T_{IR}$ $D_{100\,\%}$ (Gy) |
|---|---|---|---|---|---|---|
| **BIG** | 92.25 ± 3.63 | 80.46 ± 3.64 | 72.37 ± 3.64 | 64.99 ± 3.06* | 61.41 ± 2.53* | 59.26 ± 2.03 |
| **IBG** | 90.06 ± 0.05 | 78.81 ± 1.66 | 71.85 ± 3.09 | 66.12 ± 2.56* | 62.37 ± 2.36* | 60.18 ± 2.03 |

***Tested for the significant difference with a p-value ≤ 0.05.**

When considering the CTV-$T_{HR}$ values, the BIG approach undoubtedly outperforms the IBG approach, which is in line with published results [233]. The IBG approach still provided better dose coverage in the CTV-$T_{IR}$ volume. This can be explained by the fact that the BIG approach applied was the forward optimisation BIG technique, and the IBG approach is an inverse optimisation approach. The inverse technique gave more priority to the CTV-$T_{IR}$ doses during the optimisation process, compared to the user during forward planning and optimisation process.

**Table 38 - Average $D_{2cm^3}$ and $D_{0.1cm^3}$ values for OAR walls of BIG and IBG approach**

| | Bladder wall | Small bowel | Rectum wall | Sigmoid wall | Recto-vaginal |
|---|---|---|---|---|---|
| **Approach** | **$D_{2cm^3}$ (Gy) Average ± SD** | **$D_{2cm^3}$ (Gy) Average ± SD** | **$D_{2cm^3}$ (Gy) Average ± SD** | **$D_{2cm^3}$ (Gy) Average ± SD** | **Dose point (Gy) Average ± SD** |
| **BIG** | 75.92 ± 0.75* | 68.86 ± 7.72* | 63.89 ± 2.95 | 64.65 ± 2.95 | 67.90 ± 5.19 |
| **IBG** | 82.65 ± 3.78* | 73.96 ± 8.64* | 64.60 ± 2.67 | 64.11 ± 4.15 | 69.95 ± 4.36 |
| **Approach** | **$D_{0.1cm^3}$ (Gy)** | **$D_{0.1cm^3}$ (Gy)** | **$D_{0.1cm^3}$ (Gy)** | **$D_{0.1cm^3}$ (Gy)** | **-** |
| **BIG** | 91.68 ± 2.68* | 79.55 ± 12.30* | 72.24 ± 5.52 | 77.35 ± 5.77 | - |
| **IBG** | 102.32 ± 7.69* | 88.10 ± 13.69* | 71.65 ± 3.85 | 75.60 ± 9.45 | - |

***Tested for the significant difference with a p-value ≤ 0.05.**

[233] (Fokdal *et al.*, 2016)

The average OAR values of the BIG and IBG approach for the seven patients are shown in Table 38. The BIG approach had an immense impact on bladder wall and small bowel $D_{2cm^3}$ and $D_{0.1m3}$ values, as well as a reduction in the recto-vaginal reference point. The difference in the average bladder wall and small bowel $D_{2cm^3}$ and $D_{0.1m3}$ values tested for the significant difference with $p \leq 0.05$. The addition of a needle to the tandem and ring configuration enabled the reduction of dwell times in the IU and ring sources which had the most impact on the bladder wall and small bowel dose values. This allowed for dose de-escalation, with significant lower EUD, $D_{2cm^3}$ and $D_{0.1m3}$ values reported for the bladder wall and small bowel.

The IBG approach recorded lower average rectum and sigmoid wall $D_{0.1m3}$ values, with no significant difference. The average dose to Point A and average TRAK values are shown in Table 39. The BIG approach led to significant lower TRAK values with $p \leq 0.05$.

**Table 39 - Average dose to point A and TRAK values of BIG and IBG approach**

| Approach | $A_{Left}$ (Gy) | $A_{Right}$ (Gy) | TRAK (cGy at 1 m) |
|---|---|---|---|
| **BIG** | 80.99 ± 14.27 | 75.13 ± 5.86 | 1.70 ± 0.22* |
| **IBG** | 78.10 ± 10.81 | 76.14 ± 6.73 | 1.95 ± 0.20* |

***Tested for the significant difference with a p-value ≤ 0.05.**

From the results, it is evident that the combination of IC/IS IGABT has an immense impact on the CTV-T and OAR doses, it enables CTV-T dose escalation which improves the therapeutic ratio and results in significantly higher local control rates in large tumours. This can be achieved without adding to treatment-related late morbidity [234]. The use of IC/IS applicators significantly correlates with local tumour control for CTV-$T_{HR}$ volumes ≥ 30 $cm^3$ [235]. The patient with the smallest CTV-$T_{HR}$ volume, planned with the IC/IS technique was 41 $cm^3$. If possible, patients who are candidates for IC/IS treatment should receive this treatment.

It is foreseen that if the IHDM are adapted to allow for inverse IC/IS optimisation and planning, it will produce even better outcome compared to the forward IC/IS approach, BIG. This will allow for a combination of even better target coverage and lower OAR values in the OAR volumes of main concern.

[234] (Fokdal et al., 2016)
[235] (Fokdal et al., 2016)

### 4.2.3.2 Inverse IC/IS IGABT planning

**Biological Interstitial Greedy (BIG) vs Inverse Biological Interstitial Greedy (IBIG)**

Only one patient was selected for inverse IC/IS IGABT planning and optimisation. The outcome was compared with the forward IC/IS outcome of the same patient. As summarised in Table 40, no significant differences were observed for the CTV-T values, apart from the CTV-$T_{IR}$ $D_{98\ \%}$ and $D_{100\ \%}$ which recorded 1.21 Gy and 0.99 Gy higher dose for the IBIG approach compared to the BIG approach.

**Table 40 - A summary of the CTV-T dose results obtained by the BIG and IBIG approach for patient 12.**

| Approach | CTV-$T_{HR}$ $D_{90\ \%}$ (Gy) | CTV-$T_{HR}$ $D_{98\ \%}$ (Gy) | CTV-$T_{HR}$ $D_{100\ \%}$ (Gy) | CTV-$T_{IR}$ $D_{90\ \%}$ (Gy) | CTV-$T_{IR}$ $D_{98\ \%}$ (Gy) | CTV-$T_{IR}$ $D_{100\ \%}$ (Gy) |
|---|---|---|---|---|---|---|
| **BIG** | 106.83 | 90.03 | 79.73 | 73.31 | 72.14 | 61.97 |
| **IBIG** | 106.41 | 90.12 | 80.52 | 73.71 | 73.35 | 62.96 |
| **Difference (Gy)** | 0.42 | -0.09 | -0.79 | -0.4 | -1.21 | -0.99 |

Positive difference values indicate that the BIG approach led to higher CTV-T values, where negative values indicate that the IBIG approach led to higher CTV-T values.

The average point A dose was reported as 80.78 Gy and 85.66 Gy, for the BIG and IBIG approach, respectively. The TRAK value recorded by the IBIG approach was higher than the value recorded for the BIG approach. The values were 1.94 and 1.49 cGy at 1 m, respectively.

The OAR dose differences are displayed below in Table 41.

**Table 41 – A summary of the OAR dose results obtained by the BIG and IBIG approach for patient 12.**

| | Bladder wall | | | Small bowel | | |
|---|---|---|---|---|---|---|
| **Approach** | **EUD (Gy)** | **$D_{2cm^3}$ (Gy)** | **$D_{0.1cm^3}$ (Gy)** | **EUD (Gy)** | **$D_{2cm^3}$ (Gy)** | **$D_{0.1cm^3}$ (Gy)** |
| **BIG** | 75.61 | 74.92 | 94.95 | 72.09 | 71.13 | 86.73 |
| **IBIG** | 69.91 | 71.85 | 84.34 | 70.58 | 70.82 | 83.68 |
| **Difference (Gy)** | **5.70** | **3.07** | **10.61** | **1.51** | **0.31** | **3.05** |
| | **Rectum wall** | | | **Sigmoid wall** | | |
| **Approach** | **EUD (Gy)** | **$D_{2cm^3}$ (Gy)** | **$D_{0.1cm^3}$ (Gy)** | **EUD (Gy)** | **$D_{2cm^3}$ (Gy)** | **$D_{0.1cm^3}$ (Gy)** |
| **BIG** | 71.84 | 66.83 | 81.43 | 68.6 | 61.08 | 73.7 |
| **IBIG** | 68.44 | 65.88 | 76.78 | 69.1 | 62.31 | 74.47 |
| **Difference (Gy)** | **3.40** | **0.95** | **4.65** | **-0.50** | **-1.23** | **-0.77** |

Positive difference values indicate that the IBIG approach led to lower OAR values, where negative values indicate that the BIG approach led to lower OAR values.

Significant differences were observed between the two approaches for this patient. The IBIG approach delivered a plan with significant lower bladder wall, small bowel and rectum wall doses compared to the BIG approach. The EUD hard constraint of the bladder wall was nearly reached by the BIG approach; however, the IBIG approach led to lower EUD, $D_{2cm^3}$ and $D_{0.1cm^3}$ values of 5.7 Gy, 3.07 Gy and 10.61 Gy, respectively. The $D_{2cm^3}$ soft constraint of the small bowel was violated by both approaches, as well as the EUD hard constraint. The IBIG approach led to significant lower small bowel EUD and $D_{0.1cm^3}$ values of 1.51 Gy and 3.05 Gy. The EUD hard constraint of the rectum and the sigmoid wall was violated by the BIG and IBIG approach; however, no $D_{2cm^3}$ constraints were reached. The IBIG approach led to significant lower rectum wall EUD and $D_{0.1cm^3}$ values of 3.40 Gy and 4.65 Gy. The BIG approach still reported lower sigmoid wall dose values, a significant lower $D_{2cm^3}$ value of 1.23 Gy; however, both approaches did not reach the $D_{2cm^3}$ soft constraint of 70 Gy.

Even though only one patient was optimised and planned with the IBIG approach, this IHDM tool shows tremendous potential.

# Chapter 5 - Conclusion

The study aimed to develop a novel biological optimisation model that could be used to efficiently and automatically optimise BT plans utilising either dose-volume or biological metrics/indexes or both for fast treatment plan generation.

The IHDM can be described as an all-in-one IGABT module. The IHDM can perform forward and inverse optimisation and planning for Intracavitary IGABT and IC/IS IGABT treatment, with live dose updates throughout the optimisation process. Before the optimisation and planning processes, the IHDM automatically incorporate the dose already received during treatment and automatically calculate, display and apply fractional OAR dose constraints applicable to the current fraction. This is done without the need for a secondary calculation program. The current IHDM only lacks the ability to perform automatic contouring, an aspect that will be addressed in future studies.

The study incorporated biological metrics, which displayed promising results and emphasized the necessity to include biological metrics in IGABT treatment planning, especially in centres which lack in MRI imaging abilities with only CT imaging available. All recorded EUD values of OARs walls were higher than the EUD of the whole OAR itself. Biological planning did produce superior CTV-T doses, which led to improved dose distributions within the CTV-T. The IBG approach reported significantly higher average CTV-$T_{HR}$ $D_{98\,\%}$ values and CTV-$T_{IR}$ EUD, $D_{98\,\%}$ and $D_{100\,\%}$ values compared to conventional planning, the ICG approach. With this, the IBG approach also recorded significantly lower average bladder wall EUD and $D_{0.1cm^3}$ values. Even though the ICG approach reported significant lower average small bowel $D_{2cm^3}$ values compared to the IBG approach, both approaches were still well below the $D_{2cm^3}$ hard constraint of 75 Gy. Taking these results into account, the benefits from the IBG approach outweighs that of the ICG approach.

CTV-T and OAR dose values obtained by the IBG approach were in line with published dose constraints and planning aims. The IBG approach could exploit and incorporate all OAR into the optimisation process, ensuring that constraints exploited to their full potential and in return, deliver a better dose distribution within the CTV-T volumes.

Lastly, it was shown, as was reported by several authors, that dose escalation can be achieved in the CTV-T with a noteworthy reduction in OAR dose with the combination of IC/IS IGABT. OAR dose de-escalation was achieved in all the IC/IS IGABT plans whether the same CTV-T dose was reported or not.

A novel biological optimisation model was developed that was used to efficiently and automatically optimise BT plans by utilising either dose-volume or biological metrics/indexes or both for fast treatment plan generation.

# Chapter 6 - References


Altekruse, S. F. (2003) 'Comparison of human papillomavirus genotypes, sexual, and reproductive risk factors of cervical adenocarcinoma and squamous cell carcinoma: Northeastern United States', *American Journal of Obstetrics and Gynecology*, 188(3), pp. 657–663. doi: 10.1067/mob.2003.132.

Bacorro, W. (2017) 'Contribution of image-guided adaptive brachytherapy to pelvic nodes treatment in locally advanced cervical cancer', *Brachytherapy*, 16(2), pp. 366–372. doi: 10.1016/j.brachy.2016.11.016.

Bae, H. S. (2016) 'Predictors of radiation field failure after definitive chemoradiation in patients with locally advanced cervical cancer', *International Journal of Gynecological Cancer*, 26(4), pp. 737–742. doi: 10.1097/IGC.0000000000000662.

Banerjee, R. (2014) 'Brachytherapy in the treatment of cervical cancer: a review.', *International journal of women's health*, 6, pp. 555–64. doi: 10.2147/IJWH.S46247.

Barbera, L. (2009) 'Management of Early and Locally Advanced Cervical Cancer', *Seminars in Oncology*, 36(2), pp. 155–169. doi: 10.1053/j.seminoncol.2008.12.007.

Barker, J. L. (2004) 'Quantification of volumetric and geometric changes occurring during fractionated radiotherapy for head-and-neck cancer using an integrated CT/linear accelerator system', *International Journal of Radiation Oncology*Biology*Physics*, 59(4), pp. 960–970. doi: 10.1016/j.ijrobp.2003.12.024.

Barrett, A. (2009) *Practical Radiotherapy Planning*, *Practical Radiotherapy Planning*. Hodder Arnold. doi: 10.1201/b13373.

Batra, P. (2010) 'Utilisation and outcomes of cervical cancer prevention services among HIV-infected women in Cape Town.', *South African medical journal = Suid-Afrikaanse tydskrif vir geneeskunde*, 100(1), pp. 39–44. Available at: http://www.ncbi.nlm.nih.gov/pubmed/20429487 (Accessed: 19 October 2018).

Beriwal, S. (2009) 'Single Magnetic Resonance Imaging vs Magnetic Resonance Imaging/Computed Tomography Planning in Cervical Cancer Brachytherapy', *Clinical Oncology*, 21(6), pp. 483–487. doi: 10.1016/j.clon.2009.03.007.

Bhatla, N. (2019) 'Revised FIGO staging for carcinoma of the cervix uteri', *International Journal of Gynecology and Obstetrics*, 145(1), pp. 129–135. doi: 10.1002/ijgo.12749.

Bjelic-Radisic, V. (2012) 'Quality of life characteristics inpatients with cervical cancer', *European Journal of Cancer*, 48(16), pp. 3009–3018. doi: 10.1016/j.ejca.2012.05.011.

Bockel, S. (2019) 'Total Reference Air Kerma is Associated with Late Bowel Morbidity in Locally Advanced Cervical Cancer Patients Treated with Image-Guided Adaptive Brachytherapy', *Journal of Clinical Medicine*, 8(1), p. 125. doi: 10.3390/jcm8010125.

Botha, M. H. (2017) 'Guidelines for cervical cancer screening in South Africa', *Southern African Journal of Gynaecological Oncology*, 9(1), pp. 8–12. Available at: http://www.sajgo.co.za/index.php/sajgo/article/view/253/pdf_4.

Bruni, L. (2019) *Human Papillomavirus and Related Diseases in South Africa*. Available at: https://hpvcentre.net/statistics/reports/ZAF.pdf?t=1589461112482 (Accessed: 14 May 2020).

van de Bunt, L. (2006) 'Conventional, conformal, and intensity-modulated radiation therapy treatment planning of external beam radiotherapy for cervical cancer: The impact of tumor regression', *International Journal of Radiation Oncology*Biology*Physics*, 64(1), pp. 189–196. doi: 10.1016/j.ijrobp.2005.04.025.

Charra-Brunaud, C. (2012) 'Impact of 3D image-based PDR brachytherapy on outcome of patients treated for cervix carcinoma in France : Results of the French STIC prospective study q', *Radiotherapy and Oncology*, 103(3), pp. 305–313. doi: 10.1016/j.radonc.2012.04.007.

Chassagne, D. (1977) 'Proposals for common definitions of reference points in gynecological brachytherapy', *J. Radiol., Electrol., Med. Nucl*, 58da(5), pp. 371–373. Available at: https://inis.iaea.org/search/search.aspx?orig_q=RN:8340495 (Accessed: 14 July 2019).

Chassagne, D. (1985) 'Report 38', *Journal of the International Commission on Radiation Units and Measurements*, os20(1), p. NP-NP. doi: 10.1093/JICRU/OS20.1.REPORT38.

Chen, L. A. (2015) 'Toxicity and cost-effectiveness analysis of intensity modulated radiation therapy versus 3-dimensional conformal radiation therapy for postoperative treatment of gynecologic cancers', *Gynecologic Oncology*, 136(3), pp. 521–528. doi: 10.1016/j.ygyno.2014.12.039.

Cho, O. (2018) 'Management for locally advanced cervical cancer: New trends and controversial issues', *Radiation Oncology Journal*, 36(4), pp. 254–264. doi: 10.3857/roj.2018.00500.

Choi, K. H. (2018) 'Clinical impact of boost irradiation to pelvic lymph node in uterine cervical cancer treated with definitive chemoradiotherapy', *Medicine (United States)*, 97(16). doi: 10.1097/MD.0000000000010517.

Dappa, E. (2017) 'The value of advanced MRI techniques in the assessment of cervical cancer: a review', *Insights into Imaging*. Springer Verlag, pp. 471–481. doi: 10.1007/s13244-017-0567-0.

Datta, N. R. (2001) 'Variations of intracavitary applicator geometry during multiple HDR brachytherapy insertions in carcinoma cervix and its influence on reporting as per ICRU report 38', *Radiotherapy and Oncology*, 60(1), pp. 15–24. doi: 10.1016/S0167-8140(01)00352-8.

Datta, N. R. (2003) 'Problems in reporting doses and volumes during multiple high-dose-rate intracavitary brachytherapy for carcinoma cervix as per ICRU Report 38: a comparative study using flexible and rigid applicators', *Gynecologic Oncology*, 91(2), pp. 285–292. doi: 10.1016/S0090-8258(03)00506-7.

Datta, N. R. (2003) 'Total reference air kerma: To what extent can it predict intracavitary volume enclosed by isodose surfaces during multiple high-dose rate brachytherapy?', *Brachytherapy*, 2, pp. 91–97. doi: 10.1016/S.

Datta, N. R. (2004) 'Problems and uncertainties with multiple point A's during multiple high-dose-rate intracavitary brachytherapy in carcinoma of the cervix.', *Clinical oncology (Royal College of Radiologists (Great Britain))*, 16(2), pp. 129–37. doi: 10.1016/J.CLON.2003.10.011.

Datta, N. R. (2005) 'From "points" to "profiles" in intracavitary brachytherapy of cervical cancer.', *Current opinion in obstetrics & gynecology*, 17(1), pp. 35–41. doi: 10.1097/00001703-200502000-00007.

Datta, N. R. (2006) 'Comparative assessment of doses to tumor, rectum, and bladder as evaluated by orthogonal radiographs vs. computer enhanced computed tomography-based intracavitary brachytherapy in cervical cancer', *Brachytherapy*, 5(4), pp. 223–229. doi: 10.1016/j.brachy.2006.09.001.

Delgado, D. (2019) 'Results from chemoradiotherapy for squamous cell cervical cancer with or without intracavitary brachytherapy', *Journal of Contemporary Brachytherapy*, 11(5), pp. 417–422. doi: 10.5114/jcb.2019.88116.

Delgado, G. (1990) 'Prospective surgical-pathological study of disease-free interval in patients with stage IB squamous cell carcinoma of the cervix: A Gynecologic Oncology Group study', *Gynecologic Oncology*, 38(3), pp. 352–357. doi: 10.1016/0090-8258(90)90072-S.

Deng, X. (2017) 'Dosimetric benefits of intensity-modulated radiotherapy and volumetric-modulated

arc therapy in the treatment of postoperative cervical cancer patients', *Journal of Applied Clinical Medical Physics*, 18(1), pp. 25–31. doi: 10.1002/acm2.12003.

Denham, J. W. (2013) 'Radiation induced bowel injury: A neglected problem', *The Lancet*, pp. 2046–2047. doi: 10.1016/S0140-6736(13)61946-7.

Denny, L. (2008) 'Prevention of cervical cancer', *Reproductive Health Matters*, 16(32), pp. 18–31. doi: 10.1016/S0968-8080(08)32397-0.

Denny, L. (2017) 'Cervical cancer prevention and early detection from a South African perspective', *South African Health Review*, pp. 189–196. Available at: http://ovidsp.ovid.com/ovidweb.cgi?T=JS&CSC=Y&NEWS=N&PAGE=fulltext&D=cagh&AN=20183060901
http://oxfordsfx.hosted.exlibrisgroup.com/oxford?sid=OVID:caghdb&id=pmid:&id=doi:&issn=1025-1715&isbn=&volume=2017&issue=&spage=189&pages=189-195&date=2017&title=Sout.

Denton, A. S. (2003) 'Interventions for the physical aspects of sexual dysfunction in women following pelvic radiotherapy', *Cochrane Database of Systematic Reviews*, p. CD003750. doi: 10.1002/14651858.CD003750.

Dimopoulos, J. C. A. (2006) 'Systematic evaluation of MRI findings in different stages of treatment of cervical cancer: Potential of MRI on delineation of target, pathoanatomic structures, and organs at risk', *International Journal of Radiation Oncology*Biology*Physics*, 64(5), pp. 1380–1388. doi: 10.1016/j.ijrobp.2005.10.017.

Dimopoulos, J. C. A. (2006) 'The Vienna applicator for combined intracavitary and interstitial brachytherapy of cervical cancer: Clinical feasibility and preliminary results', *International Journal of Radiation Oncology*Biology*Physics*, 66(1), pp. 83–90. doi: 10.1016/j.ijrobp.2006.04.041.

Dimopoulos, Johannes C.A. (2009) 'Dose-Volume Histogram Parameters and Local Tumor Control in Magnetic Resonance Image-Guided Cervical Cancer Brachytherapy', *International Journal of Radiation Oncology Biology Physics*, 75(1), pp. 56–63. doi: 10.1016/j.ijrobp.2008.10.033.

Dimopoulos, Johannes C A (2009) 'Dose – effect relationship for local control of cervical cancer by magnetic resonance image-guided brachytherapy', *Radiotherapy and Oncology*, 93(2), pp. 311–315. doi: 10.1016/j.radonc.2009.07.001.

Dimopoulos, Johannes C. A. (2009) 'MRI Assessment of Cervical Cancer for Adaptive Radiotherapy', *Strahlentherapie und Onkologie*, 185(5), pp. 282–287. doi: 10.1007/s00066-009-1918-7.

E.B.Podgorsak (2005) *Radiation Oncology Physics: A Handbook for Teachers and Students*, *International Atomic Energy Agency*. doi: 10.1038/sj.bjc.6604224.

Eifel, P. J. (1994) 'The influence of tumor size and morphology on the outcome of patients with figo stage IB squamous cell carcinoma of the uterine cervix', *International Journal of Radiation Oncology, Biology, Physics*, 29(1), pp. 9–16. doi: 10.1016/0360-3016(94)90220-8.

Eifel, P. J. (2004) 'Pelvic irradiation with concurrent chemotherapy versus pelvic and para-aortic irradiation for high-risk cervical cancer: An update of Radiation Therapy Oncology Group Trial (RTOG) 90-01', *Journal of Clinical Oncology*, 22(5), pp. 872–880. doi: 10.1200/JCO.2004.07.197.

Eifel, P. J. (2006) 'Concurrent chemotherapy and radiation therapy as the standard of care for cervical cancer', *Nature Clinical Practice Oncology*. Nat Clin Pract Oncol, pp. 248–255. doi: 10.1038/ncponc0486.

Elshaikh, M. (2006) 'Advances in radiation oncology', *Annual Review of Medicine*, pp. 19–31. doi: 10.1146/annurev.med.57.121304.131431.

Eskander, R. N. (2010) 'Comparison of Computed Tomography and Magnetic Resonance Imaging in Cervical Cancer Brachytherapy Target and Normal Tissue Contouring', *International Journal of*

*Gynecological Cancer*, 20(1), pp. 47–53. doi: 10.1111/IGC.0b013e3181c4a627.

Fellner, C. (2001) 'Comparison of radiography- and computed tomography-based treatment planning in cervix cancer in brachytherapy with specific attention to some quality assurance aspects', *Radiotherapy and Oncology*, 58(1), pp. 53–62. doi: 10.1016/S0167-8140(00)00282-6.

Fokdal, L. (2013) 'Clinical feasibility of combined intracavitary/interstitial brachytherapy in locally advanced cervical cancer employing MRI with a tandem/ring applicator in situ and virtual preplanning of the interstitial component', *Radiotherapy and Oncology*, 107(1), pp. 63–68. doi: 10.1016/j.radonc.2013.01.010.

Fokdal, L. (2016) 'Image guided adaptive brachytherapy with combined intracavitary and interstitial technique improves the therapeutic ratio in locally advanced cervical cancer: Analysis from the retroEMBRACE study', *Radiotherapy and Oncology*, 120(3), pp. 434–440. doi: 10.1016/j.radonc.2016.03.020.

Fokdal, L. (2018) 'Physician assessed and patient reported urinary morbidity after radio-chemotherapy and image guided adaptive brachytherapy for locally advanced cervical cancer', *Radiotherapy and Oncology*, 127(3), pp. 423–430. doi: 10.1016/j.radonc.2018.05.002.

Fokdal, L. (2019) 'Risk Factors for Ureteral Stricture After Radiochemotherapy Including Image Guided Adaptive Brachytherapy in Cervical Cancer: Results From the EMBRACE Studies', *International Journal of Radiation Oncology Biology Physics*, 103(4), pp. 887–894. doi: 10.1016/j.ijrobp.2018.11.006.

Frumovitz, M. (2005) 'Quality of Life and Sexual Functioning in Cervical Cancer Survivors', *Journal of Clinical Oncology*, 23(30), pp. 7428–7436. doi: 10.1200/JCO.2004.00.3996.

Frumovitz, M. (2015) *Invasive cervical cencer: epidemiology, risk factors, clinical menifestations, and diagnosis*, *UpToDate*. Available at: UpToDate. (Accessed: 15 May 2020).

Fyles, A. W. (1995) 'Prognostic factors in patients with cervix cancer treated by radiation therapy: results of a multiple regression analysis', *Radiotherapy and Oncology*, 35(2), pp. 107–117. doi: 10.1016/0167-8140(95)01535-O.

Gandhi, A. K. (2013) 'Early clinical outcomes and toxicity of intensity modulated versus conventional pelvic radiation therapy for locally advanced cervix carcinoma: A prospective randomized study', *International Journal of Radiation Oncology Biology Physics*, 87(3), pp. 542–548. doi: 10.1016/j.ijrobp.2013.06.2059.

Georg, P. (2012) 'Dose effect relationship for late side effects of the rectum and urinary bladder in magnetic resonance image-guided adaptive cervix cancer brachytherapy', *International Journal of Radiation Oncology Biology Physics*, 82(2), pp. 653–657. doi: 10.1016/j.ijrobp.2010.12.029.

Girinsky, T. (1993) 'Overall treatment time in advanced cervical carcinomas: a critical parameter in treatment outcome.', *International journal of radiation oncology, biology, physics*, 27(5), pp. 1051–6. doi: 10.1016/0360-3016(93)90522-w.

Granero, D. (2006) 'A dosimetric study on the Ir-192 high dose rate Flexisource', *Medical Physics*, 33(12), pp. 4578–4582. doi: 10.1118/1.2388154.

Greimel, E. R. (2009) 'Quality of life and sexual functioning after cervical cancer treatment: a long-term follow-up study', *Psycho-Oncology*, 18(5), pp. 476–482. doi: 10.1002/pon.1426.

Grigsby, P. W. (1993) 'Anatomic variation of gynecologic brachytherapy prescription points', *International Journal of Radiation Oncology*Biology*Physics*, 27(3), pp. 725–729. doi: 10.1016/0360-3016(93)90402-H.

Gulia, A. (2013) 'Conventional four field radiotherapy versus computed tomography-based treatment planning in cancer cervix: A dosimetric study.', *South Asian journal of cancer*, 2(3), pp. 132–5. doi: 10.4103/2278-330X.114116.

Haie-Meder, C. (2005) 'Recommendations from Gynaecological (GYN) GEC-ESTRO Working Group (I): Concepts and terms in 3D image based 3D treatment planning in cervix cancer brachytherapy with emphasis on MRI assessment of GTV and CTV', *Radiotherapy and Oncology*, 74(3), pp. 235–245. doi: 10.1016/j.radonc.2004.12.015.

Han, K. (2013) 'Trends in the utilization of brachytherapy in cervical cancer in the United States', *International Journal of Radiation Oncology Biology Physics*, 87(1), pp. 111–119. doi: 10.1016/j.ijrobp.2013.05.033.

Hanks, G. E. (1983) 'Patterns of care outcome studies. Results of the national practice in cancer of the cervix.', *Cancer*, 51(5), pp. 959–67. Available at: http://www.ncbi.nlm.nih.gov/pubmed/6821861 (Accessed: 19 October 2018).

Hareyama, M. (2002) 'High-dose-rate versus low-dose-rate intracavitary therapy for carcinoma of the uterine cervix', *Cancer*, 94(1), pp. 117–124. doi: 10.1002/cncr.10207.

Haripotepornkul, N. H. (2011) 'Evaluation of intra- and inter-fraction movement of the cervix during intensity modulated radiation therapy', *Radiotherapy and Oncology*, 98(3), pp. 347–351. doi: 10.1016/j.radonc.2010.11.015.

Härkki-Sirén, P. (1998) 'Urinary tract injuries after hysterectomy.', *Obstetrics and gynecology*, 92(1), pp. 113–8. Available at: http://www.ncbi.nlm.nih.gov/pubmed/9649105 (Accessed: 21 July 2019).

Hegazy, N. (2013) 'High-risk clinical target volume delineation in CT-guided cervical cancer brachytherapy: Impact of information from FIGO stage with or without systematic inclusion of 3D documentation of clinical gynecological examination', *Acta Oncologica*, 52(7), pp. 1345–1352. doi: 10.3109/0284186X.2013.813068.

Heijkoop, S. T. (2015) 'Quantification of intra-fraction changes during radiotherapy of cervical cancer assessed with pre- and post-fraction Cone Beam CT scans', *Radiotherapy and Oncology*, 117(3), pp. 536–541. doi: 10.1016/j.radonc.2015.08.034.

Hoskin, P. J. (1996) 'Changes in applicator position with fractionated high dose rate gynaecological brachytherapy', *Radiotherapy and Oncology*, 40(1), pp. 59–62. doi: 10.1016/0167-8140(96)01746-X.

Huh, W. K. (2015) 'Use of primary high-risk human papillomavirus testing for cervical cancer screening: Interim clinical guidance', *Journal of Lower Genital Tract Disease*, 19(2), pp. 91–96. doi: 10.1097/LGT.0000000000000103.

Ingber, L. (1993) 'Simulated annealing: Practice versus theory', *Mathematical and Computer Modelling*, 18(11), pp. 29–57. doi: 10.1016/0895-7177(93)90204-C.

Jadon, R. (2014) 'A Systematic Review of Organ Motion and Image-guided Strategies in External Beam Radiotherapy for Cervical Cancer', *Clinical Oncology*, 26(4), pp. 185–196. doi: 10.1016/j.clon.2013.11.031.

Jason D Wright, M. D. (2019) 'Cervical intraepithelial neoplasia: Terminology, incidence, pathogenesis, and prevention - UpToDate', *UpTo Date*, pp. 1–20. Available at: https://www.uptodate.com/contents/cervical-intraepithelial-neoplasia-terminology-incidence-pathogenesis-and-prevention#! (Accessed: 15 May 2020).

Jensen, N. B. K. (2018) 'Bowel morbidity following radiochemotherapy and image-guided adaptive brachytherapy for cervical cancer: Physician- and patient reported outcome from the EMBRACE study.', *Radiotherapy and oncology : journal of the European Society for Therapeutic Radiology and Oncology*, 127(3), pp. 431–439. doi: 10.1016/j.radonc.2018.05.016.

Jensen, P. T. (2003) 'Longitudinal study of sexual function and vaginal changes after radiotherapy for cervical cancer', *International Journal of Radiation Oncology Biology Physics*, 56(4), pp. 937–949. doi: 10.1016/S0360-3016(03)00362-6.

Jürgenliemk-Schulz, I. M. (2009) 'MRI-guided treatment-planning optimisation in intracavitary or combined intracavitary/interstitial PDR brachytherapy using tandem ovoid applicators in locally advanced cervical cancer', *Radiotherapy and Oncology*, 93(2), pp. 322–330. doi: 10.1016/j.radonc.2009.08.014.

Jürgenliemk-Schulz, I. M. (2010) 'Variation of treatment planning parameters (D90 HR-CTV, D2ccfor OAR) for cervical cancer tandem ring brachytherapy in a multicentre setting: Comparison of standard planning and 3D image guided optimisation based on a joint protocol for dose-volume constra', *Radiotherapy and Oncology*, 94(3), pp. 339–345. doi: 10.1016/j.radonc.2009.10.011.

Kang, H.-C. (2010) '3D CT-based high-dose-rate brachytherapy for cervical cancer: Clinical impact on late rectal bleeding and local control', *Radiotherapy and Oncology*, 97(3), pp. 507–513. doi: 10.1016/j.radonc.2010.10.002.

Kapp, K. S. (1992) 'Dosimetry of intracavitary placements for uterine and cervical carcinoma: results of orthogonal film, TLD, and CT-assisted techniques.', *Radiotherapy and oncology : journal of the European Society for Therapeutic Radiology and Oncology*, 24(3), pp. 137–46. Available at: http://www.ncbi.nlm.nih.gov/pubmed/1410567 (Accessed: 13 July 2019).

Karabis, A. (2005) 'HIPO: A hybrid inverse treatment planning optimisation algorithm in HDR brachytherapy', *Radiotherapy and Oncology*, 76, p. S29. doi: 10.1016/s0167-8140(05)81018-7.

Kirchheiner, K. (2014) 'Manifestation pattern of early-late vaginal morbidity after definitive radiation (Chemo)therapy and image-guided adaptive brachytherapy for locally advanced cervical cancer: An analysis from the embrace study', *International Journal of Radiation Oncology Biology Physics*, 89(1), pp. 88–95. doi: 10.1016/j.ijrobp.2014.01.032.

Kirchheiner, K. (2015) 'Health related quality of life and patient reported symptoms before and during definitive radio(chemo)therapy using image-guided adaptive brachytherapy for locally advanced cervical cancer and early recovery - A mono-institutional prospective study', *Gynecologic Oncology*, 136(3), pp. 415–423. doi: 10.1016/j.ygyno.2014.10.031.

Kirchheiner, K. (2016) 'Dose-effect relationship and risk factors for vaginal stenosis after definitive radio(chemo)therapy with image-guided brachytherapy for locally advanced cervical cancer in the EMBRACE study', *Radiotherapy and Oncology*, 118(1), pp. 160–166. doi: 10.1016/j.radonc.2015.12.025.

Kirisits, C. (2005) 'Dose and volume parameters for MRI-based treatment planning in intracavitary brachytherapy for cervical cancer', *International Journal of Radiation Oncology*Biology*Physics*, 62(3), pp. 901–911. doi: 10.1016/j.ijrobp.2005.02.040.

Kirisits, C. (2006) 'The Vienna applicator for combined intracavitary and interstitial brachytherapy of cervical cancer: Design, application, treatment planning, and dosimetric results', *International Journal of Radiation Oncology*Biology*Physics*, 65(2), pp. 624–630. doi: 10.1016/j.ijrobp.2006.01.036.

Kirkpatrick, S. (1983) 'Optimisation by simulated annealing', *Science*, 220(4598), pp. 671–680. doi: 10.1126/science.220.4598.671.

Kitchener, H. C. (2014) 'The clinical effectiveness and cost-effectiveness of primary human papillomavirus cervical screening in England: Extended follow-up of the ARTISTIC randomised trial cohort through three screening rounds', *Health Technology Assessment*, 18(23), pp. 1–195. doi: 10.3310/hta18230.

Klee, M. (2000) 'Life after Radiotherapy: The Psychological and Social Effects Experienced by Women Treated for Advanced Stages of Cervical Cancer', *Gynecologic Oncology*, 76(1), pp. 5–13. doi: 10.1006/gyno.1999.5644.

Klopp, A. H. (2016) 'A Phase III Randomized Trial Comparing Patient-Reported Toxicity and Quality of Life (QOL) During Pelvic Intensity Modulated Radiation Therapy as Compared to Conventional

Radiation Therapy', *International Journal of Radiation Oncology*Biology*Physics*, 96(2), p. S3. doi: 10.1016/j.ijrobp.2016.06.024.

Koom, W. S. (2007) 'Computed Tomography-Based High-Dose-Rate Intracavitary Brachytherapy for Uterine Cervical Cancer: Preliminary Demonstration of Correlation Between Dose–Volume Parameters and Rectal Mucosal Changes Observed by Flexible Sigmoidoscopy', *International Journal of Radiation Oncology*Biology*Physics*, 68(5), pp. 1446–1454. doi: 10.1016/j.ijrobp.2007.02.009.

Kovalic, J. J. (1991) 'The effect of volume of disease in patients with carcinoma of the uterine cervix.', *International journal of radiation oncology, biology, physics*, 21(4), pp. 905–10. doi: 10.1016/0360-3016(91)90728-m.

Krishnatry, R. (2012) 'CT or MRI for Image-based Brachytherapy in Cervical Cancer', *Japanese Journal of Clinical Oncology*, 42(4), pp. 309–313. doi: 10.1093/jjco/hys010.

Kuipers, T. (2001) 'HDR brachytherapy applied to cervical carcinoma with moderate lateral expansion: modified principles of treatment.', *Radiotherapy and oncology : journal of the European Society for Therapeutic Radiology and Oncology*, 58(1), pp. 25–30. Available at: http://www.ncbi.nlm.nih.gov/pubmed/11165678 (Accessed: 14 July 2019).

Kumar, M. (2019) 'Impact of different dose prescription schedules on EQD2 in high-dose-rate intracavitary brachytherapy of carcinoma cervix', *Journal of Contemporary Brachytherapy*, 11(2), pp. 189–193. doi: 10.5114/jcb.2019.84586.

Lahanas, M. (2003) 'A hybrid evolutionary algorithm for multi-objective anatomy-based dose optimisation in high-dose-rate brachytherapy', *Physics in Medicine and Biology*, 48(3), pp. 399–415. doi: 10.1088/0031-9155/48/3/309.

Lang, S. (2007a) 'Treatment Planning for MRI Assisted Brachytherapy of Gynecologic Malignancies Based on Total Dose Constraints', *International Journal of Radiation Oncology Biology Physics*, 69(2), pp. 619–627. doi: 10.1016/j.ijrobp.2007.06.019.

Lang, S. (2007b) 'Treatment Planning for MRI Assisted Brachytherapy of Gynecologic Malignancies Based on Total Dose Constraints', *International Journal of Radiation Oncology Biology Physics*, 69(2), pp. 619–627. doi: 10.1016/j.ijrobp.2007.06.019.

Lertsanguansinchai, P. (2004) 'Phase III randomized trial comparing LDR and HDR brachytherapy in treatment of cervical carcinoma', *International Journal of Radiation Oncology*Biology*Physics*, 59(5), pp. 1424–1431. Available at: https://linkinghub.elsevier.com/retrieve/pii/S0360301604002068 (Accessed: 13 July 2019).

Lessard, E. (2001) 'Inverse planning anatomy-based dose optimisation for HDR-brachytherapy of the prostate using fast simulated annealing algorithm and dedicated objective function', *Medical Physics*, 28(5), pp. 773–779. doi: 10.1118/1.1368127.

LEWIS, G. C. (1960) 'Space dose relationships for points A and B in the radium therapy of cancer of the uterine cervix.', *The American journal of roentgenology, radium therapy, and nuclear medicine*, 83, pp. 432–46. Available at: http://www.ncbi.nlm.nih.gov/pubmed/14416519 (Accessed: 13 July 2019).

Lindegaard, J. C. (2013) 'MRI-guided adaptive radiotherapy in locally advanced cervical cancer from a Nordic perspective', *Acta Oncologica*, 52(7), pp. 1510–1519. doi: 10.3109/0284186X.2013.818253.

Ling, C. C. (1987) 'CT-assisted assessment of bladder and rectum dose in gynecological implants', *International Journal of Radiation Oncology*Biology*Physics*, 13(10), pp. 1577–1582. doi: 10.1016/0360-3016(87)90327-0.

Logsdon, M. (1999) 'Figo IIIB squamous cell carcinoma of the cervix: an analysis of prognostic factors emphasizing the balance between external beam and intracavitary radiation therapy.', *Int J Radiat Oncol Biol Phys*, 43(4), pp. 763–775. Available at: https://www.ncbi.nlm.nih.gov/pubmed/10098431.

Mahmoud, O. (2017) 'External beam techniques to boost cervical cancer when brachytherapy is not an option-Theories and applications', *Annals of Translational Medicine*. AME Publishing Company. doi: 10.21037/atm.2017.03.102.

Maier, U. (1997) 'Late Urological Complications and Malignancies After Curative Radiotherapy for Gynecological Carcinomas', *The Journal of Urology*, 158(3 Pt 1), pp. 814–817. doi: 10.1097/00005392-199709000-00033.

Maiman, M. (1998) 'Management of cervical neoplasia in human immunodeficiency virus-infected women.', *Journal of the National Cancer Institute. Monographs*, (23), pp. 43–9. Available at: http://www.ncbi.nlm.nih.gov/pubmed/9709302 (Accessed: 19 October 2018).

*Management of Cervical Cancer: Strategies for Limited-resource Centres - A Guide for Radiation Oncologists* (2013). Vienna: INTERNATIONAL ATOMIC ENERGY AGENCY (Human Health Reports). Available at: https://www.iaea.org/publications/8738/management-of-cervical-cancer-strategies-for-limited-resource-centres-a-guide-for-radiation-oncologists.

Martinez, A. A. (2001) 'Improvement in dose escalation using the process of adaptive radiotherapy combined with three-dimensional conformal or intensity-modulated beams for prostate cancer', *International Journal of Radiation Oncology*Biology*Physics*, 50(5), pp. 1226–1234. doi: 10.1016/S0360-3016(01)01552-8.

Mazeron, R. (2015) 'Impact of treatment time and dose escalation on local control in locally advanced cervical cancer treated by chemoradiation and image-guided pulsed-dose rate adaptive brachytherapy', *Radiotherapy and Oncology*, 114(2), pp. 257–263. doi: 10.1016/j.radonc.2014.11.045.

Mazeron, R. (2016) 'Dose–volume effect relationships for late rectal morbidity in patients treated with chemoradiation and MRI-guided adaptive brachytherapy for locally advanced cervical cancer: Results from the prospective multicenter EMBRACE study', *Radiotherapy and Oncology*, 120(3), pp. 412–419. doi: 10.1016/j.radonc.2016.06.006.

Mbulawa, Z. Z. A. (2018) 'High human papillomavirus (HPV) prevalence in South African adolescents and young women encourages expanded HPV vaccination campaigns.', *PloS one*, 13(1), p. e0190166. doi: 10.1371/journal.pone.0190166.

McIntyre, J. F. (1995) 'Ureteral stricture as a late complication of radiotherapy for stage IB carcinoma of the uterine cervix.', *Cancer*, 75(3), pp. 836–43. doi: 10.1002/1097-0142(19950201)75:3<836::aid-cncr2820750315>3.0.co;2-a.

Mittal, K. (2015) 'Complications of radiation therapy in carcinoma cervix', *International Journal of Applied Research*, 1(10), pp. 720–731.

Mohamed, S. (2015) 'Parametrial boosting in locally advanced cervical cancer: Combined intracavitary/interstitial brachytherapy vs. intracavitary brachytherapy plus external beam radiotherapy', *Brachytherapy*, 14(1), pp. 23–28. doi: 10.1016/j.brachy.2014.09.010.

Mohamed, S. (2016) 'Vaginal dose de-escalation in image guided adaptive brachytherapy for locally advanced cervical cancer', *Radiotherapy and Oncology*, 120(3), pp. 480–485. doi: 10.1016/J.RADONC.2016.05.020.

Mohammadi, S. (2015) 'A computational study on different penalty approaches for constrained optimisation in radiation therapy treatment planning with a simulated annealing algorithm', in *2015 IEEE/ACIS 16th International Conference on Software Engineering, Artificial Intelligence, Networking and Parallel/Distributed Computing, SNPD 2015 - Proceedings*. Institute of Electrical and Electronics Engineers Inc. doi: 10.1109/SNPD.2015.7176174.

Morice, P. (2003) 'Prognostic value of lymphovascular space invasion determined with hematoxylin-eosin staining in early stage cervical carcinoma: Results of a multivariate analysis', *Annals of Oncology*, 14(10), pp. 1511–1517. doi: 10.1093/annonc/mdg412.

Morris, K. AL (2015) 'Pelvic radiation therapy: Between delight and disaster', *World Journal of Gastrointestinal Surgery*, 7(11), p. 279. doi: 10.4240/wjgs.v7.i11.279.

Morris, M. (1999) 'Pelvic Radiation with Concurrent Chemotherapy Compared with Pelvic and Para-Aortic Radiation for High-Risk Cervical Cancer', *New England Journal of Medicine*, 340(15), pp. 1137–1143. doi: 10.1056/NEJM199904153401501.

Mundt, A. J. (2002) 'Intensity-modulated whole pelvic radiotherapy in women with gynecologic malignancies.', *International journal of radiation oncology, biology, physics*, 52(5), pp. 1330–7. doi: 10.1016/s0360-3016(01)02785-7.

Nag, S. (2000) 'The American Brachytherapy Society recommendations for high-dose-rate brachytherapy for carcinoma of the cervix.', *International journal of radiation oncology, biology, physics*, 48(1), pp. 201–11. doi: 10.1016/s0360-3016(00)00497-1.

Nappi, L. (2005) 'Cervical squamous intraepithelial lesions of low-grade in HIV-infected women: Recurrence, persistence, and progression, in treated and untreated women', *European Journal of Obstetrics and Gynecology and Reproductive Biology*, 121(2), pp. 226–232. doi: 10.1016/j.ejogrb.2004.12.003.

Nath, R. (1997) *Code of practice for brachytherapy physics: Report of the AAPM Radiation Therapy Committee Task Group No. 56*.

Niemierko, A. (1997) 'Reporting and analyzing dose distributions: A concept of equivalent uniform dose', *Medical Physics*, 24(1), pp. 103–110. doi: 10.1118/1.598063.

Nomden, C. N. (2013) 'Clinical outcome and dosimetric parameters of chemo-radiation including MRI guided adaptive brachytherapy with tandem-ovoid applicators for cervical cancer patients: A single institution experience', *Radiotherapy and Oncology*, 107(1), pp. 69–74. doi: 10.1016/j.radonc.2013.04.006.

Osoba, D. (2011) 'Health-related quality of life and cancer clinical trials', *Therapeutic Advances in Medical Oncology*. SAGE Publications, pp. 57–71. doi: 10.1177/1758834010395342.

Pandey, U. (2017) 'What is Cervical Cancer?', *Journal of Gynecology and Womens Health*, 2(5). doi: 10.19080/JGWH.2017.02.555599.

Patel, F. D. (1994) 'Low dose rate vs. high dose rate brachytherapy in the treatment of carcinoma of the uterine cervix: A clinical trial', *International Journal of Radiation Oncology*Biology*Physics*, 28(2), pp. 335–341. doi: 10.1016/0360-3016(94)90055-8.

Pelloski, C. E. (2005) 'Comparison between CT-based volumetric calculations and ICRU reference-point estimates of radiation doses delivered to bladder and rectum during intracavitary radiotherapy for cervical cancer', *International Journal of Radiation Oncology*Biology*Physics*, 62(1), pp. 131–137. doi: 10.1016/j.ijrobp.2004.09.059.

Perez, C. A. (1995) 'Carcinoma of the uterine cervix. I. Impact of prolongation of overall treatment time and timing of brachytherapy on outcome of radiation therapy', *International Journal of Radiation Oncology*Biology*Physics*, 32(5), pp. 1275–1288. doi: 10.1016/0360-3016(95)00220-S.

Perez, C. A. (1998) 'Tumor size, irradiation dose, and long-term outcome of carcinoma of uterine cervix', *International Journal of Radiation Oncology Biology Physics*, 41(2), pp. 307–317. doi: 10.1016/S0360-3016(98)00067-4.

Pirog, E. C. (2000) 'Prevalence of human papillomavirus DNA in different histological subtypes of cervical adenocarcinoma', *American Journal of Pathology*, 157(4), pp. 1055–1062. doi: 10.1016/S0002-9440(10)64619-6.

Pötter, R. (2006) 'Recommendations from gynaecological (GYN) GEC ESTRO working group (II): Concepts and terms in 3D image-based treatment planning in cervix cancer brachytherapy—3D dose-

volume parameters and aspects of 3D image-based anatomy, radiation physics, radiobiology', *Radiotherapy and Oncology*, 78(1), pp. 67–77. doi: 10.1016/j.radonc.2005.11.014.

Pötter, R. (2007) 'Clinical impact of MRI assisted dose-volume adaptation and dose escalation in brachytherapy of locally advanced cervix cancer', *Radiotherapy and Oncology*, 83(2), pp. 148–155. doi: 10.1016/j.radonc.2007.04.012.

Pötter, R. (2011) 'Clinical outcome of protocol based image (MRI) guided adaptive brachytherapy combined with 3D conformal radiotherapy with or without chemotherapy in patients with locally advanced cervical cancer.', *Radiotherapy and oncology : journal of the European Society for Therapeutic Radiology and Oncology*, 100(1), pp. 116–23. doi: 10.1016/j.radonc.2011.07.012.

Pötter, R. (2016) 'Value of Magnetic Resonance Imaging Without or with Applicator in Place for Target Definition in Cervix Cancer Brachytherapy', *International Journal of Radiation Oncology Biology Physics*, 94(3), pp. 588–597. doi: 10.1016/j.ijrobp.2015.09.023.

Pötter, R. (2018) 'The EMBRACE II study: The outcome and prospect of two decades of evolution within the GEC-ESTRO GYN working group and the EMBRACE studies', *Clinical and Translational Radiation Oncology*. Elsevier Ireland Ltd, pp. 48–60. doi: 10.1016/j.ctro.2018.01.001.

'Prescribing, Recording, and Reporting Brachytherapy for Cancer of the Cervix' (2013) *Journal of the ICRU*, 13(1–2), pp. 1–10. doi: 10.1093/jicru_ndw027.

Van De Putte, G. (2005) 'Risk grouping in stage IB squamous cell cervical carcinoma', *Gynecologic Oncology*, 99(1), pp. 106–112. doi: 10.1016/j.ygyno.2005.05.026.

Rijkmans, E. C. (2014) 'Improved survival of patients with cervical cancer treated with image-guided brachytherapy compared with conventional brachytherapy', *Gynecologic Oncology*, 135(2), pp. 231–238. doi: 10.1016/j.ygyno.2014.08.027.

Rivard, M. J. (2004) 'Update of AAPM Task Group No . 43 Report : A revised AAPM protocol for brachytherapy dose calculations', (43), pp. 633–674. doi: 10.1118/1.1646040.

Robadi, I. A. (2018) 'The importance of high-risk human papillomavirus types other than 16 and 18 in cervical neoplasia', *Archives of Pathology and Laboratory Medicine*, 142(6), pp. 693–695. doi: 10.5858/arpa.2017-0563-RA.

Robin, T. P. (2016) 'Disparities in standard of care treatment and associated survival decrement in patients with locally advanced cervical cancer', *Gynecologic Oncology*, 143(2), pp. 319–325. doi: 10.1016/j.ygyno.2016.09.009.

Romano, K. D. (2017) 'Transition from LDR to HDR brachytherapy for cervical cancer: Evaluation of tumor control, survival, and toxicity', *Brachytherapy*, 16(2), pp. 378–386. doi: 10.1016/j.brachy.2016.12.005.

Saha, S. (2008) 'Image-guided HDR intracavitary and interstitial brachytherapy for locally advanced cervix cancer – correlation of late toxicity with DVH data and 3-year outcome analysis', *Brachytherapy*, 7(2), p. 98. doi: 10.1016/j.brachy.2008.02.353.

Sala, E. (2013) 'The added role of MR imaging in treatment stratification of patients with gynecologic malignancies: What the radiologist needs to know', *Radiology*. Radiological Society of North America, Inc., pp. 717–740. doi: 10.1148/radiol.12120315.

Schmid, M. P. (2011) 'Local recurrences in cervical cancer patients in the setting of image-guided brachytherapy: A comparison of spatial dose distribution within a matched-pair analysis', *Radiotherapy and Oncology*, 100(3), pp. 468–472. doi: 10.1016/j.radonc.2011.08.014.

Schoeppel, S. L. (1994) 'Three-dimensional treatment planning of intracavitary gynecologic implants: Analysis of ten cases and implications for dose specification', *International Journal of Radiation Oncology*Biology*Physics*, 28(1), pp. 277–283. doi: 10.1016/0360-3016(94)90168-6.

Schover, L. R. (1989) 'Sexual dysfunction and treatment for early stage cervical cancer', *Cancer*, 63(1), pp. 204–212. doi: 10.1002/1097-0142(19890101)63:1<204::AID-CNCR2820630133>3.0.CO;2-U.

Schwarz, M. (2004) 'Sensitivity of treatment plan optimisation for prostate cancer using the equivalent uniform dose ( EUD ) with respect to the rectal wall volume parameter', 73, pp. 209–218. doi: 10.1016/j.radonc.2004.08.016.

Sharma, D. N. (2011) 'High–dose rate interstitial brachytherapy using two weekly sessions of 10Gy each for patients with locally advanced cervical carcinoma', *Brachytherapy*, 10(3), pp. 242–248. doi: 10.1016/j.brachy.2010.09.001.

Shaw, W. (2013) 'Equivalence of Gyn GEC-ESTRO guidelines for image guided cervical brachytherapy with EUD-based dose prescription.', *Radiation Oncology*, 8(1), p. 266. doi: 10.1186/1748-717X-8-266.

Shaw, W. (2017) 'Image-guided adaptive brachytherapy dose escalation for cervix cancer via fractionation compensation', *Brachytherapy*, 16(3), pp. 534–546. doi: 10.1016/j.brachy.2017.01.002.

Shin, K. H. (2006) 'CT-guided intracavitary radiotherapy for cervical cancer: Comparison of conventional point A plan with clinical target volume-based three-dimensional plan using dose–volume parameters', *International Journal of Radiation Oncology*Biology*Physics*, 64(1), pp. 197–204. doi: 10.1016/j.ijrobp.2005.06.015.

Silberstein, J. L. (2013) *Translational andrology and urology.*, *Translational Andrology and Urology*. Available at: http://tau.amegroups.com/article/view/6247/7010#B12 (Accessed: 22 July 2019).

Simonds, H. (2015) 'HIV status and acute hematologic toxicity among patients with cervix cancer undergoing radical chemoradiation', *International Journal of Gynecological Cancer*, 25(5), pp. 884–890. doi: 10.1097/IGC.0000000000000441.

Smith, J. S. (2007) 'Human papillomavirus type distribution in invasive cervical cancer and high-grade cervical lesions: A meta-analysis update', *International Journal of Cancer*, 121(3), pp. 621–632. doi: 10.1002/ijc.22527.

Snyman, L. C. (2006) 'Urine cytology as a screening test for bladder infiltration in cervical cancer', *International Journal of Gynecological Cancer*, 16(4), pp. 1587–1590. doi: 10.1111/j.1525-1438.2006.00630.x.

Snyman, L. C. (2013) 'Prevention of cervical cancer - how long before we get it right?', *South African Journal of Obstetrics and Gynaecology*, 19(1), pp. 2–3. doi: 10.7196/sajog.651.

Sobotta, B. (2011) 'On expedient properties of common biological score functions for multi-modality, adaptive and 4D dose optimisation', *Physics in Medicine and Biology*, 56(10), p. N123. doi: 10.1088/0031-9155/56/10/N01.

Spampinato, S. (2019) 'OC-0507 Risk factors for bladder fistula, bleeding and cystitis in cervix cancer: an EMBRACE analysis', *Radiotherapy and Oncology*, 133, pp. S262–S263. doi: 10.1016/S0167-8140(19)30927-2.

Srivastava, A. (2014) 'Brachytherapy in cancer cervix: Time to move ahead from point A?', *World Journal of Clinical Oncology*. Baishideng Publishing Group Inc, pp. 764–774. doi: 10.5306/wjco.v5.i4.764.

StatsSA (2018) *Mid-year population estimates - P0302*. doi: Statistical release P0302.

Stewart, A. J. (2006) 'Current controversies in high-dose-rate versus low-dose-rate brachytherapy for cervical cancer.', *Cancer*, 107(5), pp. 908–15. doi: 10.1002/cncr.22054.

Sturdza, A. (2016) 'Image guided brachytherapy in locally advanced cervical cancer: Improved pelvic control and survival in RetroEMBRACE, a multicenter cohort study', *Radiotherapy and Oncology*, 120(3), pp. 428–433. doi: 10.1016/j.radonc.2016.03.011.

Tan, L. (2011) 'Implementation of Image-guided Brachytherapy for Cervix Cancer in the UK: Progress Update', *Clinical Oncology*, 23(10), pp. 681–684. doi: 10.1016/j.clon.2011.07.011.

Tan, L. T. (2011) 'Implementation of image-guided brachytherapy for cervix cancer in the UK: Progress update', *Clinical Oncology*, 23(10), pp. 681–684. doi: 10.1016/j.clon.2011.07.011.

Tan, P. W. (2015) 'Outpatient combined intracavitary and interstitial cervical brachytherapy: barriers and solutions to implementation of a successful programme - a single institutional experience.', *Journal of contemporary brachytherapy*, 7(3), pp. 259–263. doi: 10.5114/jcb.2015.52625.

Tanderup, K. (2010) 'From point A to the sculpted pear: MR image guidancely improves tumour dose and sparing of organs at risk in brachytherapy of cervical cancer', *Radiotherapy and Oncology*, 94(2), pp. 173–180. doi: 10.1016/j.radonc.2010.01.001.

Tanderup, K. (2013) 'Uncertainties in image guided adaptive cervix cancer brachytherapy: Impact on planning and prescription', *Radiotherapy and Oncology*, 107(1), pp. 1–5. doi: 10.1016/j.radonc.2013.02.014.

Tanderup, K. (2014) 'Curative radiation therapy for locally advanced cervical cancer: Brachytherapy is NOT optional', *International Journal of Radiation Oncology Biology Physics*, 88(3), pp. 537–539. doi: 10.1016/j.ijrobp.2013.11.011.

Tanderup, K. (2016) 'Effect of tumor dose, volume and overall treatment time on local control after radiochemotherapy including MRI guided brachytherapy of locally advanced cervical cancer', *Radiotherapy and Oncology*, 120(3), pp. 441–446. doi: 10.1016/j.radonc.2016.05.014.

Tanderup, K. (2020) 'Evidence-Based Dose Planning Aims and Dose Prescription in Image-Guided Brachytherapy Combined With Radiochemotherapy in Locally Advanced Cervical Cancer', *Seminars in Radiation Oncology*, 30(4), pp. 311–327. doi: 10.1016/j.semradonc.2020.05.008.

Taylor, A. (2004) 'Intensity-modulated radiotherapy--what is it?', *Cancer imaging : the official publication of the International Cancer Imaging Society*, 4(2), pp. 68–73. doi: 10.1102/1470-7330.2004.0003.

Teshima, T. (1993) 'High-dose rate and low-dose rate intracavitary therapy for carcinoma of the uterine cervix. Final results of Osaka University Hospital.', *Cancer*, 72(8), pp. 2409–14. doi: 10.1002/1097-0142(19931015)72:8<2409::aid-cncr2820720819>3.0.co;2-n.

Tod, M. (1953) 'Treatment of Cancer of the Cervix Uteri—A Revised "Manchester Method"', *The British Journal of Radiology*, 26(305), pp. 252–257. doi: 10.1259/0007-1285-26-305-252.

Tod, M. C. (1938) 'A Dosage System for Use in the Treatment of Cancer of the Uterine Cervix', *The British Journal of Radiology*, 11(132), pp. 809–824. doi: 10.1259/0007-1285-11-132-809.

Trnková, P. (2009) 'New inverse planning technology for image-guided cervical cancer brachytherapy : Description and evaluation within a clinical frame', *Radiotherapy and Oncology*, 93(2), pp. 331–340. doi: 10.1016/j.radonc.2009.10.004.

Tyagi, N. (2011) 'Daily Online Cone Beam Computed Tomography to Assess Interfractional Motion in Patients With Intact Cervical Cancer', *International Journal of Radiation Oncology*Biology*Physics*, 80(1), pp. 273–280. doi: 10.1016/j.ijrobp.2010.06.003.

Viswanathan, A. N. (2007) 'Computed Tomography Versus Magnetic Resonance Imaging-Based Contouring in Cervical Cancer Brachytherapy: Results of a Prospective Trial and Preliminary Guidelines for Standardized Contours', *International Journal of Radiation Oncology*Biology*Physics*, 68(2), pp. 491–498. doi: 10.1016/j.ijrobp.2006.12.021.

Viswanathan, A. N. (2010) 'Radiation dose-volume effects of the urinary bladder.', *International journal of radiation oncology, biology, physics*, 76(3 Suppl), pp. S116-22. doi: 10.1016/j.ijrobp.2009.02.090.

Viswanathan, A. N. (2010) 'Three-Dimensional Imaging in Gynecologic Brachytherapy: A Survey of the American Brachytherapy Society', *International Journal of Radiation Oncology*Biology*Physics*, 76(1), pp. 104–109. doi: 10.1016/j.ijrobp.2009.01.043.

Viswanathan, A. N. (2012) 'American Brachytherapy Society consensus guidelines for locally advanced carcinoma of the cervix. Part I: General principles', *Brachytherapy*, 11(1), pp. 33–46. doi: 10.1016/j.brachy.2011.07.003.

Viswanathan, A. N. (2012) 'American Brachytherapy Society consensus guidelines for locally advanced carcinoma of the cervix. Part II: High-dose-rate brachytherapy', *Brachytherapy*, 11(1), pp. 47–52. doi: 10.1016/j.brachy.2011.07.002.

Viswanathan, A. N. (2014) 'Comparison and consensus guidelines for delineation of clinical target volume for CT- and MR-based brachytherapy in locally advanced cervical cancer', *International Journal of Radiation Oncology Biology Physics*, 90(2), pp. 320–328. doi: 10.1016/j.ijrobp.2014.06.005.

Vordermark, D. (2016) 'Radiotherapy of Cervical Cancer', *Oncology Research and Treatment*. S. Karger AG, pp. 516–520. doi: 10.1159/000448902.

Wachter-Gerstner, N. (2003) 'Bladder and rectum dose defined from MRI based treatment planning for cervix cancer brachytherapy: Comparison of dose-volume histograms for organ contours and organ wall, comparison with ICRU rectum and bladder reference point', *Radiotherapy and Oncology*, 68(3), pp. 269–276. doi: 10.1016/S0167-8140(03)00189-0.

Wagner, A. (2013) 'Intensity modulated radiotherapy in gynecologic cancers: Hope, hype or hyperbole?', *Gynecologic Oncology*, 130(1), pp. 229–236. doi: 10.1016/j.ygyno.2013.04.052.

Wanderås, A. D. (2012) 'Adaptive brachytherapy of cervical cancer , comparison of conventional point A and CT based individual treatment planning Adaptive brachytherapy of cervical cancer , comparison of conventional point A and CT based individual treatment planning', (January 2016). doi: 10.3109/0284186X.2011.626446.

Wang, J. Z. (2010) 'Sequential magnetic resonance imaging of cervical cancer: the predictive value of absolute tumor volume and regression ratio measured before, during, and after radiation therapy.', *Cancer*, 116(21), pp. 5093–101. doi: 10.1002/cncr.25260.

Wang, K.-L. (2007) 'Correlation of Traditional Point a With Anatomic Location of Uterine Artery and Ureter in Cancer of the Uterine Cervix', *International Journal of Radiation Oncology*Biology*Physics*, 69(2), pp. 498–503. doi: 10.1016/j.ijrobp.2007.03.038.

Wang, X. (2010) 'High dose rate versus low dose rate intracavity brachytherapy for locally advanced uterine cervix cancer', in Liu, R. (ed.) *Cochrane Database of Systematic Reviews*. Chichester, UK: John Wiley & Sons, Ltd, p. CD007563. doi: 10.1002/14651858.CD007563.pub2.

WHO (2018) 'WHO | Cervical cancer', *WHO*. Available at: http://www.who.int/cancer/prevention/diagnosis-screening/cervical-cancer/en/ (Accessed: 15 May 2020).

Wu, Q. (2002) 'Optimisation of intensity-modulated radiotherapy plans based on the equivalent uniform dose.', *International journal of radiation oncology, biology, physics*, 52(1), pp. 224–35. doi: 10.1016/s0360-3016(01)02585-8.

Wu, Q. (2005) 'Dose sculpting with generalized equivalent uniform dose', *Medical Physics*, 32(5), pp. 1387–1396. doi: 10.1118/1.1897464.

Yen, A. (2018) 'Risk factors for fistula formation after interstitial brachytherapy for locally advanced gynecological cancers involving vagina', *Journal of Contemporary Brachytherapy*, 10(6), pp. 510–515. doi: 10.5114/jcb.2018.80171.

Altekruse, S. F. (2003) 'Comparison of human papillomavirus genotypes, sexual, and reproductive risk factors of cervical adenocarcinoma and squamous cell carcinoma: Northeastern United States', *American Journal of Obstetrics and Gynecology*, 188(3), pp. 657–663. doi: 10.1067/mob.2003.132.

Bacorro, W. (2017) 'Contribution of image-guided adaptive brachytherapy to pelvic nodes treatment in locally advanced cervical cancer', *Brachytherapy*, 16(2), pp. 366–372. doi: 10.1016/j.brachy.2016.11.016.

Bae, H. S. (2016) 'Predictors of radiation field failure after definitive chemoradiation in patients with locally advanced cervical cancer', *International Journal of Gynecological Cancer*, 26(4), pp. 737–742. doi: 10.1097/IGC.0000000000000662.

Banerjee, R. (2014) 'Brachytherapy in the treatment of cervical cancer: a review.', *International journal of women's health*, 6, pp. 555–64. doi: 10.2147/IJWH.S46247.

Barbera, L. (2009) 'Management of Early and Locally Advanced Cervical Cancer', *Seminars in Oncology*, 36(2), pp. 155–169. doi: 10.1053/j.seminoncol.2008.12.007.

Barker, J. L. (2004) 'Quantification of volumetric and geometric changes occurring during fractionated radiotherapy for head-and-neck cancer using an integrated CT/linear accelerator system', *International Journal of Radiation Oncology*Biology*Physics*, 59(4), pp. 960–970. doi: 10.1016/j.ijrobp.2003.12.024.

Barrett, A. (2009) *Practical Radiotherapy Planning*, *Practical Radiotherapy Planning*. Hodder Arnold. doi: 10.1201/b13373.

Batra, P. (2010) 'Utilisation and outcomes of cervical cancer prevention services among HIV-infected women in Cape Town.', *South African medical journal = Suid-Afrikaanse tydskrif vir geneeskunde*, 100(1), pp. 39–44. Available at: http://www.ncbi.nlm.nih.gov/pubmed/20429487 (Accessed: 19 October 2018).

Beriwal, S. (2009) 'Single Magnetic Resonance Imaging vs Magnetic Resonance Imaging/Computed Tomography Planning in Cervical Cancer Brachytherapy', *Clinical Oncology*, 21(6), pp. 483–487. doi: 10.1016/j.clon.2009.03.007.

Bhatla, N. (2019) 'Revised FIGO staging for carcinoma of the cervix uteri', *International Journal of Gynecology and Obstetrics*, 145(1), pp. 129–135. doi: 10.1002/ijgo.12749.

Bjelic-Radisic, V. (2012) 'Quality of life characteristics inpatients with cervical cancer', *European Journal of Cancer*, 48(16), pp. 3009–3018. doi: 10.1016/j.ejca.2012.05.011.

Bockel, S. (2019) 'Total Reference Air Kerma is Associated with Late Bowel Morbidity in Locally Advanced Cervical Cancer Patients Treated with Image-Guided Adaptive Brachytherapy', *Journal of Clinical Medicine*, 8(1), p. 125. doi: 10.3390/jcm8010125.

Botha, M. H. (2017) 'Guidelines for cervical cancer screening in South Africa', *Southern African Journal of Gynaecological Oncology*, 9(1), pp. 8–12. Available at: http://www.sajgo.co.za/index.php/sajgo/article/view/253/pdf_4.

Bruni, L. (2019) *Human Papillomavirus and Related Diseases in South Africa*. Available at: https://hpvcentre.net/statistics/reports/ZAF.pdf?t=1589461112482 (Accessed: 14 May 2020).

van de Bunt, L. (2006) 'Conventional, conformal, and intensity-modulated radiation therapy treatment planning of external beam radiotherapy for cervical cancer: The impact of tumor regression', *International Journal of Radiation Oncology*Biology*Physics*, 64(1), pp. 189–196. doi: 10.1016/j.ijrobp.2005.04.025.

Charra-Brunaud, C. (2012) 'Impact of 3D image-based PDR brachytherapy on outcome of patients treated for cervix carcinoma in France : Results of the French STIC prospective study q', *Radiotherapy and Oncology*, 103(3), pp. 305–313. doi: 10.1016/j.radonc.2012.04.007.

Chassagne, D. (1977) 'Proposals for common definitions of reference points in gynecological brachytherapy', *J. Radiol., Electrol., Med. Nucl*, 58da(5), pp. 371–373. Available at: https://inis.iaea.org/search/search.aspx?orig_q=RN:8340495 (Accessed: 14 July 2019).

Chassagne, D. (1985) 'Report 38', *Journal of the International Commission on Radiation Units and Measurements*, os20(1), p. NP-NP. doi: 10.1093/JICRU/OS20.1.REPORT38.

Chen, L. A. (2015) 'Toxicity and cost-effectiveness analysis of intensity modulated radiation therapy versus 3-dimensional conformal radiation therapy for postoperative treatment of gynecologic cancers', *Gynecologic Oncology*, 136(3), pp. 521–528. doi: 10.1016/j.ygyno.2014.12.039.

Cho, O. (2018) 'Management for locally advanced cervical cancer: New trends and controversial issues', *Radiation Oncology Journal*, 36(4), pp. 254–264. doi: 10.3857/roj.2018.00500.

Choi, K. H. (2018) 'Clinical impact of boost irradiation to pelvic lymph node in uterine cervical cancer treated with definitive chemoradiotherapy', *Medicine (United States)*, 97(16). doi: 10.1097/MD.0000000000010517.

Dappa, E. (2017) 'The value of advanced MRI techniques in the assessment of cervical cancer: a review', *Insights into Imaging*. Springer Verlag, pp. 471–481. doi: 10.1007/s13244-017-0567-0.

Datta, N. R. (2001) 'Variations of intracavitary applicator geometry during multiple HDR brachytherapy insertions in carcinoma cervix and its influence on reporting as per ICRU report 38', *Radiotherapy and Oncology*, 60(1), pp. 15–24. doi: 10.1016/S0167-8140(01)00352-8.

Datta, N. R. (2003) 'Problems in reporting doses and volumes during multiple high-dose-rate intracavitary brachytherapy for carcinoma cervix as per ICRU Report 38: a comparative study using flexible and rigid applicators', *Gynecologic Oncology*, 91(2), pp. 285–292. doi: 10.1016/S0090-8258(03)00506-7.

Datta, N. R. (2003) 'Total reference air kerma: To what extent can it predict intracavitary volume enclosed by isodose surfaces during multiple high-dose rate brachytherapy?', *Brachytherapy*, 2, pp. 91–97. doi: 10.1016/S.

Datta, N. R. (2004) 'Problems and uncertainties with multiple point A's during multiple high-dose-rate intracavitary brachytherapy in carcinoma of the cervix.', *Clinical oncology (Royal College of Radiologists (Great Britain))*, 16(2), pp. 129–37. doi: 10.1016/J.CLON.2003.10.011.

Datta, N. R. (2005) 'From "points" to "profiles" in intracavitary brachytherapy of cervical cancer.', *Current opinion in obstetrics & gynecology*, 17(1), pp. 35–41. doi: 10.1097/00001703-200502000-00007.

Datta, N. R. (2006) 'Comparative assessment of doses to tumor, rectum, and bladder as evaluated by orthogonal radiographs vs. computer enhanced computed tomography-based intracavitary brachytherapy in cervical cancer', *Brachytherapy*, 5(4), pp. 223–229. doi: 10.1016/j.brachy.2006.09.001.

Delgado, D. (2019) 'Results from chemoradiotherapy for squamous cell cervical cancer with or without intracavitary brachytherapy', *Journal of Contemporary Brachytherapy*, 11(5), pp. 417–422. doi: 10.5114/jcb.2019.88116.

Delgado, G. (1990) 'Prospective surgical-pathological study of disease-free interval in patients with stage IB squamous cell carcinoma of the cervix: A Gynecologic Oncology Group study', *Gynecologic Oncology*, 38(3), pp. 352–357. doi: 10.1016/0090-8258(90)90072-S.

Deng, X. (2017) 'Dosimetric benefits of intensity-modulated radiotherapy and volumetric-modulated arc therapy in the treatment of postoperative cervical cancer patients', *Journal of Applied Clinical Medical Physics*, 18(1), pp. 25–31. doi: 10.1002/acm2.12003.

Denham, J. W. (2013) 'Radiation induced bowel injury: A neglected problem', *The Lancet*, pp. 2046–

2047. doi: 10.1016/S0140-6736(13)61946-7.

Denny, L. (2008) 'Prevention of cervical cancer', *Reproductive Health Matters*, 16(32), pp. 18–31. doi: 10.1016/S0968-8080(08)32397-0.

Denny, L. (2017) 'Cervical cancer prevention and early detection from a South African perspective', *South African Health Review*, pp. 189–196. Available at: http://ovidsp.ovid.com/ovidweb.cgi?T=JS&CSC=Y&NEWS=N&PAGE=fulltext&D=cagh&AN=20183060901
http://oxfordsfx.hosted.exlibrisgroup.com/oxford?sid=OVID:caghdb&id=pmid:&id=doi:&issn=1025-1715&isbn=&volume=2017&issue=&spage=189&pages=189-195&date=2017&title=Sout.

Denton, A. S. (2003) 'Interventions for the physical aspects of sexual dysfunction in women following pelvic radiotherapy', *Cochrane Database of Systematic Reviews*, p. CD003750. doi: 10.1002/14651858.CD003750.

Dimopoulos, J. C. A. (2006) 'Systematic evaluation of MRI findings in different stages of treatment of cervical cancer: Potential of MRI on delineation of target, pathoanatomic structures, and organs at risk', *International Journal of Radiation Oncology*Biology*Physics*, 64(5), pp. 1380–1388. doi: 10.1016/j.ijrobp.2005.10.017.

Dimopoulos, J. C. A. (2006) 'The Vienna applicator for combined intracavitary and interstitial brachytherapy of cervical cancer: Clinical feasibility and preliminary results', *International Journal of Radiation Oncology*Biology*Physics*, 66(1), pp. 83–90. doi: 10.1016/j.ijrobp.2006.04.041.

Dimopoulos, Johannes C.A. (2009) 'Dose-Volume Histogram Parameters and Local Tumor Control in Magnetic Resonance Image-Guided Cervical Cancer Brachytherapy', *International Journal of Radiation Oncology Biology Physics*, 75(1), pp. 56–63. doi: 10.1016/j.ijrobp.2008.10.033.

Dimopoulos, Johannes C A (2009) 'Dose – effect relationship for local control of cervical cancer by magnetic resonance image-guided brachytherapy', *Radiotherapy and Oncology*, 93(2), pp. 311–315. doi: 10.1016/j.radonc.2009.07.001.

Dimopoulos, Johannes C. A. (2009) 'MRI Assessment of Cervical Cancer for Adaptive Radiotherapy', *Strahlentherapie und Onkologie*, 185(5), pp. 282–287. doi: 10.1007/s00066-009-1918-7.

E.B.Podgorsak (2005) *Radiation Oncology Physics: A Handbook for Teachers and Students*, *International Atomic Energy Agency*. doi: 10.1038/sj.bjc.6604224.

Eifel, P. J. (1994) 'The influence of tumor size and morphology on the outcome of patients with figo stage IB squamous cell carcinoma of the uterine cervix', *International Journal of Radiation Oncology, Biology, Physics*, 29(1), pp. 9–16. doi: 10.1016/0360-3016(94)90220-8.

Eifel, P. J. (2004) 'Pelvic irradiation with concurrent chemotherapy versus pelvic and para-aortic irradiation for high-risk cervical cancer: An update of Radiation Therapy Oncology Group Trial (RTOG) 90-01', *Journal of Clinical Oncology*, 22(5), pp. 872–880. doi: 10.1200/JCO.2004.07.197.

Eifel, P. J. (2006) 'Concurrent chemotherapy and radiation therapy as the standard of care for cervical cancer', *Nature Clinical Practice Oncology*. Nat Clin Pract Oncol, pp. 248–255. doi: 10.1038/ncponc0486.

Elshaikh, M. (2006) 'Advances in radiation oncology', *Annual Review of Medicine*, pp. 19–31. doi: 10.1146/annurev.med.57.121304.131431.

Eskander, R. N. (2010) 'Comparison of Computed Tomography and Magnetic Resonance Imaging in Cervical Cancer Brachytherapy Target and Normal Tissue Contouring', *International Journal of Gynecological Cancer*, 20(1), pp. 47–53. doi: 10.1111/IGC.0b013e3181c4a627.

Fellner, C. (2001) 'Comparison of radiography- and computed tomography-based treatment planning in cervix cancer in brachytherapy with specific attention to some quality assurance aspects',

*Radiotherapy and Oncology*, 58(1), pp. 53–62. doi: 10.1016/S0167-8140(00)00282-6.

Fokdal, L. (2013) 'Clinical feasibility of combined intracavitary/interstitial brachytherapy in locally advanced cervical cancer employing MRI with a tandem/ring applicator in situ and virtual preplanning of the interstitial component', *Radiotherapy and Oncology*, 107(1), pp. 63–68. doi: 10.1016/j.radonc.2013.01.010.

Fokdal, L. (2016) 'Image guided adaptive brachytherapy with combined intracavitary and interstitial technique improves the therapeutic ratio in locally advanced cervical cancer: Analysis from the retroEMBRACE study', *Radiotherapy and Oncology*, 120(3), pp. 434–440. doi: 10.1016/j.radonc.2016.03.020.

Fokdal, L. (2018) 'Physician assessed and patient reported urinary morbidity after radio-chemotherapy and image guided adaptive brachytherapy for locally advanced cervical cancer', *Radiotherapy and Oncology*, 127(3), pp. 423–430. doi: 10.1016/j.radonc.2018.05.002.

Fokdal, L. (2019) 'Risk Factors for Ureteral Stricture After Radiochemotherapy Including Image Guided Adaptive Brachytherapy in Cervical Cancer: Results From the EMBRACE Studies', *International Journal of Radiation Oncology Biology Physics*, 103(4), pp. 887–894. doi: 10.1016/j.ijrobp.2018.11.006.

Frumovitz, M. (2005) 'Quality of Life and Sexual Functioning in Cervical Cancer Survivors', *Journal of Clinical Oncology*, 23(30), pp. 7428–7436. doi: 10.1200/JCO.2004.00.3996.

Frumovitz, M. (2015) *Invasive cervical cencer: epidemiology, risk factors, clinical menifestations, and diagnosis*, *UpToDate*. Available at: UpToDate. (Accessed: 15 May 2020).

Fyles, A. W. (1995) 'Prognostic factors in patients with cervix cancer treated by radiation therapy: results of a multiple regression analysis', *Radiotherapy and Oncology*, 35(2), pp. 107–117. doi: 10.1016/0167-8140(95)01535-O.

Gandhi, A. K. (2013) 'Early clinical outcomes and toxicity of intensity modulated versus conventional pelvic radiation therapy for locally advanced cervix carcinoma: A prospective randomized study', *International Journal of Radiation Oncology Biology Physics*, 87(3), pp. 542–548. doi: 10.1016/j.ijrobp.2013.06.2059.

Georg, P. (2012) 'Dose effect relationship for late side effects of the rectum and urinary bladder in magnetic resonance image-guided adaptive cervix cancer brachytherapy', *International Journal of Radiation Oncology Biology Physics*, 82(2), pp. 653–657. doi: 10.1016/j.ijrobp.2010.12.029.

Girinsky, T. (1993) 'Overall treatment time in advanced cervical carcinomas: a critical parameter in treatment outcome.', *International journal of radiation oncology, biology, physics*, 27(5), pp. 1051–6. doi: 10.1016/0360-3016(93)90522-w.

Granero, D. (2006) 'A dosimetric study on the Ir-192 high dose rate Flexisource', *Medical Physics*, 33(12), pp. 4578–4582. doi: 10.1118/1.2388154.

Greimel, E. R. (2009) 'Quality of life and sexual functioning after cervical cancer treatment: a long-term follow-up study', *Psycho-Oncology*, 18(5), pp. 476–482. doi: 10.1002/pon.1426.

Grigsby, P. W. (1993) 'Anatomic variation of gynecologic brachytherapy prescription points', *International Journal of Radiation Oncology*Biology*Physics*, 27(3), pp. 725–729. doi: 10.1016/0360-3016(93)90402-H.

Gulia, A. (2013) 'Conventional four field radiotherapy versus computed tomography-based treatment planning in cancer cervix: A dosimetric study.', *South Asian journal of cancer*, 2(3), pp. 132–5. doi: 10.4103/2278-330X.114116.

Haie-Meder, C. (2005) 'Recommendations from Gynaecological (GYN) GEC-ESTRO Working Group (I): Concepts and terms in 3D image based 3D treatment planning in cervix cancer brachytherapy with emphasis on MRI assessment of GTV and CTV', *Radiotherapy and Oncology*, 74(3), pp. 235–245. doi:

10.1016/j.radonc.2004.12.015.

Han, K. (2013) 'Trends in the utilization of brachytherapy in cervical cancer in the United States', *International Journal of Radiation Oncology Biology Physics*, 87(1), pp. 111–119. doi: 10.1016/j.ijrobp.2013.05.033.

Hanks, G. E. (1983) 'Patterns of care outcome studies. Results of the national practice in cancer of the cervix.', *Cancer*, 51(5), pp. 959–67. Available at: http://www.ncbi.nlm.nih.gov/pubmed/6821861 (Accessed: 19 October 2018).

Hareyama, M. (2002) 'High-dose-rate versus low-dose-rate intracavitary therapy for carcinoma of the uterine cervix', *Cancer*, 94(1), pp. 117–124. doi: 10.1002/cncr.10207.

Haripotepornkul, N. H. (2011) 'Evaluation of intra- and inter-fraction movement of the cervix during intensity modulated radiation therapy', *Radiotherapy and Oncology*, 98(3), pp. 347–351. doi: 10.1016/j.radonc.2010.11.015.

Härkki-Sirén, P. (1998) 'Urinary tract injuries after hysterectomy.', *Obstetrics and gynecology*, 92(1), pp. 113–8. Available at: http://www.ncbi.nlm.nih.gov/pubmed/9649105 (Accessed: 21 July 2019).

Hegazy, N. (2013) 'High-risk clinical target volume delineation in CT-guided cervical cancer brachytherapy: Impact of information from FIGO stage with or without systematic inclusion of 3D documentation of clinical gynecological examination', *Acta Oncologica*, 52(7), pp. 1345–1352. doi: 10.3109/0284186X.2013.813068.

Heijkoop, S. T. (2015) 'Quantification of intra-fraction changes during radiotherapy of cervical cancer assessed with pre- and post-fraction Cone Beam CT scans', *Radiotherapy and Oncology*, 117(3), pp. 536–541. doi: 10.1016/j.radonc.2015.08.034.

Hoskin, P. J. (1996) 'Changes in applicator position with fractionated high dose rate gynaecological brachytherapy', *Radiotherapy and Oncology*, 40(1), pp. 59–62. doi: 10.1016/0167-8140(96)01746-X.

Huh, W. K. (2015) 'Use of primary high-risk human papillomavirus testing for cervical cancer screening: Interim clinical guidance', *Journal of Lower Genital Tract Disease*, 19(2), pp. 91–96. doi: 10.1097/LGT.0000000000000103.

Ingber, L. (1993) 'Simulated annealing: Practice versus theory', *Mathematical and Computer Modelling*, 18(11), pp. 29–57. doi: 10.1016/0895-7177(93)90204-C.

Jadon, R. (2014) 'A Systematic Review of Organ Motion and Image-guided Strategies in External Beam Radiotherapy for Cervical Cancer', *Clinical Oncology*, 26(4), pp. 185–196. doi: 10.1016/j.clon.2013.11.031.

Jason D Wright, M. D. (2019) 'Cervical intraepithelial neoplasia: Terminology, incidence, pathogenesis, and prevention - UpToDate', *UpTo Date*, pp. 1–20. Available at: https://www.uptodate.com/contents/cervical-intraepithelial-neoplasia-terminology-incidence-pathogenesis-and-prevention#! (Accessed: 15 May 2020).

Jensen, N. B. K. (2018) 'Bowel morbidity following radiochemotherapy and image-guided adaptive brachytherapy for cervical cancer: Physician- and patient reported outcome from the EMBRACE study.', *Radiotherapy and oncology : journal of the European Society for Therapeutic Radiology and Oncology*, 127(3), pp. 431–439. doi: 10.1016/j.radonc.2018.05.016.

Jensen, P. T. (2003) 'Longitudinal study of sexual function and vaginal changes after radiotherapy for cervical cancer', *International Journal of Radiation Oncology Biology Physics*, 56(4), pp. 937–949. doi: 10.1016/S0360-3016(03)00362-6.

Jürgenliemk-Schulz, I. M. (2009) 'MRI-guided treatment-planning optimisation in intracavitary or combined intracavitary/interstitial PDR brachytherapy using tandem ovoid applicators in locally advanced cervical cancer', *Radiotherapy and Oncology*, 93(2), pp. 322–330. doi:

10.1016/j.radonc.2009.08.014.

Jürgenliemk-Schulz, I. M. (2010) 'Variation of treatment planning parameters (D90 HR-CTV, D2ccfor OAR) for cervical cancer tandem ring brachytherapy in a multicentre setting: Comparison of standard planning and 3D image guided optimisation based on a joint protocol for dose-volume constra', *Radiotherapy and Oncology*, 94(3), pp. 339–345. doi: 10.1016/j.radonc.2009.10.011.

Kang, H.-C. (2010) '3D CT-based high-dose-rate brachytherapy for cervical cancer: Clinical impact on late rectal bleeding and local control', *Radiotherapy and Oncology*, 97(3), pp. 507–513. doi: 10.1016/j.radonc.2010.10.002.

Kapp, K. S. (1992) 'Dosimetry of intracavitary placements for uterine and cervical carcinoma: results of orthogonal film, TLD, and CT-assisted techniques.', *Radiotherapy and oncology : journal of the European Society for Therapeutic Radiology and Oncology*, 24(3), pp. 137–46. Available at: http://www.ncbi.nlm.nih.gov/pubmed/1410567 (Accessed: 13 July 2019).

Karabis, A. (2005) 'HIPO: A hybrid inverse treatment planning optimisation algorithm in HDR brachytherapy', *Radiotherapy and Oncology*, 76, p. S29. doi: 10.1016/s0167-8140(05)81018-7.

Kirchheiner, K. (2014) 'Manifestation pattern of early-late vaginal morbidity after definitive radiation (Chemo)therapy and image-guided adaptive brachytherapy for locally advanced cervical cancer: An analysis from the embrace study', *International Journal of Radiation Oncology Biology Physics*, 89(1), pp. 88–95. doi: 10.1016/j.ijrobp.2014.01.032.

Kirchheiner, K. (2015) 'Health related quality of life and patient reported symptoms before and during definitive radio(chemo)therapy using image-guided adaptive brachytherapy for locally advanced cervical cancer and early recovery - A mono-institutional prospective study', *Gynecologic Oncology*, 136(3), pp. 415–423. doi: 10.1016/j.ygyno.2014.10.031.

Kirchheiner, K. (2016) 'Dose-effect relationship and risk factors for vaginal stenosis after definitive radio(chemo)therapy with image-guided brachytherapy for locally advanced cervical cancer in the EMBRACE study', *Radiotherapy and Oncology*, 118(1), pp. 160–166. doi: 10.1016/j.radonc.2015.12.025.

Kirisits, C. (2005) 'Dose and volume parameters for MRI-based treatment planning in intracavitary brachytherapy for cervical cancer', *International Journal of Radiation Oncology*Biology*Physics*, 62(3), pp. 901–911. doi: 10.1016/j.ijrobp.2005.02.040.

Kirisits, C. (2006) 'The Vienna applicator for combined intracavitary and interstitial brachytherapy of cervical cancer: Design, application, treatment planning, and dosimetric results', *International Journal of Radiation Oncology*Biology*Physics*, 65(2), pp. 624–630. doi: 10.1016/j.ijrobp.2006.01.036.

Kirkpatrick, S. (1983) 'Optimisation by simulated annealing', *Science*, 220(4598), pp. 671–680. doi: 10.1126/science.220.4598.671.

Kitchener, H. C. (2014) 'The clinical effectiveness and cost-effectiveness of primary human papillomavirus cervical screening in England: Extended follow-up of the ARTISTIC randomised trial cohort through three screening rounds', *Health Technology Assessment*, 18(23), pp. 1–195. doi: 10.3310/hta18230.

Klee, M. (2000) 'Life after Radiotherapy: The Psychological and Social Effects Experienced by Women Treated for Advanced Stages of Cervical Cancer', *Gynecologic Oncology*, 76(1), pp. 5–13. doi: 10.1006/gyno.1999.5644.

Klopp, A. H. (2016) 'A Phase III Randomized Trial Comparing Patient-Reported Toxicity and Quality of Life (QOL) During Pelvic Intensity Modulated Radiation Therapy as Compared to Conventional Radiation Therapy', *International Journal of Radiation Oncology*Biology*Physics*, 96(2), p. S3. doi: 10.1016/j.ijrobp.2016.06.024.

Koom, W. S. (2007) 'Computed Tomography-Based High-Dose-Rate Intracavitary Brachytherapy for Uterine Cervical Cancer: Preliminary Demonstration of Correlation Between Dose–Volume Parameters and Rectal Mucosal Changes Observed by Flexible Sigmoidoscopy', *International Journal of Radiation Oncology*Biology*Physics*, 68(5), pp. 1446–1454. doi: 10.1016/j.ijrobp.2007.02.009.

Kovalic, J. J. (1991) 'The effect of volume of disease in patients with carcinoma of the uterine cervix.', *International journal of radiation oncology, biology, physics*, 21(4), pp. 905–10. doi: 10.1016/0360-3016(91)90728-m.

Krishnatry, R. (2012) 'CT or MRI for Image-based Brachytherapy in Cervical Cancer', *Japanese Journal of Clinical Oncology*, 42(4), pp. 309–313. doi: 10.1093/jjco/hys010.

Kuipers, T. (2001) 'HDR brachytherapy applied to cervical carcinoma with moderate lateral expansion: modified principles of treatment.', *Radiotherapy and oncology : journal of the European Society for Therapeutic Radiology and Oncology*, 58(1), pp. 25–30. Available at: http://www.ncbi.nlm.nih.gov/pubmed/11165678 (Accessed: 14 July 2019).

Kumar, M. (2019) 'Impact of different dose prescription schedules on EQD2 in high-dose-rate intracavitary brachytherapy of carcinoma cervix', *Journal of Contemporary Brachytherapy*, 11(2), pp. 189–193. doi: 10.5114/jcb.2019.84586.

Lahanas, M. (2003) 'A hybrid evolutionary algorithm for multi-objective anatomy-based dose optimisation in high-dose-rate brachytherapy', *Physics in Medicine and Biology*, 48(3), pp. 399–415. doi: 10.1088/0031-9155/48/3/309.

Lang, S. (2007a) 'Treatment Planning for MRI Assisted Brachytherapy of Gynecologic Malignancies Based on Total Dose Constraints', *International Journal of Radiation Oncology Biology Physics*, 69(2), pp. 619–627. doi: 10.1016/j.ijrobp.2007.06.019.

Lang, S. (2007b) 'Treatment Planning for MRI Assisted Brachytherapy of Gynecologic Malignancies Based on Total Dose Constraints', *International Journal of Radiation Oncology Biology Physics*, 69(2), pp. 619–627. doi: 10.1016/j.ijrobp.2007.06.019.

Lertsanguansinchai, P. (2004) 'Phase III randomized trial comparing LDR and HDR brachytherapy in treatment of cervical carcinoma', *International Journal of Radiation Oncology*Biology*Physics*, 59(5), pp. 1424–1431. Available at: https://linkinghub.elsevier.com/retrieve/pii/S0360301604002068 (Accessed: 13 July 2019).

Lessard, E. (2001) 'Inverse planning anatomy-based dose optimisation for HDR-brachytherapy of the prostate using fast simulated annealing algorithm and dedicated objective function', *Medical Physics*, 28(5), pp. 773–779. doi: 10.1118/1.1368127.

LEWIS, G. C. (1960) 'Space dose relationships for points A and B in the radium therapy of cancer of the uterine cervix.', *The American journal of roentgenology, radium therapy, and nuclear medicine*, 83, pp. 432–46. Available at: http://www.ncbi.nlm.nih.gov/pubmed/14416519 (Accessed: 13 July 2019).

Lindegaard, J. C. (2013) 'MRI-guided adaptive radiotherapy in locally advanced cervical cancer from a Nordic perspective', *Acta Oncologica*, 52(7), pp. 1510–1519. doi: 10.3109/0284186X.2013.818253.

Ling, C. C. (1987) 'CT-assisted assessment of bladder and rectum dose in gynecological implants', *International Journal of Radiation Oncology*Biology*Physics*, 13(10), pp. 1577–1582. doi: 10.1016/0360-3016(87)90327-0.

Logsdon, M. (1999) 'Figo IIIB squamous cell carcinoma of the cervix: an analysis of prognostic factors emphasizing the balance between external beam and intracavitary radiation therapy.', *Int J Radiat Oncol Biol Phys*, 43(4), pp. 763–775. Available at: https://www.ncbi.nlm.nih.gov/pubmed/10098431.

Mahmoud, O. (2017) 'External beam techniques to boost cervical cancer when brachytherapy is not an option-Theories and applications', *Annals of Translational Medicine*. AME Publishing Company. doi:

10.21037/atm.2017.03.102.

Maier, U. (1997) 'Late Urological Complications and Malignancies After Curative Radiotherapy for Gynecological Carcinomas', *The Journal of Urology*, 158(3 Pt 1), pp. 814–817. doi: 10.1097/00005392-199709000-00033.

Maiman, M. (1998) 'Management of cervical neoplasia in human immunodeficiency virus-infected women.', *Journal of the National Cancer Institute. Monographs*, (23), pp. 43–9. Available at: http://www.ncbi.nlm.nih.gov/pubmed/9709302 (Accessed: 19 October 2018).

*Management of Cervical Cancer: Strategies for Limited-resource Centres - A Guide for Radiation Oncologists* (2013). Vienna: INTERNATIONAL ATOMIC ENERGY AGENCY (Human Health Reports). Available at: https://www.iaea.org/publications/8738/management-of-cervical-cancer-strategies-for-limited-resource-centres-a-guide-for-radiation-oncologists.

Martinez, A. A. (2001) 'Improvement in dose escalation using the process of adaptive radiotherapy combined with three-dimensional conformal or intensity-modulated beams for prostate cancer', *International Journal of Radiation Oncology*Biology*Physics*, 50(5), pp. 1226–1234. doi: 10.1016/S0360-3016(01)01552-8.

Mazeron, R. (2015) 'Impact of treatment time and dose escalation on local control in locally advanced cervical cancer treated by chemoradiation and image-guided pulsed-dose rate adaptive brachytherapy', *Radiotherapy and Oncology*, 114(2), pp. 257–263. doi: 10.1016/j.radonc.2014.11.045.

Mazeron, R. (2016) 'Dose–volume effect relationships for late rectal morbidity in patients treated with chemoradiation and MRI-guided adaptive brachytherapy for locally advanced cervical cancer: Results from the prospective multicenter EMBRACE study', *Radiotherapy and Oncology*, 120(3), pp. 412–419. doi: 10.1016/j.radonc.2016.06.006.

Mbulawa, Z. Z. A. (2018) 'High human papillomavirus (HPV) prevalence in South African adolescents and young women encourages expanded HPV vaccination campaigns.', *PloS one*, 13(1), p. e0190166. doi: 10.1371/journal.pone.0190166.

McIntyre, J. F. (1995) 'Ureteral stricture as a late complication of radiotherapy for stage IB carcinoma of the uterine cervix.', *Cancer*, 75(3), pp. 836–43. doi: 10.1002/1097-0142(19950201)75:3<836::aid-cncr2820750315>3.0.co;2-a.

Mittal, K. (2015) 'Complications of radiation therapy in carcinoma cervix', *International Journal of Applied Research*, 1(10), pp. 720–731.

Mohamed, S. (2015) 'Parametrial boosting in locally advanced cervical cancer: Combined intracavitary/interstitial brachytherapy vs. intracavitary brachytherapy plus external beam radiotherapy', *Brachytherapy*, 14(1), pp. 23–28. doi: 10.1016/j.brachy.2014.09.010.

Mohamed, S. (2016) 'Vaginal dose de-escalation in image guided adaptive brachytherapy for locally advanced cervical cancer', *Radiotherapy and Oncology*, 120(3), pp. 480–485. doi: 10.1016/J.RADONC.2016.05.020.

Mohammadi, S. (2015) 'A computational study on different penalty approaches for constrained optimisation in radiation therapy treatment planning with a simulated annealing algorithm', in *2015 IEEE/ACIS 16th International Conference on Software Engineering, Artificial Intelligence, Networking and Parallel/Distributed Computing, SNPD 2015 - Proceedings*. Institute of Electrical and Electronics Engineers Inc. doi: 10.1109/SNPD.2015.7176174.

Morice, P. (2003) 'Prognostic value of lymphovascular space invasion determined with hematoxylin-eosin staining in early stage cervical carcinoma: Results of a multivariate analysis', *Annals of Oncology*, 14(10), pp. 1511–1517. doi: 10.1093/annonc/mdg412.

Morris, K. AL (2015) 'Pelvic radiation therapy: Between delight and disaster', *World Journal of*

*Gastrointestinal Surgery*, 7(11), p. 279. doi: 10.4240/wjgs.v7.i11.279.

Morris, M. (1999) 'Pelvic Radiation with Concurrent Chemotherapy Compared with Pelvic and Para-Aortic Radiation for High-Risk Cervical Cancer', *New England Journal of Medicine*, 340(15), pp. 1137–1143. doi: 10.1056/NEJM199904153401501.

Mundt, A. J. (2002) 'Intensity-modulated whole pelvic radiotherapy in women with gynecologic malignancies.', *International journal of radiation oncology, biology, physics*, 52(5), pp. 1330–7. doi: 10.1016/s0360-3016(01)02785-7.

Nag, S. (2000) 'The American Brachytherapy Society recommendations for high-dose-rate brachytherapy for carcinoma of the cervix.', *International journal of radiation oncology, biology, physics*, 48(1), pp. 201–11. doi: 10.1016/s0360-3016(00)00497-1.

Nappi, L. (2005) 'Cervical squamous intraepithelial lesions of low-grade in HIV-infected women: Recurrence, persistence, and progression, in treated and untreated women', *European Journal of Obstetrics and Gynecology and Reproductive Biology*, 121(2), pp. 226–232. doi: 10.1016/j.ejogrb.2004.12.003.

Nath, R. (1997) *Code of practice for brachytherapy physics: Report of the AAPM Radiation Therapy Committee Task Group No. 56*.

Niemierko, A. (1997) 'Reporting and analyzing dose distributions: A concept of equivalent uniform dose', *Medical Physics*, 24(1), pp. 103–110. doi: 10.1118/1.598063.

Nomden, C. N. (2013) 'Clinical outcome and dosimetric parameters of chemo-radiation including MRI guided adaptive brachytherapy with tandem-ovoid applicators for cervical cancer patients: A single institution experience', *Radiotherapy and Oncology*, 107(1), pp. 69–74. doi: 10.1016/j.radonc.2013.04.006.

Osoba, D. (2011) 'Health-related quality of life and cancer clinical trials', *Therapeutic Advances in Medical Oncology*. SAGE Publications, pp. 57–71. doi: 10.1177/1758834010395342.

Pandey, U. (2017) 'What is Cervical Cancer?', *Journal of Gynecology and Womens Health*, 2(5). doi: 10.19080/JGWH.2017.02.555599.

Patel, F. D. (1994) 'Low dose rate vs. high dose rate brachytherapy in the treatment of carcinoma of the uterine cervix: A clinical trial', *International Journal of Radiation Oncology*Biology*Physics*, 28(2), pp. 335–341. doi: 10.1016/0360-3016(94)90055-8.

Pelloski, C. E. (2005) 'Comparison between CT-based volumetric calculations and ICRU reference-point estimates of radiation doses delivered to bladder and rectum during intracavitary radiotherapy for cervical cancer', *International Journal of Radiation Oncology*Biology*Physics*, 62(1), pp. 131–137. doi: 10.1016/j.ijrobp.2004.09.059.

Perez, C. A. (1995) 'Carcinoma of the uterine cervix. I. Impact of prolongation of overall treatment time and timing of brachytherapy on outcome of radiation therapy', *International Journal of Radiation Oncology*Biology*Physics*, 32(5), pp. 1275–1288. doi: 10.1016/0360-3016(95)00220-S.

Perez, C. A. (1998) 'Tumor size, irradiation dose, and long-term outcome of carcinoma of uterine cervix', *International Journal of Radiation Oncology Biology Physics*, 41(2), pp. 307–317. doi: 10.1016/S0360-3016(98)00067-4.

Pirog, E. C. (2000) 'Prevalence of human papillomavirus DNA in different histological subtypes of cervical adenocarcinoma', *American Journal of Pathology*, 157(4), pp. 1055–1062. doi: 10.1016/S0002-9440(10)64619-6.

Pötter, R. (2006) 'Recommendations from gynaecological (GYN) GEC ESTRO working group (II): Concepts and terms in 3D image-based treatment planning in cervix cancer brachytherapy—3D dose-volume parameters and aspects of 3D image-based anatomy, radiation physics, radiobiology',

*Radiotherapy and Oncology*, 78(1), pp. 67–77. doi: 10.1016/j.radonc.2005.11.014.

Pötter, R. (2007) 'Clinical impact of MRI assisted dose-volume adaptation and dose escalation in brachytherapy of locally advanced cervix cancer', *Radiotherapy and Oncology*, 83(2), pp. 148–155. doi: 10.1016/j.radonc.2007.04.012.

Pötter, R. (2011) 'Clinical outcome of protocol based image (MRI) guided adaptive brachytherapy combined with 3D conformal radiotherapy with or without chemotherapy in patients with locally advanced cervical cancer.', *Radiotherapy and oncology : journal of the European Society for Therapeutic Radiology and Oncology*, 100(1), pp. 116–23. doi: 10.1016/j.radonc.2011.07.012.

Pötter, R. (2016) 'Value of Magnetic Resonance Imaging Without or with Applicator in Place for Target Definition in Cervix Cancer Brachytherapy', *International Journal of Radiation Oncology Biology Physics*, 94(3), pp. 588–597. doi: 10.1016/j.ijrobp.2015.09.023.

Pötter, R. (2018) 'The EMBRACE II study: The outcome and prospect of two decades of evolution within the GEC-ESTRO GYN working group and the EMBRACE studies', *Clinical and Translational Radiation Oncology*. Elsevier Ireland Ltd, pp. 48–60. doi: 10.1016/j.ctro.2018.01.001.

'Prescribing, Recording, and Reporting Brachytherapy for Cancer of the Cervix' (2013) *Journal of the ICRU*, 13(1–2), pp. 1–10. doi: 10.1093/jicru_ndw027.

Van De Putte, G. (2005) 'Risk grouping in stage IB squamous cell cervical carcinoma', *Gynecologic Oncology*, 99(1), pp. 106–112. doi: 10.1016/j.ygyno.2005.05.026.

Rijkmans, E. C. (2014) 'Improved survival of patients with cervical cancer treated with image-guided brachytherapy compared with conventional brachytherapy', *Gynecologic Oncology*, 135(2), pp. 231–238. doi: 10.1016/j.ygyno.2014.08.027.

Rivard, M. J. (2004) 'Update of AAPM Task Group No . 43 Report : A revised AAPM protocol for brachytherapy dose calculations', (43), pp. 633–674. doi: 10.1118/1.1646040.

Robadi, I. A. (2018) 'The importance of high-risk human papillomavirus types other than 16 and 18 in cervical neoplasia', *Archives of Pathology and Laboratory Medicine*, 142(6), pp. 693–695. doi: 10.5858/arpa.2017-0563-RA.

Robin, T. P. (2016) 'Disparities in standard of care treatment and associated survival decrement in patients with locally advanced cervical cancer', *Gynecologic Oncology*, 143(2), pp. 319–325. doi: 10.1016/j.ygyno.2016.09.009.

Romano, K. D. (2017) 'Transition from LDR to HDR brachytherapy for cervical cancer: Evaluation of tumor control, survival, and toxicity', *Brachytherapy*, 16(2), pp. 378–386. doi: 10.1016/j.brachy.2016.12.005.

Saha, S. (2008) 'Image-guided HDR intracavitary and interstitial brachytherapy for locally advanced cervix cancer – correlation of late toxicity with DVH data and 3-year outcome analysis', *Brachytherapy*, 7(2), p. 98. doi: 10.1016/j.brachy.2008.02.353.

Sala, E. (2013) 'The added role of MR imaging in treatment stratification of patients with gynecologic malignancies: What the radiologist needs to know', *Radiology*. Radiological Society of North America, Inc., pp. 717–740. doi: 10.1148/radiol.12120315.

Schmid, M. P. (2011) 'Local recurrences in cervical cancer patients in the setting of image-guided brachytherapy: A comparison of spatial dose distribution within a matched-pair analysis', *Radiotherapy and Oncology*, 100(3), pp. 468–472. doi: 10.1016/j.radonc.2011.08.014.

Schoeppel, S. L. (1994) 'Three-dimensional treatment planning of intracavitary gynecologic implants: Analysis of ten cases and implications for dose specification', *International Journal of Radiation Oncology*Biology*Physics*, 28(1), pp. 277–283. doi: 10.1016/0360-3016(94)90168-6.

Schover, L. R. (1989) 'Sexual dysfunction and treatment for early stage cervical cancer', *Cancer*, 63(1), pp. 204–212. doi: 10.1002/1097-0142(19890101)63:1<204::AID-CNCR2820630133>3.0.CO;2-U.

Schwarz, M. (2004) 'Sensitivity of treatment plan optimisation for prostate cancer using the equivalent uniform dose ( EUD ) with respect to the rectal wall volume parameter', 73, pp. 209–218. doi: 10.1016/j.radonc.2004.08.016.

Sharma, D. N. (2011) 'High–dose rate interstitial brachytherapy using two weekly sessions of 10Gy each for patients with locally advanced cervical carcinoma', *Brachytherapy*, 10(3), pp. 242–248. doi: 10.1016/j.brachy.2010.09.001.

Shaw, W. (2013) 'Equivalence of Gyn GEC-ESTRO guidelines for image guided cervical brachytherapy with EUD-based dose prescription.', *Radiation Oncology*, 8(1), p. 266. doi: 10.1186/1748-717X-8-266.

Shaw, W. (2017) 'Image-guided adaptive brachytherapy dose escalation for cervix cancer via fractionation compensation', *Brachytherapy*, 16(3), pp. 534–546. doi: 10.1016/j.brachy.2017.01.002.

Shin, K. H. (2006) 'CT-guided intracavitary radiotherapy for cervical cancer: Comparison of conventional point A plan with clinical target volume-based three-dimensional plan using dose–volume parameters', *International Journal of Radiation Oncology*Biology*Physics*, 64(1), pp. 197–204. doi: 10.1016/j.ijrobp.2005.06.015.

Silberstein, J. L. (2013) *Translational andrology and urology.*, *Translational Andrology and Urology*. Available at: http://tau.amegroups.com/article/view/6247/7010#B12 (Accessed: 22 July 2019).

Simonds, H. (2015) 'HIV status and acute hematologic toxicity among patients with cervix cancer undergoing radical chemoradiation', *International Journal of Gynecological Cancer*, 25(5), pp. 884–890. doi: 10.1097/IGC.0000000000000441.

Smith, J. S. (2007) 'Human papillomavirus type distribution in invasive cervical cancer and high-grade cervical lesions: A meta-analysis update', *International Journal of Cancer*, 121(3), pp. 621–632. doi: 10.1002/ijc.22527.

Snyman, L. C. (2006) 'Urine cytology as a screening test for bladder infiltration in cervical cancer', *International Journal of Gynecological Cancer*, 16(4), pp. 1587–1590. doi: 10.1111/j.1525-1438.2006.00630.x.

Snyman, L. C. (2013) 'Prevention of cervical cancer - how long before we get it right?', *South African Journal of Obstetrics and Gynaecology*, 19(1), pp. 2–3. doi: 10.7196/sajog.651.

Sobotta, B. (2011) 'On expedient properties of common biological score functions for multi-modality, adaptive and 4D dose optimisation', *Physics in Medicine and Biology*, 56(10), p. N123. doi: 10.1088/0031-9155/56/10/N01.

Spampinato, S. (2019) 'OC-0507 Risk factors for bladder fistula, bleeding and cystitis in cervix cancer: an EMBRACE analysis', *Radiotherapy and Oncology*, 133, pp. S262–S263. doi: 10.1016/S0167-8140(19)30927-2.

Srivastava, A. (2014) 'Brachytherapy in cancer cervix: Time to move ahead from point A?', *World Journal of Clinical Oncology*. Baishideng Publishing Group Inc, pp. 764–774. doi: 10.5306/wjco.v5.i4.764.

StatsSA (2018) *Mid-year population estimates - P0302*. doi: Statistical release P0302.

Stewart, A. J. (2006) 'Current controversies in high-dose-rate versus low-dose-rate brachytherapy for cervical cancer.', *Cancer*, 107(5), pp. 908–15. doi: 10.1002/cncr.22054.

Sturdza, A. (2016) 'Image guided brachytherapy in locally advanced cervical cancer: Improved pelvic control and survival in RetroEMBRACE, a multicenter cohort study', *Radiotherapy and Oncology*, 120(3), pp. 428–433. doi: 10.1016/j.radonc.2016.03.011.

Tan, L. (2011) 'Implementation of Image-guided Brachytherapy for Cervix Cancer in the UK: Progress Update', *Clinical Oncology*, 23(10), pp. 681–684. doi: 10.1016/j.clon.2011.07.011.

Tan, L. T. (2011) 'Implementation of image-guided brachytherapy for cervix cancer in the UK: Progress update', *Clinical Oncology*, 23(10), pp. 681–684. doi: 10.1016/j.clon.2011.07.011.

Tan, P. W. (2015) 'Outpatient combined intracavitary and interstitial cervical brachytherapy: barriers and solutions to implementation of a successful programme - a single institutional experience.', *Journal of contemporary brachytherapy*, 7(3), pp. 259–263. doi: 10.5114/jcb.2015.52625.

Tanderup, K. (2010) 'From point A to the sculpted pear: MR image guidance significantly improves tumour dose and sparing of organs at risk in brachytherapy of cervical cancer', *Radiotherapy and Oncology*, 94(2), pp. 173–180. doi: 10.1016/j.radonc.2010.01.001.

Tanderup, K. (2013) 'Uncertainties in image guided adaptive cervix cancer brachytherapy: Impact on planning and prescription', *Radiotherapy and Oncology*, 107(1), pp. 1–5. doi: 10.1016/j.radonc.2013.02.014.

Tanderup, K. (2014) 'Curative radiation therapy for locally advanced cervical cancer: Brachytherapy is NOT optional', *International Journal of Radiation Oncology Biology Physics*, 88(3), pp. 537–539. doi: 10.1016/j.ijrobp.2013.11.011.

Tanderup, K. (2016) 'Effect of tumor dose, volume and overall treatment time on local control after radiochemotherapy including MRI guided brachytherapy of locally advanced cervical cancer', *Radiotherapy and Oncology*, 120(3), pp. 441–446. doi: 10.1016/j.radonc.2016.05.014.

Tanderup, K. (2020) 'Evidence-Based Dose Planning Aims and Dose Prescription in Image-Guided Brachytherapy Combined With Radiochemotherapy in Locally Advanced Cervical Cancer', *Seminars in Radiation Oncology*, 30(4), pp. 311–327. doi: 10.1016/j.semradonc.2020.05.008.

Taylor, A. (2004) 'Intensity-modulated radiotherapy--what is it?', *Cancer imaging : the official publication of the International Cancer Imaging Society*, 4(2), pp. 68–73. doi: 10.1102/1470-7330.2004.0003.

Teshima, T. (1993) 'High-dose rate and low-dose rate intracavitary therapy for carcinoma of the uterine cervix. Final results of Osaka University Hospital.', *Cancer*, 72(8), pp. 2409–14. doi: 10.1002/1097-0142(19931015)72:8<2409::aid-cncr2820720819>3.0.co;2-n.

Tod, M. (1953) 'Treatment of Cancer of the Cervix Uteri—A Revised "Manchester Method"', *The British Journal of Radiology*, 26(305), pp. 252–257. doi: 10.1259/0007-1285-26-305-252.

Tod, M. C. (1938) 'A Dosage System for Use in the Treatment of Cancer of the Uterine Cervix', *The British Journal of Radiology*, 11(132), pp. 809–824. doi: 10.1259/0007-1285-11-132-809.

Trnková, P. (2009) 'New inverse planning technology for image-guided cervical cancer brachytherapy : Description and evaluation within a clinical frame', *Radiotherapy and Oncology*, 93(2), pp. 331–340. doi: 10.1016/j.radonc.2009.10.004.

Tyagi, N. (2011) 'Daily Online Cone Beam Computed Tomography to Assess Interfractional Motion in Patients With Intact Cervical Cancer', *International Journal of Radiation Oncology*Biology*Physics*, 80(1), pp. 273–280. doi: 10.1016/j.ijrobp.2010.06.003.

Viswanathan, A. N. (2007) 'Computed Tomography Versus Magnetic Resonance Imaging-Based Contouring in Cervical Cancer Brachytherapy: Results of a Prospective Trial and Preliminary Guidelines for Standardized Contours', *International Journal of Radiation Oncology*Biology*Physics*, 68(2), pp. 491–498. doi: 10.1016/j.ijrobp.2006.12.021.

Viswanathan, A. N. (2010) 'Radiation dose-volume effects of the urinary bladder.', *International journal of radiation oncology, biology, physics*, 76(3 Suppl), pp. S116-22. doi: 10.1016/j.ijrobp.2009.02.090.

Viswanathan, A. N. (2010) 'Three-Dimensional Imaging in Gynecologic Brachytherapy: A Survey of the American Brachytherapy Society', *International Journal of Radiation Oncology*Biology*Physics*, 76(1), pp. 104–109. doi: 10.1016/j.ijrobp.2009.01.043.

Viswanathan, A. N. (2012) 'American Brachytherapy Society consensus guidelines for locally advanced carcinoma of the cervix. Part I: General principles', *Brachytherapy*, 11(1), pp. 33–46. doi: 10.1016/j.brachy.2011.07.003.

Viswanathan, A. N. (2012) 'American Brachytherapy Society consensus guidelines for locally advanced carcinoma of the cervix. Part II: High-dose-rate brachytherapy', *Brachytherapy*, 11(1), pp. 47–52. doi: 10.1016/j.brachy.2011.07.002.

Viswanathan, A. N. (2014) 'Comparison and consensus guidelines for delineation of clinical target volume for CT- and MR-based brachytherapy in locally advanced cervical cancer', *International Journal of Radiation Oncology Biology Physics*, 90(2), pp. 320–328. doi: 10.1016/j.ijrobp.2014.06.005.

Vordermark, D. (2016) 'Radiotherapy of Cervical Cancer', *Oncology Research and Treatment*. S. Karger AG, pp. 516–520. doi: 10.1159/000448902.

Wachter-Gerstner, N. (2003) 'Bladder and rectum dose defined from MRI based treatment planning for cervix cancer brachytherapy: Comparison of dose-volume histograms for organ contours and organ wall, comparison with ICRU rectum and bladder reference point', *Radiotherapy and Oncology*, 68(3), pp. 269–276. doi: 10.1016/S0167-8140(03)00189-0.

Wagner, A. (2013) 'Intensity modulated radiotherapy in gynecologic cancers: Hope, hype or hyperbole?', *Gynecologic Oncology*, 130(1), pp. 229–236. doi: 10.1016/j.ygyno.2013.04.052.

Wanderås, A. D. (2012) 'Adaptive brachytherapy of cervical cancer , comparison of conventional point A and CT based individual treatment planning Adaptive brachytherapy of cervical cancer , comparison of conventional point A and CT based individual treatment planning', (January 2016). doi: 10.3109/0284186X.2011.626446.

Wang, J. Z. (2010) 'Sequential magnetic resonance imaging of cervical cancer: the predictive value of absolute tumor volume and regression ratio measured before, during, and after radiation therapy.', *Cancer*, 116(21), pp. 5093–101. doi: 10.1002/cncr.25260.

Wang, K.-L. (2007) 'Correlation of Traditional Point a With Anatomic Location of Uterine Artery and Ureter in Cancer of the Uterine Cervix', *International Journal of Radiation Oncology*Biology*Physics*, 69(2), pp. 498–503. doi: 10.1016/j.ijrobp.2007.03.038.

Wang, X. (2010) 'High dose rate versus low dose rate intracavity brachytherapy for locally advanced uterine cervix cancer', in Liu, R. (ed.) *Cochrane Database of Systematic Reviews*. Chichester, UK: John Wiley & Sons, Ltd, p. CD007563. doi: 10.1002/14651858.CD007563.pub2.

WHO (2018) 'WHO | Cervical cancer', *WHO*. Available at: http://www.who.int/cancer/prevention/diagnosis-screening/cervical-cancer/en/ (Accessed: 15 May 2020).

Wu, Q. (2002) 'Optimisation of intensity-modulated radiotherapy plans based on the equivalent uniform dose.', *International journal of radiation oncology, biology, physics*, 52(1), pp. 224–35. doi: 10.1016/s0360-3016(01)02585-8.

Wu, Q. (2005) 'Dose sculpting with generalized equivalent uniform dose', *Medical Physics*, 32(5), pp. 1387–1396. doi: 10.1118/1.1897464.

Yen, A. (2018) 'Risk factors for fistula formation after interstitial brachytherapy for locally advanced gynecological cancers involving vagina', *Journal of Contemporary Brachytherapy*, 10(6), pp. 510–515. doi: 10.5114/jcb.2018.80171.

## Acknowledgements

I dedicate this work to my Mother, you gave me hope, strength and courage to never give up. I am who I am, because of you.

I would like to first and foremost thank God for the grace to have finished this study.

A big thanks to my sister Naudine, for all your wisdom, knowledge, time and support. Without you this wouldn't have been possible.

To the rest of my family and friends, thank you for the support. Especially my husband, Marnus for your endless support and patience.

Lastly, thanks for the Medical Physics Department for the assistance throughout the study.

# Appendix

**Appendix 1 - 192Ir-HDR-Flexisource Anisotropy Function F (r, Θ)**

**192Ir-HDR-Flexisource Anisotropy Function F(r,Θ)**

| | Distance from Active Source Center r (cm) | | | | | | | | | | | | | | | | | | | |
|---|---|---|---|---|---|---|---|---|---|---|---|---|---|---|---|---|---|---|---|---|
| **θ (°)** | **0.25** | **0.5** | **0.75** | **1** | **1.5** | **2** | **3** | **4** | **5** | **6** | **7** | **8** | **10** | **12** | **15** | **20** |
| **0** | --- | 0.649 | 0.619 | 0.607 | 0.602 | 0.614 | 0.634 | 0.656 | 0.680 | 0.692 | 0.717 | 0.733 | 0.760 | 0.777 | 0.802 | 0.833 |
| **1** | --- | 0.654 | 0.624 | 0.614 | 0.615 | 0.626 | 0.649 | 0.670 | 0.693 | 0.706 | 0.729 | 0.742 | 0.768 | 0.789 | 0.812 | 0.840 |
| **2** | --- | 0.659 | 0.632 | 0.625 | 0.632 | 0.642 | 0.667 | 0.686 | 0.709 | 0.725 | 0.743 | 0.756 | 0.780 | 0.803 | 0.824 | 0.848 |
| **3** | --- | 0.660 | 0.638 | 0.636 | 0.642 | 0.652 | 0.676 | 0.696 | 0.718 | 0.734 | 0.751 | 0.764 | 0.787 | 0.809 | 0.829 | 0.852 |
| **4** | --- | 0.665 | 0.648 | 0.647 | 0.655 | 0.666 | 0.689 | 0.710 | 0.729 | 0.744 | 0.760 | 0.773 | 0.796 | 0.816 | 0.837 | 0.858 |
| **5** | --- | 0.672 | 0.660 | 0.660 | 0.669 | 0.679 | 0.701 | 0.721 | 0.739 | 0.754 | 0.769 | 0.782 | 0.804 | 0.821 | 0.841 | 0.864 |
| **6** | --- | 0.681 | 0.672 | 0.673 | 0.682 | 0.692 | 0.713 | 0.732 | 0.750 | 0.764 | 0.778 | 0.791 | 0.811 | 0.825 | 0.845 | 0.867 |
| **8** | --- | 0.707 | 0.700 | 0.702 | 0.710 | 0.720 | 0.739 | 0.757 | 0.771 | 0.784 | 0.796 | 0.807 | 0.825 | 0.839 | 0.855 | 0.874 |
| **10** | --- | 0.735 | 0.729 | 0.731 | 0.739 | 0.748 | 0.764 | 0.778 | 0.791 | 0.802 | 0.813 | 0.822 | 0.839 | 0.852 | 0.868 | 0.883 |
| **15** | --- | 0.800 | 0.795 | 0.796 | 0.801 | 0.808 | 0.818 | 0.829 | 0.837 | 0.845 | 0.853 | 0.859 | 0.871 | 0.880 | 0.891 | 0.903 |
| **20** | --- | 0.851 | 0.845 | 0.845 | 0.848 | 0.852 | 0.860 | 0.868 | 0.875 | 0.880 | 0.885 | 0.890 | 0.898 | 0.905 | 0.912 | 0.920 |
| **25** | --- | 0.887 | 0.883 | 0.882 | 0.884 | 0.886 | 0.891 | 0.897 | 0.901 | 0.906 | 0.910 | 0.913 | 0.918 | 0.923 | 0.929 | 0.934 |
| **30** | --- | 0.914 | 0.909 | 0.909 | 0.911 | 0.913 | 0.917 | 0.921 | 0.924 | 0.926 | 0.930 | 0.932 | 0.936 | 0.939 | 0.943 | 0.947 |
| **40** | --- | 0.951 | 0.948 | 0.948 | 0.948 | 0.949 | 0.951 | 0.953 | 0.955 | 0.957 | 0.958 | 0.959 | 0.961 | 0.962 | 0.965 | 0.966 |
| **50** | --- | 0.972 | 0.971 | 0.971 | 0.972 | 0.972 | 0.973 | 0.974 | 0.975 | 0.975 | 0.976 | 0.976 | 0.977 | 0.978 | 0.979 | 0.979 |
| **60** | 0.99 | 0.986 | 0.985 | 0.986 | 0.986 | 0.986 | 0.986 | 0.987 | 0.987 | 0.987 | 0.987 | 0.988 | 0.987 | 0.988 | 0.988 | 0.989 |
| **70** | 0.996 | 0.993 | 0.994 | 0.994 | 0.995 | 0.994 | 0.995 | 0.995 | 0.995 | 0.995 | 0.995 | 0.995 | 0.994 | 0.995 | 0.995 | 0.995 |
| **80** | 0.999 | 0.998 | 0.999 | 0.998 | 0.998 | 0.999 | 0.999 | 0.999 | 0.999 | 0.999 | 0.999 | 0.999 | 0.999 | 0.999 | 0.999 | 0.998 |
| **90** | 1 | 1 | 1 | 1 | 1 | 1 | 1 | 1 | 1 | 1 | 1 | 1 | 1 | 1 | 1 | 1 |
| **100** | 0.999 | 0.998 | 0.998 | 0.998 | 0.998 | 0.999 | 0.999 | 0.999 | 0.999 | 0.999 | 0.999 | 0.999 | 0.999 | 0.999 | 0.999 | 0.999 |
| **110** | 0.996 | 0.993 | 0.993 | 0.993 | 0.994 | 0.994 | 0.995 | 0.996 | 0.995 | 0.995 | 0.996 | 0.996 | 0.995 | 0.995 | 0.996 | 0.995 |
| **120** | 0.991 | 0.986 | 0.985 | 0.986 | 0.986 | 0.986 | 0.987 | 0.987 | 0.987 | 0.987 | 0.987 | 0.988 | 0.988 | 0.989 | 0.989 | 0.989 |
| **130** | --- | 0.972 | 0.970 | 0.971 | 0.971 | 0.972 | 0.973 | 0.974 | 0.974 | 0.975 | 0.975 | 0.976 | 0.978 | 0.978 | 0.978 | 0.980 |
| **140** | --- | 0.951 | 0.948 | 0.948 | 0.949 | 0.950 | 0.953 | 0.955 | 0.956 | 0.957 | 0.958 | 0.959 | 0.961 | 0.963 | 0.965 | 0.966 |
| **150** | --- | 0.916 | 0.911 | 0.911 | 0.913 | 0.914 | 0.918 | 0.922 | 0.925 | 0.927 | 0.930 | 0.932 | 0.936 | 0.940 | 0.944 | 0.947 |
| **155** | --- | --- | 0.885 | 0.884 | 0.886 | 0.888 | 0.893 | 0.899 | 0.903 | 0.907 | 0.910 | 0.913 | 0.919 | 0.924 | 0.929 | 0.934 |
| **160** | --- | --- | 0.848 | 0.848 | 0.850 | 0.853 | 0.861 | 0.868 | 0.875 | 0.880 | 0.885 | 0.890 | 0.898 | 0.905 | 0.912 | 0.921 |
| **165** | --- | --- | --- | 0.799 | 0.803 | 0.807 | 0.817 | 0.828 | 0.838 | 0.845 | 0.853 | 0.859 | 0.870 | 0.880 | 0.890 | 0.902 |
| **170** | --- | --- | --- | 0.731 | 0.738 | 0.746 | 0.761 | 0.776 | 0.789 | 0.799 | 0.811 | 0.820 | 0.837 | 0.850 | 0.865 | 0.883 |
| **172** | --- | --- | --- | 0.700 | 0.706 | 0.716 | 0.734 | 0.751 | 0.766 | 0.778 | 0.791 | 0.802 | 0.820 | 0.834 | 0.852 | 0.870 |
| **174** | --- | --- | --- | 0.660 | 0.669 | 0.679 | 0.702 | 0.722 | 0.740 | 0.755 | 0.769 | 0.782 | 0.803 | 0.820 | 0.841 | 0.861 |
| **175** | --- | --- | --- | 0.639 | 0.647 | 0.658 | 0.682 | 0.705 | 0.724 | 0.741 | 0.756 | 0.770 | 0.793 | 0.810 | 0.834 | 0.856 |
| **176** | --- | --- | --- | 0.611 | 0.621 | 0.633 | 0.660 | 0.684 | 0.705 | 0.724 | 0.740 | 0.755 | 0.782 | 0.800 | 0.824 | 0.850 |
| **177** | --- | --- | --- | 0.574 | 0.588 | 0.604 | 0.635 | 0.661 | 0.685 | 0.706 | 0.722 | 0.737 | 0.769 | 0.791 | 0.814 | 0.844 |
| **178** | --- | --- | --- | 0.526 | 0.549 | 0.569 | 0.605 | 0.637 | 0.663 | 0.686 | 0.703 | 0.720 | 0.754 | 0.778 | 0.803 | 0.834 |
| **179** | --- | --- | --- | 0.487 | 0.509 | 0.532 | 0.570 | 0.606 | 0.633 | 0.659 | 0.682 | 0.700 | 0.734 | 0.763 | 0.790 | 0.817 |
| **180** | --- | --- | --- | 0.474 | 0.490 | 0.512 | 0.550 | 0.589 | 0.615 | 0.643 | 0.670 | 0.688 | 0.722 | 0.756 | 0.783 | 0.807 |

**Appendix 2 -The difference between the IHDM calculated and TG43 dose rate per unit air-kerma strength for all 70 positional coordinates.**

| Group number | Coordinates (cm) | | | Dose rate per unit air-kerma strength (cGy/hU) | | |
|---|---|---|---|---|---|---|
| | x | y | z | IHDM | TG 43 | % error TG43/IHDM |
| Group 1 | 0.00 | 0.00 | 0.25 | 15.40 | 15.56 | 1.02% |
| | 0.25 | 0.00 | 0.00 | 15.40 | 15.56 | 1.02% |
| | 0.25 | 0.25 | 0.00 | 9.07 | 9.21 | 1.51% |
| | 0.00 | 0.25 | 0.25 | 9.07 | 9.21 | 1.51% |
| | -0.25 | 0.00 | 0.00 | 15.40 | 15.56 | 1.02% |
| | 0.00 | 0.00 | -0.25 | 15.40 | 15.56 | 1.02% |
| | -0.25 | -0.25 | 0.00 | 9.10 | 9.21 | 1.24% |
| | 0.00 | -0.25 | -0.25 | 9.10 | 9.21 | 1.24% |
| Group 2 | 1.00 | 0.00 | 0.00 | 1.098 | 1.109 | 0.96% |
| | 0.00 | 1.00 | 0.00 | 0.696 | 0.703 | 1.04% |
| | 0.00 | 0.00 | 1.00 | 1.098 | 1.109 | 0.96% |
| | 1.00 | 1.00 | 0.00 | 0.536 | 0.542 | 1.03% |
| | 0.00 | 1.00 | 1.00 | 0.536 | 0.542 | 1.03% |
| | -1.00 | 0.00 | 0.00 | 1.098 | 1.109 | 0.96% |
| | 0.00 | -1.00 | 0.00 | 0.543 | 0.549 | 1.19% |
| | 0.00 | 0.00 | -1.00 | 1.098 | 1.109 | 0.96% |
| | -1.00 | -1.00 | 0.00 | 0.538 | 0.542 | 0.74% |
| | 0.00 | -1.00 | -1.00 | 0.538 | 0.542 | 0.74% |
| Group 3 | 2.00 | 0.00 | 0.00 | 0.278 | 0.281 | 1.09% |
| | 0.00 | 2.00 | 0.00 | 0.172 | 0.174 | 0.97% |
| | 0.00 | 0.00 | 2.00 | 0.278 | 0.281 | 1.09% |
| | 2.00 | 2.00 | 0.00 | 0.134 | 0.1358 | 1.06% |
| | 0.00 | 2.00 | 2.00 | 0.134 | 0.1358 | 1.06% |
| | -2.00 | 0.00 | 0.00 | 0.278 | 0.281 | 1.09% |
| | 0.00 | -2.00 | 0.00 | 0.144 | 0.145 | 1.05% |
| | 0.00 | 0.00 | -2.00 | 0.278 | 0.281 | 1.09% |
| | -2.00 | -2.00 | 0.00 | 0.135 | 0.1358 | 0.70% |
| | 0.00 | -2.00 | -2.00 | 0.135 | 0.1358 | 0.70% |
| Group 4 | 4.00 | 0.00 | 0.00 | 0.070 | 0.070 | 0.81% |
| | 0.00 | 4.00 | 0.00 | 0.046 | 0.046 | 1.12% |
| | 0.00 | 0.00 | 4.00 | 0.070 | 0.070 | 0.81% |
| | 4.00 | 4.00 | 0.00 | 0.0334 | 0.0337 | 1.00% |
| | 0.00 | 4.00 | 4.00 | 0.0334 | 0.0337 | 1.00% |
| | -4.00 | 0.00 | 0.00 | 0.070 | 0.0702 | 0.81% |
| | 0.00 | -4.00 | 0.00 | 0.041 | 0.0414 | 1.16% |
| | 0.00 | 0.00 | -4.00 | 0.070 | 0.0702 | 0.81% |
| | -4.00 | -4.00 | 0.00 | 0.0334 | 0.0337 | 0.76% |

| | | | | | | |
|---|---|---|---|---|---|---|
| | 0.00 | -4.00 | -4.00 | 0.0334 | 0.0337 | 0.76% |
| **Group 5** | 6.00 | 0.00 | 0.00 | 0.0306 | 0.0308 | 0.61% |
| | 0.00 | 6.00 | 0.00 | 0.0212 | 0.0214 | 0.91% |
| | 0.00 | 0.00 | 6.00 | 0.0306 | 0.0308 | 0.61% |
| | 6.00 | 6.00 | 0.00 | 0.0144 | 0.01451 | 0.76% |
| | 0.00 | 6.00 | 6.00 | 0.0144 | 0.01451 | 0.76% |
| | -6.00 | 0.00 | 0.00 | 0.0306 | 0.0308 | 0.61% |
| | 0.00 | -6.00 | 0.00 | 0.0197 | 0.01985 | 0.73% |
| | 0.00 | 0.00 | -6.00 | 0.0306 | 0.0308 | 0.61% |
| | -6.00 | -6.00 | 0.00 | 0.0144 | 0.0145 | 0.46% |
| | 0.00 | -6.00 | -6.00 | 0.0144 | 0.0145 | 0.46% |
| **Group 6** | 8.00 | 0.00 | 0.00 | 0.0168 | 0.01695 | 0.89% |
| | 0.00 | 8.00 | 0.00 | 0.0123 | 0.01243 | 1.06% |
| | 0.00 | 0.00 | 8.00 | 0.0168 | 0.01695 | 0.89% |
| | 8.00 | 8.00 | 0.00 | 0.0077 | 0.00773 | 0.39% |
| | 0.00 | 8.00 | 8.00 | 0.0077 | 0.00773 | 0.13% |
| | -8.00 | 0.00 | 0.00 | 0.0168 | 0.0170 | 0.65% |
| | 0.00 | -8.00 | 0.00 | 0.0116 | 0.0117 | 0.80% |
| | 0.00 | 0.00 | -8.00 | 0.0168 | 0.0170 | 0.61% |
| | -8.00 | -8.00 | 0.00 | 0.0077 | 0.0077 | 0.13% |
| | 0.00 | -8.00 | -8.00 | 0.0077 | 0.0077 | 0.13% |
| **Group 7** | 10.00 | 0.00 | 0.00 | 0.0104 | 0.0105 | 0.29% |
| | 0.00 | 10.00 | 0.00 | 0.0079 | 0.00796 | 0.45% |
| | 0.00 | 0.00 | 10.00 | 0.0104 | 0.0105 | 0.30% |
| | 10.00 | 10.00 | 0.00 | 0.0046 | 0.0046 | 0.97% |
| | 0.00 | 10.00 | 10.00 | 0.0046 | 0.0046 | 0.97% |
| | -10.00 | 0.00 | 0.00 | 0.0104 | 0.01048 | 0.29% |
| | 0.00 | -10.00 | 0.00 | 0.0075 | 0.00763 | 1.43% |
| | 0.00 | 0.00 | -10.00 | 0.0104 | 0.01048 | 0.30% |
| | -10.00 | -10.00 | 0.00 | 0.0047 | 0.00459 | 1.35% |
| | 0.00 | -10.00 | -10.00 | 0.0047 | 0.00459 | 1.29% |

**Appendix 3 - The difference between the IHDM calculated and Oncentra TPS dose rate per unit air-kerma strength for all 70 positional coordinates.**

| Group number | Coordinates (cm) | | | Dose rate per unit air-kerma strength (cGy/hU) | | |
|---|---|---|---|---|---|---|
| | x | y | z | IHDM | ONCENTRA TPS | % error IHDM/TPS |
| Group 1 | 0.00 | 0.00 | 0.25 | 15.40 | 15.76 | 2.27% |
| | 0.25 | 0.00 | 0.00 | 15.40 | 15.78 | 2.42% |
| | 0.25 | 0.25 | 0.00 | 9.07 | 9.24 | 1.82% |
| | 0.00 | 0.25 | 0.25 | 9.07 | 9.22 | 1.59% |
| | -0.25 | 0.00 | 0.00 | 15.40 | 15.21 | 1.28% |
| | 0.00 | 0.00 | -0.25 | 15.40 | 15.23 | 1.14% |
| | -0.25 | -0.25 | 0.00 | 9.10 | 9.10 | 0.07% |
| | 0.00 | -0.25 | -0.25 | 9.10 | 9.10 | 0.03% |
| Group 2 | 1.00 | 0.00 | 0.00 | 1.10 | 1.11 | 1.45% |
| | 0.00 | 1.00 | 0.00 | 0.70 | 0.71 | 1.55% |
| | 0.00 | 0.00 | 1.00 | 1.10 | 1.11 | 1.45% |
| | 1.00 | 1.00 | 0.00 | 0.54 | 0.54 | 0.94% |
| | 0.00 | 1.00 | 1.00 | 0.54 | 0.54 | 1.07% |
| | -1.00 | 0.00 | 0.00 | 1.10 | 1.10 | 0.45% |
| | 0.00 | -1.00 | 0.00 | 0.543 | 0.560 | 3.08% |
| | 0.00 | 0.00 | -1.00 | 1.10 | 1.10 | 0.45% |
| | -1.00 | -1.00 | 0.00 | 0.54 | 0.54 | 0.53% |
| | 0.00 | -1.00 | -1.00 | 0.54 | 0.54 | 0.53% |
| Group 3 | 2.00 | 0.00 | 0.00 | 0.28 | 0.28 | 1.18% |
| | 0.00 | 2.00 | 0.00 | 0.172 | 0.176 | 1.82% |
| | 0.00 | 0.00 | 2.00 | 0.28 | 0.28 | 1.18% |
| | 2.00 | 2.00 | 0.00 | 0.13 | 0.14 | 1.01% |
| | 0.00 | 2.00 | 2.00 | 0.13 | 0.14 | 1.01% |
| | -2.00 | 0.00 | 0.00 | 0.28 | 0.28 | 0.68% |
| | 0.00 | -2.00 | 0.00 | 0.144 | 0.148 | 3.07% |
| | 0.00 | 0.00 | -2.00 | 0.28 | 0.28 | 0.68% |
| | -2.00 | -2.00 | 0.00 | 0.13 | 0.14 | 0.65% |
| | 0.00 | -2.00 | -2.00 | 0.13 | 0.14 | 0.65% |
| Group 4 | 4.00 | 0.00 | 0.00 | 0.0696 | 0.0700 | 0.48% |
| | 0.00 | 4.00 | 0.00 | 0.046 | 0.047 | 2.54% |
| | 0.00 | 0.00 | 4.00 | 0.0696 | 0.0700 | 0.48% |
| | 4.00 | 4.00 | 0.00 | 0.0334 | 0.0336 | 0.65% |
| | 0.00 | 4.00 | 4.00 | 0.0334 | 0.0336 | 0.65% |
| | -4.00 | 0.00 | 0.00 | 0.0696 | 0.0700 | 0.48% |
| | 0.00 | -4.00 | 0.00 | 0.041 | 0.042 | 2.51% |
| | 0.00 | 0.00 | -4.00 | 0.0696 | 0.0700 | 0.48% |
| | -4.00 | -4.00 | 0.00 | 0.0334 | 0.0336 | 0.42% |
| | 0.00 | -4.00 | -4.00 | 0.0334 | 0.0336 | 0.42% |
| Group 5 | 6.00 | 0.00 | 0.00 | 0.0306 | 0.0308 | 0.57% |

| | | | | | | |
|---|---|---|---|---|---|---|
| | 0.00 | 6.00 | 0.00 | 0.0212 | 0.0217 | 2.23% |
| | 0.00 | 0.00 | 6.00 | 0.0306 | 0.0308 | 0.57% |
| | 6.00 | 6.00 | 0.00 | 0.0144 | 0.0147 | 2.00% |
| | 0.00 | 6.00 | 6.00 | 0.0144 | 0.0147 | 2.00% |
| | -6.00 | 0.00 | 0.00 | 0.0306 | 0.0308 | 0.57% |
| | 0.00 | -6.00 | 0.00 | 0.0197 | 0.0203 | 2.89% |
| | 0.00 | 0.00 | -6.00 | 0.0306 | 0.0308 | 0.57% |
| | -6.00 | -6.00 | 0.00 | 0.0144 | 0.0147 | 1.77% |
| | 0.00 | -6.00 | -6.00 | 0.0144 | 0.0147 | 1.77% |
| **Group 6** | 8.00 | 0.00 | 0.00 | 0.0161 | 0.0168 | 4.21% |
| | 0.00 | 8.00 | 0.00 | 0.0119 | 0.0123 | 3.29% |
| | 0.00 | 0.00 | 8.00 | 0.0161 | 0.0168 | 4.21% |
| | 8.00 | 8.00 | 0.00 | 0.0070 | 0.0077 | 9.13% |
| | 0.00 | 8.00 | 8.00 | 0.0070 | 0.0077 | 9.36% |
| | -8.00 | 0.00 | 0.00 | 0.0161 | 0.0168 | 4.43% |
| | 0.00 | -8.00 | 0.00 | 0.0112 | 0.0116 | 3.30% |
| | 0.00 | 0.00 | -8.00 | 0.0161 | 0.0168 | 4.48% |
| | -8.00 | -8.00 | 0.00 | 0.0070 | 0.0077 | 9.60% |
| | 0.00 | -8.00 | -8.00 | 0.0070 | 0.0077 | 9.60% |
| **Group 7** | 10.00 | 0.00 | 0.00 | 0.0098 | 0.0104 | 6.25% |
| | 0.00 | 10.00 | 0.00 | 0.0077 | 0.0079 | 2.88% |
| | 0.00 | 0.00 | 10.00 | 0.0098 | 0.0104 | 6.25% |
| | 10.00 | 10.00 | 0.00 | 0.0042 | 0.0046 | 9.62% |
| | 0.00 | 10.00 | 10.00 | 0.0042 | 0.0046 | 9.62% |
| | -10.00 | 0.00 | 0.00 | 0.0098 | 0.0104 | 6.25% |
| | 0.00 | -10.00 | 0.00 | 0.0077 | 0.0075 | 2.32% |
| | 0.00 | 0.00 | -10.00 | 0.0098 | 0.0104 | 6.25% |
| | -10.00 | -10.00 | 0.00 | 0.0042 | 0.0047 | 9.77% |
| | 0.00 | -10.00 | -10.00 | 0.0042 | 0.0047 | 9.72% |